نموذج رقم (1)

إقــــرار

أنا الموقع أدناه مقدم الرسالة التي تحمل العنوان:

Strengthening of RC Beams using SCC Jacketing with Wire Mesh

أقر بأن ما اشتملت عليه هذه الرسالة إنما هو نتاج جهدي الخاص، باستثناء ما تمت الإشارة إليه حيثما ورد، وإن هذه الرسالة ككل أو أي جزء منها لم يقدم من قبل لنيل درجة أو لقب علمي أو بحثي لدى أي مؤسسة تعليمية أو بحثية أخرى.

DECLARATION

The work provided in this thesis, unless otherwise referenced, is the researcher's own work, and has not been submitted elsewhere for any other degree or qualification

Student's name: اسم الطالب: محمود احمد أبو مرق

Signature: التوقيع:

Date: 10/02/2016   التاريخ:

Islamic University of Gaza

Higher Education Deanship

Faculty of Engineering

Civil Engineering Department

Design and Rehabilitation of Structures

الجامعـــــة الإسلاميـة – غــزة

عمـــــادة الـدراســـات العليـــا

كليـــــــــة الهنـــــدســـــــة

قســــــم الهنــــدسة المدنيــــة

برنامج تصميم وتأهيل المنشـآت

STRENGTHENING OF RC BEAMS USING SCC JACKETING WITH WIRE MESH

تقوية الكمرات الخرسانية المسلحة باستعمال قمصان من الخرسانة ذاتية الدمك مع شبكة أسلاك

By

MOHAMMED AHMED ABU MARAQ

Supervised By

PROF. MOHAMED ZIARA

A Thesis Submitted in Partial Fulfillment of the Requirements for the Degree of Master of Science in Civil Engineering - Design and Rehabilitation of Structures Program

1437 هـ - 2016 م

نتيجة الحكم على أطروحة ماجستير

بناءً على موافقة شئون البحث العلمي والدراسات العليا بالجامعة الإسلامية بغزة على تشكيل لجنة الحكم على أطروحة الباحث/ محمد أحمد رمضان أبو مرق لنيل درجة الماجستير في كلية ال<u>هندسة</u> قسم ال<u>هندسة المدنية-</u> <u>تصميم وتأهيل المنشآت</u> وموضوعها:

تقوية الكمرات الخرسانية المسلحة باستعمال قمصان من الخرسانة ذاتية الدمك مع شبكة أسلاك
Strengthening of RC Beams Using SCC Jacketing with Wire Mesh

وبعد المناقشة العلنية التي تمت اليوم الاثنين 29 ربيع الآخر 1437هـ، الموافق 2016/02/08م الساعة الواحدة ظهراً بمبنى القدس، اجتمعت لجنة الحكم على الأطروحة والمكونة من:

أ.د. محمد محمد زيارة	مشرفاً و رئيساً	....
أ.د. سمير محمد شحادة	مناقشاً داخلياً	....
د. بسام عبد الرحمن تايه	مناقشاً خارجياً	....

وبعد المداولة أوصت اللجنة بمنح الباحث درجة الماجستير في كلية ال<u>هندسة</u>/ قسم ال<u>هندسة المدنية-</u> <u>تصميم وتأهيل المنشآت</u>.

واللجنة إذ تمنحه هذه الدرجة فإنها توصيه بتقوى الله ولزوم طاعته وأن يسخّر علمه في خدمة دينه ووطنه.

والله ولي التوفيق ،،،

نائب الرئيس لشئون البحث العلمي والدراسات العليا

أ.د. عبدالرؤوف علي المناعمة

DEDICATIONS

To my parents, brothers, and sisters for their endless support.

To my friends, colleagues and to whom I belong to.

To all of you, I dedicate this thesis.

ACKNOWLEDGMENT

ABSTRACT

This research presents the experimental investigations of the structural behavior of reinforced concrete (RC) beams. The strengthening technique that was used section enlargement using Self-Compacting Concrete (SCC) reinforced with welded wire mesh (WWM). Different mechanical bonding between old and new concrete techniques were also investigated. These included dowels, expansion bolts and surface roughening.

Strengthening of beams was achieved by casting a SCC U-formed jacket that reinforced with small diameter of WWM to increase their shear resistance and increasing the flexural strength of concrete beams.

Four-point bending flexural tests were conducted on small-scale RC beams in the testing program up to failure. The test specimens were 1200 mm long with a cross section of 100 mm x 150 mm and after section enlargement the cross section was increased to 160 mm x 200 mm.

The test program included eighteen beams; three out of them were used as control beams; four out of these beams were used as monolithic control casted beams. While the other eleven beams were tested as strengthened beams and classified into two groups based on bonding technique and WWM properties.

The obtained results from the investigation indicated that the enlarged section using SCC jacketing with WWM improved significantly structural performance of beam measured in terms of ultimate load carrying capacity, stiffness, crack width and deflection.

The strengthened beams were able to reach their full flexural capacities comparable to their monolithic counterpart's beams. The interlaminar shear failure was prevented in all strengthened beams.

To understand the structure behavior of the strengthened beams, theoretical analysis was carried out and a simplified design procedure was presented in this thesis to predict the flexural strength and deflection at yielding and at ultimate stages. This analysis is done based on the basics of flexural theory and its assumptions and a good agreement at ultimate stage between experiment test results and prediction values was achieved.

المُــــــخص

هذا البحث يعرض نتائج الفحوصات المخبرية لدراسة التصرف الإنشائي للكمرات الخرسانية المسلحة . إن الطريقة المستخدمة لتقـــــوية هذه الكمــــرات هي تقنية القمصان الخرسانية والتي من خلالها تمت زيادة المقطع الخرساني باستخدام خرسانة ذاتية الدمك ومسلحة بشبكة من الأسلاك المعدنية الملحومة معاً وباستعمال طرق ميكانيكية مختلفة لربط الخرسانة الجديدة بالقديمة. هذه الطرق تشمل زراعة الأشاير أو استخدام براغي تتوسع أوتخشين سطح الباطون القديم.

لتحقيق عملية التقوية والتدعيم تم استعمال قميص خرساني على شكل حرف (U) باللغة الإنجليزية وصب خرسانة ذاتية الدمك , هذا القميص تم تسليحه باستعمال شبكة معدنية من الأسلاك الملحومة ذات أقطار صغيرة لزيادة مقاومة المقطع لقوى القص وكذلك لزيادة قدرة تحمل الكمرات الخرسانية لعزوم الإنحناء.

برنامج الفحص في هذه الدراسة أجري على كمرات خرسانية مسلحة ذات مقاس صغير مرتكزة على دعائم بسيطة ومعرضـة لقوتين مركزتين وقد تم فحصـها حتى الإنهيار، جميع هذه الكمــرات لها نفس الطول وهو 1200 ملم ومساحة مقطع عرضي 100 ملم x 150 ملم وبعد عملية التقوية تزداد مساحة المقطع العرضي لتصبح 160 ملم x 200 ملم.

ثماني عشرة كمرة خرسانية مسلحة تم استخدامها في برنامج الفحوصات ، ثلاث من هذه الكمرات تم فحصها كعينات قياسية ، أربع من هذه الكمرات تم فحصها ككمرات قياسية مصبوبة كوحدة واحدة ، بينما الإحدى عشرة كمرة المتبقية تمت عملية تقويتها انشائياً وقد تم تقسيم هذه الكمــرات إلى مجموعتين وذلك حسب التقنية المستخدمة للربط و كذلك حسب خصائص شبكة الأسلاك الملحومة المستخدمة.

أظهرت النتائج المخبرية التي تم الحصول عليها خلال هذه الدراسة أن تقنية زيادة المقطع باستعمال خرسانة ذاتية الدمك وشبكة معدنية من الأسلاك الملحومة تحسن وبشكل ملحوظ الأداء الإنشائي للكمرات من حيث قدرة التحمـل القصوى ، الصَلابة , عرض التشققات على الكمرات الخرسانية و قيم الترخيم والهبوط.

استطاعت الكمرات الخرسانية المقواة أن تصل لقدرة التحمل القصوى لعزوم الإنحناء مقارنة بالكمرات المناظرة لها والتي صبت كوحدة واحدة. الإنهيار عن طريق قوى القص الجانبية تم منعه في جميع الكمرات الخرسانية المقواة.

لفهم التصرف الإنشائي للكمرات المقواة انشائياً , تم عمل تحليل نظري و خطوات تصميمية مبسطة تم اشتقاقها بهذه الدراسة للتنبؤ بعزوم الإنحنـاء وقيم الترخـــيم بمرحلة اللدونة والمرحلة القصوى . هذا التحليل تم اجرائه بناءً على نظرية الإنحناء وفرضياتها وقد أظهرت النتائج المخبرية العملية للكمرات الخرسانية المقواة عند المرحلة القصوى تطابق كبير مع النتائج التي تم التنبؤ بها وتم الحصول عليها نظرياً.

TABLE OF CONTENTS

LIST OF TABLES

LIST OF FIGURES

LIST OF NOTATIONS

A_s	:	Cross sectional area of the steel bar in tension.
A_{swi}	:	Cross sectional area of the steel wires in tension at depth i.
a	:	Shear Span.
a	:	Depth of rectangular stress block, Whitney Block.
a/d	:	Shear span to depth ratio
b	:	Distance between each column of dowels, or distance to edge.
b_e	:	Width of section.
C	:	Compressive stress resultant in concrete.
c	:	Depth of neutral axis.
c	:	Distance between each row of dowels.
d	:	Effective depth of section.
d_m, d_r	:	Largest diameter of the flow spread of SCC in Abrams cone.
E_c	:	Elastic concrete modulus.
E_s	:	Elastic modulus of steel bars.
E_w	:	Elastic modulus of steel wires.
F	:	Load bearing capacity of a dowel.
F_{cr}	:	Modulus of rupture, For normal weight concrete.
fc'	:	Standard cylinder concrete compressive strength.
f_{cc}	:	Compressive strength of the concrete.
f_{ct}	:	Tensile strength of the concrete which equal to 10 % of compressive strength.
f_{st}	:	Tensile strength of the steel.
f_y	:	Yield strength of steel bars.
f_{yw}	:	Yield strength of steel wires.
f_u	:	Ultimate strength of steel bars.
f_{uw}	:	Ultimate strength of steel wires.
H_1	:	Depth of SCC in L box behind the gate.
H_2	:	Depth of SCC in L box at the end of the horizontal section.
h_{wi}	:	Depth of steel wires at level i.
I_{cr}	:	Moment of inertia of cracked section transformed to concrete.
I_e	:	Effective moment of inertia.
I_g	:	Moment of inertia for the gross section.
L	:	Distance between supports.
M_a	:	Maximum bending moment in member at sage deflection is computed.

M_{cr}	:	Cracking bending moment that causes the stress in extreme tension fiber to reach the modulus of rupture.
M_y	:	Yielding moment of beam.
M_{yC}	:	Calculated bending moment at yielding stage
M_{yE}	:	Experimental test result of bending moment at yielding stage.
M_u	:	Ultimate moment of beam.
M_{uC}	:	Calculated bending moment at ultimate stage
M_{uE}	:	Experimental test result of bending moment at ultimate stage.
PA	:	Passing ability of SCC.
T500	:	Time recorded when the flow spread of SCC reaches 500mm in diameter.
t_v	:	V-funnel flow time.
Y_t	:	Distance from the section centroid to the extreme tension fiber
Δcr	:	Mid-Span deflection at Mcr.
Δ_y	:	Mid-Span deflection at My.
Δ_{yc}	:	Calculated deflection at yielding stage
Δ_{yt}	:	Experimental results of deflection at yielding stage.
Δ_u	:	Mid-Span deflection at Mu.
Δ_{uc}	:	Calculated deflection at ultimate stage
Δ_{ut}	:	Experimental results of deflection at ultimate stage.
Δ_u/Δ_i	:	Ductility ratio defined as the ratio between the mid-spans deflections at ultimate load to that at the first crack load.
$\varnothing$	:	Diameter of one dowel.
ε_c	:	Concrete strain at the extreme fiber.
ε_{ywi}	:	Wire strain at bottom face must be equal or larger than 0.005 to be in tension control section.
ρ	:	Longitudinal reinforcement ratio.

LIST OF ABBREVIATIONS

ACI   American Concrete Institute.

ASTM   American Society for Testing and Materials.

EFNARC European Federation of National Trade Association

FEM   Finite Element Method.

FRP   Fiber Reinforced Polymers.

GFRP   Glass Fiber Reinforced Polymers.

HPFRC   High Performance Reinforced Concrete.

IUG   Islamic University of Gaza.

LP   Limestone Powder

LVDT   Linear Variable Displacement Transducer.

MAS   Maximum Aggregate Size.

PCC   Plain Cement Concrete.

RC   Reinforced Concrete.

RSW   Resistive Spot Welding

SCC   Self-Compacting Concrete.

SL   Service Load

SWM   Steel Wire Mesh.

UL   Ultimate Load

VMA   Viscosity Modifying Admixture.

WWM   Welded Wire Mesh.

1

CHAPTER
INTRODUCTION

CHAPTER 1

INTRODUCTION

1.1 GENERAL BACKGROUND

A varietal strengthening techniques are used in practice for reinforced concrete (RC) structures (**Ziara, 2014**). The strengthening technique becomes necessary for RC structures during their service life if the structures cannot meet the code of practice requirements due to different types of deterioration. A large number of structures constructed in the past using the older design codes are structurally unsafe according to the new design codes and hence need strengthening.

The main causes of deterioration depending on its cause can be classified into two categories. The first one is sudden damages which include natural disasters, wars and accidental damages, the other one is progressive damages which attributed to abuse use, neglect particularly the historical building and harmful environmental factors (**Ziara et al., 1996**).

Beams are paramount structural elements for sustaining loads, thus finding the efficient strengthening techniques are necessary in terms of maintaining the safety of the structures.

The application of steel welded wire mesh (WWM) to the surface of RC members as external reinforcement is a promising and recent new technique for strengthening and rehabilitating damaged concrete elements (**Xing, et al, 2010**).

Nowadays, it is necessary to find strengthening techniques suitable in terms of low costs and fast processing time particularly in Gaza Strip due to the abnormal conditions caused by the Israeli aggression which causes additional damages to RC structures.

In this research, the focus has been placed on the investigation of structural behavior of rectangular RC beams strengthened with galvanized steel WWM embedded in Self-Compacting Concrete (SCC) jacketing, which is recently considered a new technique for strengthening damaged concrete elements.

1.2 STATEMENT OF THE PROBLEM

This study deals with the problem of structural strengthening of rectangular RC beams when their conditions of use cannot be guaranteed during the service life and their fitness and strength can no longer to sustain the applied loads.

Needs for strengthening and upgrading of RC beams may be attributed to increasing applied load, modification of structural system, design errors, construction faults, accidental damages and improvements in suitability for use due to limitation of deflections and reduction of stress in steel reinforcement .

In this study, a method of strengthening of beams using galvanized steel WWM and SCC jacketing will be investigated to answer the following:

1- Is it possible to strengthen the flexural strength of existing beams by this technique?
2- Is the type of bonding between concrete substrate and new one a significant factor in strengthening process?
3- Does the WWM properties play a significant role through increasing the structural capacity of strengthened beams?
4- Is the U-jacketing of strengthening scheme can be used in rehabilitation process to reach full structural capacity?
5- Does the strengthened beams comply with code of practice requirements especially the Serviceability Limit State based on the crack width and deflections?
6- Does the strengthened beams will behave in a ductile manner up to failure or not?
7- Can the strengthened beams reach its full flexural capacity using the mechanical bonding or not?
8- What would be the design model for strengthening to match the existing beams in the practice?

To answer all above mentioned questions this research presents an experimental investigation and test program were prepared based on a set of beams that were subjected to pre-loading. Then the beams were strengthened using thin reinforced jacketing in different schemes and retested by the same flexural loading.

1.3 SCOPE OF WORK

The research scope focuses on strengthening method that is applied to rectangular RC beams. The main scope of this research is to understand the behavior of beams with the proposed different mechanically bonded methods of steel WWM embedded in SCC jacketing that can help designers and practitioners based on comprehensive experimental test program.

1.4 RESEARCH GOAL

The main goal of the research is to develop a more cost-effective strengthening technique for RC beams that can be applied in repairing RC structures especially in Gaza Strip.

Also this research produced a simplified design procedure that can predict the flexural strength of RC beams strengthened with WWM composites to reach good agreement between experiment and predicted values that achieved.

1.5 RESEARCH OBJECTIVES

The main objective of this research is to address the effectiveness of strengthening RC rectangular beams with WWM and SCC jacketing and to study the construction technology involved for further development. Within the main objective, sub objectives are:

1- To propose new method relative jacketing technique reinforced with galvanized WWM application to strengthening RC member.
2- To study the flexural behavior of RC beams under static loading condition.
3- To examine the effect of jacketing strengthening scheme and different wire mesh properties on the response of beam in terms of failure modes, enhancement of load carrying capacity and load deflection behavior.
4- To investigate the methods of anchorage of the WWM in strengthened beams.
5- To study the contribution of externally WWM on the flexural behavior of RC beams.

1.6 METHODOLOGY

To achieve the objectives of this research, the following tasks will be executed according to Figure 1.1. The Methodology steps are briefly described as follows:

1
Conducting a literature review.

2
Identifying research specifics and testing parameters.

3
Design the test program and selecting materilas.

4
Performing the experimental works.

5
Recording the results.

6
Analysis of test results and prepare the design approach of sterengthening.

7
Prepare the conclusions and recommendations.

8
Writing of M.Sc. Thesis.
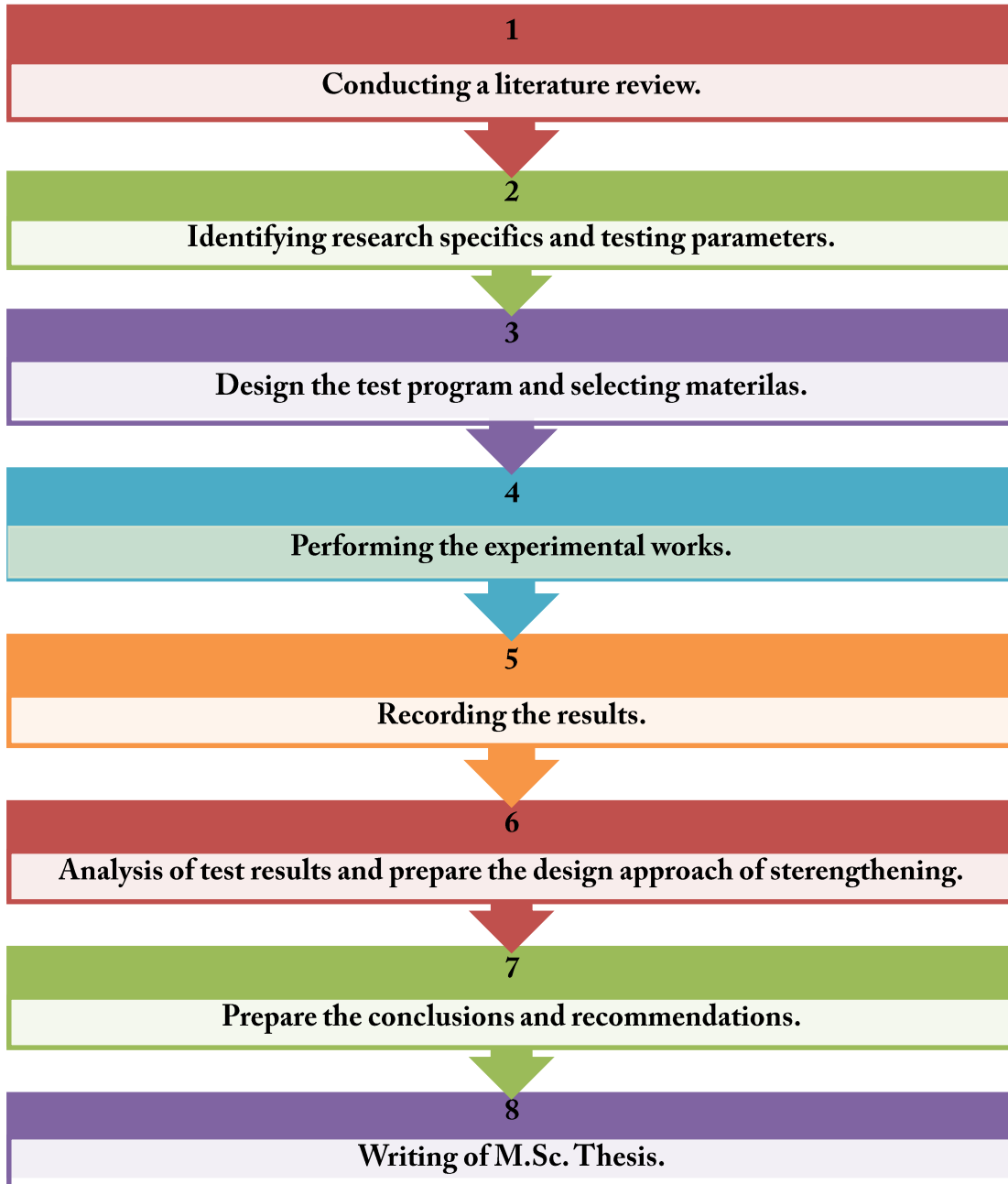
Figure 1.1 Methodology Tasks.

1.6.1. Conducting a Literature Review

In this section previous research works related to the subject undertaken research are reviewed to identify main concern aspects of the problem and its strengthening.

1.6.2. Identifying Research Specifics and Testing Parameters

In this section research specifics and testing parameters has been determined based on collected data related to testing facilities and material availability. In this stage the testing parameters should be wisely selected since they determine the extent of the program.

1.6.3. Design the Test Program and Selecting Materials

The test program is developed based on full understanding of the problem. It is designed to achieve the research problem. The details of the test program are addressed in this step. These include testing equipment, number and size of test beams, bonding mechanisms, selecting suitable materials which comply with American Society for Testing and Materials (ASTM) standards, casting, jacketing, curing, etc.

1.6.4. Performing the Experimental Works

In this section full testing procedure has been carried out based on the tentative test program. Also the experiment works comply with applicable standards.

1.6.5. Recording the Results

The test results are obtained and recorded using suitable devices such as take series of photo, measurements of load, deflection, cracking etc., make movies for the process of beams crushing and hand writing of the collected test results.

1.6.6. Analysis of the Test Results and Prepare Design Approach of Beams

The test results has been analyzed and discussed to achieve the targeted objectives, then the design approach of beams has been prepared to reach good agreement between experiment and predicted values that achieved.

1.6.7. Prepare the Conclusions and Recommendations

Conclusions and recommendations reached based on the test results were prepared for use by engineers in Gaza Strip to decide on an optimum and effective way for strengthening of RC beams in the real life application.

1.6.8. Writing of M.Sc. Thesis

M.Sc. thesis has been written during and after the experimental works as a draft copy, then it has been revised and finalized.

1.7 THESIS STRUCTURE

The research consists of seven chapters and five appendices organized as follows:

Chapter 1 (Introduction)

This chapter gives a general background about strengthening of RC beams using SCC with galvanized steel WWM, research problem and scope of work, objectives and methodology used to achieve the research objectives. Also it describes the structure of the research.

Chapter 2 (Literature Review)

This chapter reviews the necessity of strengthening of RC elements and the strengthening techniques of RC beams particularly the concrete jacketing.

This chapter discusses previous research works related to the undertaken research to identify main concern aspects of the problem and its strengthening.

Chapter 3 (Test Program)

This chapter illustrates the description of test program, parameters that determine the extent of the program, structural design of tested beams according to American Concrete Institute (ACI) 318-14, and the test program obstacles. It also presents the description for each beam in this research.

Chapter 4 (Laboratory Works)

This chapter reviews the materials used for constructing beams such as cement, reinforcement steel, fine aggregate, coarse aggregate etc., and concrete job mix design.

It also describes the experimental set-up, tested beams preloading stage, beam strengthening set-up and beams flexure testing procedure.

It also includes the materials were used in tested beams strengthening like producing SCC and their properties, mix design, and equipment used in the testing procedures. In addition to strengthening materials such as WWM properties and welding process, expansion bolt properties, anchoring resin, and others.

Also this chapter illustrates the test results for test program materials including the fresh and hardened results for both concrete and SCC, reinforcement steel properties such as yielding, elongation etc., WWM properties, and others.

Chapter 5 (Test Results and Discussions)

This chapter illustrates the test results for tested beams specimens including the investigated structural behavior for the flexural strengths, ductility expressed by the middle span deflection, crack development of tested beams, crack width, and visual inspection of cracks pattern.

Chapter 6 (Theoretical Analysis of Strengthened Beams)

This chapter describes a simplified design approach to predict the flexural strength of rectangular RC beams strengthened using WWM based on the analyzed test results of the tested beams.

Chapter 7 (Conclusions and Recommendation)

This chapter includes the concluded remarks, main conclusions and recommendations drawn from this research for future works.

References

Lists of reviewed references.

Appendixes

Lists the appendixes.

Appendix **A** Repair materials specifications

Appendix **B** Deflection derivation of two point loading

Appendix **C** SCC test methods according to EFNARC

Appendix **D** Shear connectors calculations

Appendix **E** Theoretical Analysis

2

CHAPTER
LITERATURE REVIEW

CHAPTER 2

LITERATURE REVIEW

2.1 INTRODUCTION

An overview of previous studies related to several strengthening techniques of RC beams are presented in this chapter, with particular attention devoted to strengthening RC beams by concrete jacketing. Also there are many different kinds of strengthening techniques of RC beams are discussed in literature.

The sophistication of strengthening techniques ranges from simple methods of enlargement of cross section (i.e. concrete jacketing, overlays, underlays, etc.) to advanced methods in which strengthening is achieved using carbon fibers, external posttensioning, steel plates and others (**Ziara, 2014**).

Structural engineers are frequently faced with the task of strengthening an existing structure. Nowadays, strengthening of damaged RC buildings has become an important issue. This research is concerned with strengthening of RC beams with jacketing. Therefore, to guide the research, relevant literatures on beams and beam strengthening techniques are discussed in the following sections.

2.2 NECESSITY OF STRENGTHENING RC ELEMENTS

Concrete structures need to be strengthened for any of the following reasons (**Mishra G., 2014**):

1. Load increases due to higher live loads, increased wheel loads, installations of heavy machinery, or vibrations.
2. Damage to structural parts due to aging of construction materials or fire damage, corrosion of steel reinforcement, and/or impact of vehicles.
3. Improvements in suitability for use due to limitation of deflections, reduction of stress in steel reinforcement and/or reduction of crack widths.

4. Modification of structural system due to elimination of walls/columns and/or openings cut through slabs.

5. Errors in planning or construction due to insufficient design dimensions and/or insufficient reinforcing steel.

2.3 DAMAGES IN BEAMS IN GAZA STRIP

Gaza strip is costal area which has 40 Km coastline on the Mediterranean Sea. This location with the associated environmental conditions may have a considerable influence on the deterioration of existing concrete structures (**El-Ebweini, 2009**).

A survey of forty case studies for assessment of existing damaged structures in Gaza Strip showed that the main cause of defects in RC beams are as follows (**Abu Hamam, 2008**):

1. Reinforcement corrosion as a result of improper concrete cover, Chloride attack and carbonation.

2. Vertical flexural cracks as a result of over loads, section deficiency and low strength materials.

3. Diagonal shear cracks as a result of over loads, foundation settlement and section deficiency.

4. Damages due to accidental events such as fire and manmade destruction.

According to the study which conducted in 2008, 9.6% of the deficiencies in Gaza strip are structural cracks in slabs and drop beams

2.4 STRENGTHENING TECHNIQUES OF RC BEAMS

In this section, most used strengthening techniques of RC beams are reviewed.

There are many common techniques for strengthening of various RC elements in use worldwide (**Ziara, 2014**). Regardless the type of the strengthening techniques used, the following considerations should be observed:

i.   Apply additional measures to carry existing loads during strengthening.

ii.   The new loads are applied after strengthening.

iii.   Ensure full interaction between new and old materials (Compatibility of strains).

2.4.1. Compression Concrete Overlay

This technique can be achieved through roughening the original concrete surface then adding a new concrete overlay reinforced with light shrinkage reinforcement as shown in Figure 2.1, to ensure full interaction between new and old materials one of the following method must be done (**Abu Almjd, 1988**):

i.   Using of shear connectors to prevent inter laminar shear

ii.   Making concrete keys for the original concrete surface and painting it with bonding agent.

iii.   Bonding of stirrups with original concrete through drilling holes and installing the ends of stirrups into these holes using epoxy resin, the fixation length must be sufficient to transfer the shear stresses.
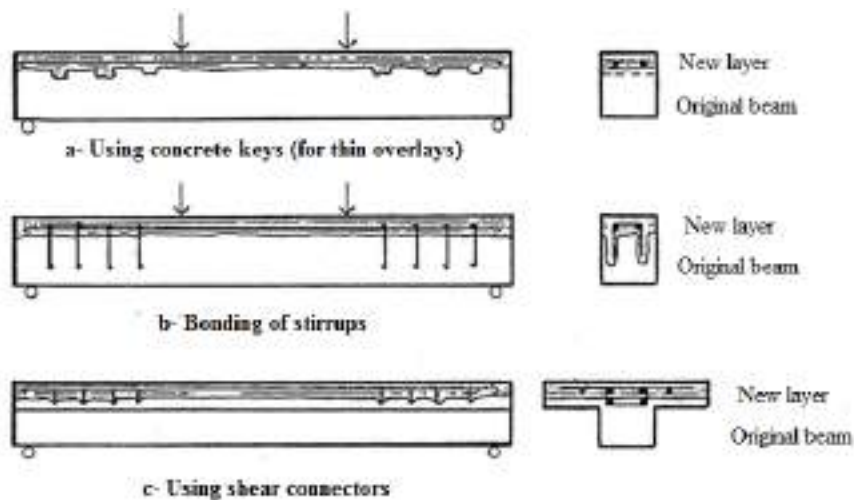
Figure 2.1 Addition of concrete overlay in compression zone (Source: Abu Almjd, 1988).

In order to accomplish force transfer between old and new concrete, roughening of the surface of the old concrete is required, as well as welding of connecting bars to the existing bars and new reinforcement.

2.4.2. Strengthening for Flexural

2.4.2.1. Addition of Steel Reinforcement (Concrete Underlay)

RC beams can be strengthened by adding new concrete to lower face of the beam. In this technique the beam depth increased due to strengthening of the tension zone of a beam through concrete underlays. In order to accomplish force transfer between old and new concrete, roughening of the surface of the old concrete is required, as well as welding of connecting bars to the existing bars and new reinforcement.

Reinforced underlays on the lower face of the beam (Figure 2.2) can only increase its flexural capacity. Existing reinforcement is connected to the new reinforcement by welding.
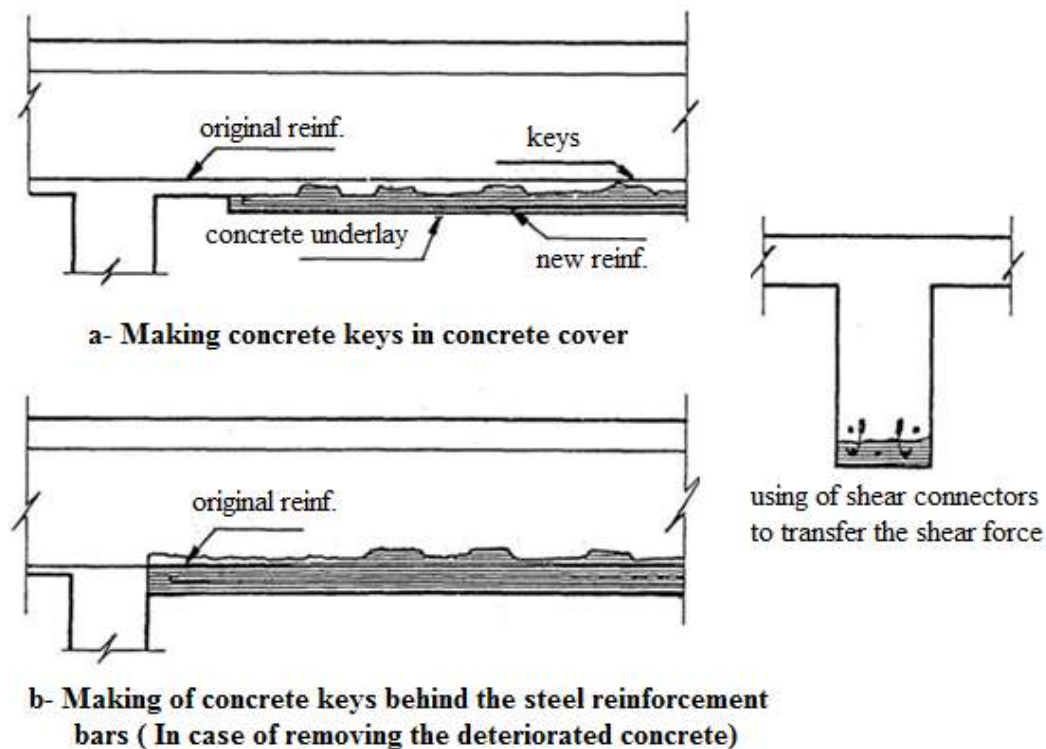
Figure 2.2 Addition of concrete underlay in tension zone (Source: Abu Almjd, 1988).

Due to the fact that using forms and pouring the concrete from the top is not possible, the feasible solutions are shotcrete or using SCC.

2.4.2.2. Addition of External Steel Plates

The technique of bonding steel plates to the surface of concrete has been used on a number of structures throughout the world to enhance load carrying capacity (**Rehabcon, Annex K, 2004**).With this technique, the bonded steel plates act as external reinforcement. The effect of bonding a plate to the tension face of a RC beam is to increase the depth from the compression face to the neutral axis and the area of effective reinforcement, thus, increasing the moment of resistance of the section. The operation can be undertaken without additional support to the member.

The bonding of steel plates to concrete members has been undertaken by several methods, using epoxy adhesives or using bolts. The choice of method being dependent upon the particular circumstances. Figure 2.3 shows the strengthening of a bridge girder using externally bolted steel plate.

Figure 2.3 Strengthening using externally bolted steel plate (Source: Khalaf, 2015).

2.4.2.3. Addition of Carbon Fibers

The strengthening or repair of concrete structures using externally bonded Fiber Reinforced Polymers (FRP) provides an alternative solution to traditional methods of strengthening such as externally bonded steel plates (**Rehabcon, Annex J, 2004**). FRP

materials are currently being used for upgrading existing structures because of their resistance to corrosion and their light weight. Different types of fiber can be used, i.e., glass, carbon and aramid. The FRP is applied to different RC elements such as beams, columns, and slabs, to provide substantial increase in strength and durability.

For flexural strengthening of RC beams the FRP is bonded to the tension zones with the fibers parallel to the principal stress direction. The effect of bonding a FRP to the tension face of a RC beam is to increase the depth from the compression face to the neutral axis and the area of effective reinforcement, thus, increasing the moment of resistance of the section. Figure 2.4 shows the strengthening of a bridge girder using externally bonded FRP.

Figure 2.4 Strengthening using bonded FRP (Source: Carbon Fiber Wrapping, n.d.).

2.4.2.4. Addition of Steel Sections (Composite Section)

The technique addition of steel sections such as (C channel, I beams, L angles and etc.) as shown in Figure 2.5 can increase the flexural capacity, ductility and stiffness of RC beams. These sections are bonded on the lower face of the beam for strengthening of the tension zone.
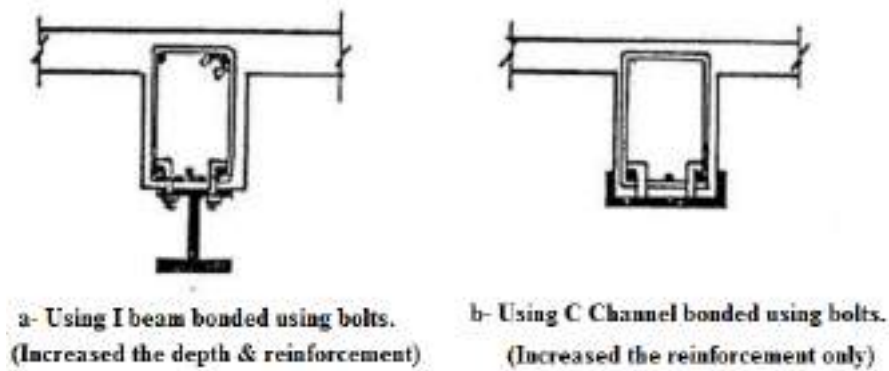
Figure 2.5 Addition of steel sections (Source: Abu Almjd, 1988)

The bonding of steel sections to concrete members has been undertaken by several methods, using epoxy adhesives, using bolts and using welding. The choice of method being dependent upon the particular circumstances.

2.4.3. Strengthening for Shear and Torsion

2.4.3.1. Addition of External Stirrups

The technique of addition of external stirrups can be accomplished using high strength steel bolts that distributed along the beam length at predetermined distances (represent stirrups) connected with steel plates or steel sections such as C- channel as shown in Figure 2.6. These bolts and steel sections must be protected against environmental condition and from corrosion with a coating. Also the new reinforcement is encased in conventionally placed concrete or in shotcrete if there is no aesthetic restrictions.
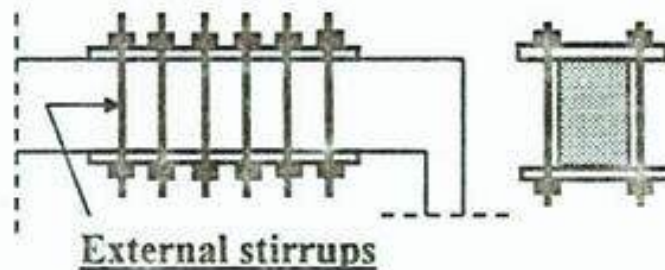
Figure 2.6 Addition of external stirrups (Source: Ziara, 2014).

2.4.3.2. Addition of External Steel Plates

With this technique, the bonded steel plates act as external shear and/ or torsion reinforcement. The effect of bonding a plate to the two side faces of a RC beam is to increase its shear resistance, thus, increasing the load carrying capacity of the section. This technique have many advantages such as, speed and simplicity of installation, simple operation, and minimal disruption during installation.

The bonding of steel plates to concrete members has been undertaken by several methods, using epoxy adhesives or using bolts (Figure 2.7). The choice of method being dependent upon the particular circumstances.

The new reinforcement may be encased with concrete (**ACI 546R-04, 2004**), shotcrete, mortar, plaster, waterproofing, fireproofing, or other product, or it may be left exposed and protected from corrosion with a coating.
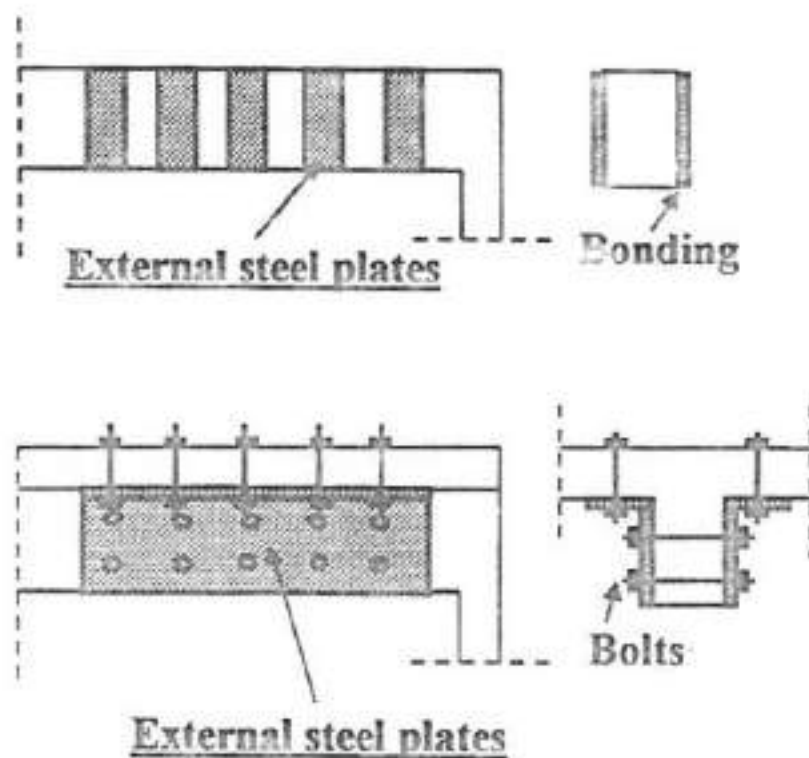
Figure 2.7 Addition of external steel plates (Source: Ziara, 2014).

The beams can be strengthen in shear by bonding external FRP of different types, with different forms and by different configurations as shown in the Figure 2.8 and 2.9.
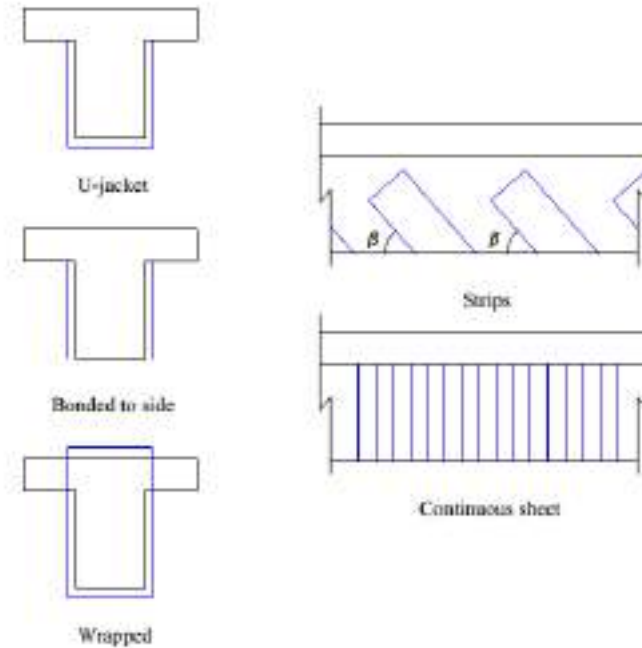
Figure 2.8 Configurations of FRP for shear (Source: Rehabcon, Annex J, 2004).

Shear strengthening of RC elements using FRP may usually be provided by bonding the external reinforcement with the principal fibre orientation either 45º or 90º (**Rehabcon, Annex J, 2004**) as shown in Figure 2.8. The strengthening will be more efficient when its fibers are parallel to the maximum principal tensile stress.

The shear contribution of FRP to the strengthened element is influenced by many factors such as size and geometry of the member, properties of concrete, internal shear and flexural reinforcements, loading conditions, method of strengthening, properties of the bond, anchorage length, type of anchorage, thickness of the FRP, rigidity of the FRP, the fibre orientation and etc.

Figure 2.9 Shear Strengthening by FRP (Source: SIKA Carbodur, n.d.).

2.4.4. Jacketing of Beams

RC jackets can be applied by adding new concrete to three or four sides of the beam (**Penelis and Kappos, 1997**). In order to accomplish force transfer between old and new concrete, roughening of the surface of the old concrete is required, as well as welding of connecting bars to the existing bars and new reinforcement as illustrated in Figure 2.10.
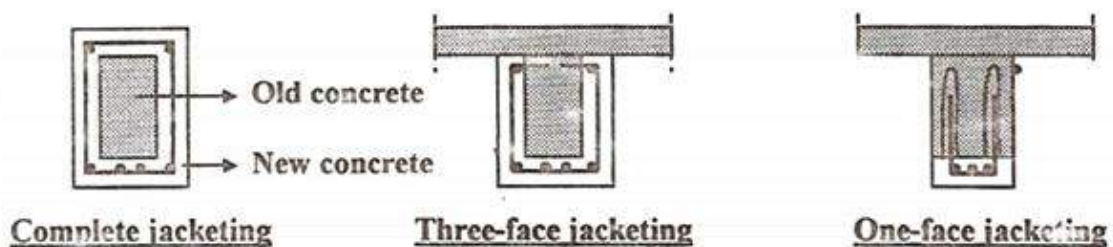
Figure 2.10 RC beam jacketing technique (Source: Ziara, 2014)

Jacketing On all four sides of the beam is the most effective solution. The thickness of the concrete that is added to the upper face is such that it can be accommodated within the floor thickness (maximum: 50—70 mm). The placement of the ties is achieved through holes, which are opened in the slab at closely spaced distances and are a so used for

pouring the concrete. The longitudinal reinforcement bars of the jacket are welded to those of the old concrete.

Jackets on three sides of the beam are used to increase the flexural and shear capacity of the beam for vertical loading, but not for seismic actions, given that strengthening of the load-bearing capacity of the section near the supports is impossible. The key to the success of such an intervention is the appropriate anchorage of the stirrups at the top of the sides of the jacket.

2.4.5. Span Shortening

Supplemental members are new columns, beams, braces, or infilled walls that are installed to support strengthened structural members, as illustrated in Figure 2.11.The supplemental members are typically placed below the failure or deflected areas to stabilize the structural framing.
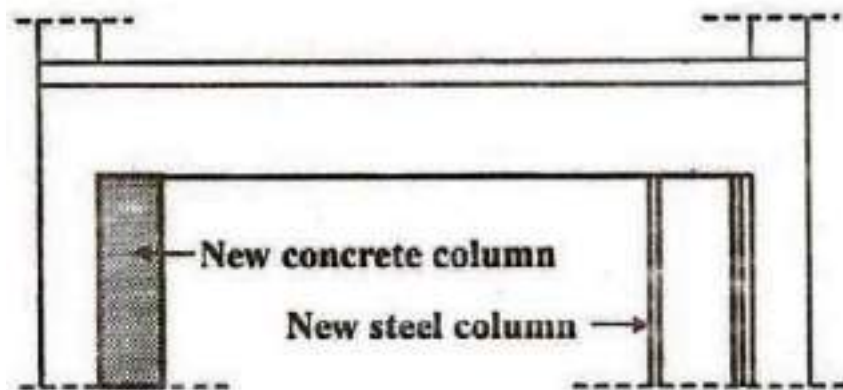
Figure 2.11 Span shortening technique (Source: Ziara, 2014).

Span shortening can be used if none of the other strengthening techniques is adequate for repair or if the structural configuration precludes use of other techniques (**ACI 546R-04, 2004**). Supplemental members are quickly installed and, therefore, are suitable temporary emergency repair solutions. Typically, new members are installed to support seriously cracked and deflected flexural members. Often, the use of supplemental members may be the most economical alternative.

2.5 DESCRIPTION OF PREVIOUS RESEARCH ON SECTION ENLARGEMENT

2.5.1. Scope

Section enlargement is one of the methods used in strengthening concrete members. Placing additional layer of concrete surrounding an existing beam is called section enlargement. Jacketing by RC could improve resistance against applied loads and enhances the durability at same time. Furthermore, section enlargement and concrete jacketing may be easier and cheaper compared to other approaches such as steel plate jacketing.

2.5.2. Previous Research Related to Section Enlargement

Diab (1998) carried out an experimental program to evaluate the effectiveness of repairing RC beams with a layer of sprayed concrete. Nine specimens (three series) were tested in total. The first series includes the testing of three reference beams (PR1-PR3) to failure. In series two, three beams (PR1-PR3) were loaded, damaged and repaired by the addition of two reinforcing steel-bar and a layer of sprayed concrete then loaded to failure; the beams of the third series three beams (PR4-PR6) have same dimension with P1 and tested in the same manner with series two, except that the reinforcing layer was performed with fibrous concrete.

The experimental results indicate that jacketing using sprayed concrete to strengthen RC beams can effectively increase their load carrying capacity or stiffness and the strengthened beams showed high ductility before failure as shown in Figure 2.12. Furthermore, additional metallic glass ribbon fibers in sprayed concrete improved the crack pattern and ultimate capacity of RC beams. Adding metallic glass ribbon fibers to RC beams improved flexural strength, enhanced cracking pattern, reduced tensile stress and greatly increased the first cracking moment.
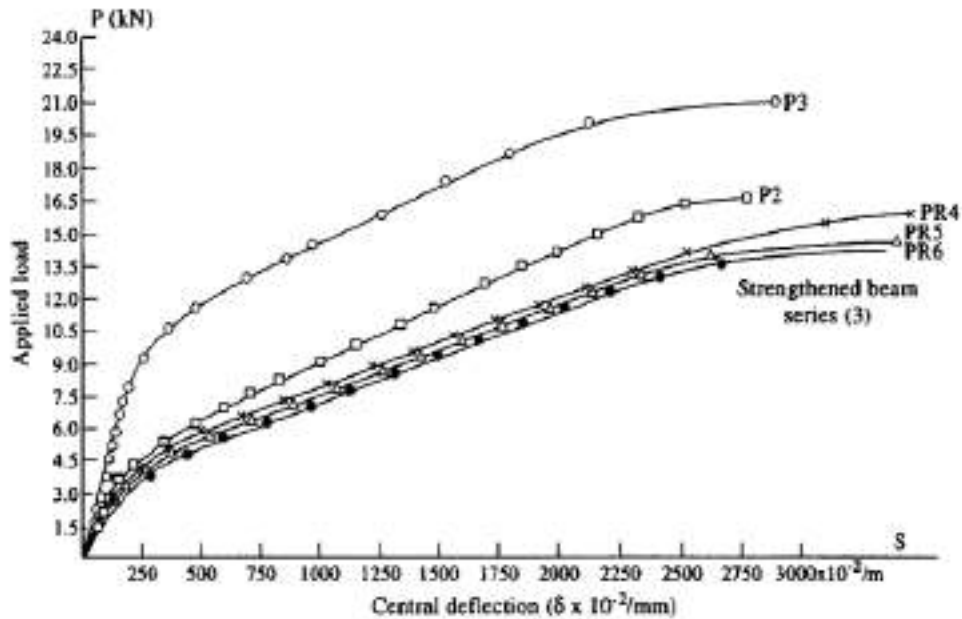
Figure 2.12 Load-central deflection curve for strengthened beams (Source: Diab 1998).

Mahdy et al. (2004) conducted an experimental study to evaluate the role of adding U-shape RC jacket in upgrading RC beams, Eleven RC beams tested under 3-PB were experimentally evaluated. The specimens strengthened by three-faces RC jackets (U-shape, 50mm at the bottom and 37.5 at each side of the beam) with and without additional stirrups.

Details of strengthening technique exhibited in Figure 2.13 and Figure 2.14.
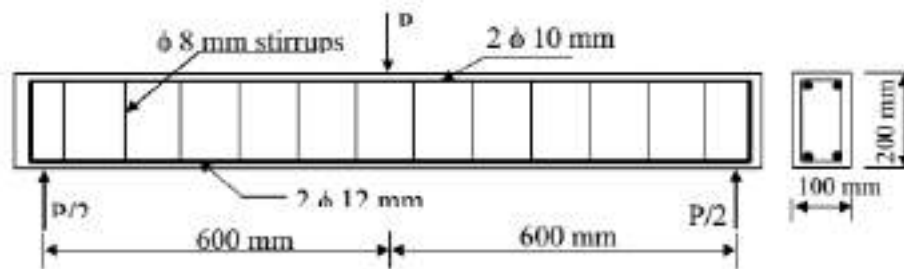
Figure 2.13 Dimensions and reinforcement of the control (Source: Mahdy et al., 2004).
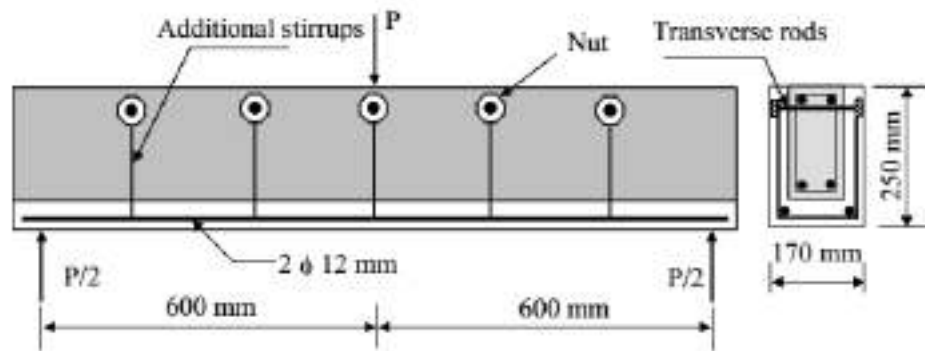
Figure 2.14 Dimensions and reinforcement of jacketing (Source: Mahdy et al., 2004).

The test results showed that the strengthened beams of additional stirrups exhibit typical failure with a ductile manner and with enhancement in strength reach 233% of the control beam. While, the strengthened beam without additional stirrups fail in brittle manner and by separation of the added concrete layer with strength enhancement reach 132% of the control beam.

Altun (2004) compared the mechanical properties of RC beams before and after jacketing under bending test. Altun categorized nine 1800 mm long RC beams with 20 MPa concrete strength, 420 MPa steel strength in three groups based on their three different cross sections and then loading them until full failure. The other nine beams that have the same dimensions were strengthened with 100 mm thick RC jackets on all four sides as shown in Figure 2.16, loaded them to full plastic yield. Typical test beam is shown in Figure 2.15.

The results revealed that damaged RC beams would behave similar to the ordinary RC beams of same dimensions with added RC jackets. However, the beam with highest ductility ratio is the most efficient since the section area is relatively less as compared to the section resisting the maximum Ultimate Load (UL). This reduces the amount of cost of the jacketing material.
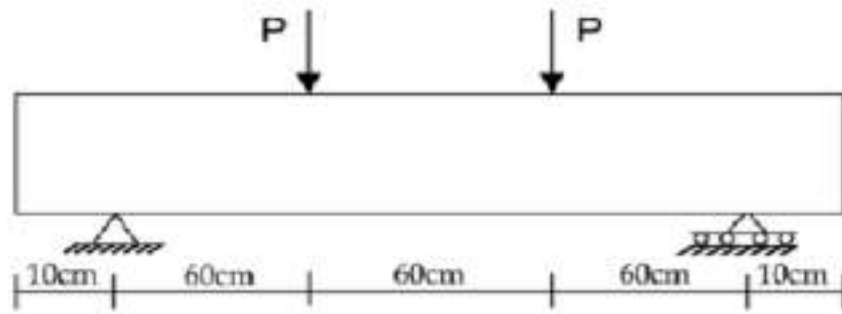
Figure 2.15 loading configuration of the jacketed RC beam (Source: Altun, 2004).
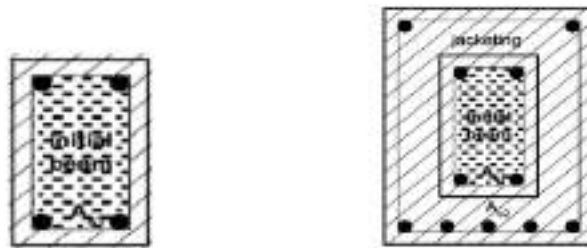
Figure 2.16 Cross-section of beams before and after jacketing (Source: Altun, 2004).

Shehata and Shehata (2008) investigated the behavior of RC beams strengthened by partial jacketing using expansion bolts as shear connectors. They categorized eight beams, which were 150 mm wide, 400 mm deep and 4500 mm long, in three groups A, B and reference group C. The three unstrengthened reference beams were in the group C and the other five partially jacketed beams were in group A and group B.

After two initial loading cycles the beams cracked, applied two lines of expansion bolts to the five beams on each side as shown in Figures 2.17 and 2.18. The holes were close to the inner stirrups and just above the main longitudinal steel.

The experimental results showed that partial jacketing is an effective strengthening method. In order to get proper anchorage, the inserted depth of the expansion bolts should be greater than five times the bolt diameter and not less than 50 mm. Exposed part of expansion bolts should be left without the extension. Exposed part and holes of expansion bolts should be as close as possible to the original stirrups and original main longitudinal steel of beams.
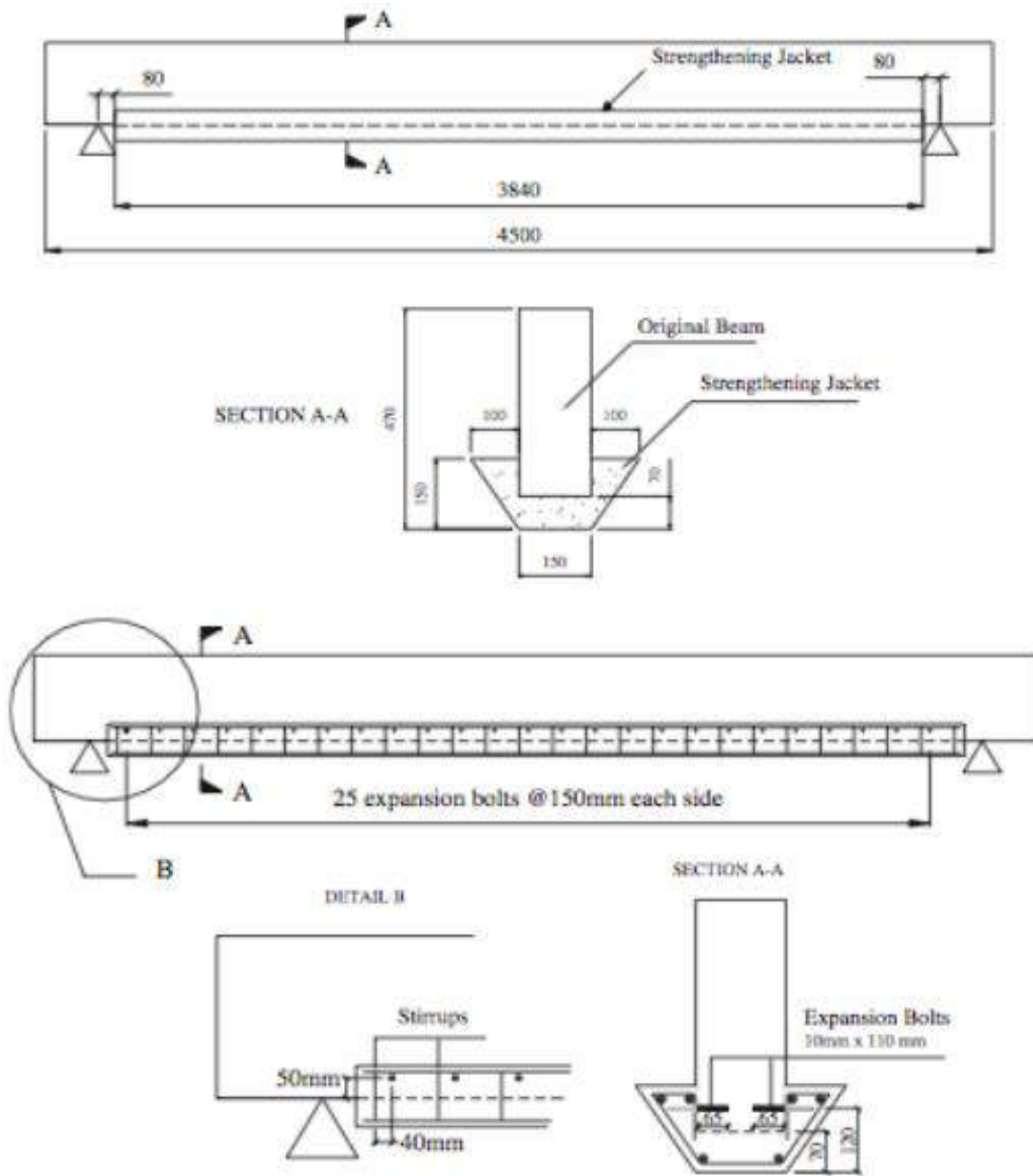
Figure 2.17 Strengthening details of specimen tested (Source: Shehata and Shehata, 2008).
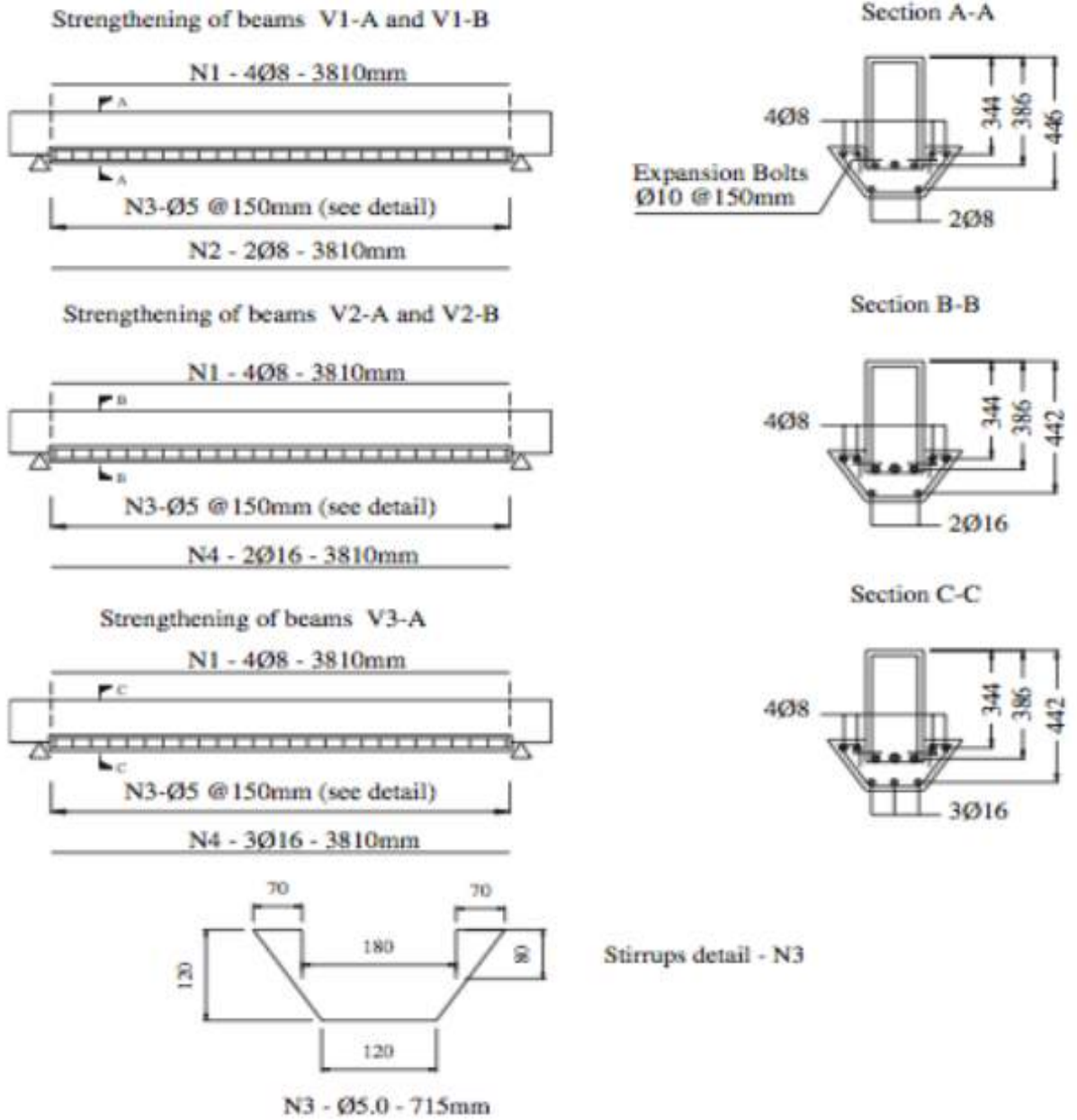
Figure 2.18 Details of reinforcement in the jackets (Source: Shehata and Shehata, 2008).

AL-Kuaity (2010) conducted an experimental study on the behavior and strength of reinforced concrete T-beams before and after strengthening by using RC jacket. Four full-scale beams were first loaded to certain levels of ultimate capacity (0, 60%, 77%, 100% of failure load). Typical test beam is exhibited in Figure 2.19. After formation of cracks or failure, the beams were strengthened by 50mm RC jackets and tested again up to failure.
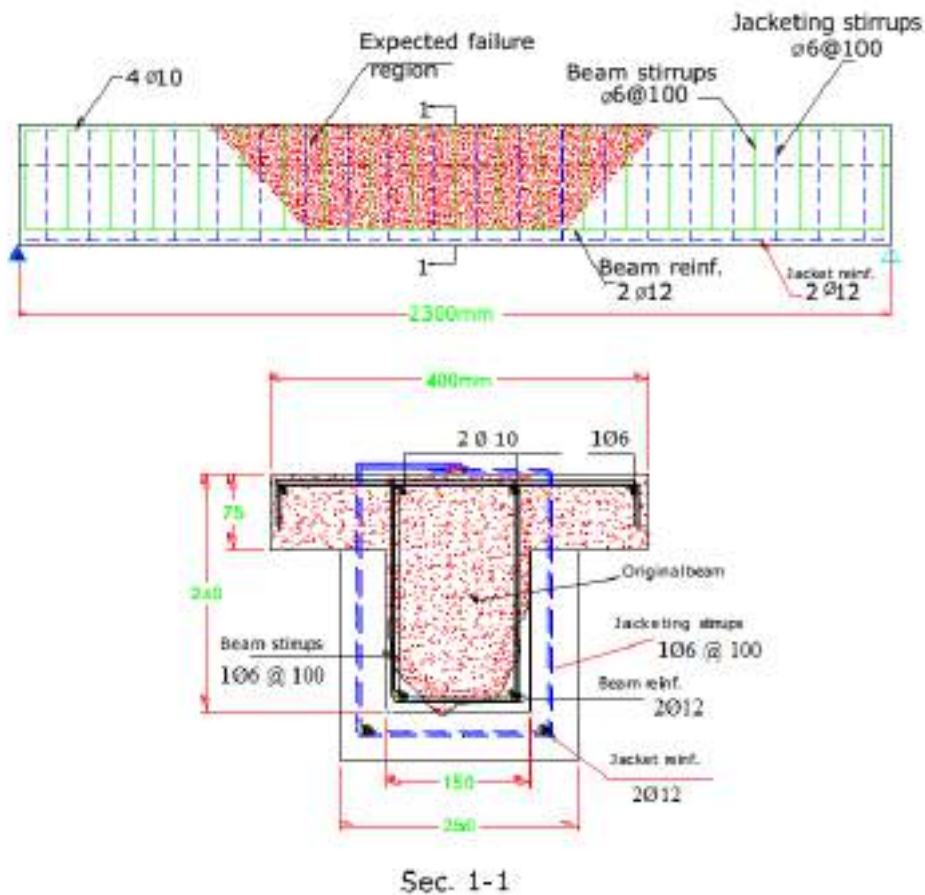
Figure 2.19 Typical jacketing of test beams (Source: AL-Kuaity, 2010).

The main objective of this study was to recover the full capacity of the beams which failed by flexure and to strengthen the cracked beams. In addition, it aimed to investigate the effect of loading condition on beams before repair on the ultimate capacity after repair. The main factor considered here is the effect of the level of loading percentages (percentages of UL before repair) on the strength and behaviors of the beam after repair.

Test results showed that the repairing by reinforced jacketing can effectively restore more than 150% of the full flexural capacity of the original beam as showed in Figure 2.20.
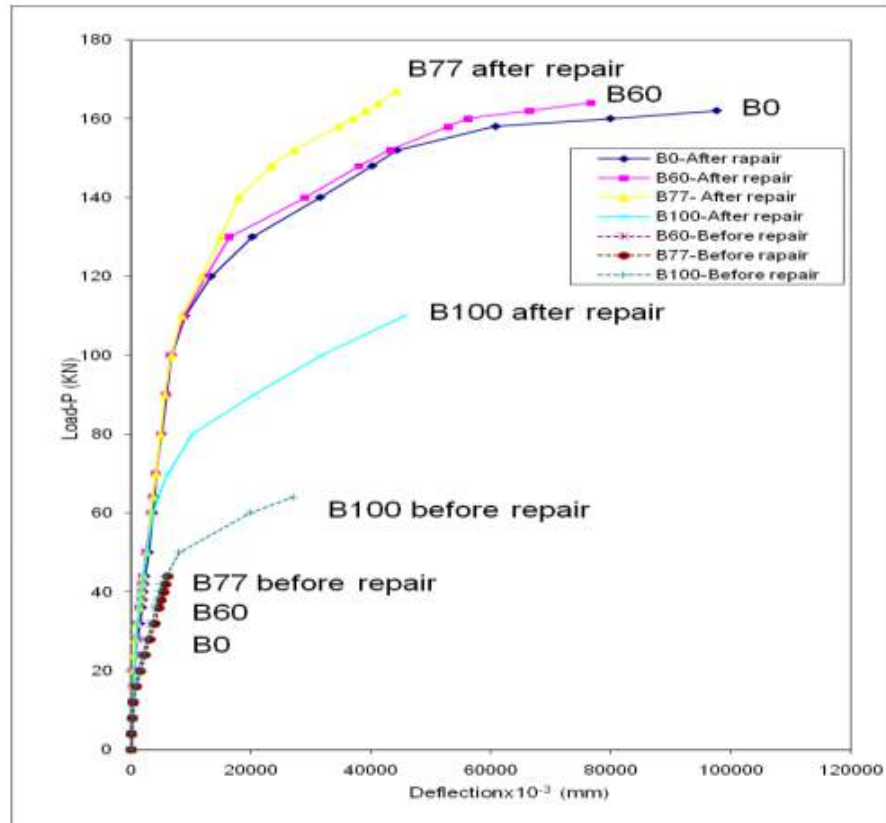
Figure 2.20 Load-deflection curves before and after jacketing (Source: AL-Kuaity, 2010).

In addition, reinforced jacket can effectively increase the ultimate capacity of cracked T-beam after repair up to 250%. Furthermore, the use of reinforced jackets for the cracked or failed beams is greatly improved the serviceability, deformation behavior, cracking behavior as well as ductility of T- beams compared to those of the original beams. The researcher concluded that the ultimate flexural strength of T-beams failed by flexure and repaired by RC jackets can accurately be predicted using conventional ultimate strength method of reinforced concrete.

The investigation showed the effectiveness of jacketing method in restoring the flexural strength of T-beams.

2.6 DESCRIPTION OF PREVIOUS RESEARCH ON STRENGTHENING WITH SCC

2.6.1. Scope

SCC is a kind of concrete with excellent deformability and segregation resistance, was first developed at Japan in 1980 (**Panda and Bal, 2013**). It is able to flow under its own weight and can completely fill the formwork even within congested reinforcement. SCC has favorable characteristics such as high fluidity, good segregation resistance and the compactibility without vibration so noiseless construction. The use of SCC has gained a wider acceptance in recent years.

2.6.2. Previous Research Related to SCC

Chalioris and Constantin (2012) investigated the application of a reinforced SCC jacket for the structural rehabilitation of shear damaged RC beams. Five beams were constructed and subjected to monotonic loading in order to exhibit shear failure. The damaged specimens were restored using relatively thin reinforced jackets and retested by the same four-point bending loading. The SCC jacket applied, encasing the bottom width and both vertical sides of the initially tested beams (U-formed jacketing), has a small thickness 25 mm and includes small Ø5 steel bars and U-formed stirrups as shown in Figure 2.21.
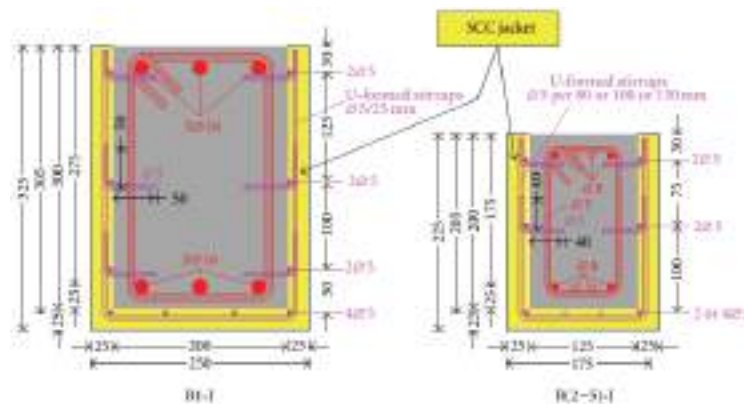
Figure 2.21 Dimensions and reinforcement of the beams. (Source: Chalioris and Constantin, 2013).

Test results indicated that the application of reinforced SCC jacketing in shear damaged RC beams is a promising rehabilitation technique since the capacity of the retrofitted beams was fully restored with respect to the initial specimens. All the jacketed beams showed enhanced of the loading bearing capacity that varied from 35% to 200% for the retrofitted beams with respect to the corresponding initial beams was observed. Further, the overall structural performance of the jacketed beams is substantially ameliorated regarding the initial shear-damaged specimens in most of the examined cases

2.7 DESCRIPTION OF PREVIOUS RESEARCH ON STRENGTHENING WITH WIRE MESH

2.7.1. Scope

SWM is a type of building materials consists of closely placed, evenly distributed and electrically welded rods to form a continuous uniformly distributed mesh. The use of Steel Wire Mesh (SWM) has an advantages because of its relative ease of placement, bending and handling. It has also save the time and money due to reduction of labors and waste parts.

The application of SWM as external reinforcement is a promising and recent new technique for strengthening and rehabilitating damaged concrete elements (**Xing et al., 2010**)

2.7.2. Previous Research Related to SWM

Pansal et al. (2006) investigated the effect of wire mesh orientation on strength of beams retrofitted using ferrocement jackets. To carry out the investigation, eight prototype beams were tested as shown in Figure 2.22. Out of these eight beams, two were used as control beams and tested to failure to find out the safe load carrying capacity. The other six beams were stressed to 75 percent of the safe load obtained from the testing of the control beams and were then retrofitted with 25 mm thick ferrocement jackets made with 1:2 cement sand mortar and w/c ratio 0.40 as shown in Figure 2.23.
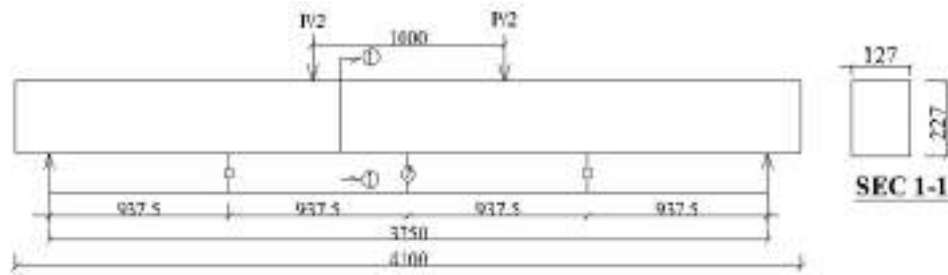
Figure 2.22 Loading arrangement for all beam specimens. (Source: Pansal et al., 2006).
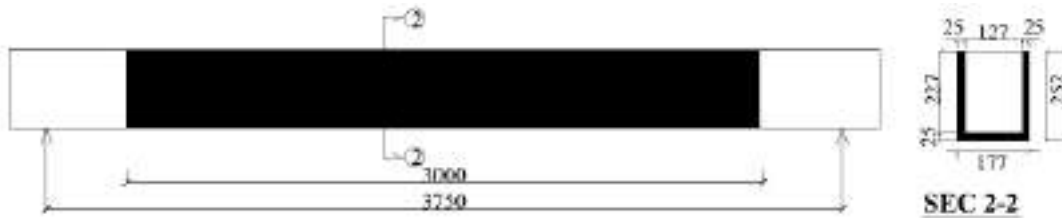
Figure 2.23 Longitudinal and cross-section of retrofitted beams (Source: Pansal et al., 2006).

The set of beams (two each) were divided into four categories depending upon the orientation of wire mesh in the jacket. Retrofitted beams having welded wire mesh oriented at 0 degree, 45 degrees and 60 degrees .

The results show that the percent increase in load carrying capacity for beam retrofitted with ferrocement jackets with wire mesh at 0, 45, 60 degree angle with longitudinal axis of beam, varies from 45.87 to 52.29 percent.

Also a considerable increase in energy absorption is observed for all orientations. However, orientation at 45 degree shows higher percentage increase in energy absorption followed by 60 and 0 degree respectively. However, the ductility ratio and energy absorption capacity is highest in case of beams retrofitted wire mesh at 0 degree followed by 45 degrees and 60 degrees.

The increase in ductility ratio and energy absorption of beams retrofitted using ferrocement jacket having WWM at different orientations, as reinforcement are makes the retrofitted beams suitable for dynamic load applications.

Xing et al. (2010) conducted an experimental investigation of RC T-beams strengthened with SWM embedded in polymer mortar overlay. Five one-third-scale simply supported RC T-beams were tested in this study. Four-point bending flexural tests were conducted up to failure on one control beam and on four strengthened beams with different load histories.

For the strengthened T-beams, the SWM composites were bonded to the bottom and the vertical sides of the web along the full length of the beam (U-jacketing). Two steel wires were placed at the bottom surface of each specimen for the tensile reinforcement, and another two steel wires at a height of 30 mm from the bottom were specified in the tension zone. Details of strengthened beams are exhibited in Figure 2.24.
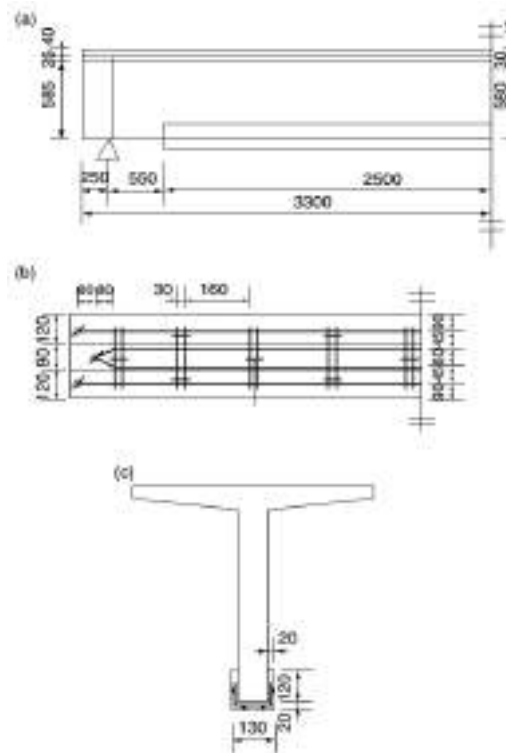
Figure 2.24 Details of strengthened beams. (Source: Xing et al., 2010).

The test results indicated that the use of SWM composites is an effective means of strengthening RC beams in flexure. The results demonstrate the feasibility of rehabilitating and strengthening RC members with SWM composites and indicate that the

ultimate strength of RC T-beams, strengthened with SWM composites, is almost the same regardless of the load history at the time of strengthening. The researchers presented a design procedure with aim to predict the flexural strength of T-beams strengthened with SWM composites and a good agreement between experiment and predicted values was achieved.

Mostosi et al. (2011) investigated the shear strengthening of RC beams with high performance jacket. The strengthening RC elements for increasing the bearing capacity under shear actions is an important issue in the retrofitting field. The researchers analyzed a possibility of low thickness high performance jackets for shear strengthening purposes.

The jackets are made with a High Performance Fiber Reinforced Concrete (HPFRC), with or without an additional 2mm diameter steel-wire mesh.

The beam specimens have a length of 2.85 m and 200 x 450 mm section, as shown in Figure 2.25.
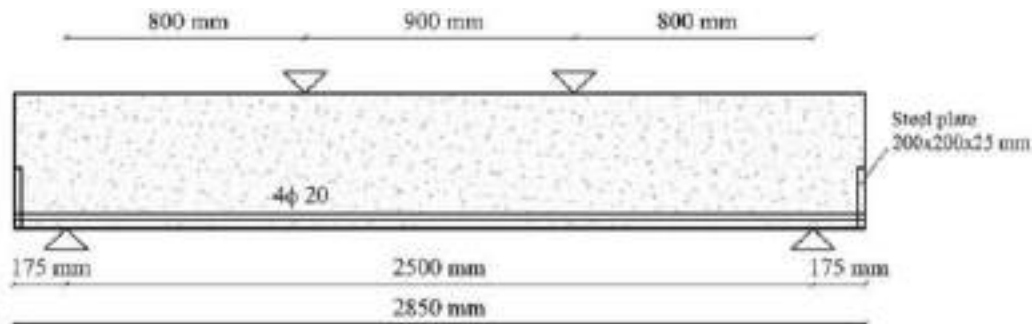
Figure 2.25 Beam geometry (Source: Mostosi et al., 2011).

The beams were tested under a four point bending configuration, by adopting a steel reacting frame. The beams were placed on roller steel supports with a span of 2.5 m. A steel beam was placed between the jacket and the specimen in order to apply the load in two points having a distance of 0.90 m. Thus the shear span ratio resulted equal to 1.90. One beam was used as reference specimen while the other three beams were strengthened by applying a high performance jacket . The summary of test specimens is shown in Table 2.1. Within the thickness of the jacket was placed a wire mesh. This mesh is made of 2.05 mm diameter bent wires, assembled with a spacing of 25.4 mm.

Table 2.1 Specimen characteristics.

Beam Cross Section	Surface	Thickness	Material	Bond Properties	Mesh Type
Un-reinforced beam	Lower Surface	No Reinforced	-	-	-
	Lateral Surfaces	No Reinforced	-	-	
Beam B	Lower Surface	50 mm	Self levelling	No primer	Welded wire mesh U bent
	Lateral Surfaces	50 mm	Self levelling	No primer	
Beam D	Lower Surface	50 mm	Self levelling	No primer	Welded wire mesh U bent
	Lateral Surfaces	50 mm	thixotropic	Epoxy primer	
Beam E	Lower Surface	50 mm	Self levelling	No primer	Welded wire mesh U bent to a height of 20 cm on the lateral surfaces
	Lateral Surfaces	30 mm	thixotropic	No primer	

Test results clearly indicate that the application of the HPFRC jacket has provided an increase of the maximum load of RC beams and an increase of its stiffness. In addition, the proposed technique, which involves the use of self levelling and thixotropic material, can be easily used in structural application for create the jacket.

For the beams D and B that have the same 50 mm jacket thickness the capacity increases 1.7 times, while if the jacket have a thickness of 30 mm on the lateral surfaces (beam E), the maximum load increases 1.5 times.

Arote et al. (2014) conducted an experimental study on the effect of the use of different types of wire mesh jacketing to the Plain Cement Concrete (PCC) beams. The experimental work is mainly concerned with the study of flexural strength of concrete by different types of wire mesh jacketing.

To carry out the investigation, there were two series. PCC beams with one side wire mesh other is three side wire mesh PCC beams. For each series six beams (150mm x 150mm x 700mm) in that three are of hexagonal openings and other is rectangular openings, were cast as control specimens.

The results show that all the jacketed beams are failed in ductile manner, as the bending stresses transmit from concrete to wire mesh which further increase a flexural strength and improve overall behavior of concrete.

Also, the results show that flexural strength of beams that have one side of rectangular wire mesh is increased by 10.92% than that of beams that have one side of hexagonal wire mesh and flexural strength of beams that have three side of rectangular wire mesh is increased by 4.23% than beams that have three side of hexagonal wire mesh.

Qeshta et al. (2014) investigated the use of wire mesh–epoxy composite for enhancing the flexural performance of concrete beams. A plain concrete beam was externally bonded with wire mesh–epoxy composite using one to five wire mesh layers. The flexural performance of the beam specimens bonded with wire mesh layers was compared with the beam specimens bonded with carbon fibre as well as a hybrid of wire mesh–epoxy– carbon fibre composite.

Concrete beam specimens with 100 mm width, 100 mm depth and 500 mm length were used. The specimens were divided into three groups. Group A included specimens with a different number of wire mesh layers, group B included specimens bonded with carbon fibre sheets of different widths and group C included specimens bonded with a hybrid of two wire mesh layers and a carbon fibre sheet. All bonded materials had an equal length of 270 mm.

All specimens were tested in four-point bending until failure at a span of 300 mm. Figure 2.26 shows the details of the test set-up. The two concentrated loads were applied at an equal distance of 100 mm from the supporting rollers. The tests were carried out under displacement control at a constant displacement rate of 0.05 mm/min. The mid-span deflection was monitored by a Linear Variable Displacement Transducer (LVDT).
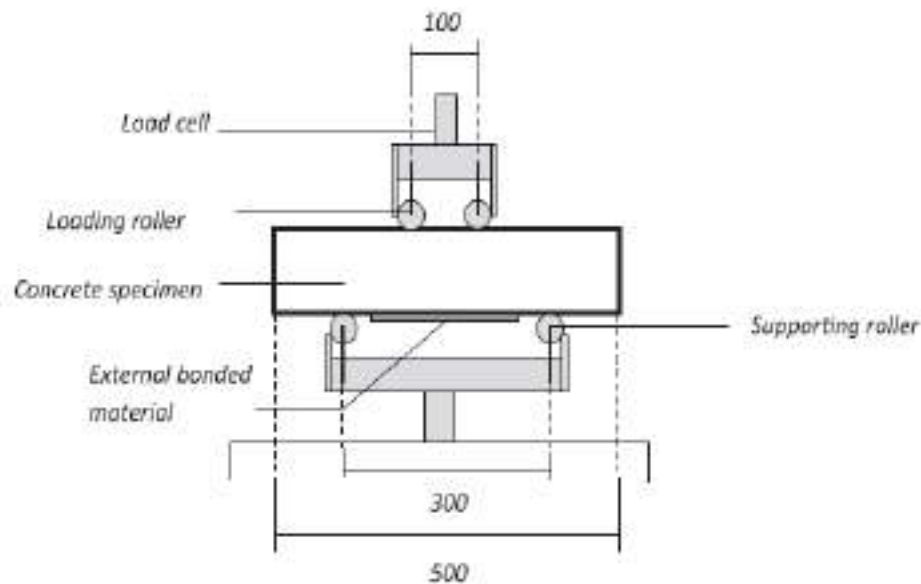
Figure 2.26 Test set-up details (mm) (Source: Qeshta et al., 2014).

The test results show that the use of wire mesh with epoxy is an efficient way to improve the flexural performance of concrete beam specimens. The increase in wire mesh layers significantly enhances the flexural strength, cracking behavior and energy absorption capability. In comparison with carbon fibre, wire mesh–epoxy composite is more efficient in flexural strength and ductility.

In addition, it was found that a concrete beam bonded with a hybrid wire mesh–epoxy–carbon fibre composite has significantly more energy absorption capability compared to specimens bonded with only carbon fibre.

Jaishankar and Prathima (2015) conducted a study about an experimental investigation done on beam prototype made of RC overlaid by a thin section of wire mesh over the main reinforcement. Wire mesh is a form of reinforcement that differs from conventional reinforcement primarily by the manner in which the reinforcing elements are dispersed and arranged. The well distributed and aligned reinforcement has made wire mesh to behave like steel plates.

The experiment includes testing of 4 prototype beams under a static loading. The beams were tested under the two point loading system. The major parameters used were type of mesh reinforcement, namely spacing and diameter of wire mesh used as an additional reinforcement. These beams are compared with a control beam and with one another. Three different kind of wire mesh used.

All the beams were rectangular cross section: width, depth and length of the beam were 100mm, 120mm, 200mm and 1000mm respectively.

Test results clearly indicate that the use of wire mesh layers as an additional reinforcement significantly enhances the flexural strength, cracking behavior and energy absorption capability. Obtained results are compared with the control specimen.

Figure 2.27 shows the load-deflection curves for beams tested. It can be observed that, the ultimate strength increases up to 37% with the use of wire mesh. Compared to the control beam, the peak load increased by 17%, 26% and 37% for beam W-1, W-2 and W-3 respectively. This shows that the beam has significant effect on spacing and diameter of the rod. Rectangular wire mesh performed better than square type wire mesh.
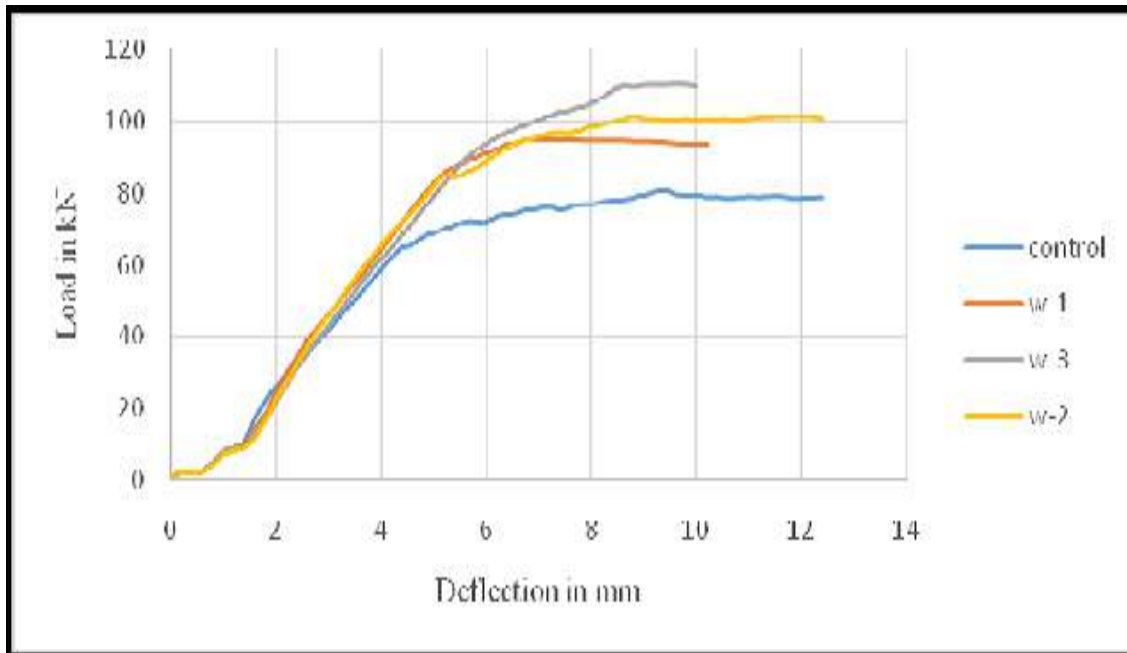
Figure 2.27 Load-deflection curve for beams. (Source: Jaishankar and Prathima, 2015).

The test results show that the use of wire mesh with closely spacing provides the higher energy absorption capacity and flexural strength and decreases the crack width among those concrete beam specimens. The results obtained from this work is expected to be useful in determining the strength, energy absorption capacity and crack width.

2.8 CONCLUDED REMARKS

Strengthening of RC structures is one of the most important tasks normally associated with the maintenance of concrete structures. The aim of strengthening is to increase the capacity of an existing structural element. A number of strengthening materials are available in the market. These include normal concrete, sprayed concrete, ferrocement, steel plate and FRP .etc.

Jacketing by RC and section enlargement may be the relatively easy and economic strengthening method compared to attachment of an external steel, external post-tensioning, wrapping with FRP or externally bonded composite system. It effectively increases the load carrying capacity, ductility and stiffness. However, the addition of concrete and steel to repair beams increases the weight of beams. So, the lightweight concrete may be considered as better applied when strengthening the beams.

Strengthening with concrete and steel rebar might lead to corrosion in beams. Hence, section enlargement and concrete jacketing are limited to use in harsh environment and the protecting corrosion is important work. The main advantages of jacketing can be concluded as:

i.   Strengthening of RC beams by ''jacketing'' is a well-established and frequently used technique. Jacketing is casting new RC shell around the damage member.

ii. RC jacket has greatly increased the flexural capacity of beams cracked and failed in flexural.

iii. RC jacketing has greatly improved the cracking behavior of beams irrespective to cracking condition before repair.

iv. Reinforced jacket increased, significantly, the flexural stiffness of the original beams resulting in less deflection under Service Load (SL).

v.   Reinforced jacket increased, significantly, shear strength by transverse fibre reinforcement.

vi. Wire mesh is a form of reinforcement that differs from conventional reinforcement primarily by the manner in which the reinforcing elements are dispersed and arranged.

vii. The previous studies show that the use of wire mesh with closely spacing provides the higher energy absorption capacity and flexural strength and decreases the crack width significantly.

viii. There have been a few studies on the behavior of RC beams strengthened with WWM including beam flexural and shearing tests.

ix. The main advantages of the WWM as materials and methods (**Ajin and Gokularm, 2015**):

    a. Higher characteristic design strength

    b. Better bonding behavior

    c. Better and economic crack fighting with tinny wires and nearer spacing.

    d. Savings of labor, time and binding wire.

    e. Flexibility of handling and placing

x. From the literature review it is concluded that there are some disadvantages of other strengthening techniques as follows:

    a. The using of steel plates and external stirrups in external strengthening suffered from corrosion.

    b. The main obstacles of widespread of FRP are the high cost and lack of confidence in long term durability.

    c. The main obstacles of widespread of span shortening and addition of steel sections are the architectural restrictions such as spaces, heights and the aesthetic view.

A few studies have been carried out on flexural strengthening of RC beams using externally bonded WWM but still the structural performance of WWM strengthened beams not be fully understood. The present study therefore explores the prospect of structurally strengthening of RC beams using SCC jacketing with externally bonded WWM.

3

CHAPTER
TEST PROGRAM

CHAPTER 3

TEST PROGRAM

3.1 INTRODUCTION

The literature review indicated that limited research has been carried out on strengthening of RC beams using WWM jacketing.

Very limited research has been conducted on the effects galvanized steel WWM on flexural behavior of RC members. The use of WWM as external reinforcement is a promising and recently developed technique for strengthening and rehabilitation projects (**Xing et al., 2010**).

In particular, the cost factor is the more important (**Huang et al., 2006**). WWM embedded in mortar overlays are less expensive composites than those which are currently considered for applications in civil engineering, such as for bridge and building repairs.

This research presents the experimental investigations of the structural behavior of RC beams. The strengthening technique that was used section enlargement using SCC reinforced with WWM. Different mechanical bonding techniques were also investigated, In addition, the flexural behavior of beams in general is briefly examined.

Section enlargement for reinforced concrete members can be defined as a method of strengthening and rehabilitations for any RC member by increasing the section's dimensions and adding additional reinforcement, taking into consideration the adequate type of bonding to ensure the compatibility between old and repaired sections (**PMFSEL Report, 1991**).

The use of SCC facilitate this type of strengthening due its good workability, passing ability and remarkable filling make SCC a reliable material for the strengthening of concrete members particularly the RC beams. Further SCC flows through congested reinforcements without causing honeycombing or vacuums in the concrete element or any discontinuity at the interface between concrete substrate and new concrete.

3.2 DESCRIPTION OF TEST PROGRAM

An experimental test program consisted of designing, constructing, strengthening and testing for flexural and shear of eighteen RC beams was carried out using SCC, which are tested under static loading condition. The test program consist of two groups divided according to the mesh properties based on mesh opening and nominal diameter.

3.2.1. Test Program Aim and Objectives

The aim of the undertaken research is to prove the possibility of strengthening existing RC beams using SCC U – jacketing. An experimental test program was designed to reach the purposed research objectives, which are:

a. To design and construct small scaled RC beams.
b. To strengthen the RC beams using section enlargement (U-Jacketing).
c. To apply the strengthening of these beams using the SCC and WWM.
d. To use different type of mechanical bonding techniques.
e. To investigate the flexural behavior of the strengthened beams.
f. To compare the real lab results with the theoretical analysis results.
g. To reach the best type of bonding between the strengthened beams and original beams.
h. To investigate the bonding between the two layers.

3.2.2. Design of Original Beam Specimens According to ACI 318-14

In this test program the main beam dimension are 1200 mm in length and 100 x 150 mm in cross section of rectangular beams as shown in Figure 3.1. The beams had a shear span to depth ratio 3.49, i.e. normal size beams, it is possible to study both the shear and the flexural strengths of the test beams.
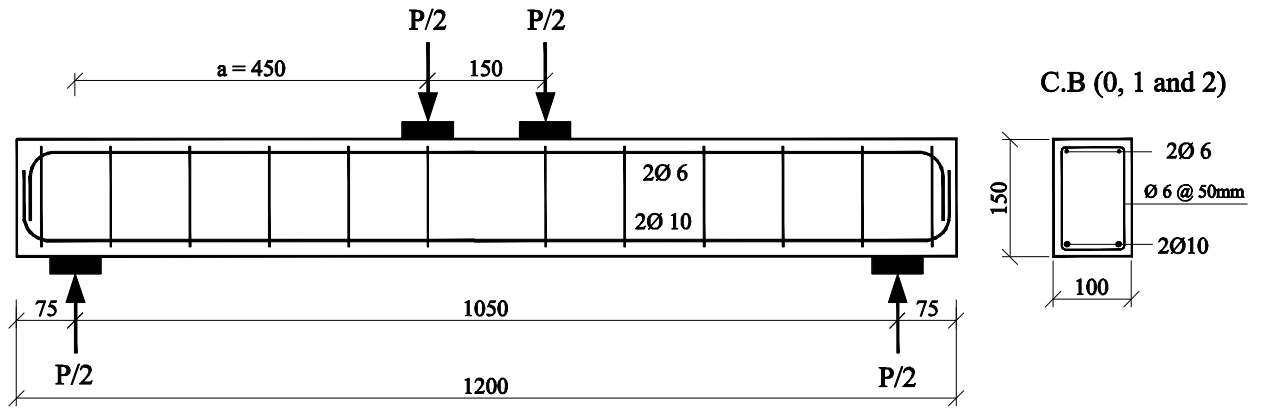
Figure 3.1 Main section geometry (All dimensions are in mm).

These beams were designed according to the (**ACI 318-14**). A nominal bending moment M_n= 8.186 KN.m was calculated. All design limitations to prevent shear failure according to the code were considered using Ø6 mm stirrups @ 50 mm.

3.3 DESIGN OF TEST PROGRAM

The test program was carried out using eighteen beams which are tested under static loading condition. Eleven out of them were strengthened using U-jacketing technique to improve the structural behavior particularly the flexural strength, the beams were tested as simply supported beams subjected to two concentrated point loading. Seven beams were used as control beams. Three out of these six beams were acted as control beams without jacketing have a cross section 100 x 150 mm to investigate UL in KN. The other four control beams were casted monolithically with different WWM properties; so that the final enlarged cross section is 160 x 200 mm. Table 3.1 illustrates the test program.

3.3.1. Main Test Parameter

The strengthened specimens are divided into two groups based on two parameters. The first is the method of anchorage of WWM to concrete substrate which have three types which are dowels, expansion bolts and roughed the beams without anchors. The other parameter is the mesh properties based on mesh opening and nominal diameter.

3.3.2. Design for Laminar Shear

Steel-to-concrete or concrete-to-concrete connections can be accomplished through the use of several types of anchorage systems. In this research strengthened beams have been done using three method of anchorage, the first one is using of an expansion bolts that are used as shear connectors. Holes with a specific diameter at the required spacing are to be drilled into the beams to a depth of about 50 mm, then the WWM assembled and the expansion bolts will be secured into the drilled holes. The second method is using of deformed steel bars 8mm diameter as shear connectors. Holes at the required spacing are to be drilled into the beams to a depth of about 50 mm and hardened by epoxy resin. Then the WWM assembled. The last method is installing the WWM on a roughed surface of the specimen without anchors.

The laminar shear is developed between two concrete layers of the main and strengthened beams. Laminar shear has been resisted only by roughening the surface and anchors. The shear capacity of the anchors is calculated according to REHABCON ANNEX I strengthening with RC specifications see Appendix D.

A certain number of required anchors made from 8 mm steel deformed bar with length of 75 mm are to be bonded using epoxy resin for the beams which bonded with anchors distributed according to their own category. Figure 3.2 shows the distribution of anchors along the entire interacted surface.

A certain number of required anchors made standard stud anchor – (HSA M8 35/25/-) Hilti type for the beams which bonded with anchors distributed according to their own category. Figure 3.3 shows the distribution of anchors along the entire interacted surface.

Figure 3.2 Distribution of 8 mm steel deformed bar anchors.

Figure 3.3 Distribution of (HSA M8 35/25/-) Hilti type anchors.

Table 3.1 Characteristics of the control beams and strengthened beams.

No.	Beam Name	Description	b x h mm x mm	a / d	Longitudinal Reinforcement Up	Longitudinal Reinforcement Bottom	Stirrups @ mm	Strengthening Tech.	Bonding Mechanism	Mesh Diameter (mm)	Mesh Open (mm)
All beam specimens will be preloaded up to 30 % of Pu (UL of Control Beam)											
1	C.B0	Control beam over reinforced in shear to examine flexural capacity	100 x 150	3.49	2Φ6mm	2Φ10mm	Φ6@50	-	-	-	-
2	C.B1										
3	C.B2										
4	MA.B1	Monolithic Control beam casted with mesh 1	160 x 200	2.48	2Φ6mm	2Φ10mm	Φ6@50	-	Monolithic Casting	3.50	25 x 25
5	MA.B2										
6	MB.B1	Monolithic Control beam casted with mesh 2	160 x 200	2.48	2Φ6mm	2Φ10mm	Φ6@50	-	Monolithic Casting	5.50	50 x 50
7	MB.B2										
8	GA.B1	Beam with U jacketing have an expansion bolts (Group A)	160 x 200	2.48	2Φ6mm	2Φ10mm	Φ6@50	U Jacketing with S.C.C with WWM	Expansion Bolts	3.50	25 x 25
9	GA.B2										
10	GA.B3	Beam with U jacketing have dowel (Group A)	160 x 200	2.48	2Φ6mm	2Φ10mm	Φ6@50		Dowels	3.50	25 x 25
11	GA.B4										
12	GA.B5	Beam with U jacketing with roughened surface (Group A)	160 x 200	2.48	2Φ6mm	2Φ10mm	Φ6@50		Roughening	3.50	25 x 25
13	GA.B6										
14	GB.B1	Beam with U jacketing have an expansion bolts (Group B)	160 x 200	2.48	2Φ6mm	2Φ10mm	Φ6@50		Expansion Bolts	5.50	50 x 50
15	GB.B2										
16	GB.B3	Beam with U jacketing have dowel (Group B)	160 x 200	2.48	2Φ6mm	2Φ10mm	Φ6@50		Dowel	5.50	50 x 50
17	GB.B4										
18	GB.B5	Beam with U jacketing with roughened surface (Group B)	160 x 200	2.48	2Φ6mm	2Φ10mm	Φ6@50		Roughening	5.50	50 x 50

3.3.3. Description of Control Beams

There are two types of control beams the first one have original sample section which is 100 x 150 x 1200 mm in dimension, and provided with flexural and shear reinforcement. The other type of control beam is the monolithically casted control beams that have 160 x 200 x 1200 mm in dimension and provided with flexural and shear reinforcement in addition to WWM. The main goal of control beams is to make a comparative study of the values obtained from the control beams with the values obtained from the strengthened specimens.

3.3.3.1. Original Control Beam (CB0, CB1, CB2)

Semi full-scale tests are performed on 1200 mm long beams with a depth of 150 mm and a width of 100 mm as shown in Figure 3.4. Three beams were casted and reinforced with two bottom longitudinal reinforcement (Φ= 10 mm), two top longitudinal reinforcement (Φ= 6 mm) and stirrups at the beam ends, having a diameter of 6 mm and a spacing of 50 mm. The bars are hooked at 90 degree to insure a good bonding and to avoid slipping out during loading. The beams were casted with concrete having a nominal cylinder compressive strength of 35 MPa.
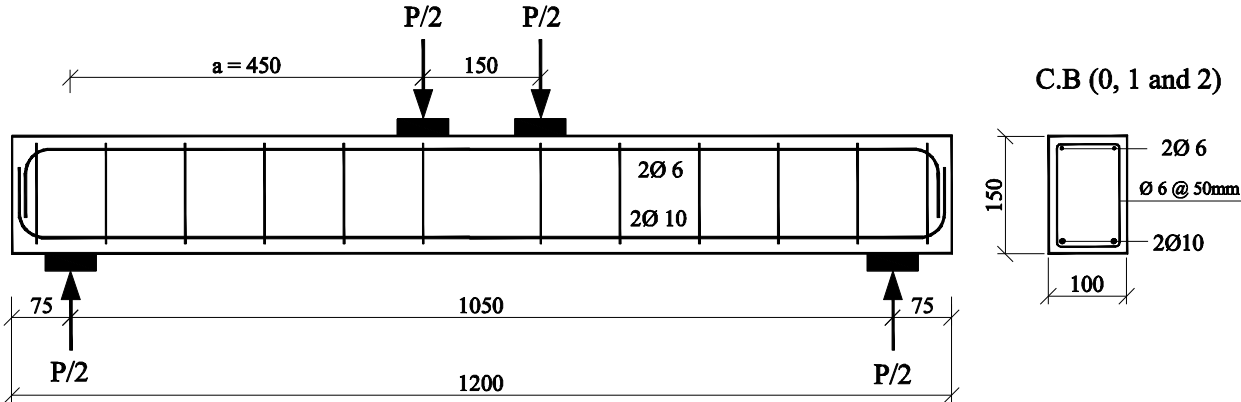
Figure 3.4 CB0, CB1 and CB2 geometry (dimensions are given in mm).

3.3.3.2. Monolithic Control Beam (MA.B1, MA.B2)

The monolithic control beams (MA.B1 and MA.B2) cross section is 1200 mm in length and 160 x 200 mm in cross section of rectangular beams as shown in Figure 3.5. The beams had a shear span to depth ratio 2.48, i.e. normal size beams, it is possible to study both the shear and the flexural strengths of the test beams. Two beams were casted and reinforced with two bottom longitudinal reinforcement (Φ= 10 mm), two top longitudinal reinforcement (Φ= 6 mm) and stirrups at the beam ends, having a diameter of 6 mm and a spacing of 50 mm. Also this beams were strengthened using WWM which consist of 3.5 mm wire diameters and 25 mm mesh opening.

The beams were casted with concrete having a nominal cylinder compressive strength of 35 MPa.
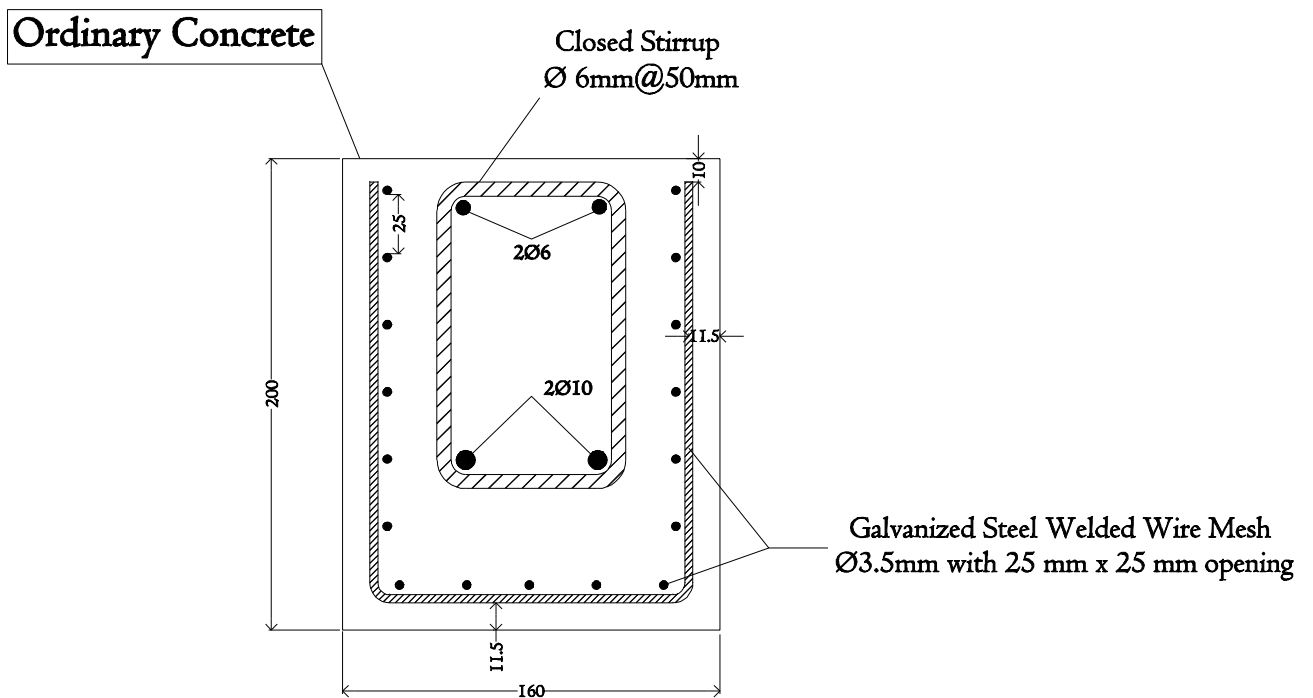
Figure 3.5 Monolithic beams MA.B1 and MA.B2 cross section (mm).

3.3.3.3. Monolithic Control Beam (MB.B1, MB.B2)

The monolithic control beams (MB.B1 and MB.B2) cross section is 1200 mm in length and 160 x 200 mm in cross section of rectangular beams as shown in Figure 3.6. The beams had a shear span to depth ratio 2.48, i.e. normal size beams, it is possible to study both the shear and the flexural strengths of the test beams. Two beams were casted and reinforced with two bottom longitudinal reinforcement (Φ= 10 mm), two top longitudinal reinforcement (Φ= 6 mm) and stirrups at the beam ends, having a diameter of 6 mm and a spacing of 50 mm. Also this beams were strengthened using WWM which consist of 5.5 mm wire diameters and 50 mm mesh opening. The beams were casted with concrete having a nominal cylinder compressive strength of 35 MPa.
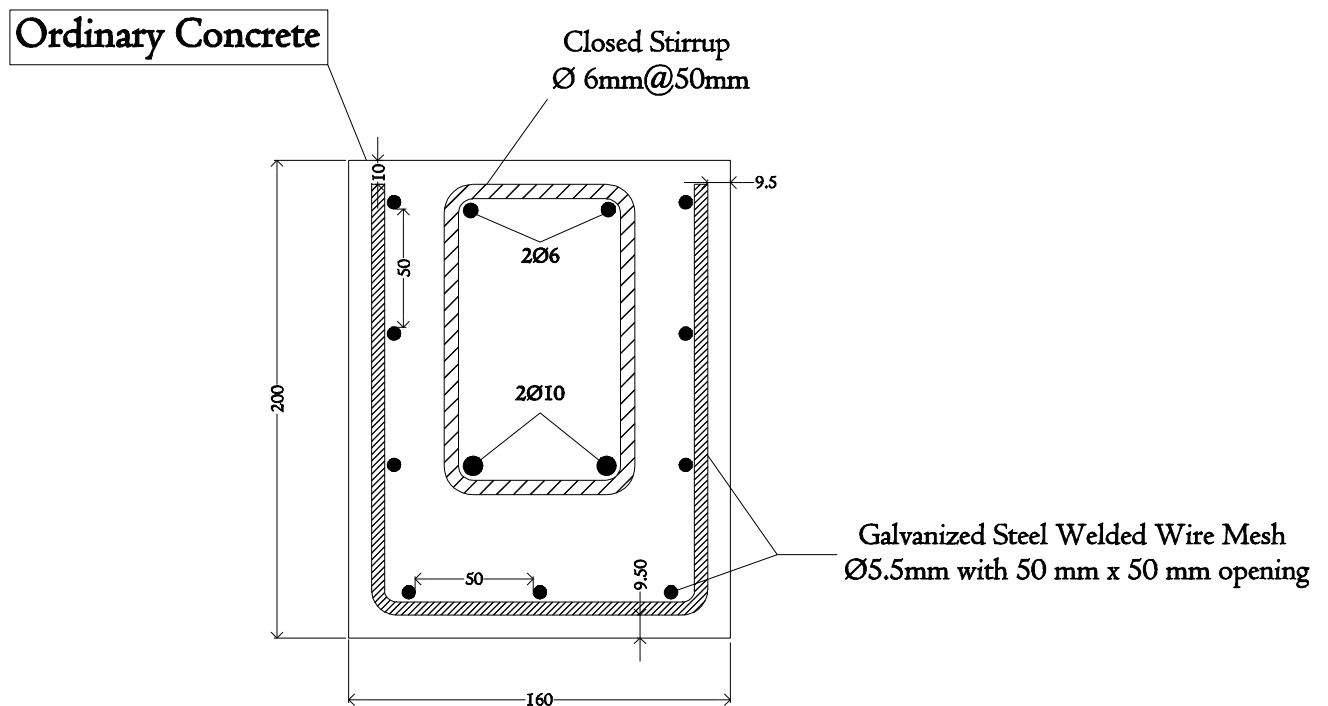
Figure 3.6 Monolithic beams MB.B1 and MB.B2 cross section (mm).

3.3.4. Description of First Group Beam Specimen (Group A)

After the pre-loading stage, the original specimens were strengthened using relatively thin reinforced jacket made of SCC reinforced with WWM. Group A contained jacketing the original beam by SCC using structural expansion anchors, steel reinforcement dowels as shear connectors and surface roughening to improve the bond between the substrate and the SCC. The reinforcement of the jackets consists of $\emptyset 3.5$ mm of 25 mm opening galvanized WWM straight and U-formed shapes.

Jackets encased the bottom width with 50 mm SCC and both vertical sides of the original beams (U-formed jacketing) with 30 mm SCC, thus the final cross section dimension of jacketed beams will be 160 x 200 mm, and also all beams have the same overall length 1200mm and load arrangement.

The beams had a shear span to depth ratio 2.48, i.e. normal size beams, it is possible to study both the shear and the flexural strengths of the test specimens.

3.3.4.1. Beams GA.B1 and GA.B2

As mentioned before the original specimens were strengthened using relatively thin reinforced jacket made of SCC reinforced with WWM. Jackets encased the bottom width with 50 mm SCC and both vertical sides of the original beams with 30 mm SCC. The strengthened beams (GA.B1 and GA.B2) cross section is 1200 mm in length and 160 x 200 mm in cross section of rectangular beams as shown in Figure 3.7.

The beams (GA.B1 and GA.B2) strengthened with jackets consist of $\emptyset 3.5$ mm of 25 mm opening as reinforcement and Hilti structural expansion anchors to prevent inter laminar shear between the concrete substrate and SCC jacket.

A certain number of required Hilti shear connectors has been determined as detailed in Appendix D.
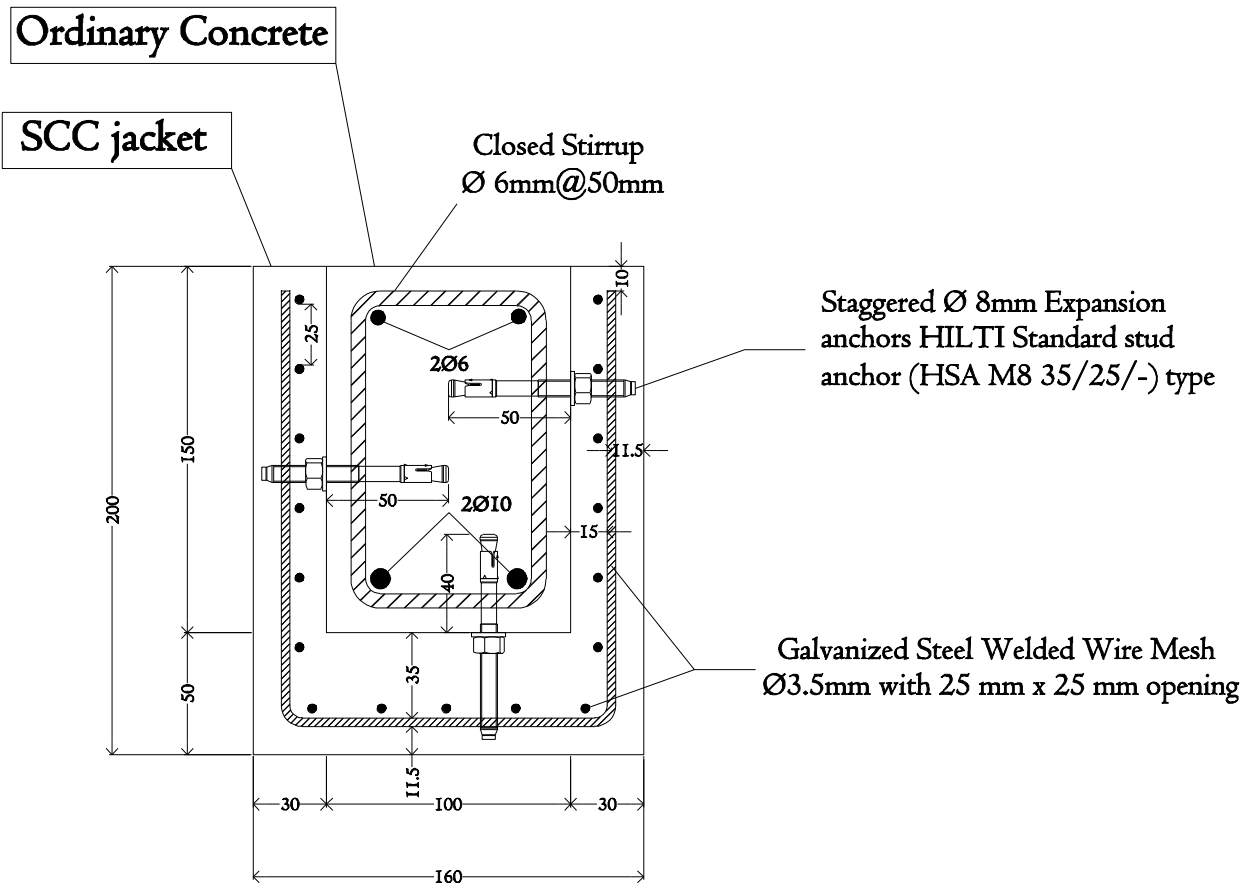
Figure 3.7 Strengthened beams GA.B1 and GA.B2 cross section (mm).

3.3.4.2. Beams GA.B3 and GA.B4

The strengthened beams (GA.B3 and GA.B4) are the same as the beams (GA.B1 and GA.B2) in cross section, overall length, jacketing scheme, jacketing reinforcement and thicknesses except the adhesion between substrate and the new concrete was ensured using Ø8 mm shear connectors.

The beams (GA.B3 and GA.B4) strengthened with jackets consist of Ø3.5 mm of 25 mm opening as reinforcement and deformed Ø8 mm steel reinforcement dowels to prevent inter laminar shear between the concrete substrate and SCC jacket as shown in Figure 3.8.

A certain number of required Ø8 mm shear connectors has been determined as detailed in Appendix D.
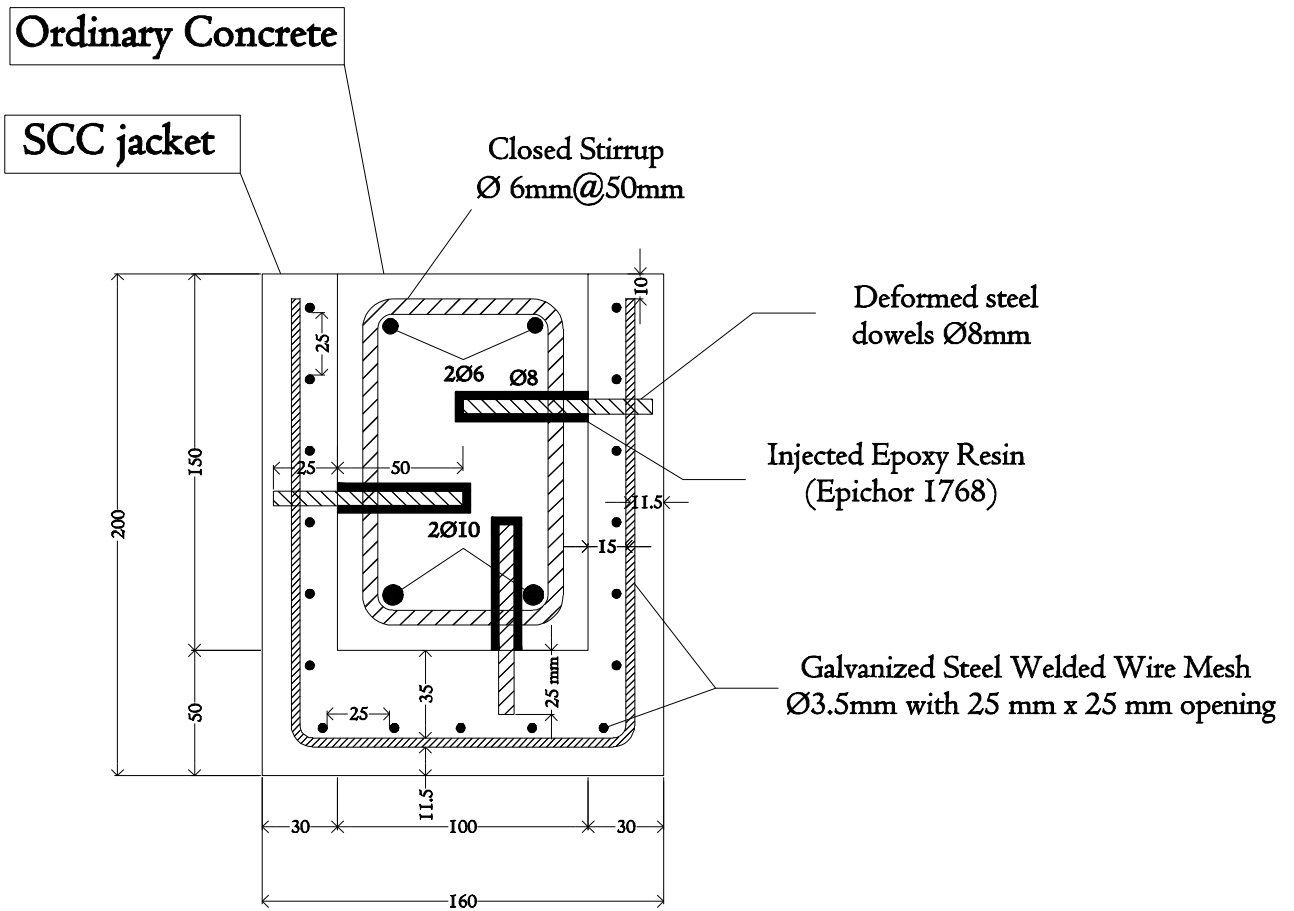
Figure 3.8 Strengthened beams GA.B3 and GA.B4 cross section (mm).

3.3.4.3. Beams GA.B5 and GA.B6

The strengthened beams (GA.B5 and GA.B6) are the same as the beams (GA.B1 and GA.B2) in cross section, overall length, jacketing scheme, jacketing reinforcement and thicknesses except the adhesion between substrate and the new concrete was ensured using surface roughening as shown in Figure 3.9. The beams (GA.B5 and GA.B6) strengthened with jackets consist of Ø3.5 mm of 25 mm opening as jacketing reinforcement.

The choice of surface treatment is related to the fact that, using grinding with rotating lamella to roughen concrete, can create a highly rough surface. Also, this treatment is mostly for economic reasons, common practice in many countries, and can be operated by unskilled labor.
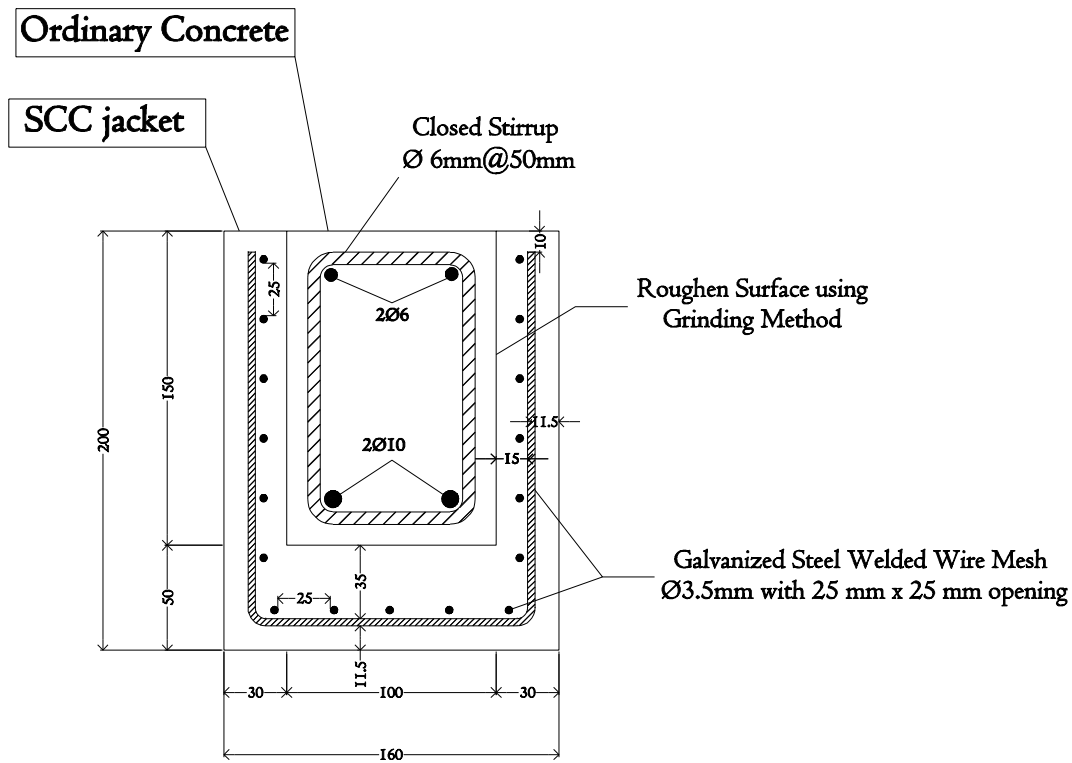
Figure 3.9 Strengthened beams GA.B5 and GA.B6 cross section (dimensions in mm).

3.3.5. Description of Second Group Beam Specimen (Group B)

After the pre-loading stage, the original specimens were strengthened using relatively thin reinforced jacket made of SCC reinforced with WWM. Group B contained jacketing the original beam by SCC using structural expansion anchors, steel reinforcement dowels as shear connectors and surface roughening to improve the bond between the substrate and the SCC. The reinforcement of the jackets consists of Ø5.5 mm of 50 mm opening galvanized WWM straight and U-formed shapes.

Jackets encased the bottom width with 50 mm SCC and both vertical sides of the original beams (U-formed jacketing) with 30 mm SCC, thus the final cross section dimension of jacketed beams will be 160 x 200 mm, and also all beams have the same overall length 1200mm and load arrangement. The beams had a shear span to depth ratio 2.48, i.e. normal size beams, it is possible to study both the shear and the flexural strengths of the test specimens.

3.3.5.1. Beams GB.B1 and GB.B2

The strengthened beams (GB.B1 and GB.B2) cross section is 1200 mm in length and 160 x 200 mm in cross section of rectangular beams as shown in Figure 3.10. Jackets encased the bottom width with 50 mm SCC and both vertical sides of the original beams with 30 mm SCC.

The beams (GB.B1 and GB.B2) strengthened with jackets consist of Ø5.5 mm of 50 mm opening as reinforcement and Hilti structural expansion anchors to prevent inter laminar shear between the concrete substrate and SCC jacket.

A certain number of required Hilti shear connectors has been determined as detailed in Appendix D.
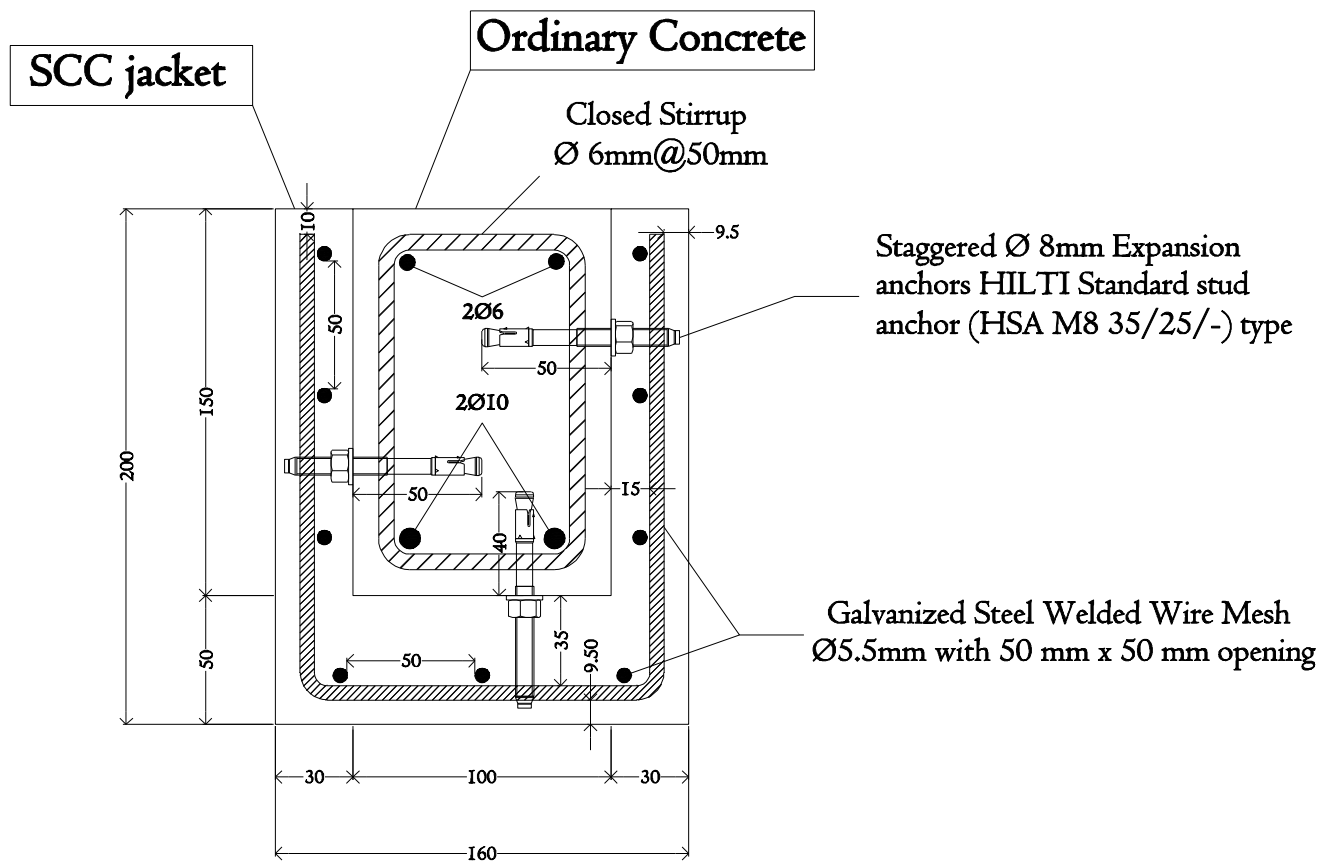
Figure 3.10 Strengthened beams GB.B1 and GB.B2 cross section (mm).

3.3.5.2. Beams GB.B3 and GB.B4

The strengthened beams (GB.B3 and GB.B4) are the same as the beams (GB.B1 and GB.B2) in cross section, overall length, jacketing scheme, jacketing reinforcement and thicknesses except the adhesion between substrate and the new concrete was ensured using Ø8 mm shear connectors.

The beams (GB.B3 and GB.B4) strengthened with jackets consist of Ø5.5 mm of 50 mm opening as reinforcement and deformed Ø8 mm steel reinforcement dowels to prevent inter laminar shear between the concrete substrate and SCC jacket as shown in Figure 3.11. A certain number of required Ø8 mm shear connectors has been determined as detailed in Appendix D.
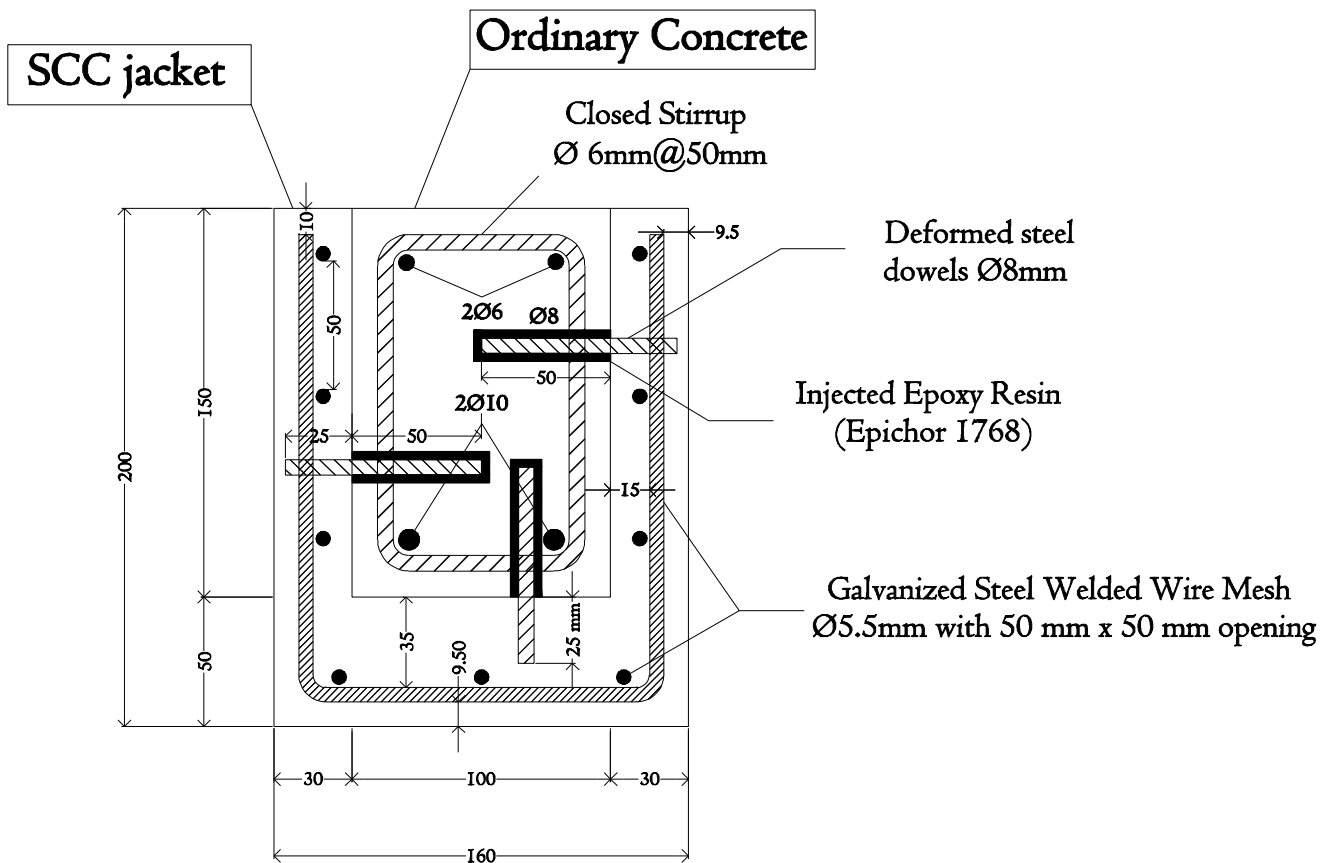
Figure 3.11 Strengthened beams GB.B3 and GB.B4 cross section (mm).

3.3.5.3. Beam GB.B5

The strengthened beam (GB.B5) is the same as the beams (GB.B1 and GB.B2) in cross section, overall length, jacketing scheme, jacketing reinforcement and thicknesses except the adhesion between substrate and the new concrete was ensured based on surface roughening using grinding with rotating lamella as shown in Figure 3.12. The beam (GB.B5) strengthened with jackets consists of Ø5.5 mm of 25 mm opening as jacketing reinforcement.
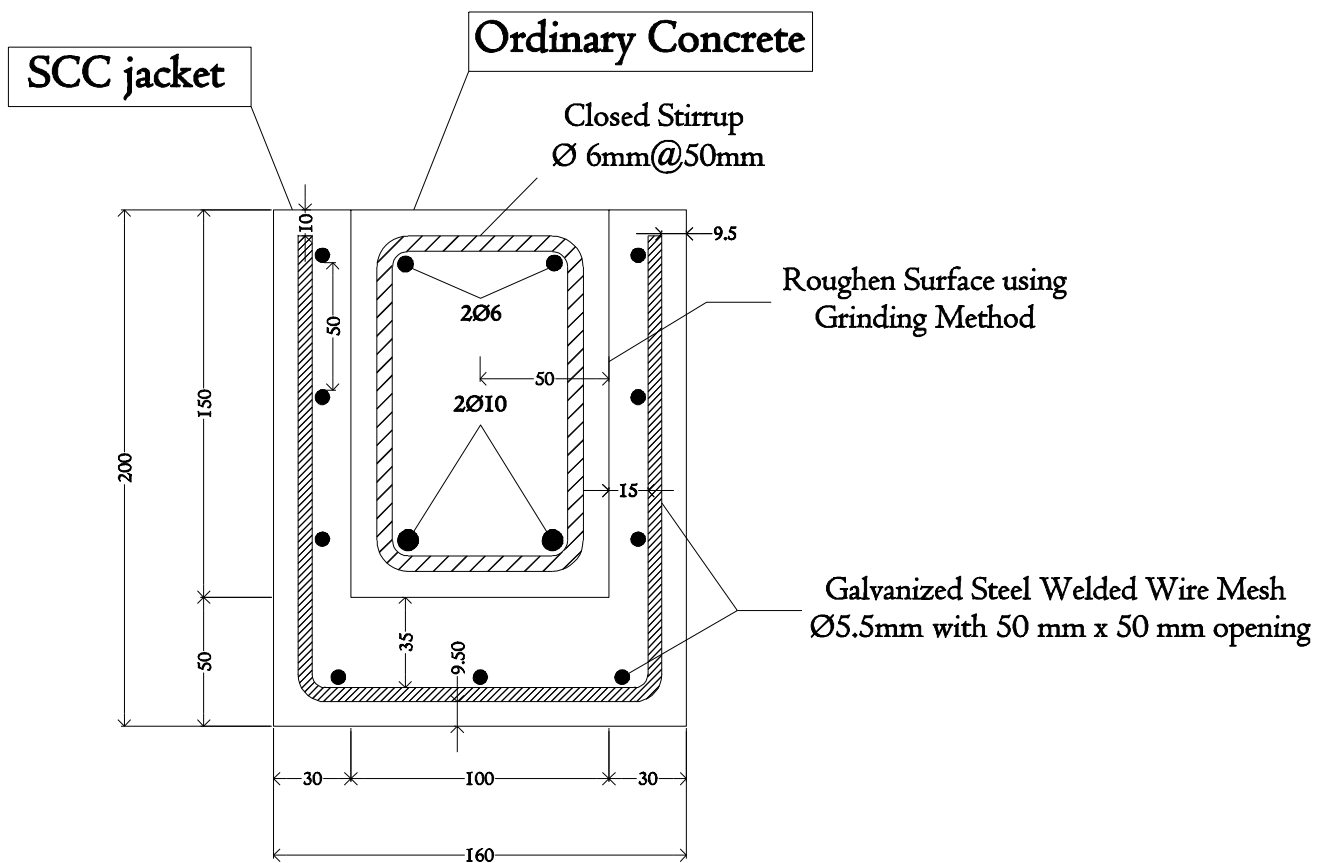
Figure 3.12 Strengthened beams GB.B5 cross section (mm).

4

CHAPTER
LABORATORY WORKS

CHAPTER 4

LABORATORY WORKS

4.1 INTRODUCTION

Laboratory works are presented in this chapter. A planned experimental work was carried out, in order to reach the research main objectives. After preparing the research's materials, all experimental work and testing took place at the Islamic University of Gaza (IUG) Lab.

4.2 MATERIALS TO BE USED BEFORE JACKETING

4.2.1. Cement

Ordinary Portland cement (CEM II/AM-SVL 42.5N) grade was used in this study as shown in Figure 4.1.

The Physical properties of cement was shown in Table 4.1.

Figure 4.1 Cement II/AM-SLV 42.5N.

Table 4.1 Physical properties of cement.

Properties	Cement	ASTM Requirements
Density (Kg/m^3)	2960	ASTM C188-87
Fineness ($cm^2/gm.$)	3500	ASTM C150-95 Min. 2800
Vicat set times(hr:min) **Initial** **Final**	2:30 5:00	ASTM C150-95 ≥ 45 min ≤ 375 min
Mortar Compressive Strength (N/mm^2)at **2 days** **28 days**	25 58	ASTM C150-95 >10 >42.5

4.2.2. Water

Potable tap water with PH of 7.1 was used for the experimentation and for the curing process.

4.2.3. Coarse Aggregate

According to the local market surveying, three types of coarse aggregate were found. Table 4.2 illustrates the sieve analysis and the properties of these types.

Table 4.2 Coarse aggregate types, sieves and properties.

Sample Description	Type (1) Foulia	Type (2) Adasia	Type (3) Simsimia
Sieve Size (mm)	% Passing	% Passing	% Passing
25	100.00	100.00	100.00
19	51.95	100.00	100.00
12.5	0.00	62.85	100.00
9.5	0.00	21.51	94.91
4.75	0.00	0.00	27.53
2.00	0.00	0.00	4.78
1.18	0.00	0.00	3.88
0.6	0.00	0.00	3.55
0.3	0.00	0.00	2.63
0.15	0.00	0.00	0.85
0.075	0.00	0.00	0.00
Pan	0.00	0.00	0.00
Dry Unit Weight (Kg/m3)	1430.20	1451.20	1597.80
Dry Specific Gravity	2.461	2.539	2.501
Saturated Specific Gravity	2.552	2.607	2.593
Absorption (%)	3.693	2.696	3.697

To achieve the ASTM C33-03 standard requirements for coarse aggregate, a mix design of these three types was prepared as shown in Table 4.3 and Figure 4.2.

Table 4.3 Coarse aggregate sieve and analysis according to ASTM C33-03

Aggregate Type	Type (1) Foulia	Type (2) Adasia	Type (3) Simsimia
% Percent	**21.2121**	**48.4848**	**31.3030**
Sample Description	**Coarse Aggregate**	**ASTM C33-03**	
	Mix of the three types	**Minimum**	**Maximum**
Sieve Size (mm)	**% Passing**	**% Passing**	**% Passing**
25	100.0	100.0	100.0
19	90.00	90.0	100.0
12.5	60.78	40.0	72.0
9.5	39.19	20.0	55.0
4.75	8.342	0.0	10.0
2.00	1.448	0.0	5.0
1.18	1.176	0.0	3.0
0.60	1.076	0.0	3.0
0.3	0.797	0.0	2.0
0.15	0.258	0.0	2.0
0.075	0.0	0.0	1.0
Dry Unit Weight (Kg/m3)	1491.07		
Dry Specific Gravity	2.51		
Saturated Specific Gravity	2.591		
Absorption (%)	3.21		
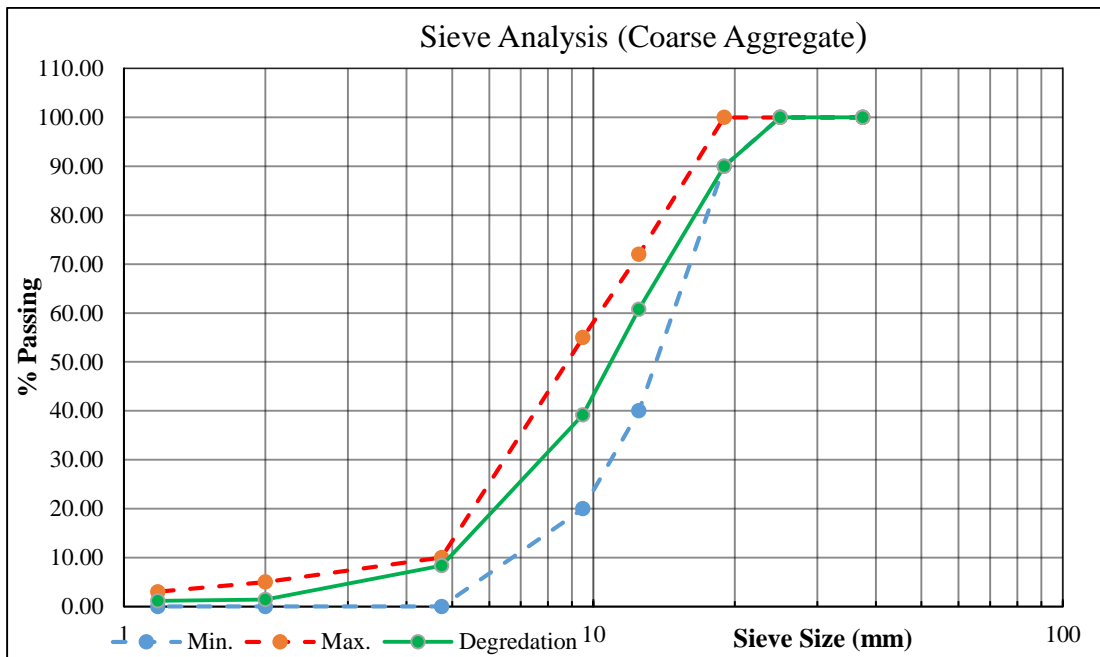
Figure 4.2 Coarse aggregate sieve analysis according to ASTM C33-03 limitation.

4.2.4. Fine Aggregate

According to the local market surveying, dune sand type were found, Table 4.4 illustrates the sieve analysis and the properties of this material.
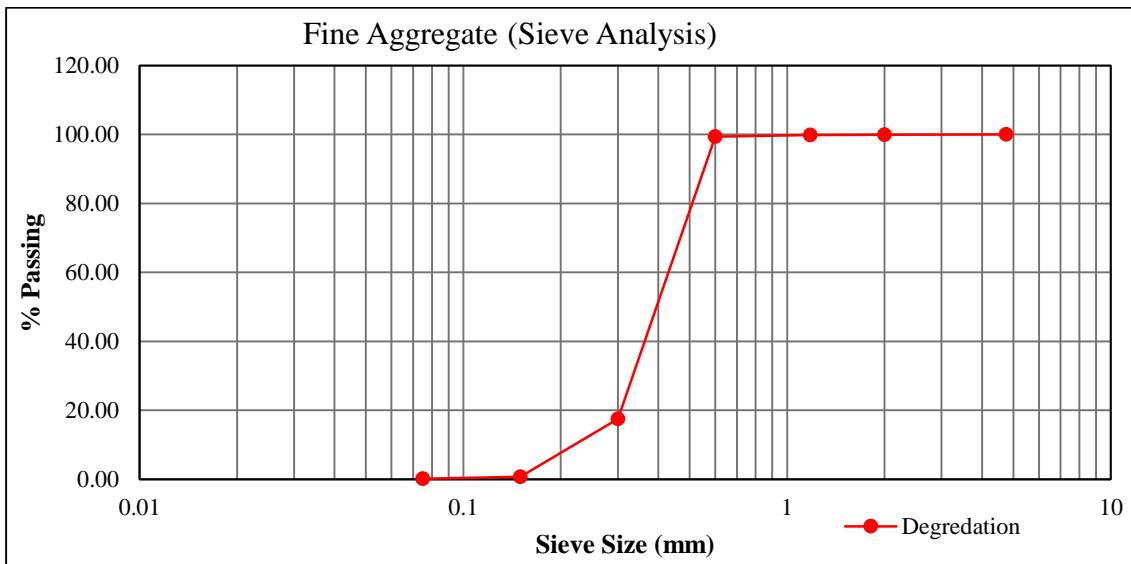
Figure 4.3 Fine aggregate sieve analysis.

Table 4.4 Fine aggregate sieve and analysis

Sample Description	Dune Sand
Sieve Size (mm)	% Passing
4.75	100.00
2.00	100.00
1.18	100.00
0.6	100.00
0.3	17.46
0.15	0.58
0.075	0.15
Pan	0.00
Dry Unit Weight (Kg/m3)	1634.93
Dry Specific Gravity	2.629
Saturated Specific Gravity	2.642
Absorption (%)	0.51
Fineness Modulus	1.82

4.2.5. Concrete Mix Design

A concrete mix was designed to obtain 28-day compressive strength fc'= 35 MPa, 25-100 mm slump, a Maximum Size of Aggregate (MSA) of 19 mm, and w/c ratio of 0.50.

Table 4.5 illustrates the mix design proportions for each cubic meter of concrete. While Table 4.6 reports the results of trail sample concrete cubes to check up the compression strength results as shown in Figure 4.4.

Table 4.5 Mix design proportion for each cubic meter of concrete.

No.	Material Type	Weight (Kg) / m³	Notes
1.	Cement	**350**	(CEM II/AM-SVL 42.5N)
2.	Water	**175**	Potable tap water
3.	Coarse Aggregate	**1197.90**	Coarse aggregate consist of the following proportions according to Table 4.3: a. 254.10 (Kg) Type 1 (Foulia) b. 580.80 (Kg) Type 2 (Adasia) c. 363.00 (Kg) Type 3 (Simsimia)
4.	Fine Aggregate	**616.60**	Clean dune sand

Table 4.6 Sample concrete cubes compression strength results.

No.	Dimension (**mm**)			Weight (**gm**.)	28 days Failure (**KN**)	Cube Stress (**MPa**)	Cylinder Stress (**MPa**) (80% Cube Stress)*	Slump (**mm**)
	Length	Width	High					
1	100	101	103	2531	521.32	51.62	41.29	
2	100	100	103	2474	457.81	45.78	36.62	35
3	101	101	100	2448	478.54	47.38	37.90	
Avg.	**100.33**	**100.67**	**102**	**2484.33**	**485.89**	**48.26**	**38.607**	**35**
* The cylinder stress equal **80 %** of the cube stress theoretically.								

Figure 4.4 IUG Lab compressive strength test machine.

4.2.6. Steel Reinforcement Bars

The steel reinforcing bars used for the construction of the beams consisted of 6 mm diameter steel bar were used for both stirrups and secondary top reinforcement. 10 mm diameter steel bar were used for main bottom reinforcement. Samples from the 10 mm reinforcing bars were tested using the standard tension test as shown in Figure 4.5, an average yielding strength of 444.70 MPa.

Ultimate strength of 689.90 MPa and 18.33 % average elongation were obtained as illustrated in Table 4.7. Samples from the 6 mm reinforcing bars were tested using the standard tension test, an average ultimate strength of 749.51 MPa and 18.00 % average elongation were obtained as illustrated in Table 4.7.

Table 4.7 Steel reinforcement bars test results.

Nominal Size (**mm**)	Cross Sectional Area (**mm²**)	Yield Stress (**MPa**)	Ultimate Stress (**MPa**)	**%** Elongation	Bending Test (**90°**)	Re-bending Test (**20°**)
10.30	83.32	440.10	689.90	18.50	Pass	Pass
10.20	81.71	452.00	689.90	20.00	Pass	Pass
10.30	83.32	442.00	689.90	16.50	Pass	Pass
5.90	27.34	-	731.24	17.50	Pass	Pass
5.90	27.34	-	767.80	18.50	Pass	Pass
5.90	27.34	-	749.50	18.00	Pass	Pass

Figure 4.5 IUG lab. standards tensile strength test machine.

4.3 MATERIALS TO BE USED FOR ENLARGED SECTION (JACKETING MATERIALS)

4.3.1. Expansion Screws (Anchor Bolts)

Steel to concrete or concrete to concrete connections can be accomplished through the use of several types of anchorage systems. Anchorage to concrete is well-known and has detailed design procedures such as (**ACI 318-14, Appendix D**), Anchor bolts play a main

role in reaching to fully composite action, Also to prevent the inter-laminar shear failure between concrete substrate and SCC jacketing. The expansion screws (standard stud anchor - HSA M8 35/25/-) Hilti type has been used in this research as shown in Figure 4.6 and For further information about these material specifications and instructions you can see Appendix A.

Figure 4.6 Hilti standard stud anchor (HSA M8 35/25/-).

This anchor bolts provides a positive anchorage between two concrete parts, a certain number of required anchors has been determined as detailed in Appendix D.

Any fewer than this number may permit occurrence of some slippage between the two concrete layers.

4.3.2. Shear Connectors (Ø8mm)

The steel reinforcing bars used for construction were used as shear connectors consisted of deformed 8mm diameter steel bars. Sample from 8 mm diameter reinforcing bars with weight of 180g and length of 47.5mm was tested using the standard tension test, yielding strength of 676.41 MPa with an ultimate strength of 835.56 MPa and 16% elongation were obtained. A certain number of required anchors has been determined as detailed in Appendix D. Any fewer than this number may permit occurrence of some slippage between the two concrete layers.

4.3.3. Chemical Adhesive (EPICHOR 1768)

EPICHOR 1768 is two component solvent free clear epoxy product, Part A (Resin) and Part B (Hardener) as shown in Figure 4.7, can be mixed with graded sand to be used as a fixing dowels in concrete and repairing mortar, it has quick initial setting time and has thyrotrophic effect, thus suitable for fixing steel dowels to concrete especially to soffits and vertical surfaces which ensures monolithic behavior with concrete. Delivered from YASMO MISR Company of Egypt. For further information see Appendix A.

Figure 4.7 EPICHOR 1768 chemical adhesive.

4.3.4. Galvanized Steel WWM

WWM are introduced to enhance the overall performance of RC beams, it has many advantages, such as high strength to weight ratio, crack resistance, ductility, durability and high degree of toughness.

WWM comprises of a smooth galvanized steel wires with 3.5 mm and 5.5 mm nominal diameter, with spacing 25x25 and 50x50 mm respectively, Spot welding was used, and the yield strength in average 203.63 MPa and 270.72 MPa respectively. Stress strain diagram of WWM were measured as shown in Figure 4.8 and Figure 4.9 for both wire diameters.
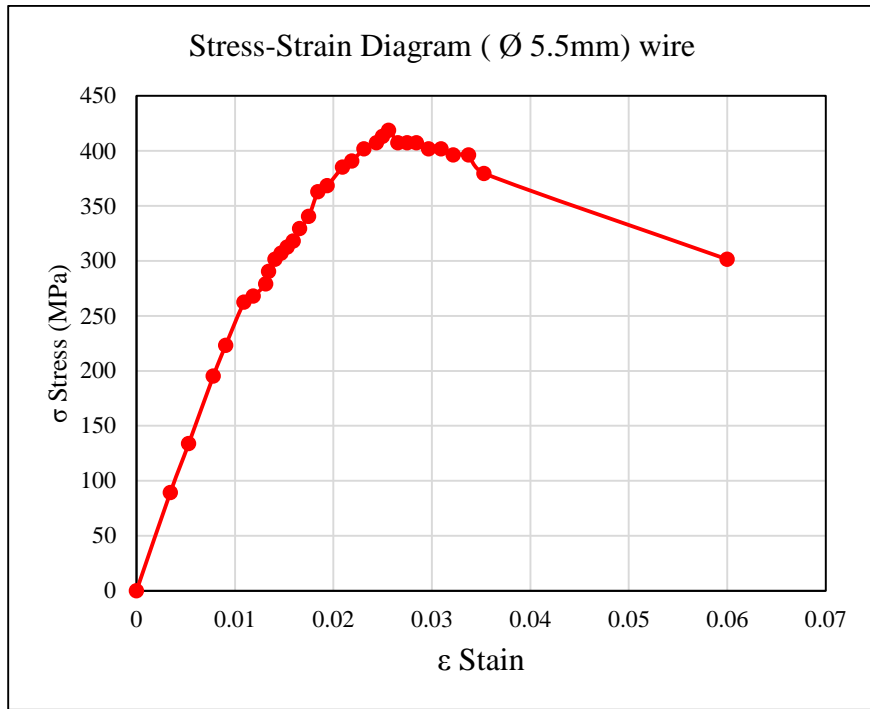
(a)
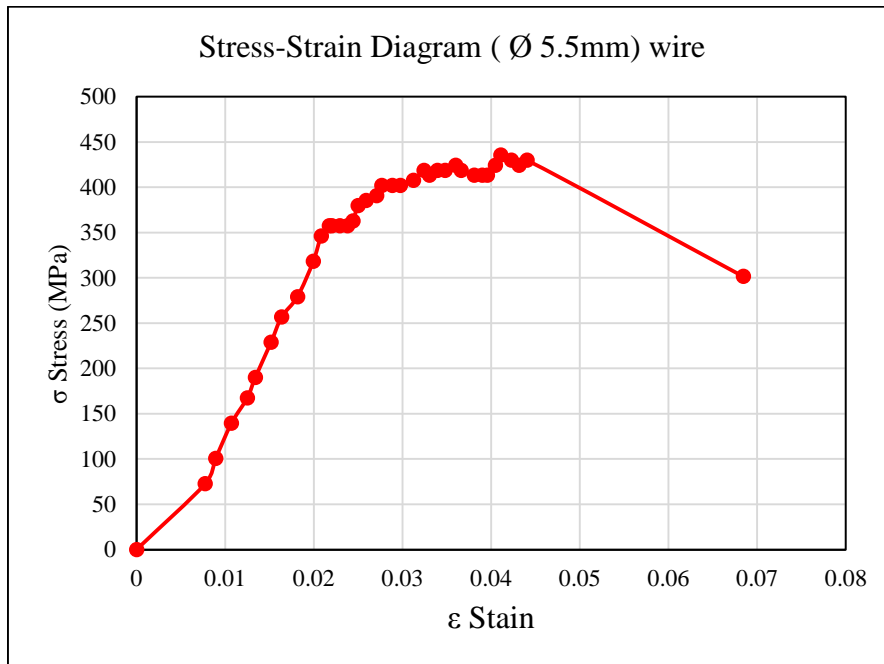
(b)

Figure 4.8 Stress strain curve of (Ø5.5 mm) wires (a) 1st wire, (b) 2nd wire.
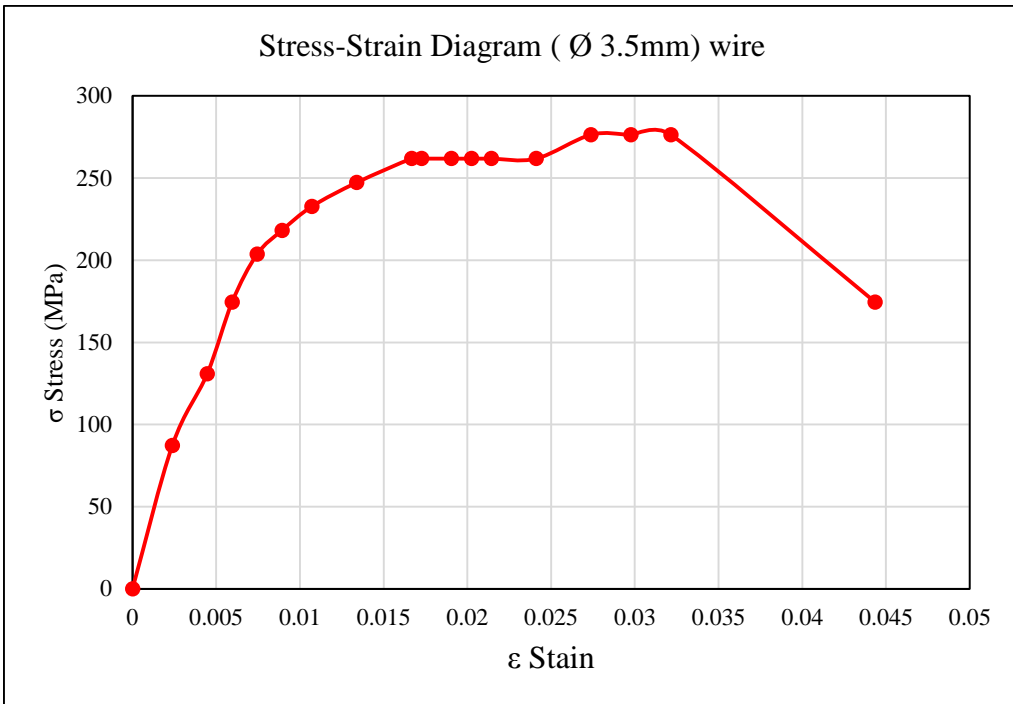
(a)
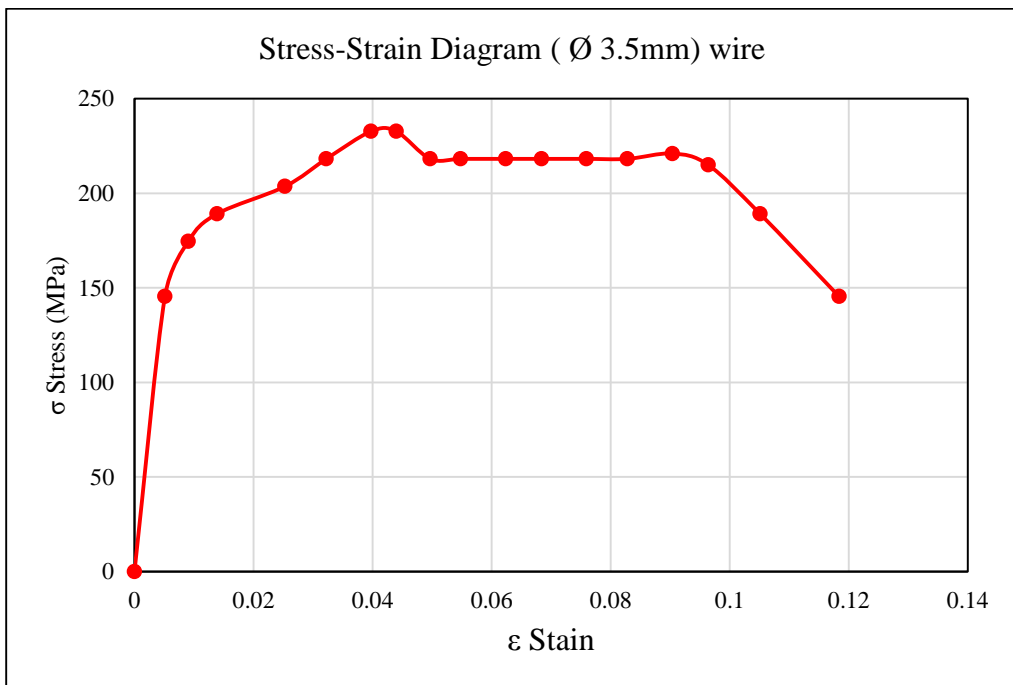
(b)

Figure 4.9 Stress strain curve of (Ø3.5 mm) wires (a) 1st wire, (b) 2nd wire.

Samples from the 5.5 mm wires were tested using the standard tension test, an average ultimate strength of 421.42 MPa and 6.42 % average elongation were obtained, in other hand as samples from the 3.5 mm wires were also tested using the standard tension test, an average ultimate strength of 261.82 MPa and 8.20 % average elongation were obtained as illustrated in Table 4.8.

Table 4.8 Galvanized steel wires test results.

Specified Size (mm)	Nominal Size (mm)	Cross Sectional Area (mm²)	Yield Stress (MPa)	Yield Stress @ offset 0.2% (MPa)	Ultimate Stress (MPa)	% Elong.	Bending Test (90°)
5.50	5.65	25.07	262.34	300	418.63	6.00	Pass
5.50	5.65	25.07	279.10	320	424.20	6.84	Pass
Average	**5.65**	**25.07**	**270.72**	**310**	**421.415**	**6.42**	Pass
3.50	3.50	9.62	203.63	248	276.36	4.57	Pass
3.50	3.50	9.62	203.63	232	247.27	11.84	Pass
Average	**3.50**	**9.62**	**203.63**	**240**	**261.815**	**8.20**	Pass

4.3.5. Resistive Spot Welding

Wikipedia (2015) reported that Resistive Spot Welding (RSW) is a process in which contacting metal surfaces are joined by the heat obtained from resistance to electric current. RSW is one of the oldest of electric welding process in use by industry today. The weld is made by a combination of heat, pressure and time.

As the name resistance welding implies, it is the resistance of the material to be welded to causes current to flow and localized heating in the part. The pressure exerted by the tongs and electrode tips, through which the current flows, hold the parts to be welded in intimate contact before, during and after the welding current time cycle.

The required amount of time to current to flow in the joint is determined by material thickness and type, the amount of current flowing and the cross-section area of the welding tip contact surfaces. Figure 4.10 is schematic diagram that illustrates the principle of RSW.
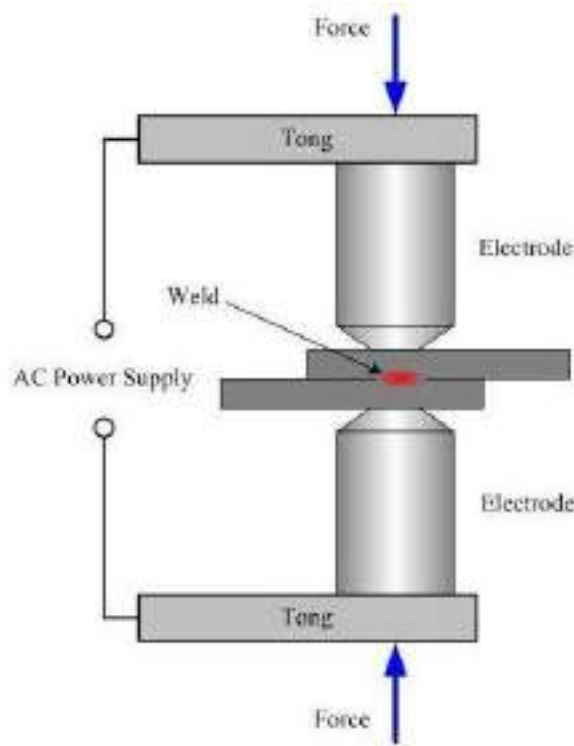
Figure 4.10 Schematic diagram of RSW. (Source: Spot Welding, 2015)

4.3.6. SCC

SCC is defined by European Federation of National Trade Association (EFNARC) "concrete that is able to flow and consolidate under its own weight, completely fill the formwork even in the presence of dense reinforcement, whilst maintaining homogeneity and without the need for any additional compaction" **(EFNARC, 2005)**.

 Figure 4.11 shows that how far can SCC flows under its own weight and does not require any external vibration for compaction.

Figure 4.11 Self-Compacting Concrete. (Source: Technical Bulletin, 2005, P1)

Good workability, passing ability and remarkable filling make SCC a reliable material for the rehabilitation of concrete members particularly the RC beams. Further SCC flows through congested reinforcements without causing honeycombing or vacuums in the concrete element or any discontinuity at the interface between concrete substrate and new concrete.

To adjust these properties chemical admixtures in SCC are a synthetic high-range water reducer (Superplasticizer) and a Viscosity Modifying Admixture (VMA) must be used. These more admixtures commonly used together **(Yang F., 2004)**.

Due to the lack of space in the jacket; the enlarged part of the specimens should have high strength, shrinkage offset, high fluidity and small diameter aggregates which is satisfied in SCC experimentally and practically.

SCC consists of these main materials: coarse aggregates, fine aggregates, cement, and water, high-range water reducing admixture (Superplasticizer) and Stone powder (finely crushed limestone) as mineral admixture.

4.3.6.1. Cement

Ordinary Portland cement (CEM II/AM-SVL 42.5N) grade was used in preparation of SCC .The physical properties of cement was shown in Table 4.1.

4.3.6.2. Water

Potable tap water with PH of 7.1 was used for the experimentation and for the curing process.

4.3.6.3. Fine Aggregate

According to the local market surveying, dune sand type were found, Table 4.4 illustrates the sieve analysis and the properties of this material.

4.3.6.4. Coarse Aggregate

Aggregate is relatively inexpensive and strong making material for concrete. It is treated customarily as inert filler. For producing SCC, selection of very strong aggregate with rough texture is significantly more important the crushed basalt (coarse aggregate). The nominal size ranges from 2 to 9 mm as shown in Figure 4.12.

Figure 4.12 Coarse aggregate (crushed basalt) ranges from 2-9 mm.

The density of the aggregate, water content, absorption and unit weight are required in mix proportions to establish weight volume relationships. Table 4.9 shows the physical properties of basalt according to ASTM standards.

Table 4.9 The physical properties of basalt.

Coarse Aggregate size (Basalt) (mm)	S.G (Dry)	S.G (SSD)	Unit Weight (Kg/m3) (Dry)	Unit Weight (Kg/m3) (SSD)	Water Content (%)	Absorption (%)
2-9	3.03	3.07	3053	3076	0.55	2.1

4.3.6.5. High Range Water Reducing Admixture (Sika ViscoCrete 5920)

Sika ViscoCrete -5920 is a third generation super plasticizer for concrete and mortar (Figure 4.13). It meets the requirements for super plasticizers according to ASTM-C- 494 Types G and F and BS EN 934 part 2: 2001.

Figure 4.13 Sika Viscocrete 5920 (Superplasticizer) used in SCC preparation.

Superplasticizer is an essential component of SCC to provide the necessary workability and improves the properties of fresh and hardened concrete. This plasticizing effect can be used to increase the flowability (resulting in highly reduced placing and compacting efforts), reduce energy cost for stream cured precast elements, improve shrinkage and creep behavior, also it reduce the rate of carbonation of the concrete and finally improve water impermeability. For further information about these repair material specifications and instructions you can see Appendix A.

4.3.6.6. Mineral Admixture

Locally available fine crushed limestone powder (LP) is used as partial cement replacement material as mineral admixture in SCC. Due to the special rheological requirements of SCC finely stone powder crushed limestone is used to increase the amount of powder, the fraction less than 0.075 mm.

The Superplasticizer is necessary for producing a highly fluid concrete mix, while the powder materials or viscosity modifying agents are required to maintain sufficient stability/cohesion of the mix, hence reducing bleeding, segregation and settlement (**Beeralingegowda and Gundakalle, 2013**). As an increase in cement content leads to a significant rise in material cost and often has other negative effects on concrete properties (e.g., increased thermal stress and shrinkage, etc.), the requirement for increased powder content in SCC is usually met by the use of pozzolanic or less reactive filler materials. These may include pulverized fuel ash, granulated ground blast Furnace slag, lime stone powder and others. LP is produced as by-product of limestone crushers.

4.4 EXPERIMENTAL WORKS

4.4.1. Preparing of SCC

Series of tests were carried out on the concrete cubes to evaluate the fresh and hardened properties of SCC. The first step in the mix design comprises developing five trial mixes to obtain the best mix of SCC.

Table 4.10 shows the mix composition for one cubic meter components of the best mix design of SCC which satisfied (**EFNARC, 2005**) guidelines.

Table 4.10 Mix proportions of SCC and the acceptance criteria of EFNARC 2005

Mix Constituents	SCC Compositions	EFNARC 2005 Requirements [*]
Powder content = (Cement +LP) (Kg/m^3)	550.00	380-600
Paste volume [**] (Liter/ m^3)	384.07	300-380
Free water (kg/m3)=(liter/ m^3)	151.47	150-210
Basalt coarse aggregate (Kg/ m^3)	868.85	750-1000
Basalt coarse aggregate (Liter/ m^3)	285.70	270-360
Aggregate (% total weight of Aggregate)	48.17	48-55 %
Fine aggregate (Kg/ m^3)	894.26	-
Fine aggregate (Liter/ m^3)	330.22	-
(Water/Powder) by volume	0.89	0.85-1.10
[*] These proportions are in no way restrictive and many SCC mixes will fall outside this range for one or more constituents. [**] Paste Volume (Liter/m3) =∑ Volume (Cement, water, Superplasticizer and the LP)		

The mixing procedure for SCC included the following steps:

   i.   Adding all quantity of Superplasticizer (100 %) to the mixing water, then mix them manually with steel rod.

  ii.   Placing the dry materials (cement and the fine crushed limestone powder), then mix them manually with trowel.

 iii.   Placing fine aggregate with coarse aggregate in the mixer pan, and mixing for 1 minute.

  iv.   Adding 35 % of water (with Superplasticizer) to the aggregate in the mixer pan, and mixing for 2 minutes.

   v.   Adding the dry material (cement and mineral admixture) to the placing fine and coarse aggregate in the mixer pan, and mixing for 2 minutes.

  vi.   Adding 35 % of water (with Superplasticizer) gradually to the mixture, and mixing for 2 minutes.

 vii.   Waiting 1 minute to mix manually using trowel in the mixer pan, then adding the remaining water (with Superplasticizer) gradually to the mix for 1 minute.

Fresh SCC test was conducted as per EFNARC 2005 guidelines as shown in Table 4.11. Slump flow, T500, V-funnel and L-Box tests were conducted for all trial mix proportion of SCC. For further information about SCC test methods according to EFNARC 2005 you can see Appendix C. The results of the best mix design were satisfied with the EFNARC 2005 guidelines. Figures 4.14, 4.15 and 4.16 illustrate the fresh SCC tests.

Table 4.11 Fresh SCC test results of the best mix design.

	Testing Method	Unit	SCC (Best Mix Design)	EFNARC 2005 Requirements	
				Min.	Max.
1	Slump Flow Test	mm	765	550	850
2	T500 Slump Flow	Sec.	2.95	2	6
3	L Box Test	H2/H1	1.00	0.80	1.00
4	V-Funnel Test	Sec	5	2	9

Figure 4.14 T500 and slump flow test.

Figure 4.15 L-Box test.

Figure 4.16 V-Funnel test.

The hardened concrete specimens were tested after 7 and 28 days of curing. The test specimens were cast in steel mold without compaction and demolded after 48 hours. The cubes specimen were cured till the day of testing under water at normal temperature and humidity conditions. The compressive strength is measured using cube specimens. The size of the cube specimen is 100 mm × 100 mm × 100 mm. twelve concrete cubes were casted for each concrete mix proportions. The compressive strength of three cubes of SCC were measured after 7, and 28 days as shown in Figure 4.17. Table 4.12 shows the properties of hardened SCC of a trial sample.

Table 4.12 Properties of hardened SCC of a trial sample.

Sample No.	Dimension (**mm**)			Weight (**gm**.)	Failure (**KN**)	Cube Stress (**MPa**)	Cylinder Stress (**MPa**) (80% Cube Stress)
	Length	Width	High				
7 Days							
1	100	101	102	2555	441.74	43.74	34.99
2	100	100	100	2515	417.11	41.71	33.37
3	100	101	102	2585	434.41	43.01	34.41
Average	**100.00**	**100.67**	**101.33**	**2551.67**	**431.09**	**42.82**	**34.26**
28 Days							
4	101	101	103	2540	585.65	57.41	45.93
5	101	99	101	2535	598.62	59.87	47.89
6	101	101	102	2575	586.77	57.52	46.02
Average	**101**	**100.33**	**102**	**2550**	**590.35**	**58.27**	**46.61**

Figure 4.17 SCC compressive strength test.

4.4.2. Beam Specimen Casting and Curing

The beam specimens have a length of 1200 mm and 100 x 150 mm section. Forms of wood for constructing beams was prepared as seen in Figure 4.18.

Figure 4.18 Wood form and reinforcement details

The wooden molds were cast with a concrete, having an average compressive strength, measured on 100 mm side cubes, equal to 39.24 N/mm2. Regarding the reinforcement, the steel rebars exhibited an average yielding strength equal to 444.70 N/mm2 and an average maximum strength equal to 689.90 N/mm2.

Figure 4.19 shows the casting process. All specimens were cured from the first day after casting with clean water properly for 14 days and saved with temperature of 25°C. Figure 4.20 shows the cured beams.

Figure 4.19 Casting process.

Figure 4.20 Curing process of RC beams.

4.4.3. Strengthening of Beam Specimens

The beam specimens were preloaded up to 30 % of UL of control beams before strengthening process in order to represent the subjected SL in nature which is 30-60 % of ultimate beam capacity, then the strengthening process was done as follows:

1- The interacted surface of the specimen was cleaned from dusts using clean water and brush.

2- The three beams (GA.B5, GA.B6 and GB.B5) were roughened in order to reach a roughness of about 1 mm using rotating lamella, able to ensure a perfect bond between the existing concrete and the applied SCC.

3- The four beams (GA.B3, GA.B4, GB.B3 and GB.B4) were drilled with thirty holes with 10 mm diameter and 50 mm depth. The holes distributed equally and staggered for the three subjected surface of each beam, these holes were cleaned with air compressor and injected with concrete-reinforcement bonding epoxy resin that mixed with sand, then the $\emptyset 8$ mm shear connectors of length 80mm were installed in each hole for the beams according to their own category. Figure 4.21 illustrates the shear connector distribution.

Figure 4.21 Shear connector distribution.

4- The specimens were left for 24 hours to ensure that epoxy is completely dried and reach its high strength.

5- The four beams (GA.B1, GA.B2, GB.B1, and GB.B2) were drilled with thirty holes with 8 mm diameter and 50 mm depth. The holes distributed equally and staggered for the three subjected surface of each beam, these holes were cleaned with air compressor, then the $\emptyset 8$ mm Hiliti shear connectors of length 80mm were installed in each hole for the beams according to their own category. Figure 4.22 illustrates the Hiliti shear connector distribution.

Figure 4.22 Hilti shear connector distribution.

6- The wooden shutters were painted using mold release oil and prepared, the WWM cage reinforcement is installed then the main specimens were placed and installed in a manner that the lower surface of jacket was upward to facilitate the casting process, addition to maintain the concrete cover for the other sides of jacket. Figure 4.23 illustrates these steps clearly.

Figure 4.23 Wooden molds with specimen preparation.

7- SCC was casted until complete filling of the wooden mold. The mold was gently stroked to ensure that air bubbles is released. Figure 4.24 shows the SCC casting process.

Figure 4.24 SCC casting process.

8- The four monolithic control beams (MA.B1, MA.B2, MB.B1, and MB.B2) were casted with an ordinary concrete, having an average compressive strength, measured on 100 mm side cubes, equal to 38.274 N/mm2. The WWM cage and the ordinary reinforcement is installed as shown in Figure 4.25.

Figure 4.25 Control beam MA.B1 casting process.

9- The wooden molds were removed after 24 hours of casting, then all specimens were cured from the first day after casting with clean water properly for 14 days and saved with temperature of 25°C.

10- For any casting day a certain number of standards cubes of (100×100×100) mm were prepared for each casting mix to obtain the actual compressive strength of the beam specimen as soon as it was tested.

4.4.4. Preparing of Standard Cubes of Trial Mixes

For ordinary concrete that were used for beam specimens before strengthening three pairs of cubes of (100×100×100) mm were prepared for each casting mix to obtain the compressive strength of concrete after 28-days. Those cubes were prepared according to (ASTM C109, 2004) standard test method for cubes. The cubes were immersed in water until the time of the test. Before the tests, the specimens were air dried for 10 to15 minutes and any loose sand grains or incrustations from the faces that will be in contact with the bearing plat of the testing machine are removed.

For SCC that used in strengthening jacketing the hardened cubes specimens were tested after 7 and 28 days of curing. The test specimens were cast in steel mold without compaction and demolded after 48 hours. The cubes specimen were cured till the day of testing under water at normal temperature and humidity conditions. The size of the cube specimen is 100 mm × 100 mm × 100 mm.

4.5 TESTING WORK PROCEDURES

4.5.1. Instrumentation and Flexural Testing

The Beams were loaded in the same flexural machine in Material and soil Laboratory at IUG as shown in Figure 4.26. The hydraulic jack that ran the machine had a compressive strength of 20 tons ($\simeq$ 200KN).

The beams were all carefully positioned in the machine manually and using the man powers. Efforts have been made to maintain manually the hydraulic jack machine in an even constant slow speed during applying the loads.

Figure 4.26 Flexural machine at IUG and deflection dial gauge fixation.

The hydraulic pressure load was recorded manually and the mid span deflection caused by changing of the applied load was monitored using mechanical dial gauge that was mounted on the jack at the mid-span of each beams as seen in Figure 4.26.

Flexural testing is considered as the main test applied for the hardened strengthened beams. Control and strengthened beams were tested under static loading condition as simply supported beams with two concentrated loads using the flexural testing machine, the deflection was recorded for each load increment.

The flexural testing machine can provide loading stages allowing many other observations to be apply in parallel during the flexural loading capacity test such as crack width observation and deflection measurement for beams during the flexural test.

4.5.2. Preloading Stage

The beam specimens before strengthening process were preloaded up to 30 % of UL of control in order to represent the subjected SL in nature which is 30-60 % of ultimate beam capacity. Then the specimens are restored using relatively thin reinforced jackets and retested by the same bending loading. The SCC concrete jacket applied, encasing both vertical sides (U formed jackets), has a small thickness 30mm and 50 mm.

4.5.3. Main Testing Procedure

The well-studied procedure was performed to meet the research testing objectives start in with preparation and testing of suitable and reliable mix design for ordinary concrete and SCC to apply the strengthening for beams by section enlargement technique (U-Jacketing), then the strengthened beams will be applied to parallel tests and measurements which are; the flexural load capacity of beam, the serviceability measurements of crack width and deflections and finally failure mode observation and crack pattern. This procedure is summarized in the following:

1- Preparing a mix design for ordinary concrete and SCC including fresh and hardened tests.
2- Apply the Strengthening for the Beams using SCC with WWM.
3- Parallel tests and measurements that must be done for each specimen are:
    i.   The flexural and capacity of the beams.
    ii. The Serviceability measurements of crack width and deflection.
    iii. Failure mode observation and crack pattern.

4.5.4. Testing Work Procedure of Strengthened Beam Specimens

After 28-days of curing for the under-layer section of the specimens, the overall beam specimens were tested for several testing parameter which were discussed previously. The specimen were tested under static loading condition as simply supported beams with two concentrated loads using hydraulic flexural loading test machine in

IUG lab facility. Deflection was measured using dial displacement gauge and the crack width were measured using micro-crack scope. Figure 4.27 shows the IUG's measurement tool instruments.

Figure 4.27 IUG's displacement gauge and microscope meter.

➢ **Prior The Testing Process**

a. The beam specimens were cleaned from debris and colored with white paint.

b. Lines were drawn on beam specimens every 50 mm on the long and the height directions to obtain the crack development during the test.

c. The position of support in IUG's flexural loading machine was checked to provide the clear span distance.

d. The specimen was installed on the IUG's flexural loading machine and positioned on its support.

e. Load spreader was placed in touch with the top beam surface to obtain two concentrated loads.

f. Deflection gauge was attached at the mid span using magnetic clamp base.

➢ **During Testing**

a. Increment of 2.35 KN load was applied to beam specimen.

b. The load was recorded.

c. Deflections were measured and recorded using displacement gauge at every load increment.

d. The maximum hair line crack occurrence was measured using micro-crack scope at every load increment.

e. The process was repeated until the failure occurrence.

➢ **After Testing**

a. The load spreader was released from the specimen.

b. Maximum crack width was measured

c. Crack pattern was drawn and checked.

d. Pack up crack pattern was checked by taking photos that illustrate the scale using ruler.

5

CHAPTER
TEST RESULTS AND DISCUSSION

CHAPTER 5

TEST RESULTS AND DISCUSSION

5.1 INTRODUCTION

Results and discussion are presented in this chapter. During testing, data and results were recorded for all the samples. This discussion includes a constructed theoretical analysis to verify the experimental works for each specimen.

5.2 TEST RESULTS OF STANDARD GROUP

5.2.1. Control Beams

CB0, (the control beam No. zero) failed in flexure with UL equal 34.31 KN. CB1, CB2 (the control beams No.1 & No.2) failed in flexure and provided UL of 44.124 KN and 38.775 KN respectively. Figures 5.1, 5.2 and 5.3 show the sample after testing and the crack pattern for CB0, CB1 & CB2 respectively.
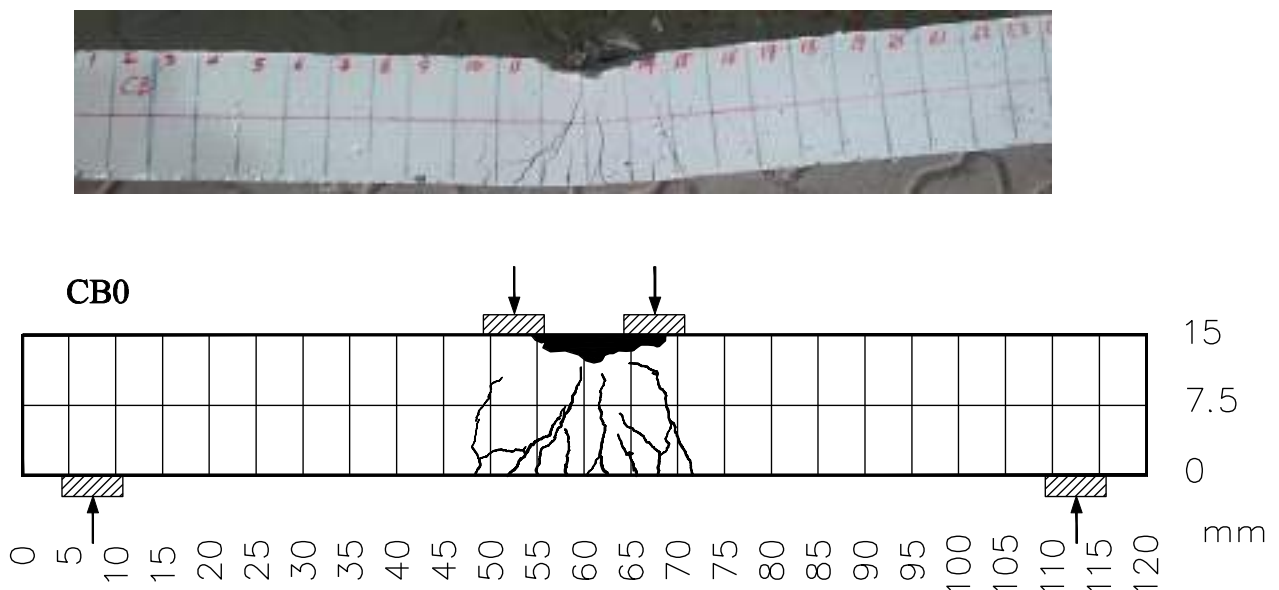
Figure 5.1 Failure mode and crack pattern of CB0.

Figure 5.2 Failure mode and crack pattern of CB1.

Figure 5.3 Failure mode and crack pattern of CB2.

Figure 5.4 shows the load-deflection curves of the three control beams. Average mid-span deflection for the three samples at the failure deflection equal 9.267 mm. Table 5.1 summarized the test results of the three control beam specimens.

Figure 5.4 Load Deflection curves of CB0, CB1 and CB2.

Table 5.1 Test results of the three control beam specimens.

Description	CB0	CB1	CB2	Average	Standard Deviation
First cracking noticed at (KN)	28.764	28.67	24.06	27.165	2.689
First cracking moment at (KN.m)	6.472	6.451	5.414	6.112	0.605
Mid-Span deflection at first cracking (mm)	4.01	3.73	3.45	3.73	0.280
Crack thickness at first cracking (mm)	0.025	0.02	0.02	0.02167	0.003
Failure load (KN)	34.31	44.124	38.775	39.0697	4.914
Failure moment (KN.m)	7.72	9.93	8.725	8.791	1.107
Total deflection at failure (mm)	9.05	10.10	8.65	9.267	0.749
Widest crack at failure (mm)	2.3	1.1	2.8	2.067	0.874
Ductility Ratio ($\Delta u/\Delta i$) [*]	2.26	2.71	2.51	2.493	0.225

[*] Ductility ratio is defined here in this investigation as the ratio between the mid-span deflection at UL to that at the first crack load.

5.2.2. Control Beams Casted Monolithically with 3.5 mm Mesh

Specimens MA.B1 and MA.B2 were the control specimens that casted monolithically using ordinary concrete with 3.5 mm mesh and (1200×200×160 mm) in dimension. The mode of failure observed was flexural failure. The crushing of concrete compression zone for MA.B1 was observed at13.765 mm of 81.883 KN and for MA.B2 it was observed at 13.11 mm of 87.180 KN. Figures 5.5 and 5.6 show the sample after testing and the crack pattern for the both specimens respectively.

Figure 5.5 Failure mode and crack pattern of MA.B1.

Figure 5.6 Failure mode and crack pattern of MA.B2.

Figure 5.7 shows the load-deflection curves of the two beam specimens. Average mid-span deflection for the two samples at the failure deflection equal 13.438 mm. Table 5.2 summarized the test results of the two monolithic control beam specimens.

For MA.B1, mid span deflection corresponding to P_{max} was 13.765 mm. The serviceability deflection limit (L/360) of 2.92 mm was reached at load of 41.5 KN or 50.71% of P_{max}. The serviceability deflection limit (L/180) of 5.833 mm was reached at load of 68.50 KN or 83.71% of P_{max}. The deflection at the working load which predicted at 70% of P_{max} was 4.65 mm.

For MA.B2, mid span deflection corresponding to P_{max} was 13.110 mm. The serviceability deflection limit (L/360) of 2.92 mm was reached at load of 37.20 KN or 42.67% of P_{max}. The serviceability deflection limit (L/180) of 5.833 mm was reached at load of 67.50 KN or 77.426% of P_{max}. The deflection at the working load which predicted at 70% of P_{max} was 5.13 mm.

Figure 5.7 Load Deflection curves of MA.B1 and MA.B2.

Table 5.2 Test results of monolithic control beam MA.B1 and MAB2.

Description	MA.B1	MA.B2	Average	Standard Deviation
First cracking noticed at (KN)	28.247	31.960	30.104	2.625
First cracking moment at (KN.m)	6.356	7.191	6.773	0.590
Mid-Span deflection at first cracking (mm)	1.820	2.31	2.065	0.346
Crack thickness at first cracking (mm)	0.02	0.022	0.021	0.001
Failure load (KN)	81.833	87.180	84.510	3.781
Failure moment (KN.m)	18.424	19.652	19.038	0.868
Total deflection at failure (mm)	13.765	13.110	13.438	0.463
Widest crack at failure (mm)	4.10	3.51	3.805	0.417
Ductility Ratio	7.56	5.68	6.51	1.329

5.2.3. Control Beams Casted Monolithically with 5.5 mm Mesh

Specimens MB.B1 and MB.B2 were the control specimens that casted monolithically using ordinary concrete with 5.5 mm mesh and (1200×200×160 mm) in dimension. The mode of failure observed was flexural failure. The crushing of concrete compression zone for MB.B1 was observed at 13.47 mm of 110.553 KN and for MB.B2 it was observed at 12.196 mm of 103.654KN.

Figures 5.8 and 5.9 show the sample after testing and the crack pattern for the both specimens respectively.

Figure 5.8 Failure mode and crack pattern of MB.B1.

Figure 5.9 Failure mode and crack pattern of MB.B2.

Figure 5.10 shows the load-deflection curves of the two beam specimens. Average mid-span deflection for the two samples at the failure deflection equal 12.833 mm. Table 5.3 summarized the test results of the two monolithic control beam specimens.

For MB.B1, mid span deflection corresponding to P_{max} was 13.47 mm. The serviceability deflection limit (L/360) of 2.92 mm was reached at load of 43.7 KN or 39.53% of P_{max}. The serviceability deflection limit (L/180) of 5.833 mm was reached at load of 78.5 KN or 71.00 % of P_{max}. The deflection at the working load which predicted at 70% of P_{max} was 5.70 mm.

For MB.B2, mid span deflection corresponding to P_{max} was 12.196 mm. The serviceability deflection limit (L/360) of 2.92 mm was reached at load of 41.00 KN or 39.55 % of P_{max}. The serviceability deflection limit (L/180) of 5.833 mm was reached at load of 79.00 KN or 76.22 % of P_{max}. The deflection at the working load which predicted at 70% of P_{max} was 5.32 mm.

Control Beams Casted Monolithically with 5.5 mm Mesh
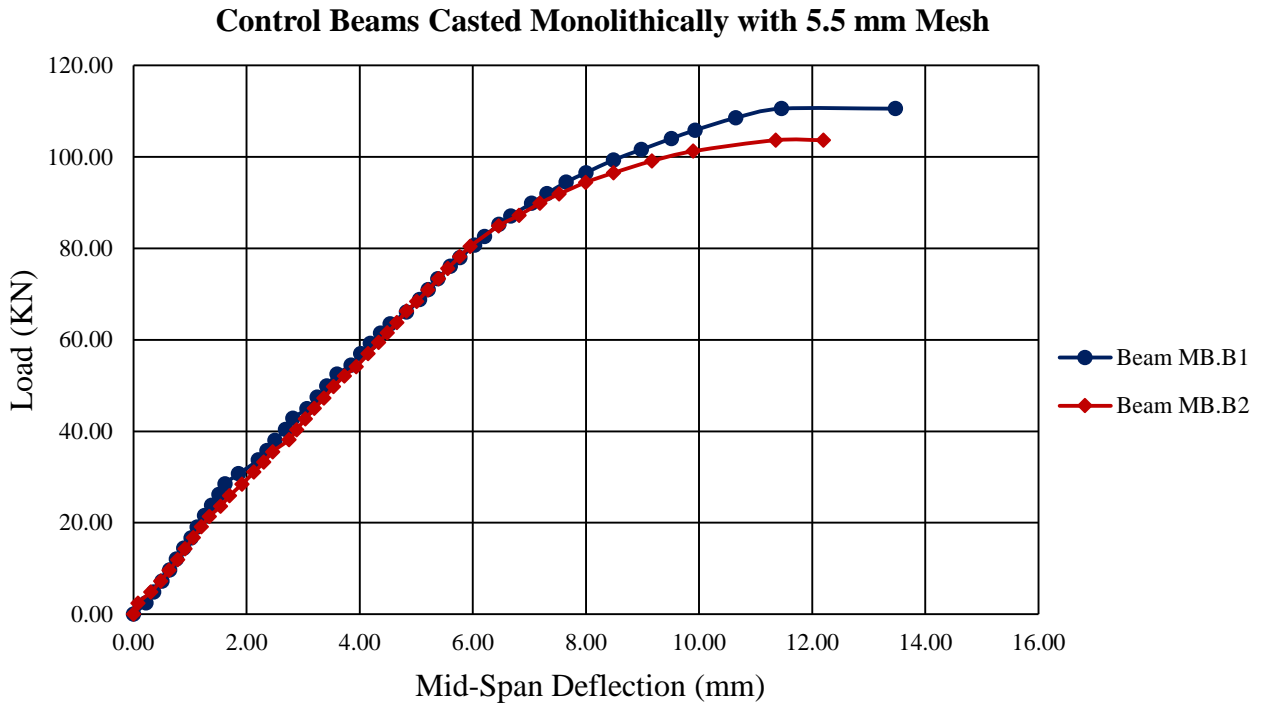
Figure 5.10 Load Deflection curves of MB.B1 and MB.B2.

Table 5.3 Test results of monolithic control beam MB.B1 and MB.B2.

Description	MB.B1	MB.B2	Average	Standard Deviation
First cracking noticed at (KN)	28.51	31.06	29.785	1.803
First cracking moment at (KN.m)	6.415	6.988	6.702	0.405
Mid-Span deflection at first cracking (mm)	1.62	2.13	1.875	0.361
Crack thickness at first cracking (mm)	0.02	0.024	0.022	0.003
Failure load (KN)	110.553	103.654	107.104	4.878
Failure moment (KN.m)	24.875	23.322	24.104	1.098
Total deflection at failure (mm)	13.47	12.196	12.833	0.901
Widest crack at failure (mm)	2.31	3.6	2.955	0.912
Ductility Ratio	8.31	5.72	6.85	1.831

5.3 TEST RESULTS OF FIRST GROUP

5.3.1. Beam with U Jacketing have an Expansion Bolts with 3.5 mm Mesh

Specimens GA.B1 and GA.B2 were the specimens that strengthened using SCC U-jacketing with 3.5 mm mesh and (1200×200×160 mm) in dimension. To prevent inter laminar shear between the concrete substrate and SCC jacket Hilti structural expansion anchors have been used. The mode of failure observed was flexural failure.

The crushing of concrete compression zone for GA.B1 was observed at 12.75 mm of 79.994 KN and for GA.B2 it was observed at 14.815mm of 82.88 KN.

Figures 5.11 and 5.12 show the sample after testing and the crack pattern for the both specimens respectively.
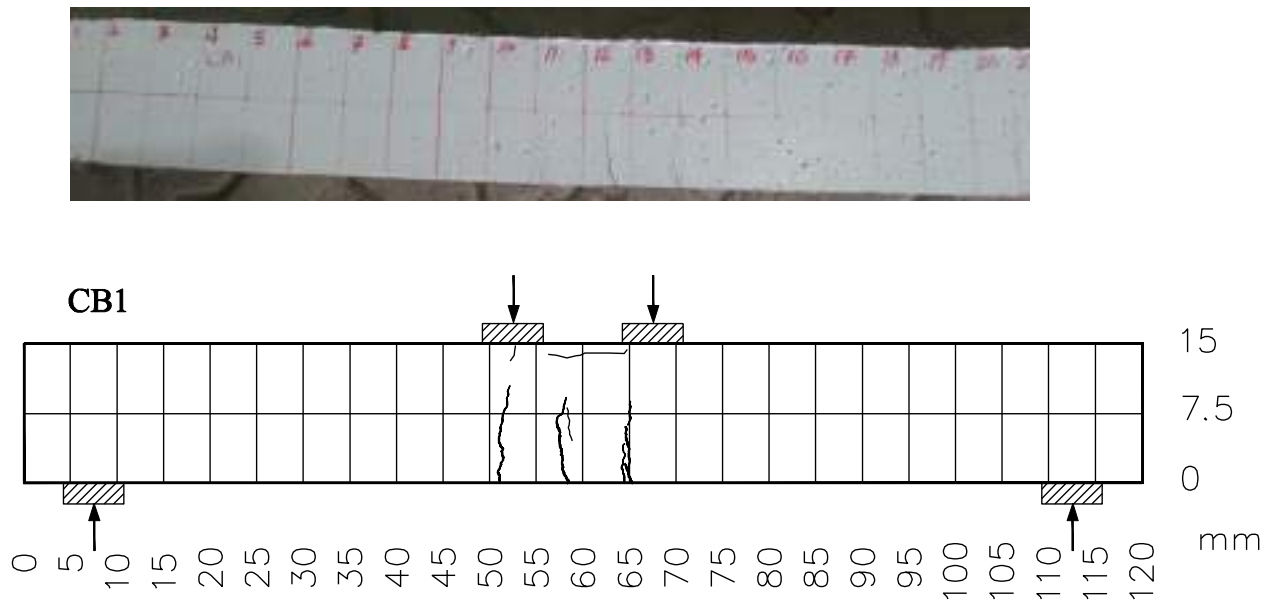

Figure 5.11 Failure mode and crack pattern of GA.B1.

Figure 5.12 Failure mode and crack pattern of GA.B2.

Figure 5.13 shows the load-deflection curves of the two beam specimens. Average mid-span deflection for the two samples at the failure deflection equal 13.783 mm. Table 5.4 summarized the test results of the two specimens.

Figure 5.13 Load Deflection curves of GA.B1 and GA.B2.

For GA.B1, mid span deflection corresponding to P_{max} was 12.75 mm. The serviceability deflection limit (L/360) of 2.92 mm was reached at load of 38.5 KN or 48.12 % of P_{max}. The serviceability deflection limit (L/180) of 5.833 mm was reached at load of 68.578 KN or 85.73 % of P_{max}. The deflection at the working load which predicted at 70% of P_{max} was 4.45 mm.

For GA.B2, mid span deflection corresponding to P_{max} was 14.815 mm. The serviceability deflection limit (L/360) of 2.92 mm was reached at load of 37.00 KN or 44.64 % of P_{max}. The serviceability deflection limit (L/180) of 5.833 mm was reached at load of 67.5 KN or 81.44 % of P_{max}. The deflection at the working load which predicted at 70% of P_{max} was 4.80 mm.

Table 5.4 Test results of strengthened beams GA.B1 and GA.B2.

Description	GA.B1	GA.B2	Average	Standard Deviation
First cracking noticed at (KN)	35.617	30.921	33.269	3.321
First cracking moment at (KN.m)	8.014	6.96	7.487	0.745
Mid-Span deflection at first cracking (mm)	2.69	2.315	2.5015	0.265
Crack thickness at first cracking (mm)	0.018	0.02	0.019	0.001
Failure load (KN)	79.994	82.880	81.437	2.041
Failure moment (KN.m)	17.998	18.648	18.323	0.460
Total deflection at failure (mm)	12.75	14.815	13.783	1.460
Widest crack at failure (mm)	1.40	3.71	2.555	1.633
Ductility Ratio	4.74	6.40	5.51	1.174

5.3.2. Beam with U Jacketing have Dowels with 3.5 mm Mesh

Specimens GA.B3 and GA.B4 were the specimens that strengthened using SCC U-jacketing with 3.5 mm mesh and (1200×200×160 mm) in dimension. To prevent inter laminar shear between the concrete substrate and SCC jacket deformed Ø8 mm steel reinforcement dowels have been used. The mode of failure observed was flexural failure.

The crushing of concrete compression zone for GA.B3 was observed at 12.85 mm of 79.463 KN and for GA.B4 it was observed at 12.465 mm of 84.976 KN.

Figures 5.14 and 5.15 show the sample after testing and the crack pattern for the both specimens respectively.

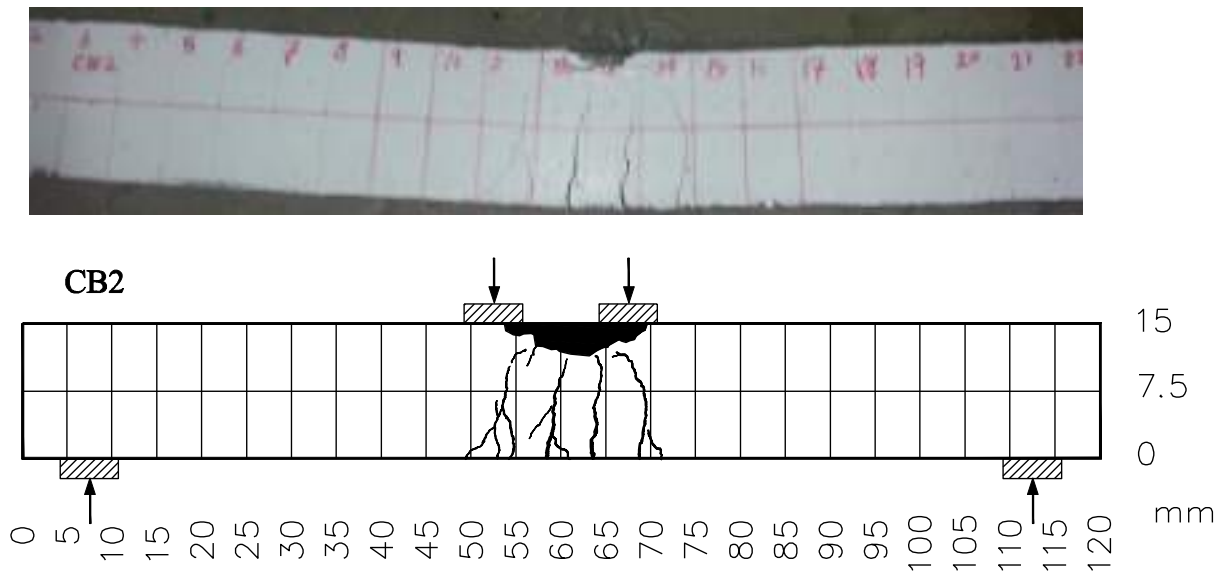Figure 5.14 Failure mode and crack pattern of GA.B3.

Figure 5.15 Failure mode and crack pattern of GA.B4.

Figure 5.16 shows the load-deflection curves of the two beam specimens. Average mid-span deflection for the two samples at the failure deflection equal 12.66 mm. Table 5.5 summarized the test results of the two specimens.
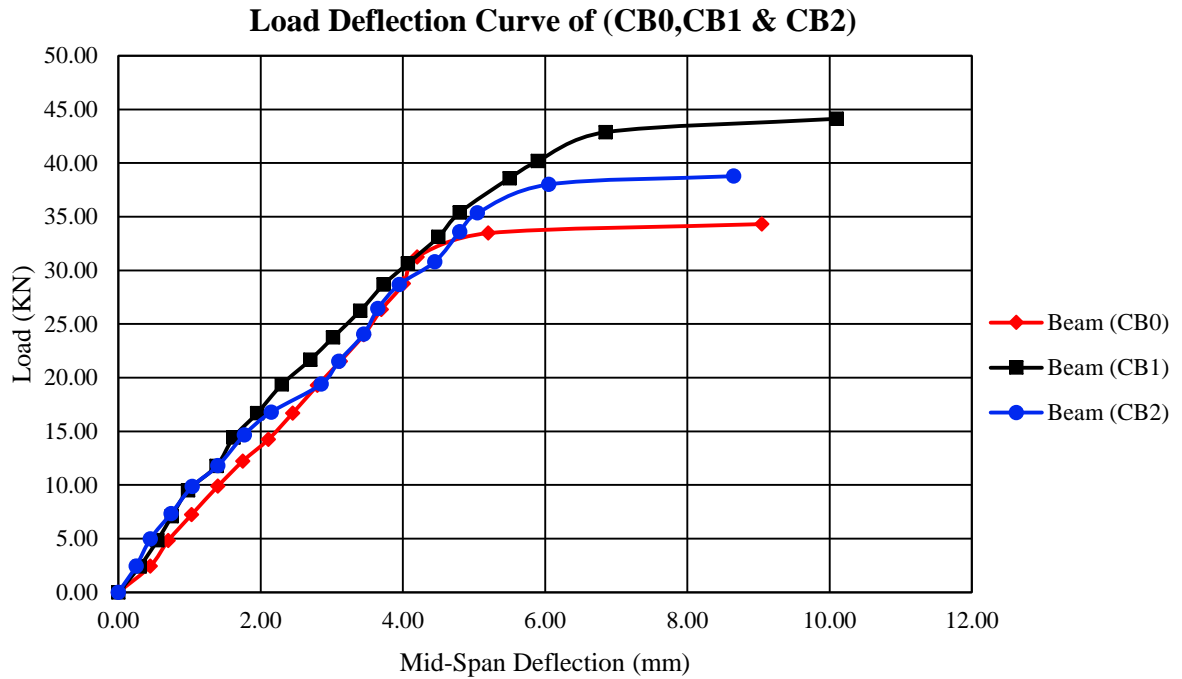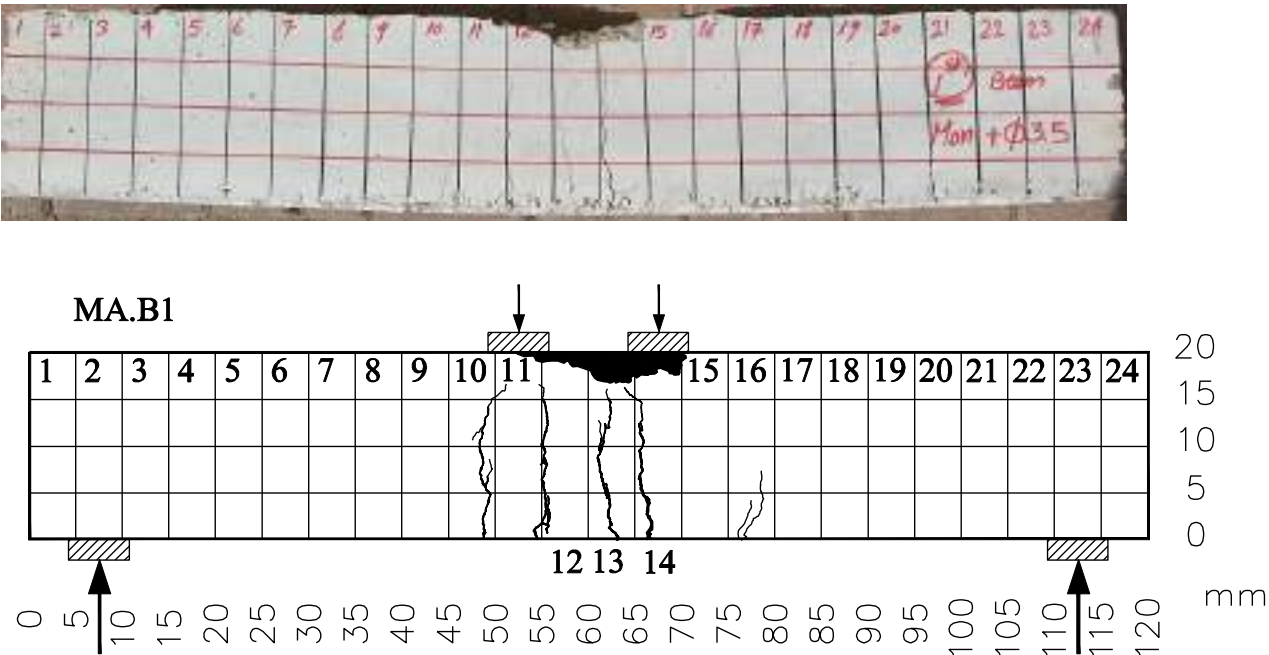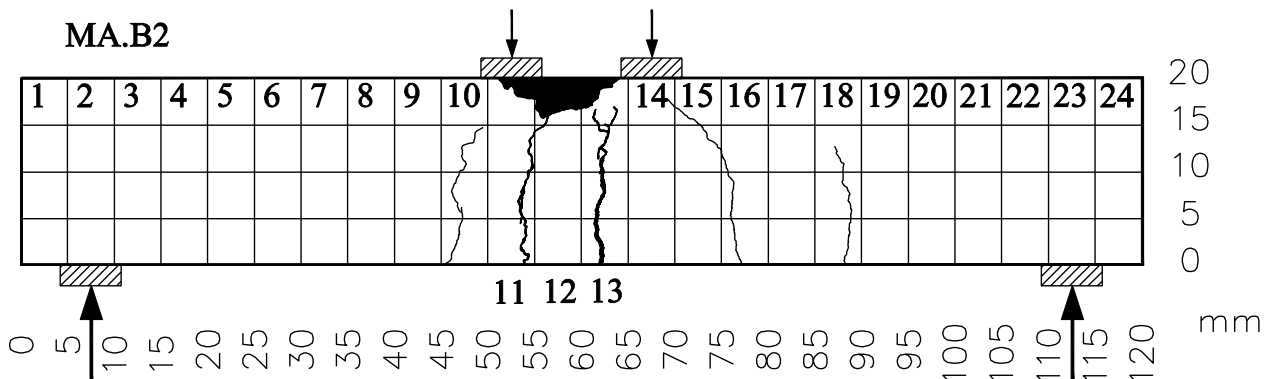

Figure 5.16 Load Deflection curves of GA.B3 and GA.B4.

For GA.B3, mid span deflection corresponding to P_{max} was 12.85 mm. The serviceability deflection limit (L/360) of 2.92 mm was reached at load of 39.5 KN or 49.71 % of P_{max}. The serviceability deflection limit (L/180) of 5.833 mm was reached at load of 68.00 KN or 85.57 % of P_{max}. The deflection at the working load which predicted at 70% of P_{max} was 4.55 mm.

For GA.B4, mid span deflection corresponding to P_{max} was 14.815 mm. The serviceability deflection limit (L/360) of 2.92 mm was reached at load of 41.00 KN or 48.25 % of P_{max}. The serviceability deflection limit (L/180) of 5.833 mm was reached at load of 72.00 KN or 84.73 % of P_{max}. The deflection at the working load which predicted at 70% of P_{max} was 4.68 mm.

Table 5.5 Test results of strengthened beams GA.B3 and GA.B4.

Description	GA.B3	GA.B4	Average	Standard Deviation
First cracking noticed at (KN)	28.529	30.931	29.73	1.698
First cracking moment at (KN.m)	6.42	6.96	6.69	0.382
Mid-Span deflection at first cracking (mm)	2.03	2.135	2.083	0.074
Crack thickness at first cracking (mm)	0.025	0.02	0.023	0.004
Failure load (KN)	79.463	84.976	82.220	3.898
Failure moment (KN.m)	17.88	19.12	18.50	0.877
Total deflection at failure (mm)	12.85	12.465	12.658	0.272
Widest crack at failure (mm)	1.80	3.22	2.51	1.004
Ductility Ratio	6.33	5.84	6.09	0.346

5.3.3. Beam with U jacketing have a Roughened Surface with 3.5 mm Mesh

Specimens GA.B5 and GA.B6 were the specimens that strengthened using SCC U-jacketing with 3.5 mm mesh and (1200×200×160 mm) in dimension. To prevent inter laminar shear between the concrete substrate and SCC jacket surface roughening has been used. The mode of failure observed was flexural failure.

The crushing of concrete compression zone for GA.B5 was observed at 20.95 mm of 84.60 KN and for GA.B6 it was observed at 15.29 mm of 80.92 KN.

Figures 5.17 and 5.18 show the sample after testing and the crack pattern for the both specimens respectively.
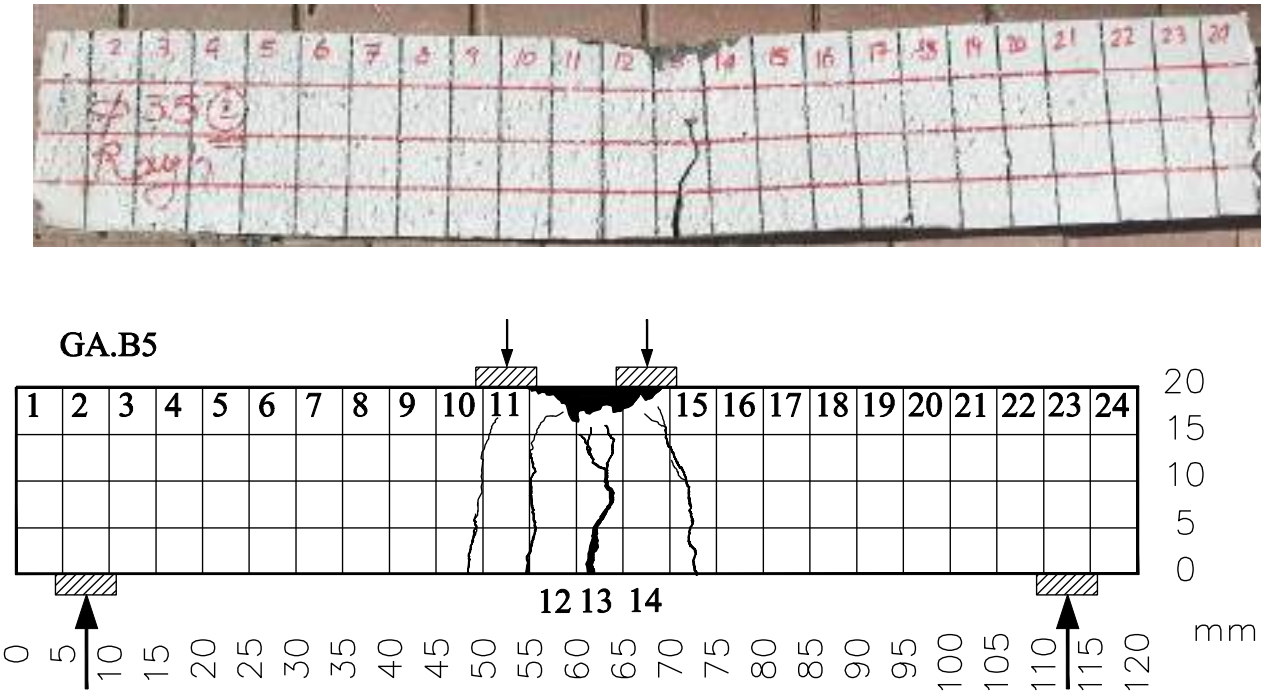
Figure 5.17 Failure mode and crack pattern of GA.B5.
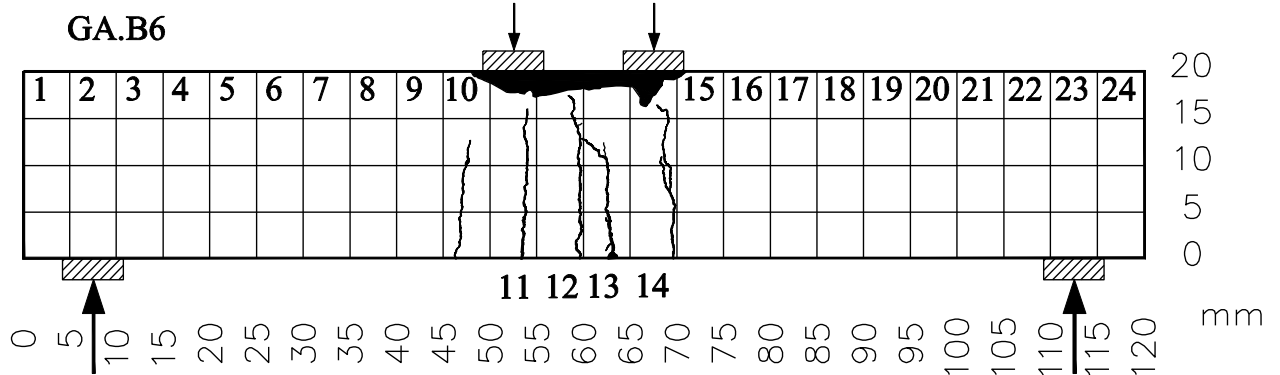
Figure 5.18 Failure mode and crack pattern of GA.B6.

Figure 5.19 shows the load-deflection curves of the two beam specimens. Average mid-span deflection for the two samples at the failure deflection equal 18.12 mm. Table 5.6 summarized the test results of the two specimens.
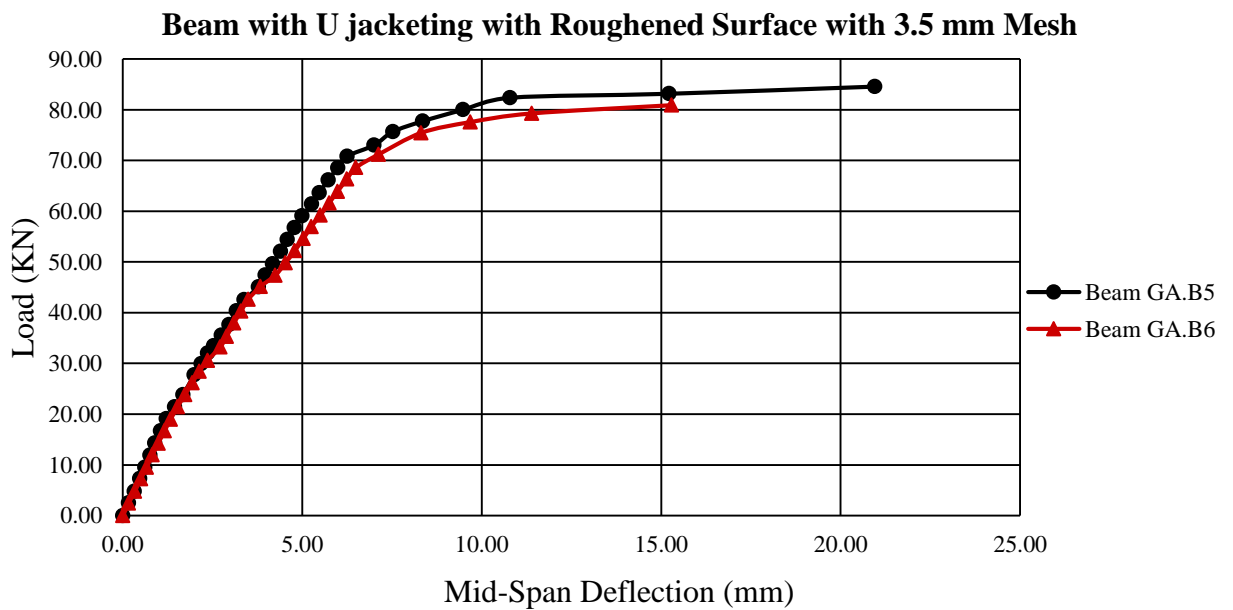
Figure 5.19 Load Deflection curves of GA.B5 and GA.B6.

For GA.B5, mid span deflection corresponding to P_{max} was 20.95 mm. The serviceability deflection limit (L/360) of 2.92 mm was reached at load of 37.1 KN or 43.85 % of P_{max}. The serviceability deflection limit (L/180) of 5.833 mm was reached at load of 67.00 KN or 79.19 % of P_{max}. The deflection at the working load which predicted at 70% of P_{max} was 5.00 mm.
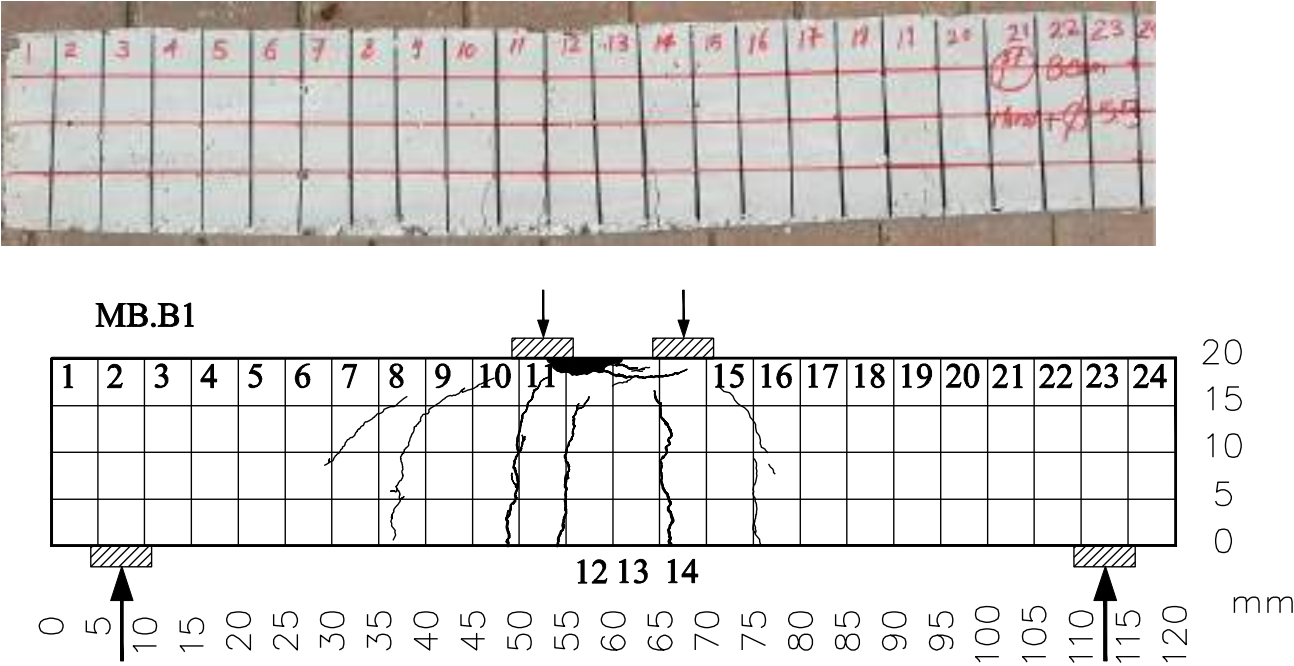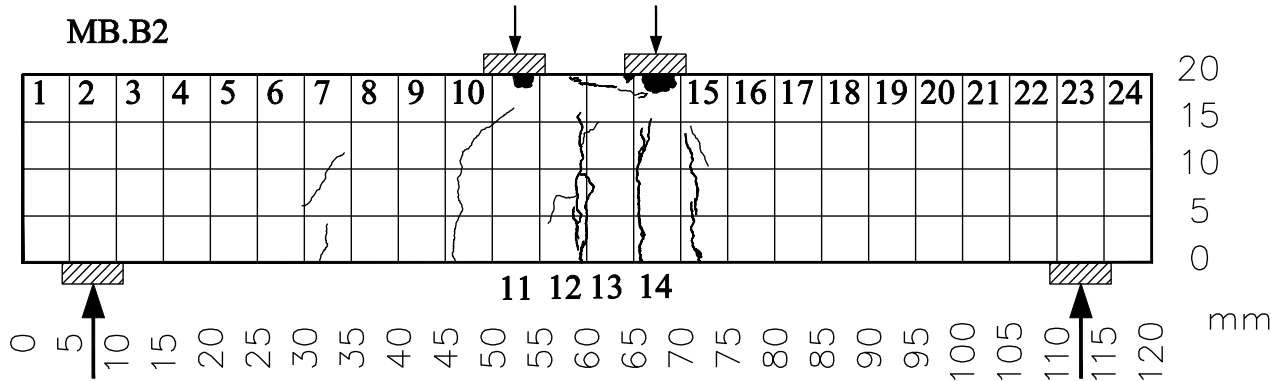
For GA.B6, mid span deflection corresponding to P_{max} was 15.29 mm. The serviceability deflection limit (L/360) of 2.92 mm was reached at load of 35.70 KN or 44.11 % of P_{max}. The serviceability deflection limit (L/180) of 5.833 mm was reached at load of 62.50 KN or 77.24 % of P_{max}. The deflection at the working load which predicted at 70% of P_{max} was 5.20 mm.

Table 5.6 Test results of strengthened beams GA.B5 and GA.B6.

Description	GA.B5	GA.B6	Average	Standard Deviation
First cracking noticed at (KN)	27.754	26.165	26.960	1.124
First cracking moment at (KN.m)	6.25	5.88	6.065	0.262
Mid-Span deflection at first cracking (mm)	1.99	1.93	1.960	0.042
Crack thickness at first cracking (mm)	0.03	0.02	0.025	0.007
Failure load (KN)	84.60	80.92	82.760	2.602
Failure moment (KN.m)	19.04	18.207	18.624	0.589
Total deflection at failure (mm)	20.95	15.29	18.120	4.002
Widest crack at failure (mm)	7.08	5.60	6.34	1.047
Ductility Ratio	10.53	7.92	9.23	1.846

5.4 TEST RESULTS OF SECOND GROUP

5.4.1. Beam with U Jacketing have an Expansion Bolts with 5.5 mm Mesh

Specimens GB.B1 and GB.B2 were the specimens that strengthened using SCC U-jacketing with 5.5 mm mesh and (1200×200×160 mm) in dimension. To prevent inter laminar shear between the concrete substrate and SCC jacket Hilti structural expansion anchors have been used. The mode of failure observed was flexural failure. The crushing of concrete compression zone for GB.B1 was observed at 15.70 mm of 99.151 KN and for GB.B2 it was observed at 16.99 mm of 107.978 KN.

Figures 5.20 and 5.21 show the sample after testing and the crack pattern for the both specimens respectively.
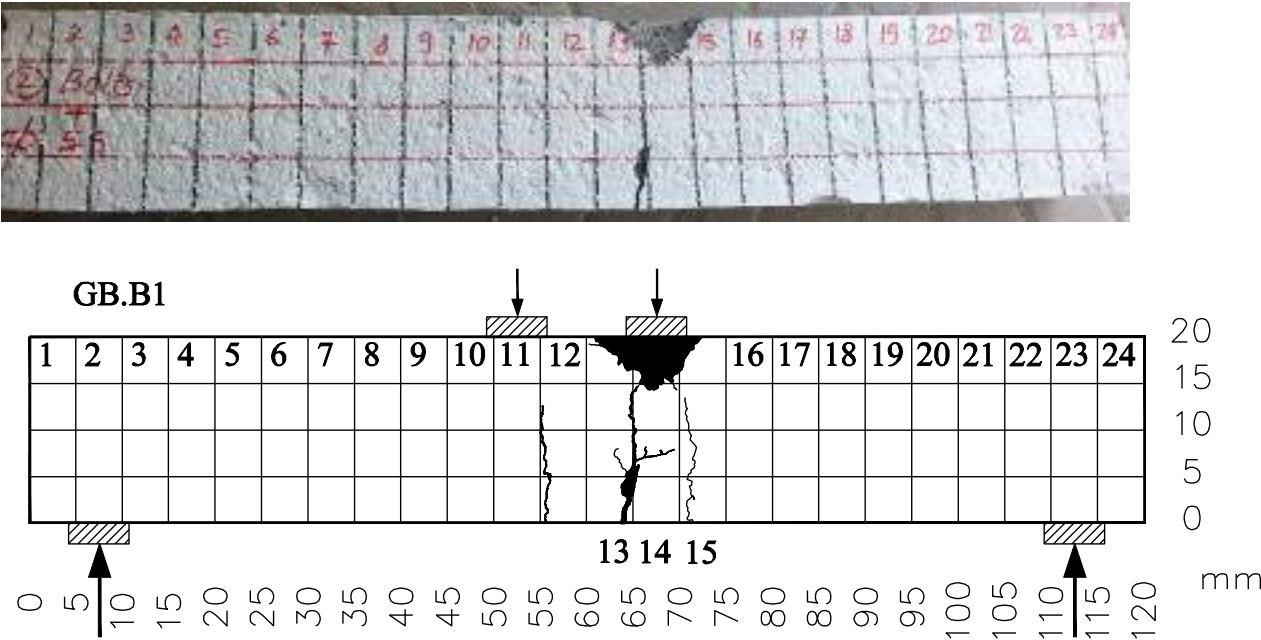
Figure 5.20 Failure mode and crack pattern of GB.B1.
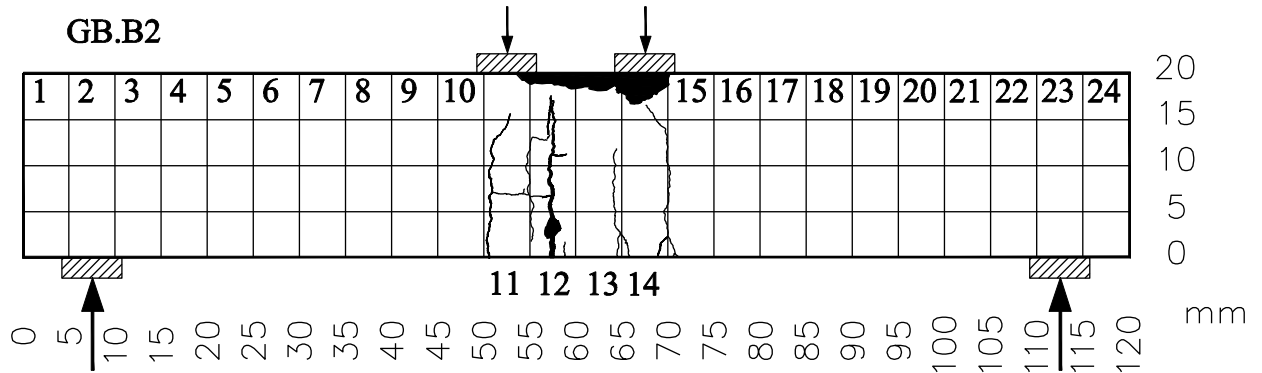
Figure 5.21 Failure mode and crack pattern of GB.B2.

Figure 5.22 shows the load-deflection curves of the two beam specimens. Average mid-span deflection for the two samples at the failure deflection equal 16.345 mm. Table 5.7 summarized the test results of the two specimens.
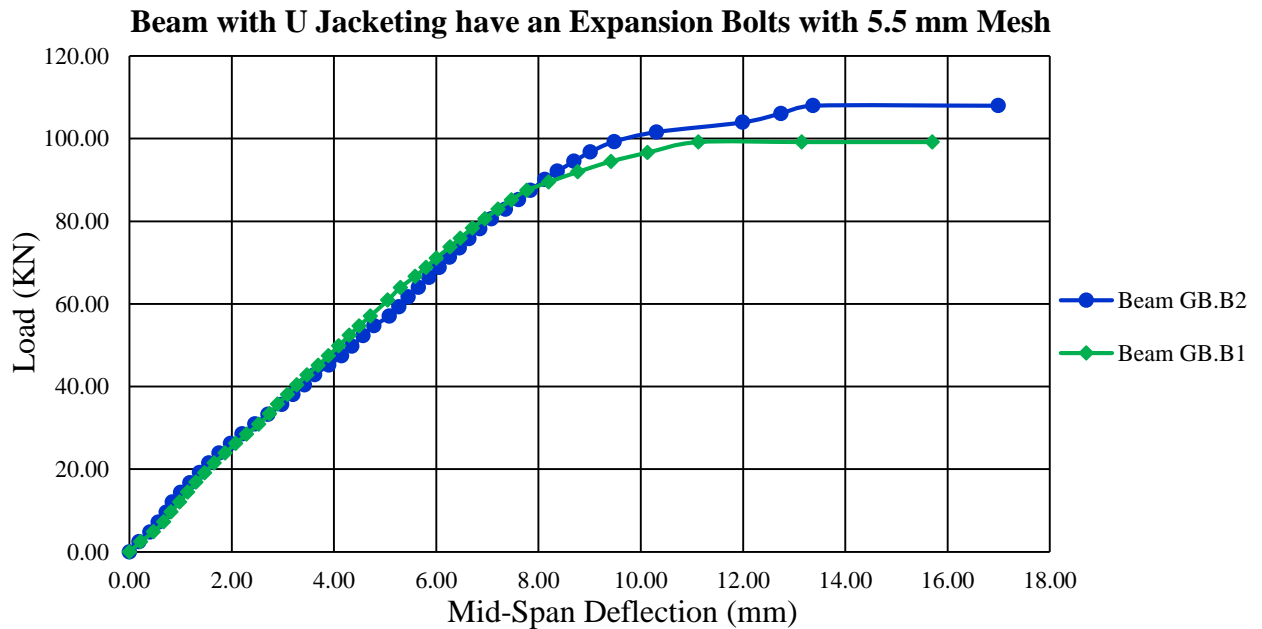
Figure 5.22 Load Deflection curves of GB.B1 and GB.B2.

For GB.B1, mid span deflection corresponding to P_{max} was 15.70 mm. The serviceability deflection limit (L/360) of 2.92 mm was reached at load of 35.734 KN or 36.04 % of P_{max}. The serviceability deflection limit (L/180) of 5.833 mm was reached at load of 68.82 KN or 69.41 % of P_{max}. The deflection at the working load which predicted at 70% of P_{max} was 5.85 mm.
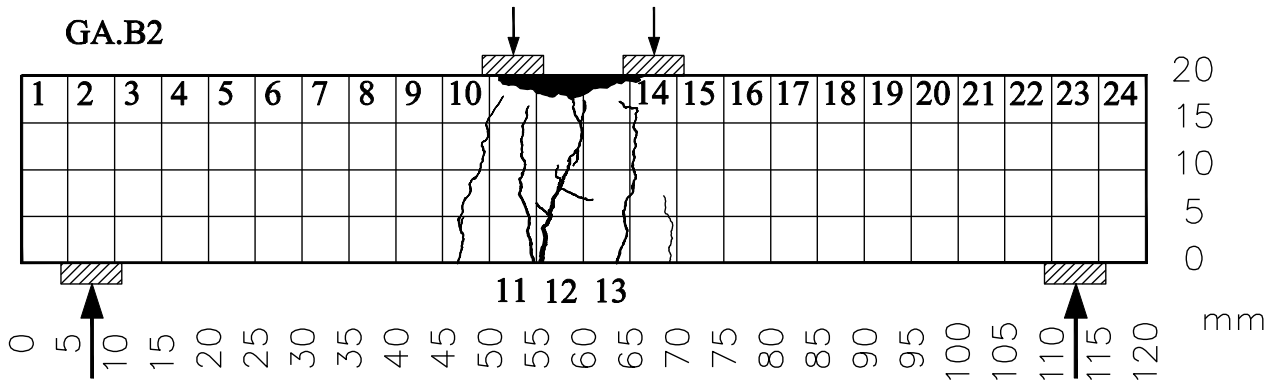
For GB.B2, mid span deflection corresponding to P_{max} was 16.99 mm. The serviceability deflection limit (L/360) of 2.92 mm was reached at load of 34.50 KN or 31.95 % of P_{max}. The serviceability deflection limit (L/180) of 5.833 mm was reached at load of 66.00 KN or 61.12 % of P_{max}. The deflection at the working load which predicted at 70% of P_{max} was 6.60 mm.

Table 5.7 Test results of strengthened beams GB.B1 and GB.B2.

Description	GB.B1	GB.B2	Average	Standard Deviation
First cracking noticed at (KN)	26.188	35.650	30.919	6.691
First cracking moment at (KN.m)	5.892	8.021	6.957	1.505
Mid-Span deflection at first cracking (mm)	2.075	2.980	2.528	0.640
Crack thickness at first cracking (mm)	0.015	0.02	0.018	0.004
Failure load (KN)	99.151	107.978	103.565	6.242
Failure moment (KN.m)	22.310	24.295	23.303	1.404
Total deflection at failure (mm)	15.700	16.990	16.345	0.912
Widest crack at failure (mm)	4.33	4.05	4.190	0.198
Ductility Ration	7.57	5.70	6.64	1.322

5.4.2. Beam with U Jacketing have Dowels with 5.5 mm Mesh

Specimens GB.B3 and GB.B4 were the specimens that strengthened using SCC U-jacketing with 5.5 mm mesh and (1200×200×160 mm) in dimension. To prevent inter laminar shear between the concrete substrate and SCC jacket deformed Ø8 mm steel reinforcement dowels have been used. The mode of failure observed was flexural failure.

The crushing of concrete compression zone for GB.B3 was observed at 14.42 mm of 95.965 KN and for GB.B4 it was observed at 13.08 mm of 107.329 KN.

Figures 5.23 and 5.24 show the sample after testing and the crack pattern for the both specimens respectively.
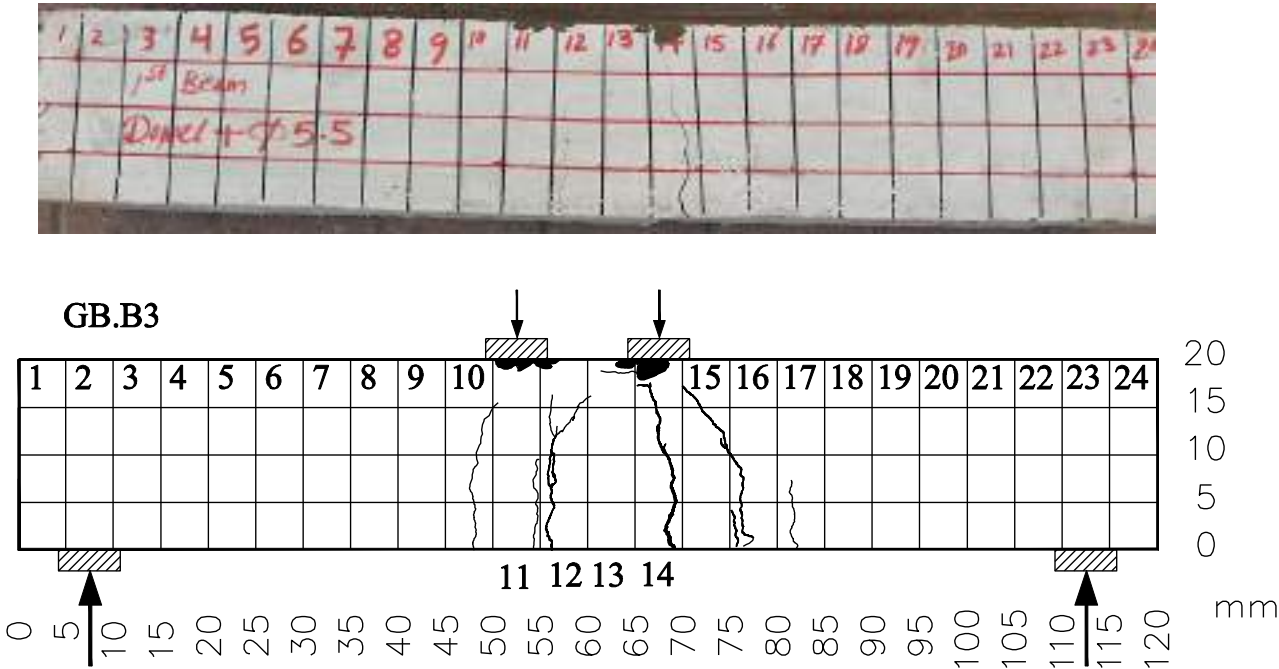
Figure 5.23 Failure mode and crack pattern of GB.B3.
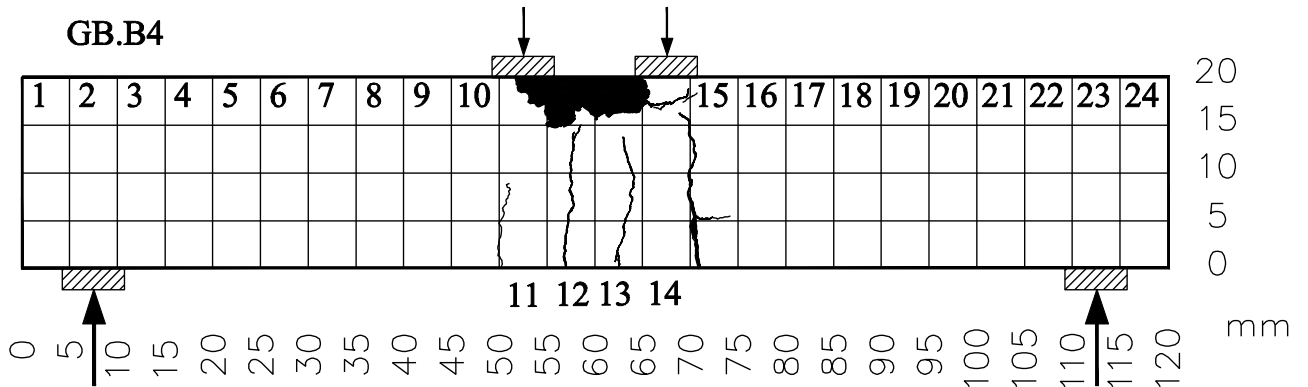
Figure 5.24 Failure mode and crack pattern of GB.B4.

Figure 5.25 shows the load-deflection curves of the two beam specimens. Average mid-span deflection for the two samples at the failure deflection equal 13.75 mm. Table 5.8 summarized the test results of the two specimens.
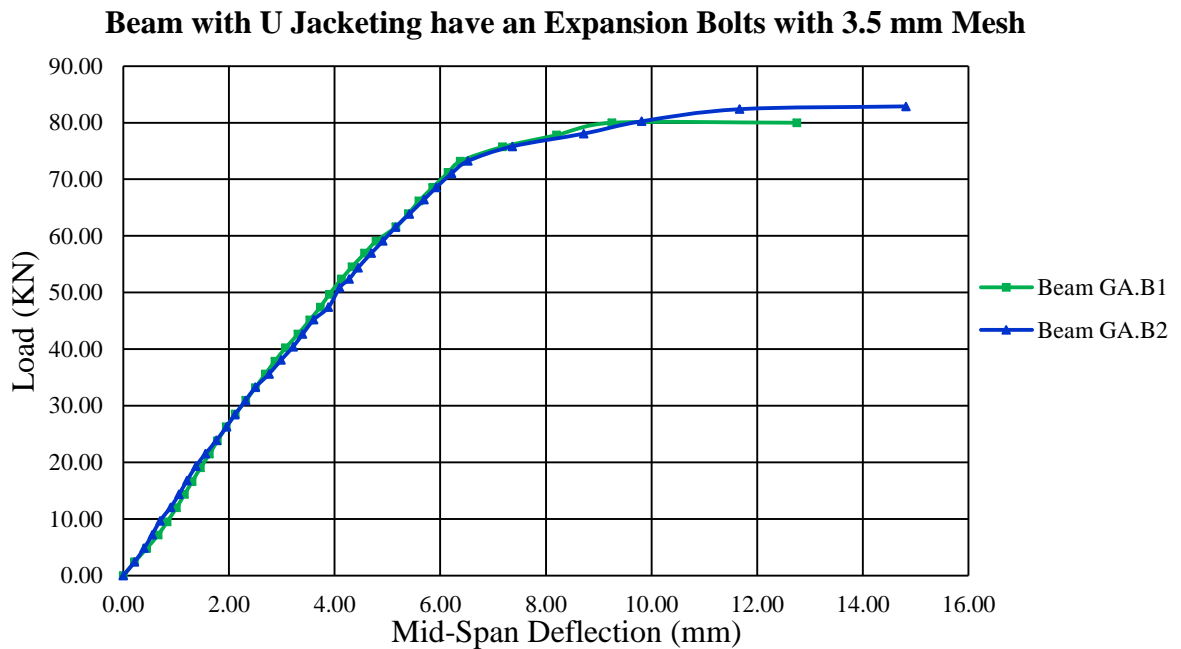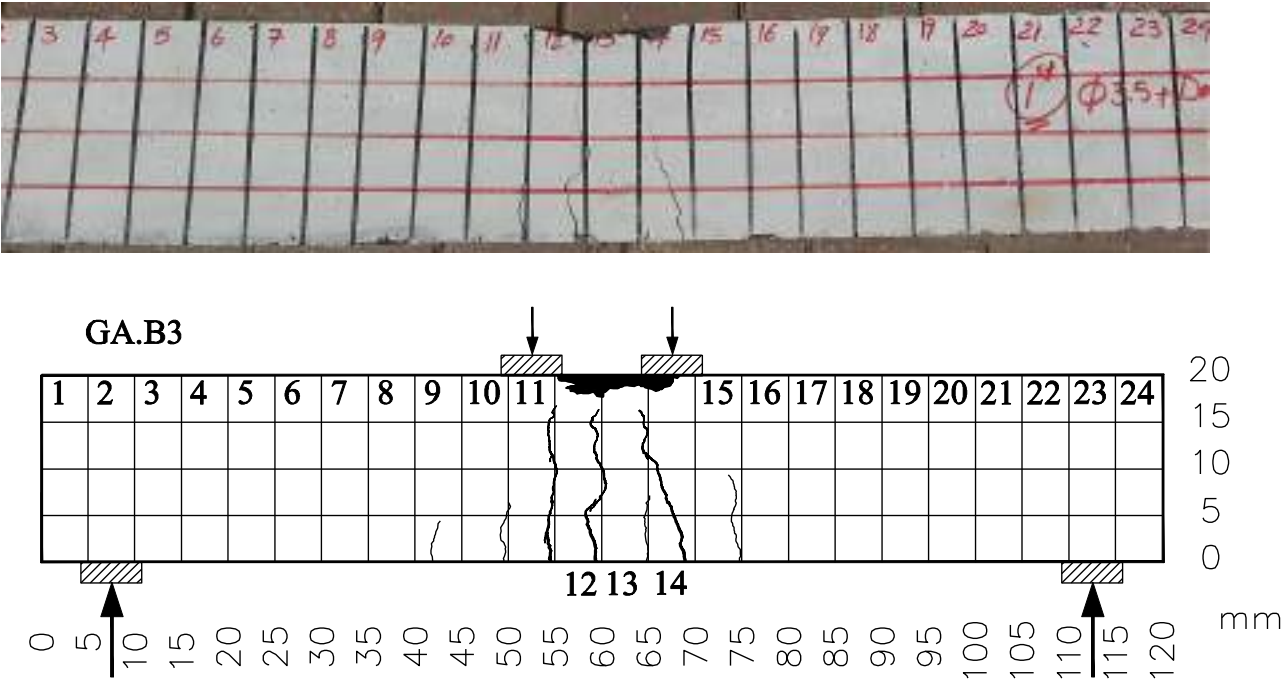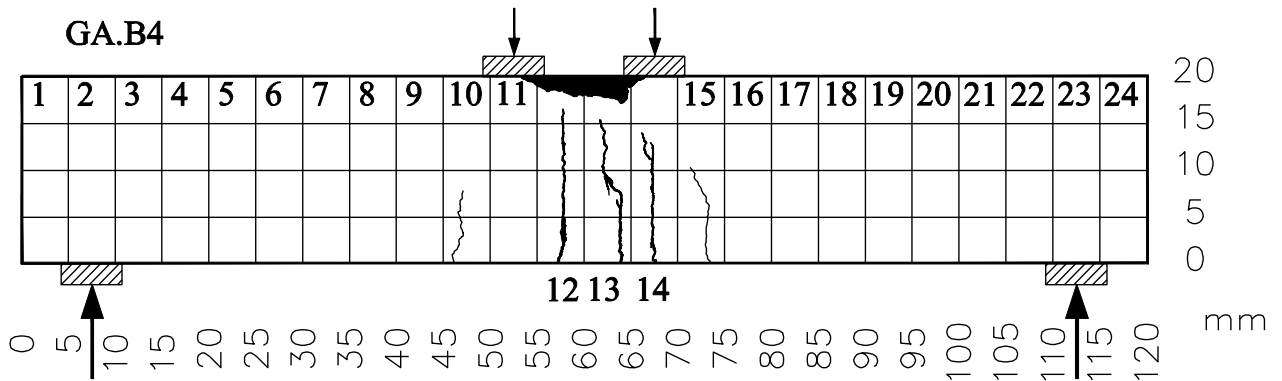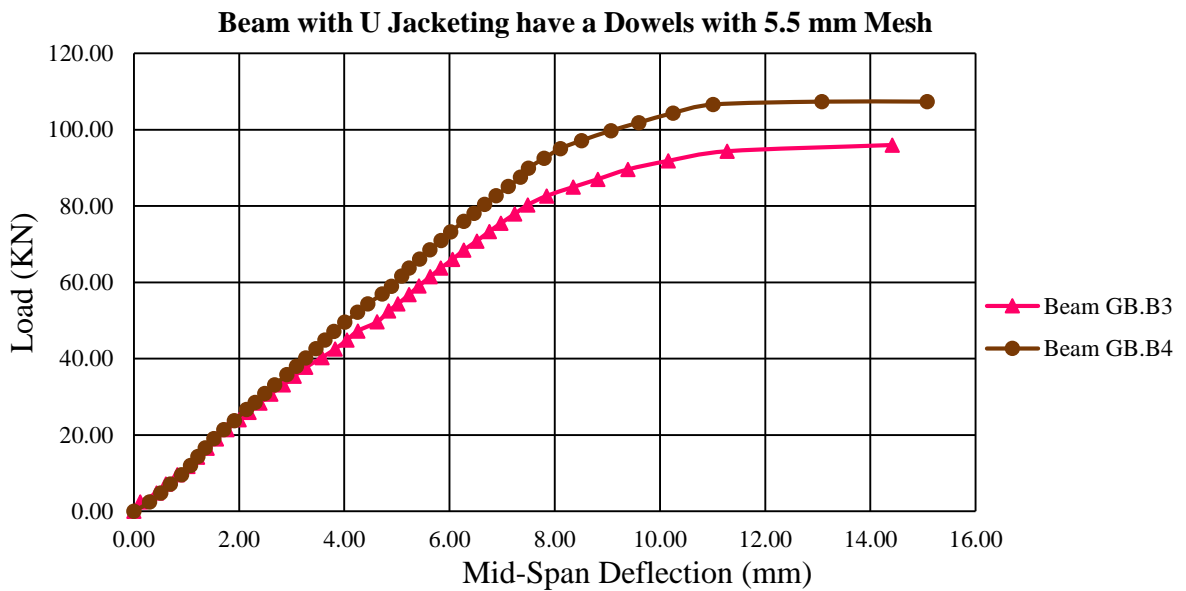

Figure 5.25 Load Deflection curves of GB.B3 and GB.B4.

For GB.B3, mid span deflection corresponding to P_{max} was 14.42 mm. The serviceability deflection limit (L/360) of 2.92 mm was reached at load of 34.00 KN or 35.43 % of P_{max}. The serviceability deflection limit (L/180) of 5.833 mm was reached at load of 63.737 KN or 66.42 % of P_{max}. The deflection at the working load which predicted at 70% of P_{max} was 6.15 mm.

For GB.B4, mid span deflection corresponding to P_{max} was 15.08 mm. The serviceability deflection limit (L/360) of 2.92 mm was reached at load of 35.856 KN or 33.41 % of P_{max}. The serviceability deflection limit (L/180) of 5.833 mm was reached at load of 70.947 KN or 66.10 % of P_{max}. The deflection at the working load which predicted at 70% of P_{max} was 6.18 mm.

Table 5.8 Test results of strengthened beams GB.B3 and GB.B4.

Description	GB.B3	GB.B4	Average	Standard Deviation
First cracking noticed at (KN)	33.840	33.135	33.488	0.499
First cracking moment at (KN.m)	7.614	7.455	7.535	0.112
Mid-Span deflection at first cracking (mm)	2.900	2.68	2.790	0.156
Crack thickness at first cracking (mm)	0.027	0.022	0.025	0.004
Failure load (KN)	95.965	107.329	101.647	8.036
Failure moment (KN.m)	21.592	24.149	22.871	1.808
Total deflection at failure (mm)	14.420	13.080	13.750	0.948
Widest crack at failure (mm)	2.73	2.31	2.520	0.297
Ductility Ratio	4.97	4.88	4.93	0.064

5.4.3. Beam with U jacketing have a Roughened Surface with 5.5 mm Mesh

Specimen GB.B5 was the beam that strengthened using SCC U-jacketing with 5.5 mm mesh and (1200×200×160 mm) in dimension. To prevent inter laminar shear between the concrete substrate and SCC jacket surface roughening has been used. The mode of failure observed was flexural failure.

The crushing of concrete compression zone for GB.B5 was observed at 13.91 mm of 103.268 KN.

Figure 5.26 shows the sample after testing and the crack pattern.
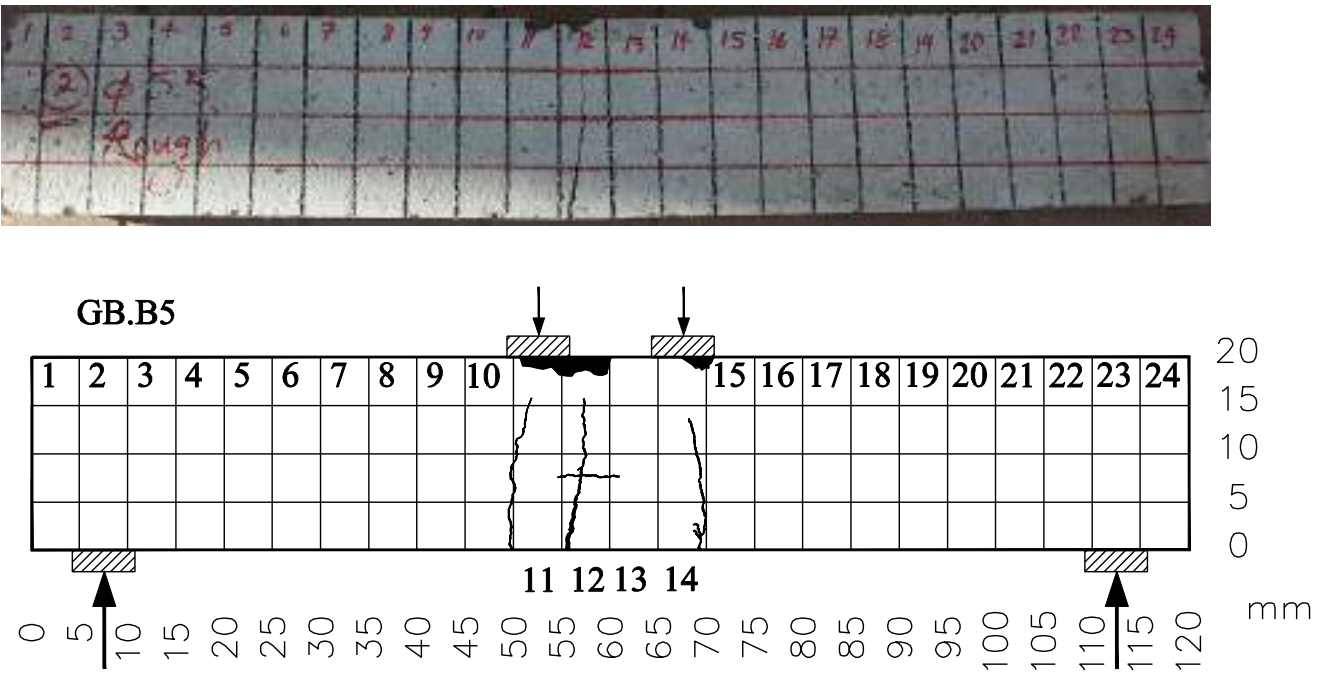
Figure 5.26 Failure mode and crack pattern of GB.B5.

Figure 5.27 shows the load-deflection curves of the beam. Also Table 5.9 summarized the test results.
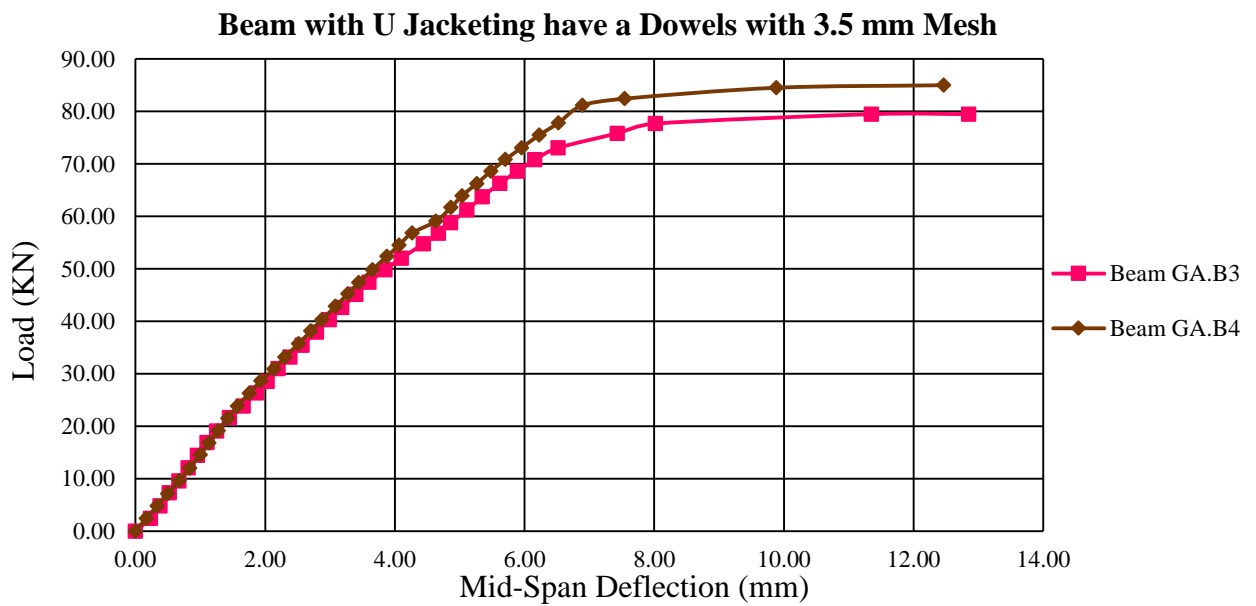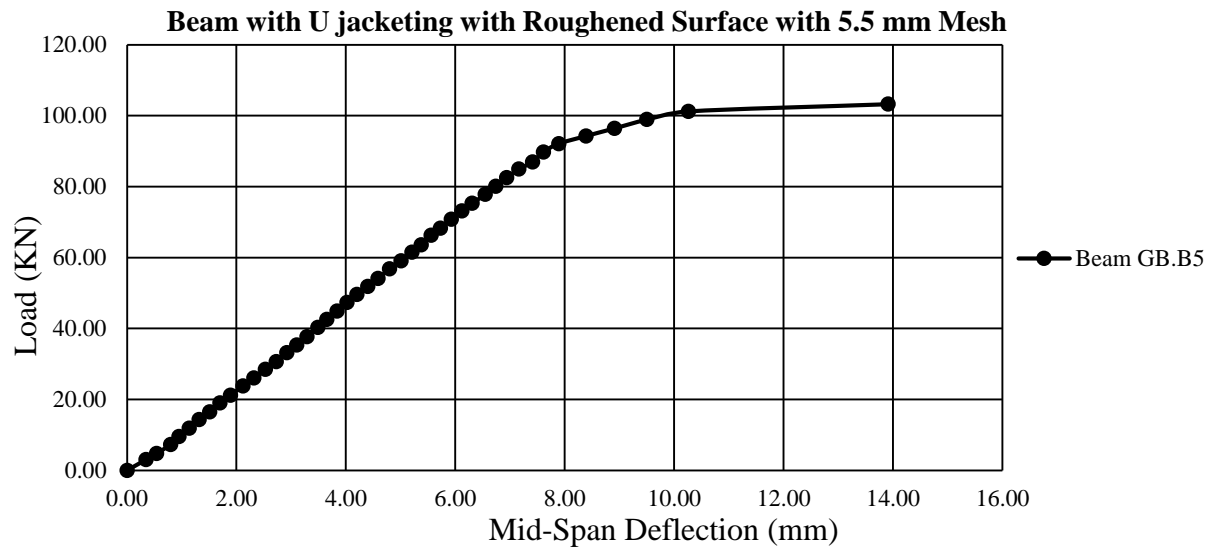
Figure 5.27 Load deflection curves of GB.B5.

For GB.B5, mid span deflection corresponding to P_{max} was 13.91 mm. The serviceability deflection limit (L/360) of 2.92 mm was reached at load of 33.168 KN or 32.12 % of P_{max}. The serviceability deflection limit (L/180) of 5.833 mm was reached at load of 67.30 KN or 65.17 % of P_{max}. The deflection at the working load which predicted at 70% of P_{max} was 6.05 mm.

Table 5.9 Test results of strengthened beam GB.B5.

Description	GB.B5
First cracking noticed at (KN)	40.345
First cracking moment at (KN.m)	9.078
Mid-Span deflection at first cracking (mm)	3.49
Crack thickness at first cracking (mm)	0.018
Failure load (KN)	103.268
Failure moment (KN.m)	23.235
Total deflection at failure (mm)	13.910
Widest crack at failure (mm)	4.92
Ductility Ratio	3.98

5.5 COMPARISON BETWEEN TECHNIQUES

5.5.1. Effect of Wire Mesh Diameters and Opening

Strengthened beams using Ø 3.5mm of 25 mm opening galvanized WWM show an average increments by more than 110.24 % of its failure load capacity compared with control beams during the flexural test as seen in Figure 5.28. The increasing in the flexural capacity was due to the addition of WWM reinforcement within the jacket and the increase in the beam effective depth. This indicates that the strengthening technique satisfies its aim to increase the flexural capacity of the strengthened beams.

The average deflection of the strengthened beams was 14.60 mm and for the control beams were 9.27 mm, which indicates that the ductility of the strengthened beams were increased significantly compared with control beams during the flexural test, The increasing in the ductility was due to the addition of WWM reinforcement within the jacket, which indicates that the strengthening process satisfies its aim.

Regardless of the type of method of anchorage employed between old and new concrete, all strengthened beams stiffness have increased more significantly compared to control beam specimens this can be clearly seen from the ascending parts of load deflection curves of strengthened beams.

Control Beams V.s Strengthened beams using Ø3.5 mm WWM

Legend:
- Beam C.B0
- Beam C.B1
- Beam C.B2
- Beam GA.B1
- Beam GA.B2
- Beam GA.B3
- Beam GA.B4
- Beam GA.B5
- Beam GA.B6

Figure 5.28 Load deflection curves for each of the beams.

Beam	Load (KN)	Percentage
CB0	34.310	
CB1	44.124	
CB2	38.775	
GA.B1	79.994	(104.75%)
GA.B2	82.880	(112.13%)
GA.B3	79.463	(103.39%)
GA.B4	84.976	(117.50%)
GA.B5	84.600	(116.54%)
GA.B6	80.920	(107.12%)
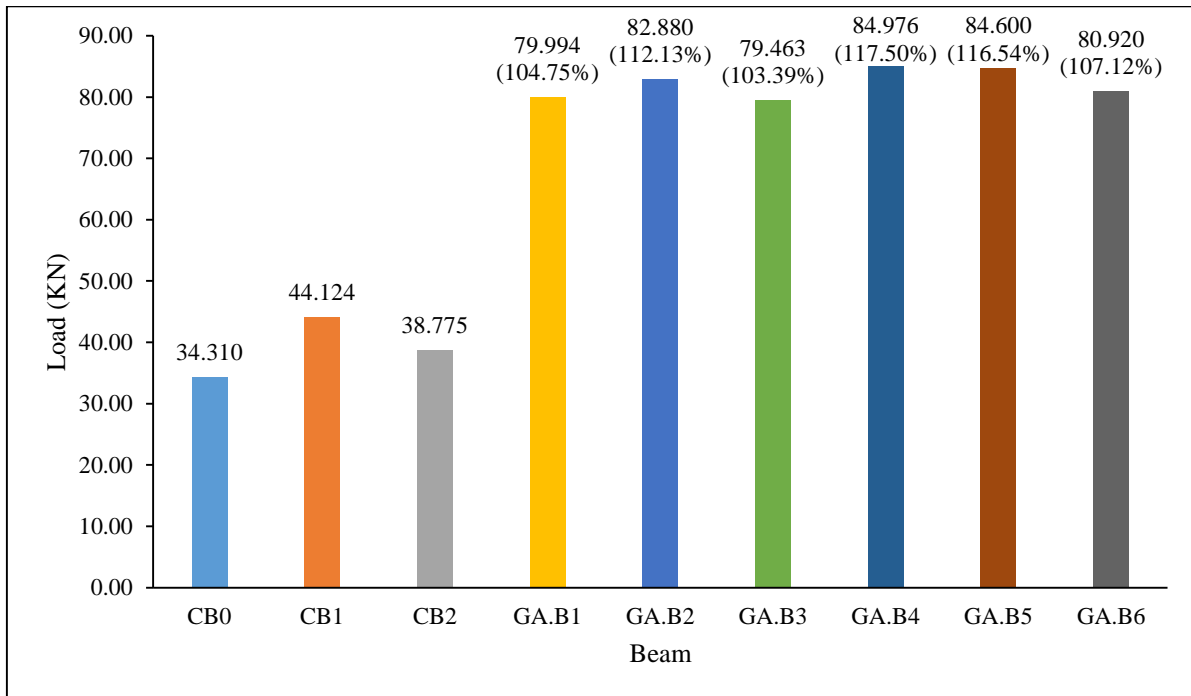
Figure 5.29 Ultimate loads for beams.

Figure 5.29 shows the ultimate failure loads for all the beam specimens. It could be observed that all the strengthening techniques used in this study are capable of restoring the ultimate capacity of control beams. The ultimate capacity of beams GA.B4 and GA.B5 respectively, show 117.50% and 116.54% higher UL capacities compared to the average UL of control beams.

All the strengthened concrete beams exhibit higher cracking load compared to the control beam, except GA.B6. The strengthened specimen GA.B1 is the highest one that show 31.12% increase in the cracking loads compared to the average cracking loads of control beams. While the strengthened specimen GA.B6 show decrease in the cracking load by -3.68% compared to the average cracking loads of control beams. Figure 5.30 shows the first cracking loads of beams.
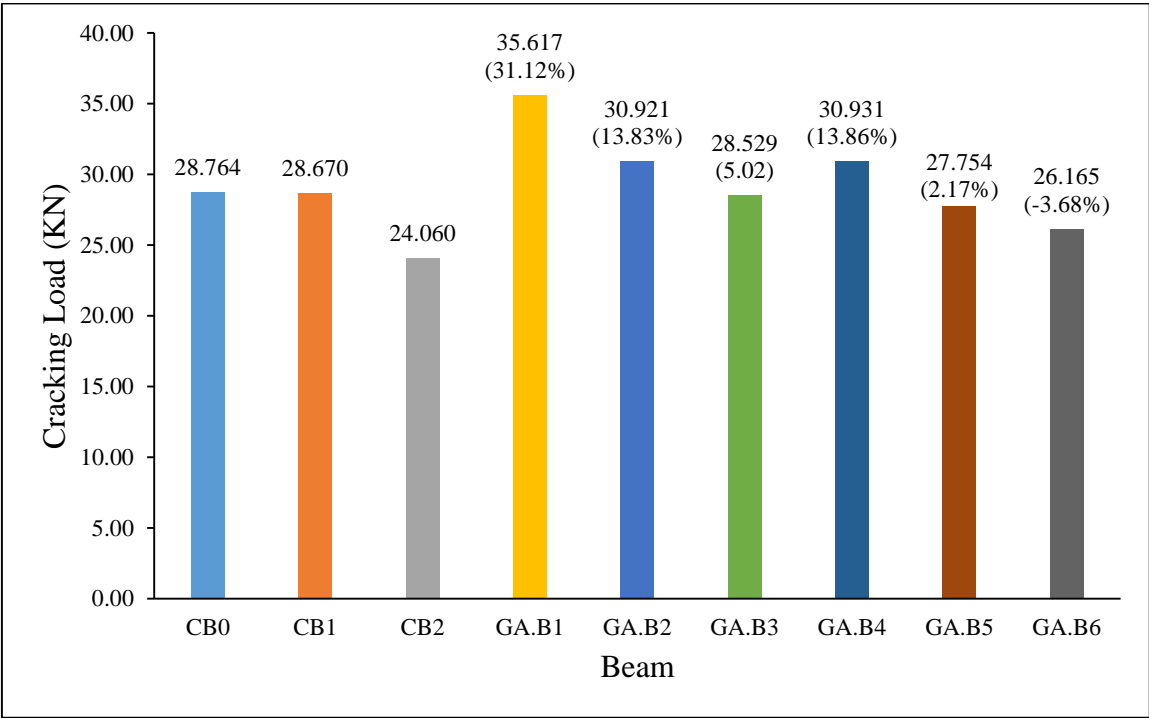
Figure 5.30 1st Cracking loads for beams.

Figure 5.31 shows the calculated ductility ratio of strengthened beams in group A compared to control beams. The ductility ratio for the test groups ranged from 2.26 to 10.53. Ductility ratio is defined here in this investigation as the ratio between the mid-

spans deflections at UL to that at the first crack load (Δu/Δi). All strengthened beams have more ductility ratio compared to control beams. Beam GA.B5 have the highest ductility ratio equal to 10.53.
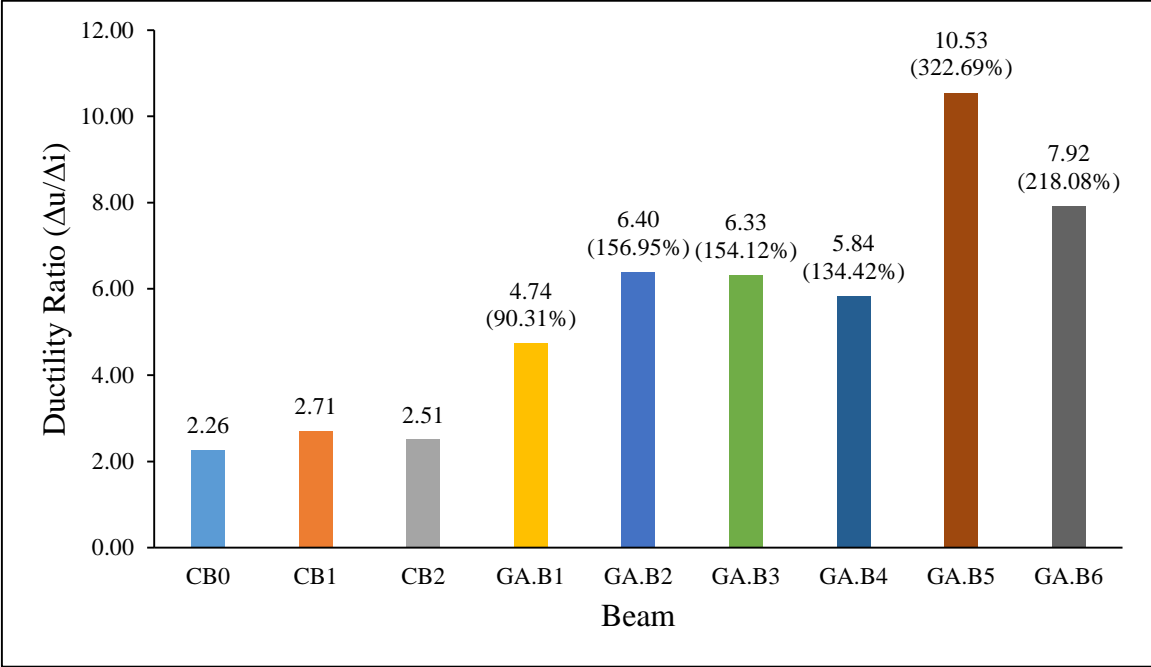
Figure 5.31 Ductility Ratio for beams.

Strengthened beams using Ø 5.5mm of 50 mm opening galvanized WWM show an average increments by more than 162.96 % of its failure load capacity compared with control beams during the flexural test as seen in Figure 5.32. The increasing in the flexural capacity was due to the addition of WWM reinforcement within the jacket and the increase in the beam effective depth. This indicates that the strengthening technique satisfies its aim to increase the flexural capacity of the strengthened beams.

The average deflection of the strengthened beams was 14.37 mm and for the control beams were 9.27 mm, which indicates that the ductility of the strengthened beams were increased significantly compared with control beams during the flexural test, The increasing in the ductility was due to the addition of WWM reinforcement within the jacket, which indicates that the strengthening process satisfies its aim.

Regardless of the type of method of anchorage employed between old and new concrete, all strengthened beams stiffness have increased more significantly compared to control beam specimens this can be clearly seen from the ascending parts of load deflection curves of strengthened beams.

Control Beams V.s Strengthened beams using Ø5.5 mm WWM

Figure 5.32 Load deflection curves for each of the beams.

Figure 5.33 shows the ultimate failure loads for all the beam specimens. It could be observed that all the strengthening techniques used in this study are capable of restoring the ultimate capacity of control beams. The ultimate capacity of beams GB.B2 and GB.B4 respectively, show 183.32% and 181.61% higher UL capacities compared to the average UL of control beams.
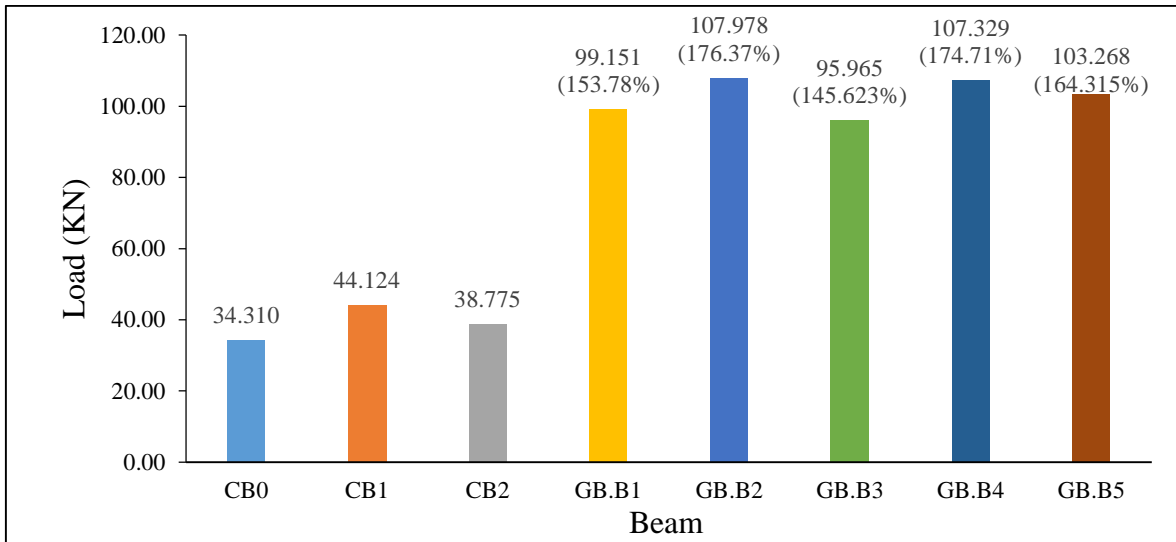
Figure 5.33 Ultimate loads for beams.

All the strengthened concrete beams exhibit higher cracking load compared to the control beam, except GB.B1. The strengthened specimen GB.B5 is the highest one that show 48.52% increase in the cracking loads compared to the average cracking loads of control beams. While the strengthened specimen GB.B1 shows decrease in the cracking load by -3.60% compared to the average cracking loads of control beams. Figure 5.34 shows the first cracking loads of beams.
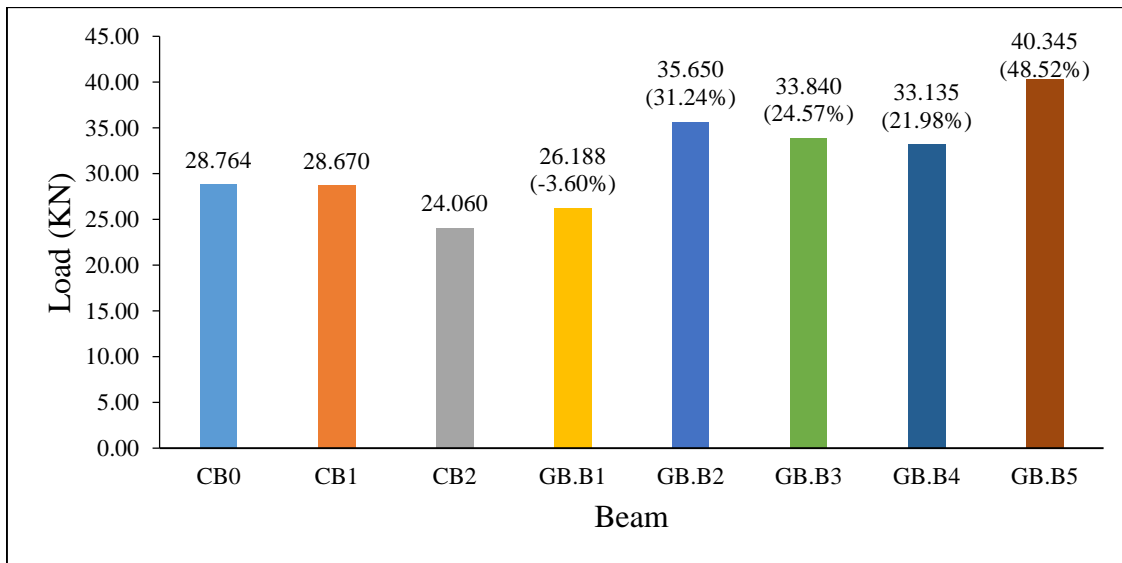
Figure 5.34 1st Cracking loads for beams.

Figure 5.35 shows the calculated ductility ratio of strengthened beams in group B compared to control beams. The ductility ratio for the test groups ranged from 2.26 to 7.57. Ductility ratio is defined here in this investigation as the ratio between the mid-spans deflections at UL to that at the first crack load ($\Delta u/\Delta i$). All strengthened beams have more ductility ratio compared to control beams. Beam GA.B5 have the highest ductility ratio equal to 7.57.
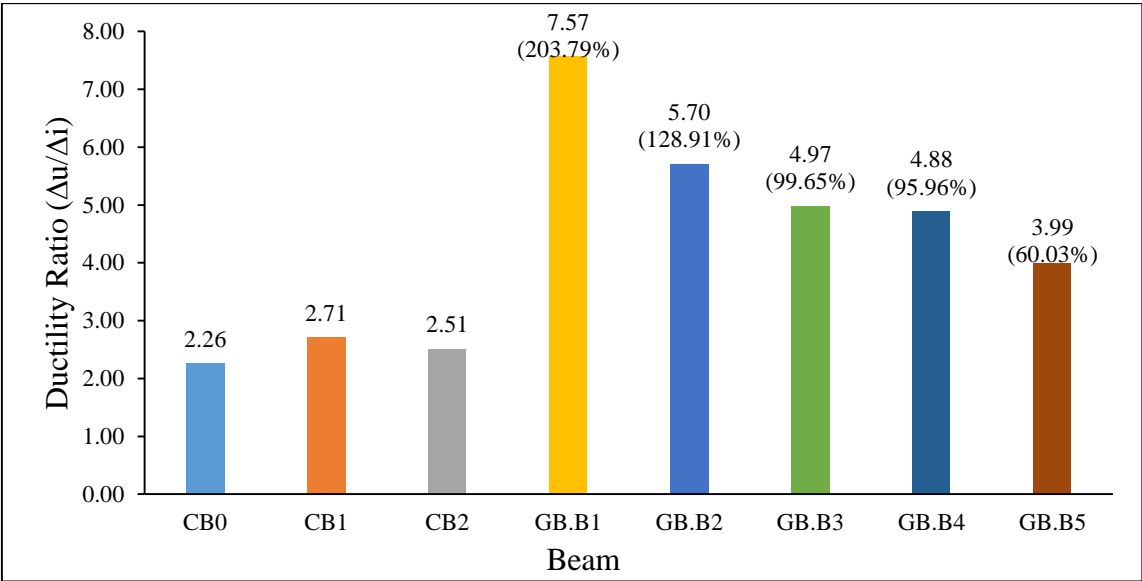
Figure 5.35 Ductility Ratio for beams.

The test results showed that all beams in the two test groups achieved their full flexural capacity and failed in a ductile manner. This is attributed to the increased confinement provided by jacketing reinforcement with WWM.

The test results showed that in the two test groups when the diameter of the galvanized steel WWM increases as in group B the failure load capacity and ductility significantly will increase compared to other group.

The test results indicate that in the two test groups the opening between bars of WWM does not play a main role in decreasing the ultimate capacity of beams.

5.5.2. Effect of Method of Bonding between New and Old Concrete

The comparison between specimens which strengthened with different type of bonding technique can be performed by evaluation of the percentage of the flexural load capacity of each specimen to the flexural load capacity of monolithic control specimen.

Table 5.10 shows the restoration percentages for each bonding technique of Group A.

Table 5.10 Comparison between bonding techniques behavior of Group A.

Specimen Name	Bonding Technique	Failure Load (KN)	Percentage of flexural load to Monolithically control specimen (%)
MA.B1	Monolithically specimen	81.883	-
MA.B2	Monolithically specimen	87.180	-
Average	Monolithically specimen	84.532	100.00
GA.B1	Expansion Bolts	79.994	94.63
GA.B2	Expansion Bolts	82.880	98.05
GA.B3	Ø 8 mm dowels	79.463	94.00
GA.B4	Ø 8 mm dowels	84.976	100.53
GA.B5	Surface Roughening	84.600	100.08
GA.B6	Surface Roughening	80.920	95.73

Figure 5.36 illustrates the comparison between bonding techniques behavior of Group A.

It is noted that the best bonding technique is by adding Ø 8 mm dowels as shear connectors at the interacted surface to connect between old and new concrete, the strengthened specimen GA.B4 restored 100.53% of flexural load compared to monolithically control specimen. While the strengthened specimen GA.B6 show the lowest restoration percentage which is 95.73%.

The restoration percentage of beams GA.B5 and GA.B6 respectively, show 100.08% and 95.73%. Ones can say that surface roughening technique either works similar to expansion bolts or dowels bonding technique.

Also, there are no significant change occurred due to roughening the substrate surface compared to two other bonding technique. Moreover, during the experimental works inter laminar shear between the concrete substrate and SCC jacket has been prevented and there is no bond failure was observed in these beams up to the UL.

It is noted that most of the specimens reach the 100% of the flexural load capacity of the monolithically specimen, which indicates that the bonding technique satisfies its aim.
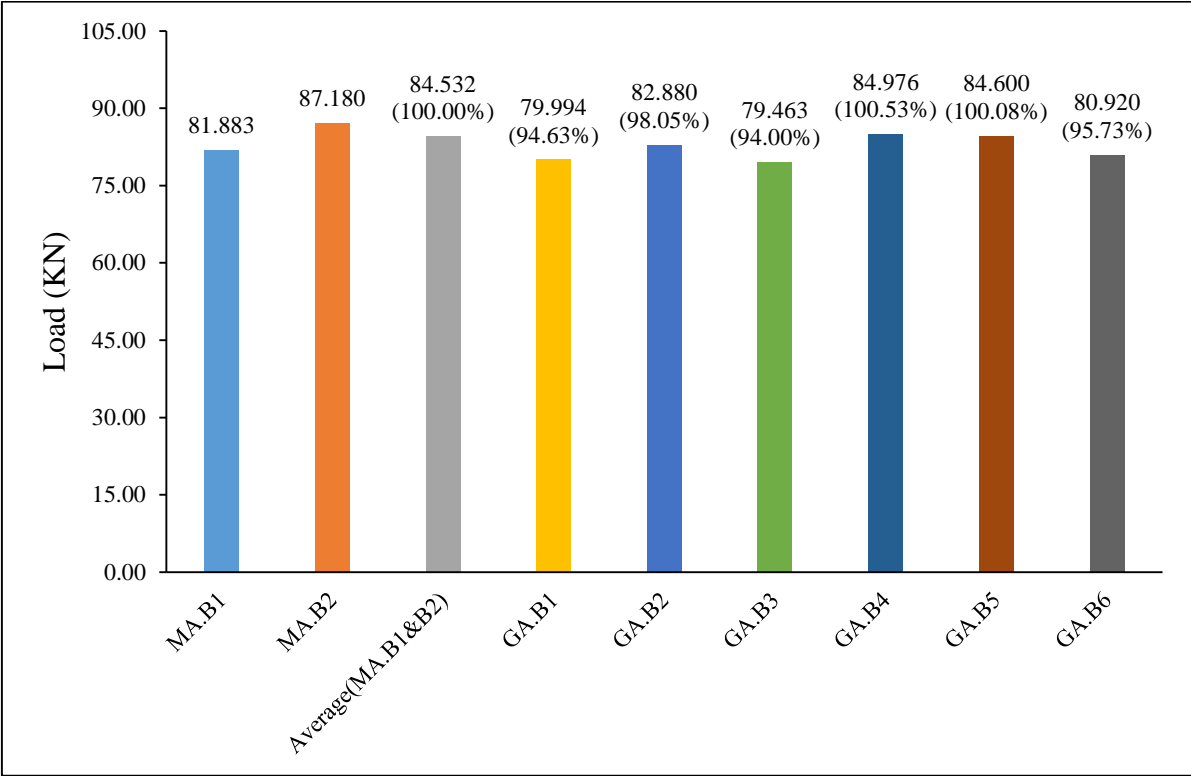
Figure 5.36 Comparison between bonding techniques behavior (Group A).

The comparison between specimens for Group B of strengthened beams using $\emptyset$ 5.5mm of 50 mm opening galvanized WWM was reported in Table 5.11.

Table 5.11 Comparison between bonding techniques behavior of Group B.

Specimen Name	Bonding Technique	Failure Load (KN)	Percentage of flexural load to Monolithically control specimen (%)
MB.B1	Monolithically specimen	110.553	-
MB.B2	Monolithically specimen	103.654	-
Average (MA.B1 & MA.B2)	Monolithically specimen	107.104	100.00
GB.B1	Expansion Bolts	99.151	92.58
GB.B2	Expansion Bolts	107.978	100.82
GB.B3	Ø 8 mm dowels	95.965	89.60
GB.B4	Ø 8 mm dowels	107.329	100.21
GB.B5	Surface Roughening	103.268	96.42

Figure 5.37 illustrates the comparison between bonding techniques behavior of Group B.
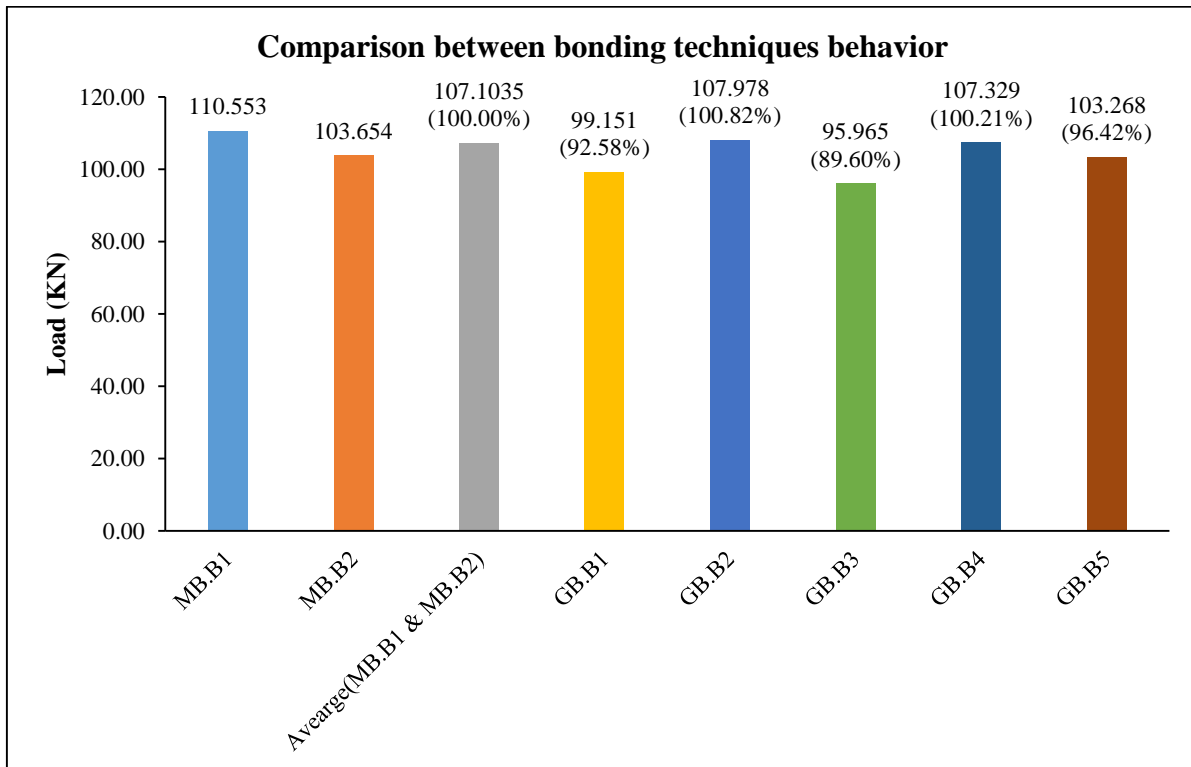
Figure 5.37 Comparison between bonding techniques behavior (Group B).
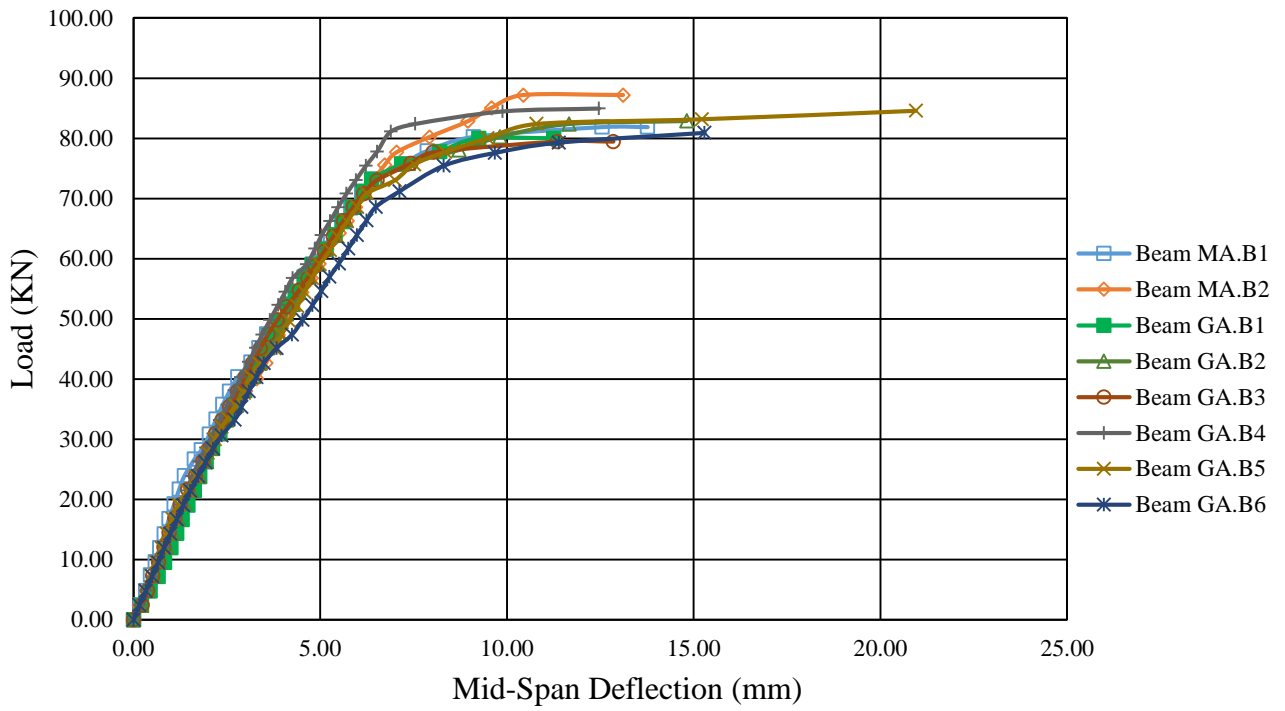
Figure 5.38 Load deflection curve of strengthened beams V.s monolithic beams (Group A).
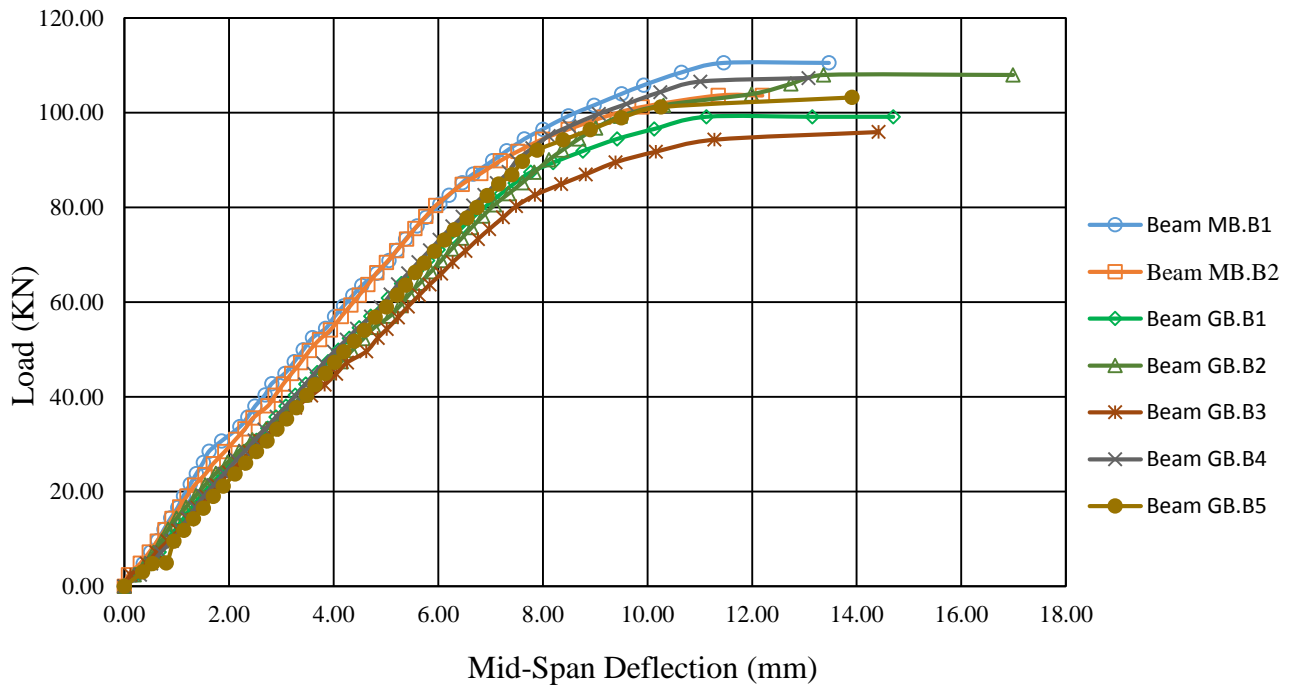
Figure 5.39 Load deflection curve of strengthened beams V.s monolithic beams (Group B).

Figures 5.38 and 5.39 show the load deflection curves of strengthened beams against the monolithic control beams for the both groups.

It is noted that the best bonding technique is by adding Hilti expansion bolts as shear connectors at the interacted surface to connect between old and new concrete, the strengthened specimen GB.B2 restored 100.82% of flexural load compared to monolithically control specimen. While the strengthened beam GB.B3 show the lowest restoration percentage which is 89.60%.

The restoration percentage of beams GB.B5, shows 96.42%. Ones can say that surface roughening technique either works similar to expansion bolts or dowels bonding technique. Also, there are no significant change occurred due to roughening the substrate surface compared to two other bonding technique. Moreover, during the experimental works inter laminar shear between the concrete substrate and SCC jacket has been prevented and there is no bond failure was observed in these beams up to the UL.

It is noted that most of the specimens reach the 100% of the flexural load capacity of the monolithically specimen, which indicates that the bonding technique satisfies its aim.

The experimental results clearly proved that jacketing can upgrade the structural properties for the RC beams, which make the strengthened beams perform as monolithic construction beams.

The test results indicated that the bonding technique by adding Ø 8 mm dowels as shear connectors can works as same as bonding technique by adding Hilti expansion bolts at the interacted surface to connect between old and new concrete. Moreover the bonding using expansion bolts are easier, faster and cheaper when compared with other technique. In other hand the surface roughening bonding technique restored a significant percent of flexural capacity in the both group.

Regardless of the type of method of bonding employed between old and new concrete and the properties of WWM, all strengthened beams restored a significant percentage of the monolithic control beam flexural load capacity.

5.5.3. Stiffness and Deflection at Service Load

The value of stiffness considered to be the slope of the line between the origin point and the coordination of the value of 70% of the UL (which have been assumed). Tables 5.12 and 5.13 show the deflection, stiffness and increasing of stiffness over the control beam at SL of the first and the second groups respectively.

Table 5.12 Deflection and stiffness at SL of the first group

Sample	Load @ SL (KN)	Deflection @ SL (mm)	Stiffness @ SL (KN/mm)	Stiffness increasing over control Beam (%)	Restoration over monolithic control beam (%)
CB0	24.020	3.500	6.86	-	-
CB1	30.644	4.070	7.59	-	-
CB2	27.150	3.700	7.34	-	-
MA.B1	57.283	4.650	12.32	-	-
MA.B2	61.026	5.050	12.08	-	-
GA.B1	55.996	4.450	12.58	65.82	102.15
GA.B2	58.016	4.800	12.09	59.27	98.11
GA.B3	55.624	4.550	12.23	61.10	99.24
GA.B4	59.483	4.680	12.71	67.49	103.17
GA.B5	59.220	5.000	11.84	56.07	96.14
GA.B6	56.644	5.200	10.89	43.54	88.43

Table 5.13 Deflection and stiffness at SL of the second group

Sample	Load @ SL (KN)	Deflection @ SL (mm)	Stiffness @ SL (KN/mm)	Stiffness increasing over control Beam (%)	Restoration over monolithic control beam (%)
CB0	24.020	3.500	6.860	-	-
CB1	30.644	4.070	7.59	-	-
CB2	27.150	3.700	7.338	-	-
MB.B1	77.387	5.700	13.577	-	-
MB.B2	72.558	5.300	13.690	-	-
GB.B1	69.410	5.850	11.865	56.35	86.67
GB.B2	75.585	6.600	11.452	50.91	83.65
GB.B3	67.176	6.150	10.923	43.94	79.79
GB.B4	75.131	6.18	12.157	60.20	88.80
GB.B5	72.288	6.05	11.948	57.45	87.28

Figures 5.40 and 5.41 show the comparison between the samples on the base of stiffness compared with control beams at the SL for the first and the second groups respectively.
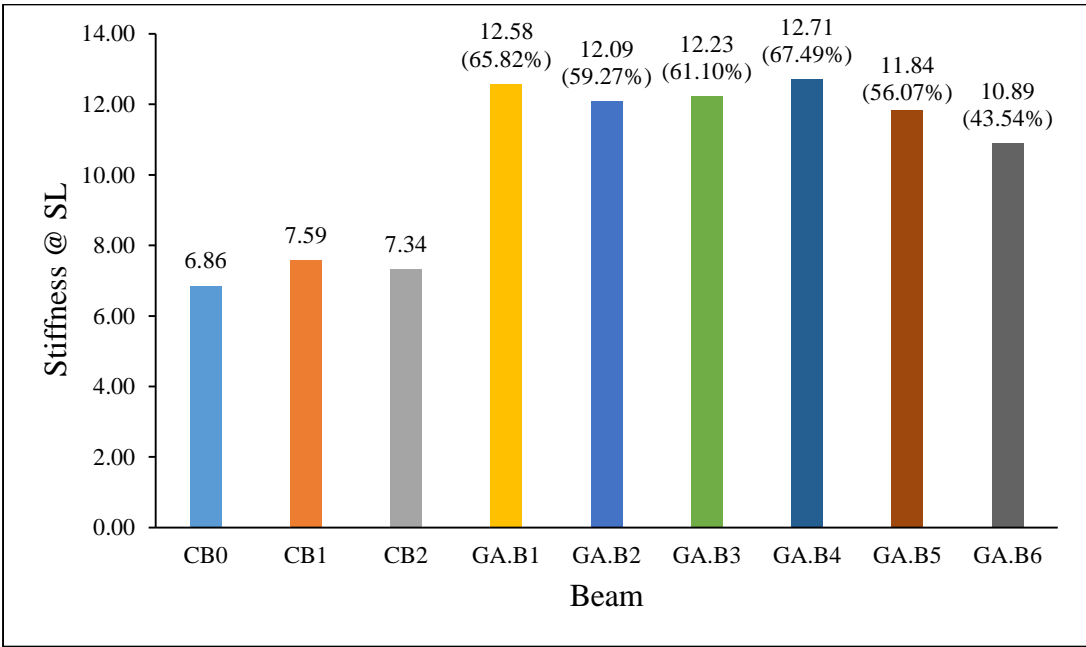
Figure 5.40 Comparative stiffness for the first group at the SL.
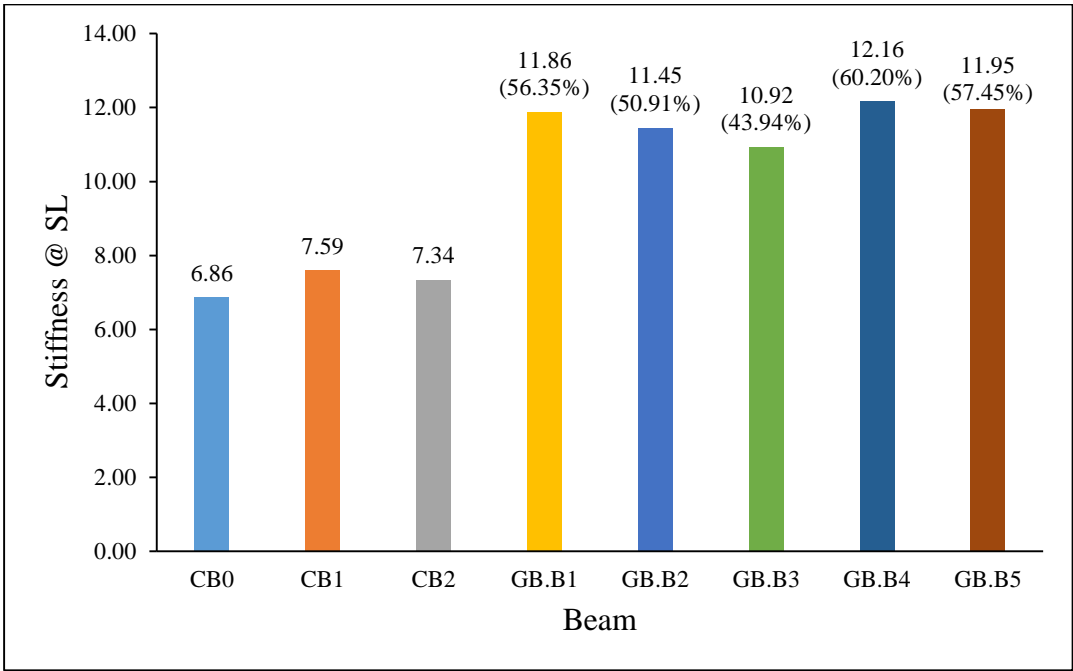
Figure 5.41 Comparative stiffness for the second group at the SL.

Figures 5.42 and 5.43 show the comparison between the samples on the base of stiffness and restoration percentage compared with monolithic control beams at the SL for the first and the second groups respectively.
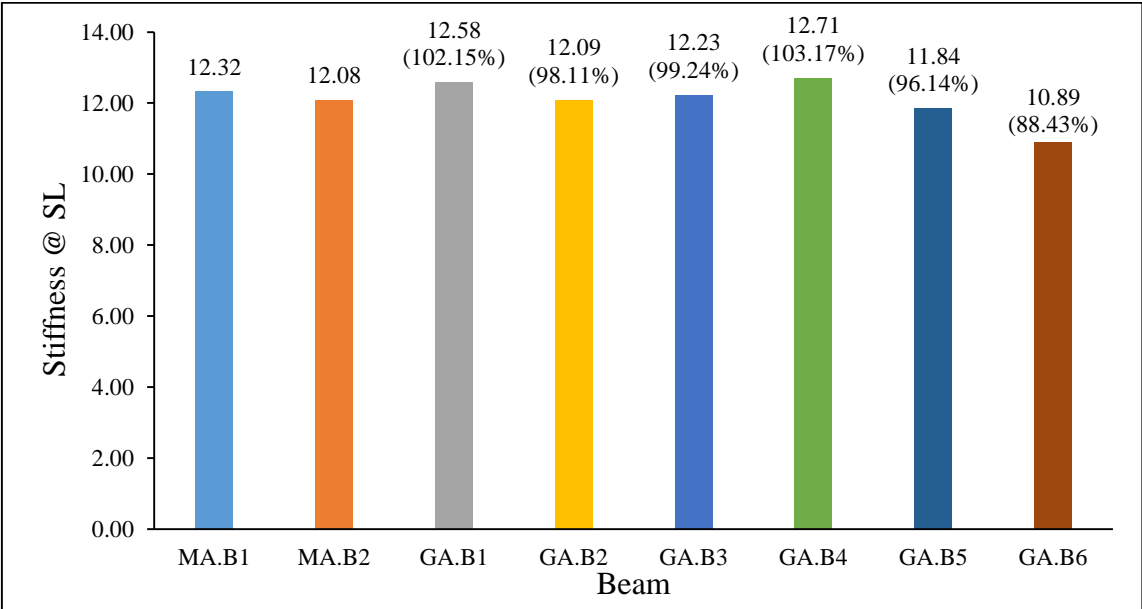
Figure 5.42 Stiffness and restoration percentage for the first group at the SL.
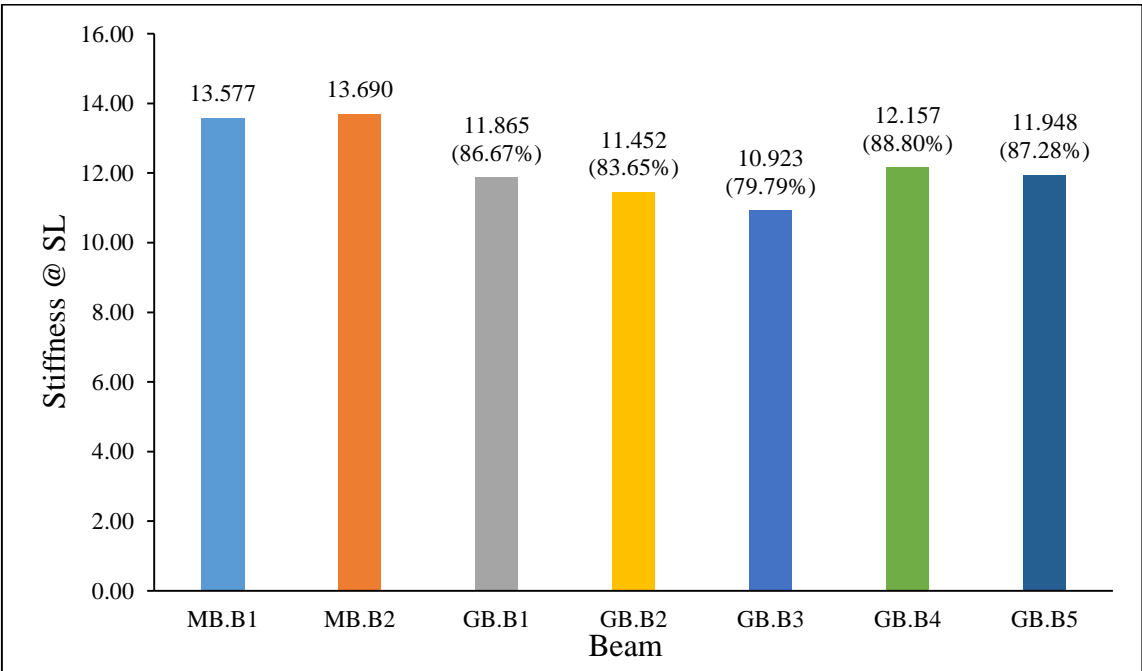
Figure 5.43 Stiffness and restoration percentage for the second group at the S

In general and as shown in the figures and the tables, the following pointes can be summarized:

i. Larger values of stiffness means larger stiffness.

ii. The strengthened beams in group A of Ø3.5 mm of 25 mm opening have higher stiffness than strengthened beams in group B of Ø5.5 mm of 50 mm opening galvanized WWM when compared with the control beams.

iii. In group A the strengthened beams in which roughening surface bonding technique is used have the lowest specimens stiffness's compared with other two bonding technique.

iv. In group A & B the strengthened beams in which the shear connector is used either Ø8 mm dowels or expansion bolts are stiffer than the strengthened beams with roughening surface technique.

v. All the strengthened test beams were stiffer than the control beam and all were able to resist loads which exceeded the flexural capacity of the control beam.

vi. The strengthened beams of group A restored 97.87 % in average, while group B strengthened beams restored 85.24 % in average compared with monolithic control beams at SL stage.

5.5.4. Stiffness and Failure Mode at Ultimate Load

Ductility is defined as the ability of structure to withstand deformation up to failure, this give alerting and enough signs of failure before the critical state is reached. Tables 5.14 and 5.15 show the values of deflection and stiffness at UL and the manner by which the samples failed for the first and the second groups respectively.

The stiffness calculated as the slope of the line between the 70% of load and the UL. Larger values of stiffness means less ductility and vice versa. Figures 5.44 and 5.45 show the comparison between the samples on the base of stiffness at the UL for the first and the second groups respectively.

In both group A & B the strengthened beams GA.B4 & GB.B4 have the highest stiffness
values at UL which mean they are the less ductile behavior.

Table 5.14 Deflection and stiffness at UL of the first group.

Sample	Load @ UL (KN)	Deflection @ UL (mm)	Stiffness @ UL (KN/mm)	Stiffness increasing over control Beam (%)	Failure Mode
CB0	10.290	5.550	1.85	-	Flexural Failure
CB1	13.237	6.030	2.20	-	Flexural Failure
CB2	11.625	4.950	2.35	-	Flexural Failure
GA.B1	23.998	8.300	2.89	23.11	Flexural Failure
GA.B2	24.864	10.015	2.48	5.71	Flexural Failure
GA.B3	23.839	8.300	2.87	22.30	Flexural Failure
GA.B4	25.493	7.785	3.27	39.44	Flexural Failure
GA.B5	25.380	15.950	1.59	-32.24	Flexural Failure
GA.B6	24.276	10.090	2.41	2.45	Flexural Failure

Table 5.15 Deflection and stiffness at UL of the second group.

Sample	Load @ UL (KN)	Deflection @ UL (mm)	Stiffness @ UL (KN/mm)	Stiffness increasing over control Beam (%)	Failure Mode
CB0	10.290	5.550	1.85	-	Flexural Failure
CB1	13.238	6.030	2.20	-	Flexural Failure
CB2	11.625	4.950	2.35	-	Flexural Failure
GB.B1	29.741	9.85	3.02	28.57	Flexural Failure
GB.B2	32.393	10.390	3.12	32.76	Flexural Failure
GB.B3	28.79	8.27	3.48	48.23	Flexural Failure
GB.B4	32.198	6.90	4.67	98.70	Flexural Failure
GB.B5	30.98	7.86	3.94	67.83	Flexural Failure
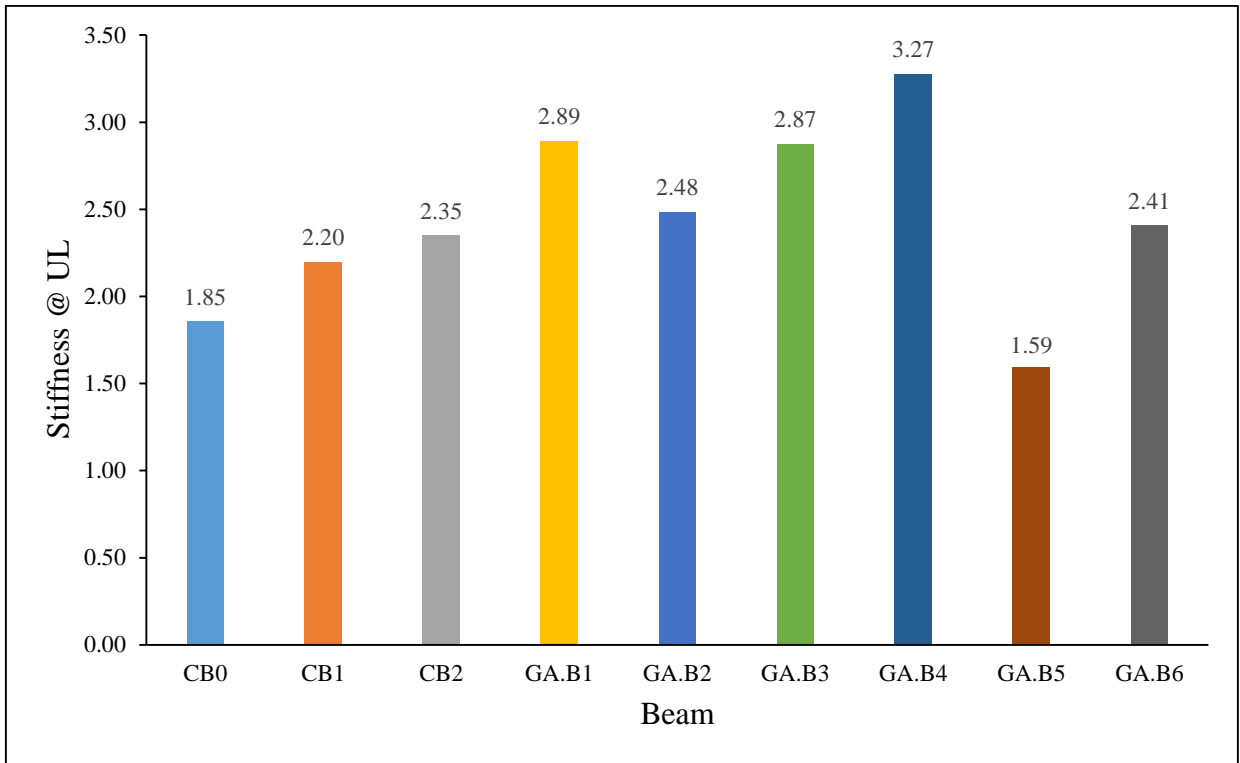
Figure 5.44 Comparative stiffness for the first group at the UL.
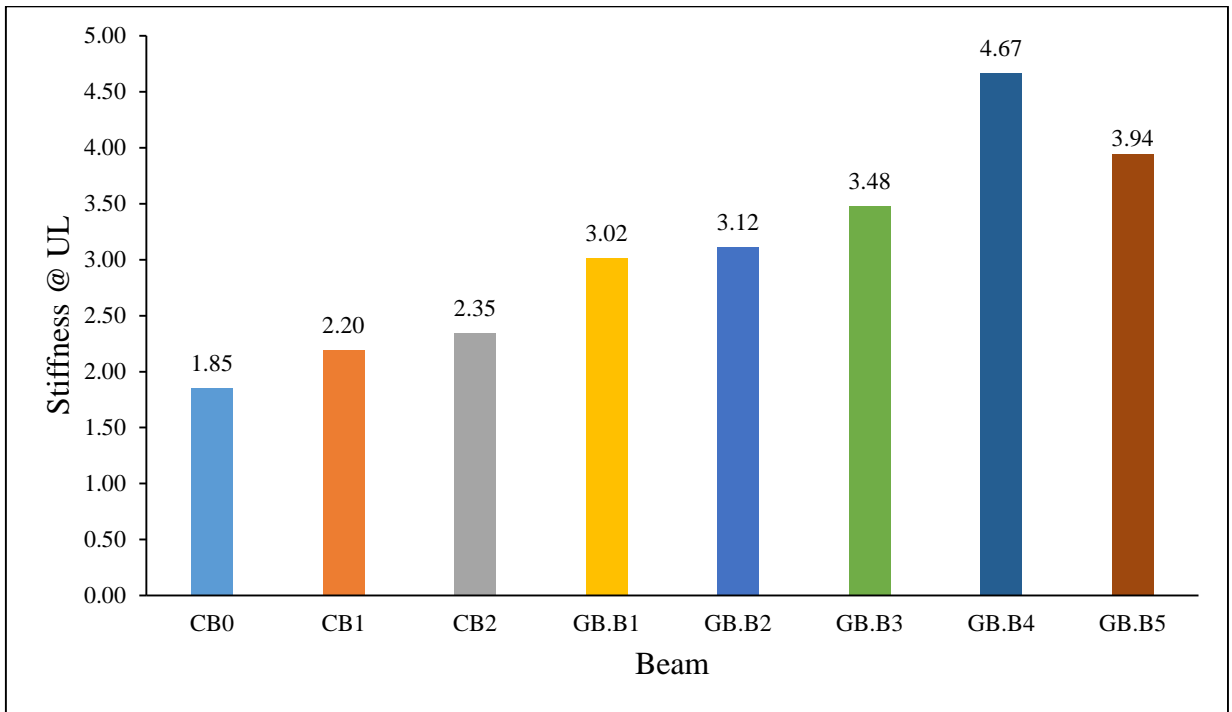
Figure 5.45 Comparative stiffness for the second group at the UL.

5.5.5. Analysis of Deflection for Specimens

The average deflection of strengthened specimens in first group is 14.85 mm which is more than the average deflection of first monolithic control specimen by 10.49%, while the average deflection of strengthened specimens in second group is 14.82 mm which is more than the average deflection of second monolithic control specimen by 15.48%.

The average deflection of strengthened specimens in first group is more than the average deflection of control specimen by 60.25%, while the second group of strengthened beams is more by 59.93%. Figure 5.46 shows the deflection of each specimen at failure of the flexural loading tests.

Regardless of the bonding type used in both groups, the strengthened beams have shown deflection values similar to that obtained from the monolithic controlled beams and at the same time have shown a deflection values more than that obtained from the controlled beams. Strengthened beam GA.B5 have the highest deflection value 20.95 mm at failure, which may attributed to the surface roughening bonding technique at interacted surfaces is not sufficient in the real-word application.
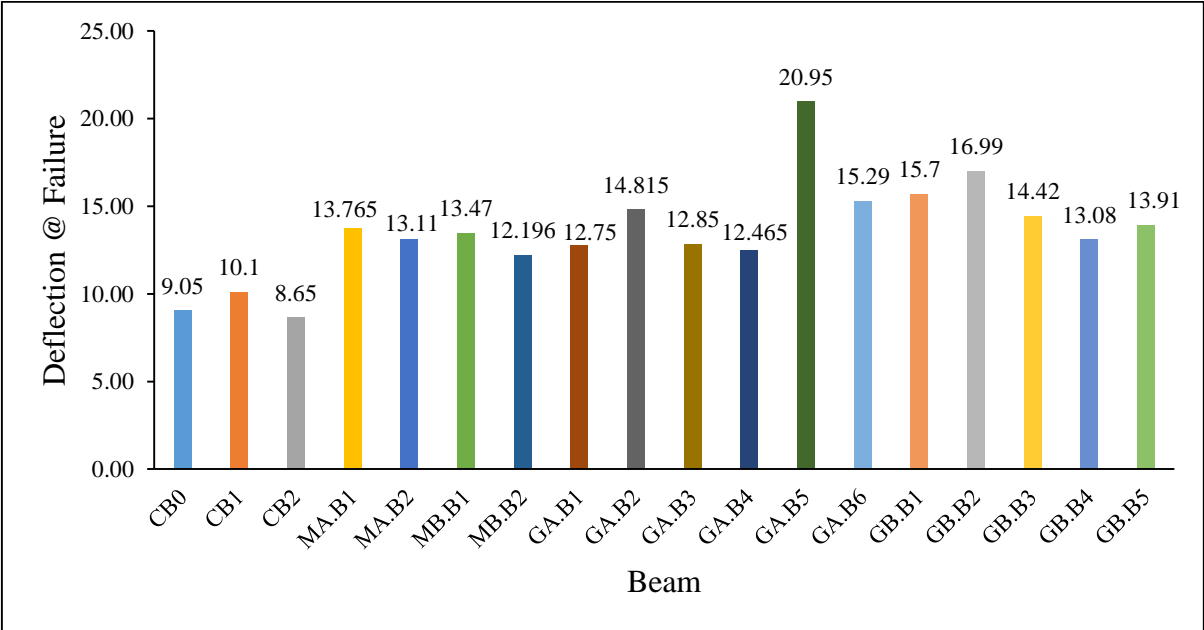
Figure 5.46 Deflections of specimens at failure.

5.5.6. Analysis of Crack Patterns for Specimens

Before testing the beams were whitewashed for easier identification of cracks during loading sequences. From Figures 5.1 through 5.26, the following results can be noted:

i. For all specimens cracks propagated from the bottom surface of the specimen to the center of the bearing plate.

ii. flexural cracks located at the mid span where the maximum flexural moment occurs that indicates jacketed beams exhibited pure flexural cracking patterns and ductile failure mode.

iii. The crack development for the strengthened beams shows normal flexural failure crack pattern compared with the control beams.

iv. Separation cracks at the common interface did not occur even upon failure during the flexural test between the concrete substrate and the SCC jacket for all strengthened beams in both groups, thus inter laminar has been prevented. This indicates that the strengthened beams perform as one unit regardless the kind bonding technique used. This may be a result for using a certain number of shear connectors which make the strengthened beams perform as monolithic construction beams. It is concluded that full interaction did develop between the jackets and the existing beam.

v. Strengthened beams GA.B5, GA.B6 & GB.B5 have the highest crack width value at SL 4.248, 3.36, and 2.952 mm respectively, which attributed to the surface roughening bonding technique at interacted surfaces is not sufficient in the real-word application (Figure 5.47).

vi. Regardless of the bonding type used in both groups, the strengthened beams have shown cracking widths and patterns similar to that obtained from the monolithic controlled beams except the strengthened beams of roughened surface they have crack width larger than others compared with monolithic control beams as shown in Figure 5.47 .
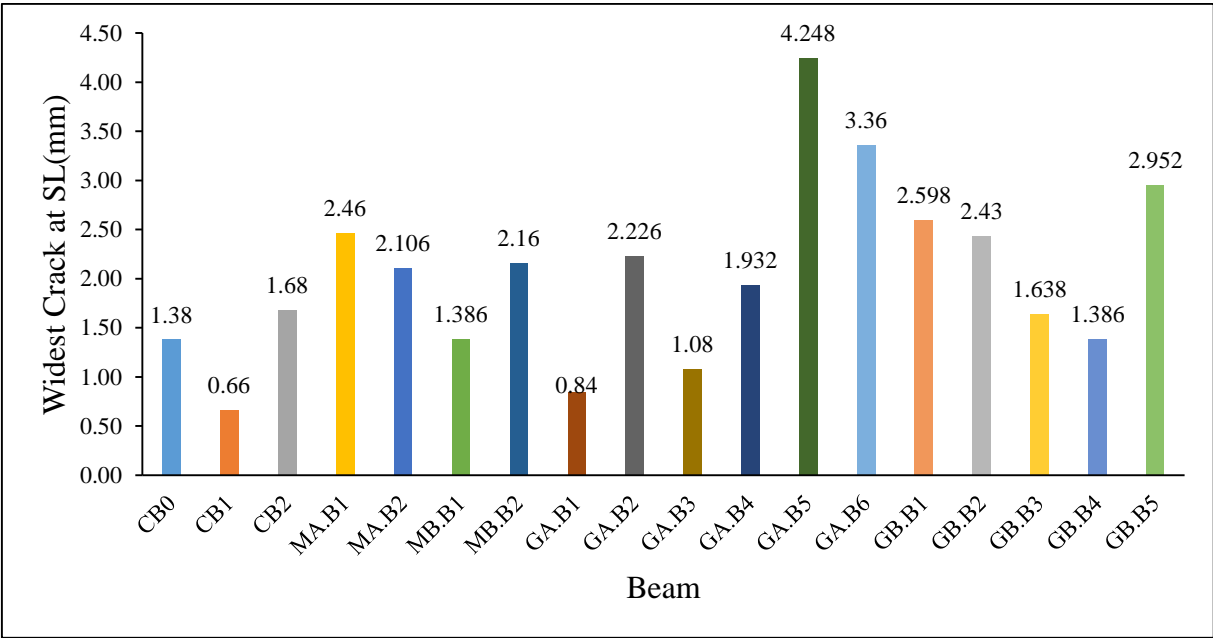
Figure 5.47 Widest crack at SL of specimens.

6

CHAPTER

THEORETICAL ANALYSIS OF STRENGTHENED BEAMS

CHAPTER 6

THEORETICAL ANALYSIS OF STRENGTHENED BEAMS

6.1 INTRODUCTION

Structural members are to be designed to satisfy strength and serviceability requirements. The strength requirement provides safety against possible failure, while the serviceability requirement ensures adequate performance at SL without excessive deflection and cracking.

A simplified design approach is presented in this chapter to predict the flexural strength and deflection at yielding and ultimate stages of rectangular RC beams strengthened using WWM based on the analyzed test results of the tested beams.

To understand the structure behavior of the strengthened beams, theoretical analysis was carried out to evaluate the flexural load capacity of the beams. This analysis is done based on the basics of flexural theory and its assumptions. So that the calculation methods for predicting the moment capacity of the strengthened beams in both group will be also provided and show a good agreement with the experimental tested results.

In this chapter a simplified design approach has been derived for the strengthened beams in both groups A and B.

6.2 STRUCTURAL ANALYSIS OF GROUP A

As shown in Figure 6.1 the assumed internal stresses and strains in a RC beam of Group A are illustrated in which the strengthened beams have jacketing reinforcement $\emptyset$ 3.5mm of 25 mm opening galvanized steel WWM.

The moment deflection curve can be schematically divided into three straight lines **(Xing, et al, 2010)**. The controlling points of the moment deflection are (Δ_{cr}, M_{cr}), (Δ_y, M_y) and (Δ_u, M_u) as seen in Figure 6.2
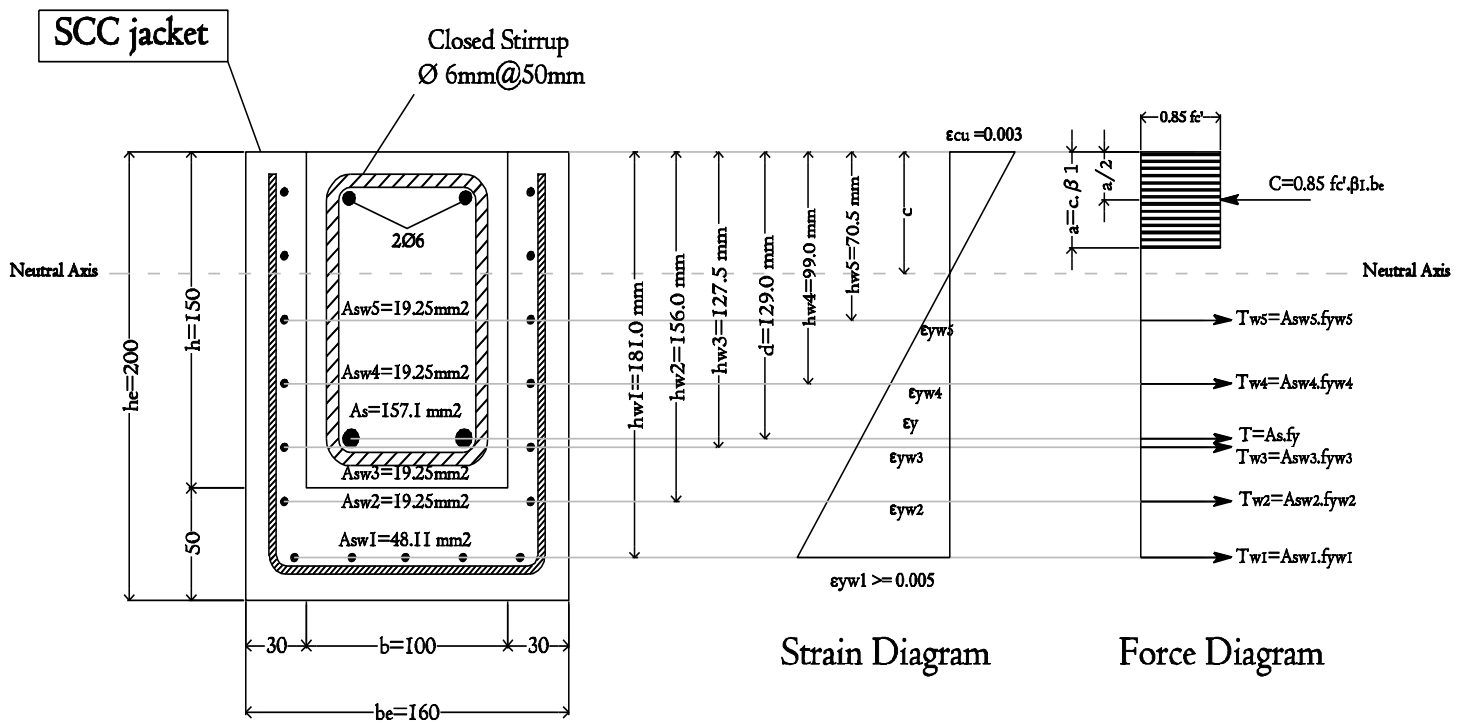
Figure 6.1 Stresses and strains of beam cross section (Group A).
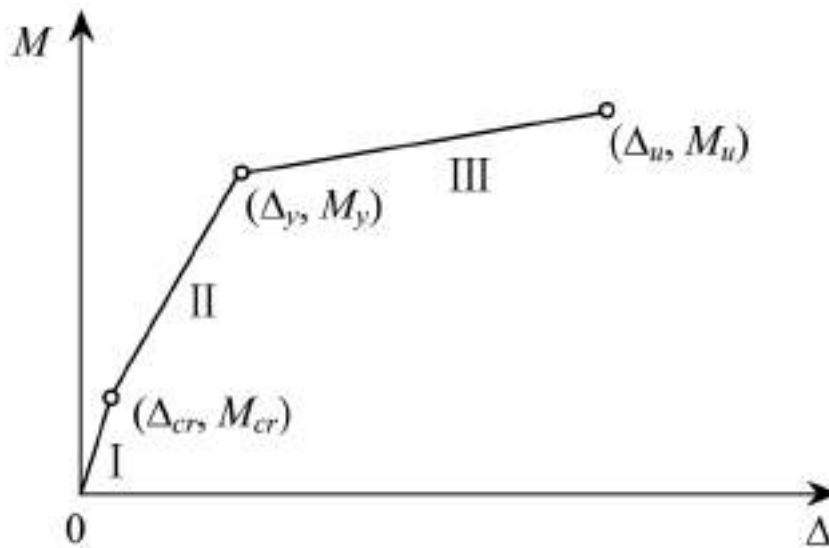
Figure 6.2 Schematic model of moment deflection curve. (Source: **Xing, et al, 2010**)

Stage I (Cracking Stage): When the maximum moment increases from zero to the cracking moment M_{cr}, the mid-span deflection increases from zero to Δcr

$$M_{cr} = \frac{I_g \times f_{cr}}{Y_t}$$
ACI Eq. (9-9)

Where:

M_{cr}: Cracking bending moment that causes the stress in extreme tension fiber to reach the modulus of rupture.

I_g: Moment of inertia for the gross section (mm^4) $= \frac{b_e.h_e^3}{12}$

F_{cr}: Modulus of rupture$= 0.62\sqrt{f_c'}$ (MPa),
ACI Eq. (9-10)

Y_t: Distance from the section centroid to the extreme tension fiber (mm) $= \frac{h_e}{2}$

Mid-span deflection of beams occur immediately on the application of load can be calculated as follows

$$\Delta_{cr} = \frac{M_{cr}}{24.I_g.E_c}(3L^2 - 4a^2)$$
Appendix B (B-1)

Where:

a: Shear span (mm) as shown Figure 6.3.

L: Distance between supports (mm) as shown Figure 6.3.

E: Elastic concrete modulus $= 4700\sqrt{f_c'}$ (MPa)
ACI Section (8.5.1)

Δ_{cr}: Mid-Span deflection at M_{cr} (mm).

I_g: Moment of inertia of gross concrete section about centroidal axis, neglecting reinforcement (mm^4) $= \frac{b_e.h_e^3}{12}$.

Figure 6.3 Beam layout and cross section geometry.

Stage II (Yielding Stage):

When the maximum moment increases from M_{cr} to the moment corresponding to steel yield M_y, mid-span deflection increases from Δ_{cr} to Δ_y as shown in Figure 6.2. To find the bending moment at yielding stage use the force diagram equilibrium (Figure 6.1).

$$+ \rightarrow \sum F_x = 0$$

$$0.85 f'_c . \beta_1 . c . b_e = A_s . f_y + A_{sw1} . f_{yw} + A_{sw2} . f_{yw} + A_{sw3} . f_{yw} + A_{sw4} . f_{yw} + A_{sw5} . f_{yw}$$

$$so \implies c = \frac{A_s . f_y + f_{yw}[A_{sw1} + A_{sw2} + A_{sw3} + A_{sw3} + A_{sw4} + A_{sw5}]}{0.85 f'_c . \beta_1 . b_e}$$

The previous equation can be simplified as

$$c = \frac{A_s . f_y + f_{yw} \sum_{i=1}^{5} A_{swi}}{0.85 f'_c . \beta_1 . b_e} \tag{6-1}$$

Where:

c: Depth of neutral axis (mm).

A$_s$: Cross sectional area of the steel bar in tension (mm^2).

A$_{swi}$: Cross sectional area of the steel wires in tension at depth i (mm^2).

f$_y$: Yield strength of steel bars (MPa).

f$_{yw}$: Yield strength of steel wires (MPa).

f$_{c'}$: Standard cylinder concrete compressive strength at 28 days (MPa).

b$_e$: Width of section (mm).

$$\beta 1 = 0.85 \qquad\qquad for\ (f_c' \leq 28\ Mpa)$$

$$\beta 1 = \left[0.85 - \frac{0.05(f_c' - 28)}{7}\right] \qquad for\ (f_c' > 28\ Mpa)$$

$$+\circlearrowleft \sum M_{@\ force\ C} = 0$$

$$M_y = \left\{A_s.f_y\left(d - \frac{a}{2}\right) + A_{sw1}.f_{yw}\left(h_{w1} - \frac{a}{2}\right) + A_{sw2}.f_{yw}\left(h_{w2} - \frac{a}{2}\right)\right.$$
$$\left. + A_{sw3}.f_{yw}\left(h_{w3} - \frac{a}{2}\right) + A_{sw4}.f_{yw}\left(h_{w4} - \frac{a}{2}\right) + A_{sw5}.f_{yw}\left(h_{w5} - \frac{a}{2}\right)\right\}$$

The previous equation can be simplified as

$$M_y = A_s.f_y\left(d - \frac{a}{2}\right) + f_{yw}.\Sigma_{i=1}^{5} A_{swi}\left(h_{wi} - \frac{a}{2}\right) \qquad\qquad \textbf{(6-2)}$$

Where:

M$_y$: Yielding moment of beam (N.mm).

d: Effective depth of section (mm).

a: Depth of rectangular stress block, Whitney Block (mm).

h$_{wi}$: Depth of steel wires at level i (mm).

ε$_{ywi}$: Wire strain at bottom face must be equal or larger than 0.005 to be in tension control section (i.e. to be ductile behavior).

From strain diagram we get that

$$\frac{\epsilon_{cu} = 0.003}{c} = \frac{\epsilon_{yw1}}{(h_{w1} - c)}$$

$$\Rightarrow \epsilon_{yw1} = \left[\frac{0.003}{c}(h_{w1} - c)\right] \geq 0.005 \qquad\qquad \textbf{(6-3)}$$

At yeilding stage the mid-span deflection can be calculated as follows

$$\Delta_y = \frac{M_y}{24.E_c.I_e}(3L^2 - 4a^2)$$ **Appendix B Eq. (B-1)**

Where:

a: Shear span (mm).

L: Distance between supports (mm).

E: Elastic concrete modulus = $4700\sqrt{f_c'}$ (MPa)   **ACI Section (8.5.1)**

$\mathbf{\Delta_y}$: Mid-span deflection at M_y (mm).

$\mathbf{I_e}$: Effective moment of inertia (mm^4), given as follows

$$I_e = \left\{ \left(\frac{M_{cr}}{M_a}\right)^3 I_g + \left[1 - \left(\frac{M_{cr}}{M_a}\right)^3\right] I_{cr} \right\} \leq I_g$$ **ACI Eq. (9-10)**

Where:

$\mathbf{M_{cr}}$: Cracking bending moment that causes the stress in extreme tension fiber to reach the modulus of rupture (N.mm).

$\mathbf{I_g}$: Moment of inertia of gross concrete section about centroidal axis, neglecting reinforcement (mm^4) = $\frac{b_e.h_e^3}{12}$.

$\mathbf{M_a}$: Maximum bending moment in member at stage deflection is computed = $\mathbf{M_y}$ (N.mm).

$\mathbf{I_{cr}}$: Moment of inertia of cracked section transformed to concrete (mm^4), I_{cr} given as follows when taking the moment of areas about the neutral axis as shown in Figure 6.4:

$$I_{cr} = \frac{1}{3}b_e.c^3 + \frac{E_s}{E_c}A_s(d-c)^2 +$$

$$\frac{E_w}{E_c}\left[\begin{array}{c} A_{sw1}(h_{w1} - c)^2 + A_{sw2}(h_{w2} - c)^2 + A_{sw3}(h_{w3} - c)^2 \\ + A_{sw4}(h_{w4} - c)^2 + A_{sw5}(h_{w5} - c)^2 \end{array}\right]$$

Figure 6.4 Cracked transformed Section.

The previous equation can be written as

$$I_{cr} = \frac{1}{3}b_e.c^3 + \frac{E_s}{E_c}A_s(d-c)^2 + \frac{E_w}{E_c}\sum_{i=1}^{5} A_{swi}(h_{wi}-c)^2 \qquad \textbf{(6-4)}$$

Where:

E$_s$: Elastic modulus of steel bars (MPa).

E$_w$: Elastic modulus of steel wires (MPa).

E$_c$: Elastic concrete modulus (MPa).

d: Effective depth of section (mm).

c: Depth of neutral axis (mm).

A$_{swi}$: Cross sectional area of the steel wires in tension at depth i (mm^2).

h$_{wi}$: Depth of steel wires at level i (mm).

Stage III (Ultimate Stage):

To find the bending moment at ultimate stage use the force diagram equilibrium

$$+ \rightarrow \sum F_x = 0$$

$$0.85 f_c' . \beta_1 . c . b_e = A_s . f_y + A_{sw1} . f_{yw} + A_{sw2} . f_{yw} + A_{sw3} . f_{yw} + A_{sw4} . f_{yw} + A_{sw5} . f_{yw}$$

$$so \Rightarrow c = \frac{A_s . f_y + f_{yw}[A_{sw1} + A_{sw2} + A_{sw3} + A_{sw4} + A_{sw5}]}{0.85 f_c' . \beta_1 . b_e}$$

The previous equation can be simplified as

$$c = \frac{A_s . f_y + f_{yw}\left(\sum_{i=1}^{5} A_{swi}\right)}{0.85 f_c' . \beta_1 . b_e} \tag{6-5}$$

Where:

c: Depth of neutral axis (mm)

A$_s$: Cross sectional area of the steel bar in tension (mm^2).

A$_{swi}$: Cross sectional area of the steel wires in tension at depth i (mm^2).

f$_y$: Yield strength of steel bars (MPa).

f$_{yw}$: Yield strength of steel wires (MPa).

f$_{c'}$: Standard cylinder concrete compressive strength at 28 days (MPa).

b$_e$: Width of section.

$$\beta1 = 0.85 \qquad\qquad for\ (f_c' \leq 28\ Mpa)$$

$$\beta1 = \left[0.85 - \frac{0.05(f_c' - 28)}{7}\right] \qquad for\ (f_c' > 28\ Mpa)$$

$$+ \circlearrowleft \sum M_{@\ force\ c} = 0$$

$$M_u = A_s . f_u \left(d - \frac{a}{2}\right) + A_{sw1} . f_{uw} \left(h_{w1} - \frac{a}{2}\right) + A_{sw2} . f_{uw} \left(h_{w2} - \frac{a}{2}\right)$$

$$+ A_{sw3} . f_{uw} \left(h_{w3} - \frac{a}{2}\right) + A_{sw4} . f_{uw} \left(h_{w4} - \frac{a}{2}\right) + A_{sw5} . f_{uw} \left(h_{w5} - \frac{a}{2}\right)$$

The previous equation can be simplified as

$$M_u = A_s . f_u \left(d - \frac{a}{2}\right) + f_{uw} . \sum_{i=1}^{5} A_{swi} \left(h_{wi} - \frac{a}{2}\right) \tag{6-6}$$

Where:

M_u: Ultimate moment of beam (N.mm).

d: Effective depth of section (mm).

a: Depth of rectangular stress block, Whitney Block (mm).

h_{wi}: Depth of steel wires at level i (mm).

f_u: Ultimate strength of steel bars (MPa).

f_{uw}: Ultimate strength of steel wires (MPa)

At ultimate stage the mid-span deflection can be calculated as follows

$$\Delta_u = \frac{M_u}{24.E_c.I_e} (3L^2 - 4a^2)$$ **Appendix B Eq. (B-1)**

Where:

a: Shear span (mm).

L: Distance between supports (mm).

E: Elastic concrete modulus $= 4700\sqrt{f_c'}$ (MPa)   **ACI Section (8.5.1)**

Δ_u: Mid-Span deflection at M_u (mm).

I_e: Effective moment of inertia (mm^4), given as follows

$$I_e = \left\{ (\frac{M_{cr}}{M_a})^3 I_g + [1 - (\frac{M_{cr}}{M_a})^3] I_{cr} \right\} \le I_g$$ **ACI Eq. (9-10)**

Where:

M_{cr}: Cracking bending moment that causes the stress in extreme tension fiber to reach the modulus of rupture (N.mm).

I_g: Moment of inertia of gross concrete section about centroidal axis (mm^4), neglecting reinforcement $= \frac{b_e.h_e^3}{12}$.

M_a: Maximum bending moment in member at stage deflection is computed $= M_u$ (N.mm).

I_{cr}: Moment of inertia of cracked section transformed to concrete I_{cr} (mm⁴), given as follows when taking the moment of areas about the neutral axis as shown in Figure 6.4:

$$I_{cr} = \frac{1}{3} b_e . c^3 + \frac{E_w}{E_c} [A_{sw1}(h_{w1} - c)^2 + A_{sw2}(h_{w2} - c)^2 + A_{sw3}(h_{w3} - c)^2$$
$$+ A_{sw4}(h_{w4} - c)^2 + A_{sw5}(h_{w5} - c)^2]$$

The previous equation can be written as

$$I_{cr} = \frac{1}{3} b_e . c^3 + \frac{E_w}{E_c} \left(\sum_{i=1}^{5} A_{swi}(h_{wi} - c)^2 \right) \tag{6-7}$$

the term $\left\{ \frac{E_s}{E_c} A_s (d - c)^2 \right\}$ icreased the stiffness of the section so that it is neglected in ultimate stage to get an accept value of mid-span deflection.

Where:

E_s: Elastic modulus of steel bars (MPa).

E_w: Elastic modulus of steel wires (MPa).

E_c: Elastic concrete modulus (MPa).

d: Effective depth of section (mm).

c: Depth of neutral axis (mm).

A_{swi}: Cross sectional area of the steel wires in tension at depth i (mm²).

h_{wi}: Depth of steel wires at level i (mm).

6.3 STRUCTURAL ANALYSIS OF GROUP B

As shown in Figure 6.5 the assumed internal stresses and strains in a RC beam of Group B are illustreted in which the strengthend beams have jacketing reinforcement Ø 5.5mm of 50 mm opening galvanized steel WWM.

The moment deflection curve can be schematically divided into three straight lines (**Xing, et al, 2010**). The controlling points of the moment deflection are (Δ_{cr}, M_{cr}), (Δ_y, M_y) and (Δ_u, M_u) as seen in Figure 6.2.
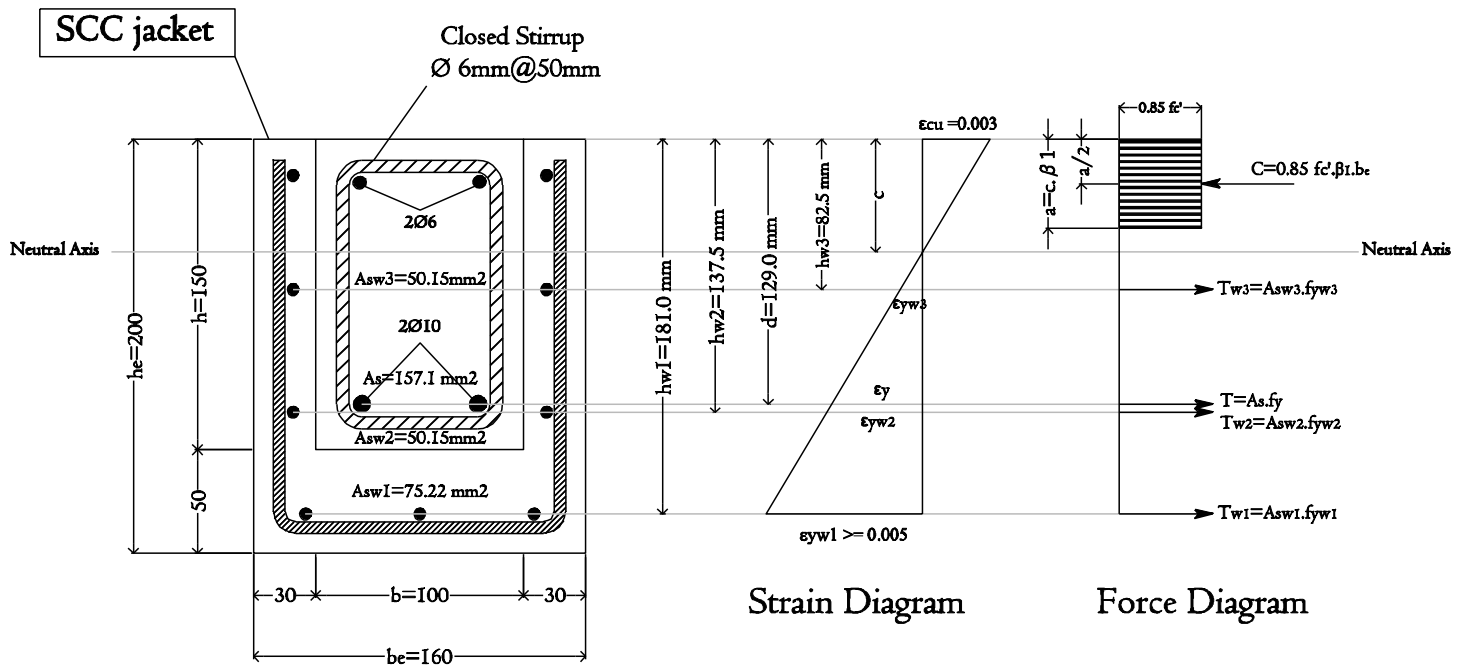
Figure 6.5 Stresses and strains of beam cross section (Group B).

Stage I (Cracking Stage): When the maximum moment increases from zero to the cracking moment M_{cr}, the mid-span deflection increases from zero to Δcr.

$$M_{cr} = \frac{I_g \times f_{cr}}{Y_t}$$
<div align="right">**ACI Eq. (9-9)**</div>

Where:

M_{cr}: Cracking bending moment that causes the stress in extreme tension fiber to reach the modulus of rupture (N.mm).

I_g: Moment of inertia for the gross section (mm^4) $= \frac{b_e.h_e^3}{12}$

F_{cr}: Modulus of rupture $= 0.62\sqrt{f_c'}$ (MPa),   **ACI Eq. (9-10)**

Y_t: Distance from the section centroid to the extreme tension fiber (mm) $= \frac{h_e}{2}$

Mid-span deflection of beams occur immediately on the application of load can be calculated as follows

$$\Delta_{cr} = \frac{M_{cr}}{24.I_g.E_c}(3L^2 - 4a^2)$$ **Appendix B Eq. (B-1)**

Where:

a: Shear span (mm) as shown Figure 6.6.

L: Distance between supports (mm) as shown Figure 6.6.

E: Elastic concrete modulus $= 4700\sqrt{f_c'}$ (MPa)   **ACI Section (8.5.1)**

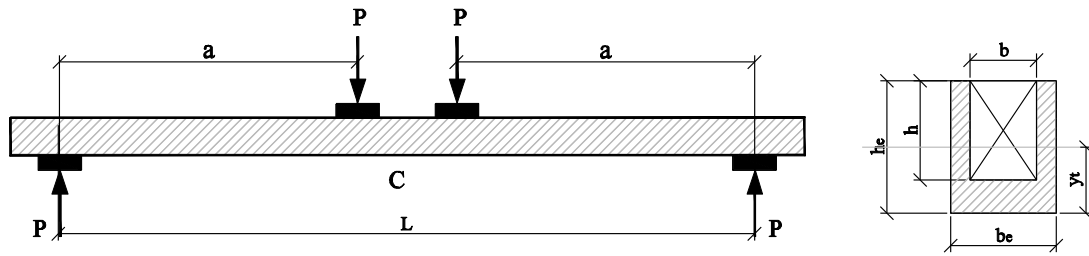Δ_{cr}: Mid-span deflection at M_{cr} (mm).
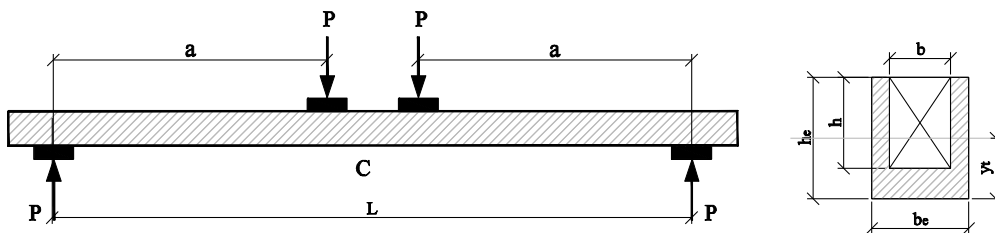
Figure 6.6 Beam layout and cross section geometry.

Stage II (Yielding Stage):

When the maximum moment increases from M_{cr} to the moment corresponding to steel yield M_y, the mid-span deflection increases from Δ_{cr} to Δ_y as shown in Figure 6.2. To find the bending moment at yielding stage use the force diagram equilibrium (Figure 6.5).

$$+ \rightarrow \sum F_x = 0$$

$$0.85 f_c' . \beta_1 . c . b_e = A_s . f_y + A_{sw1} . f_{yw} + A_{sw2} . f_{yw} + A_{sw3} . f_{yw}$$

$$so \Rightarrow c = \frac{A_s . f_y + f_{yw}[A_{sw1} + A_{sw2} + A_{sw3}]}{0.85 f_c' . \beta_1 . b_e}$$

The previous equation can be simplified as

$$c = \frac{A_s . f_y + f_{yw} \sum_{i=1}^{3} A_{swi}}{0.85 f_c' . \beta_1 . b_e} \qquad\qquad \textbf{(6-8)}$$

Where:

c: Depth of neutral axis (mm)

A$_s$: Cross sectional area of the steel bar in tension (mm^2).

A$_{swi}$: Cross sectional area of the steel wires in tension at depth I (mm^2).

f$_y$: Yield strength of steel bars (MPa).

f$_{yw}$: Yield strength of steel wires (MPa).

f$_{c'}$: Standard cylinder concrete compressive strength at 28 days (MPa).

b$_e$: Width of section (mm).

$$\beta 1 = 0.85 \qquad\qquad for\ (f_c' \le 28\ Mpa)$$

$$\beta 1 = \left[0.85 - \frac{0.05(f_c' - 28)}{7}\right] \qquad for\ (f_c' > 28\ Mpa)$$

$$+ \circlearrowleft \sum M_{@\ force\ C} = 0$$

$$M_y = \left\{ M_y = A_s . f_y \left(d - \frac{a}{2}\right) + A_{sw1} . f_{yw} \left(h_{w1} - \frac{a}{2}\right) + A_{sw2} . f_{yw} \left(h_{w2} - \frac{a}{2}\right) \right.$$
$$\left. + A_{sw3} . f_{yw} \left(h_{w3} - \frac{a}{2}\right) \right\}$$

The previous equation can be simplified as

$$M_y = A_s \cdot f_y \left(d - \frac{a}{2} \right) + f_{yw} \cdot \Sigma_{i=1}^{3} A_{swi} \left(h_{wi} - \frac{a}{2} \right) \qquad \text{(6-9)}$$

Where:

M_y: Yielding moment of beam (N.mm).

d: Effective depth of section (mm).

a: Depth of rectangular stress block ,Whitney Block (mm).

h_{wi}: Depth of steel wires at level i (mm).

ε_{ywi}: wire strain at bottom face must be equal or larger than 0.005 to be in tension control section (i.e. to be ductile behavior).

From strain diagram we get that

$$\frac{\epsilon_{cu} = 0.003}{c} = \frac{\epsilon_{yw1}}{(h_{w1} - c)}$$

$$\Rightarrow \epsilon_{yw1} = \left[\frac{0.003}{c} (h_{w1} - c) \right] \geq 0.005 \qquad \text{(6-10)}$$

At yielding stage the mid-span deflection can be calculated as follows

$$\Delta_y = \frac{M_y}{24.E_c.I_e} (3L^2 - 4a^2) \qquad \textbf{Appendix B Eq. (B-1)}$$

Where:

a: Shear span (mm).

L: The Distance between supports (mm).

E: Elastic concrete modulus $= 4700\sqrt{f_c'}$ (MPa)   **ACI Section (8.5.1)**

Δ_y: Mid-span deflection at M_y (mm).

I_e: Effective moment of inertia (mm^4), given as follows

$$I_e = \left\{ (\frac{M_{cr}}{M_a})^3 I_g + [1 - (\frac{M_{cr}}{M_a})^3] I_{cr} \right\} \leq I_g \qquad \textbf{ACI Eq. (9-10)}$$

Where:

M_{cr}: Cracking bending moment that causes the stress in extreme tension fiber to reach the modulus of rupture (N.mm).

I_g: Moment of inertia of gross concrete section about centroidal axis, neglecting reinforcement $(mm^4) = \frac{b_e.h_e^3}{12}$.

M_a: Maximum bending moment in member at stage deflection is computed $= M_y$ (N.mm).

I_{cr}: Moment of inertia of cracked section transformed to concrete (mm^4), I_{cr} given as follows when taking the moment of areas about the neutral axis as shown in Figure 6.7:

$$I_{cr} = \frac{1}{3}b_e.c^3 + \frac{E_s}{E_c}A_s(d-c)^2 + \frac{E_w}{E_c}[A_{sw1}(h_{w1}-c)^2 + A_{sw2}(h_{w2}-c)^2 +$$
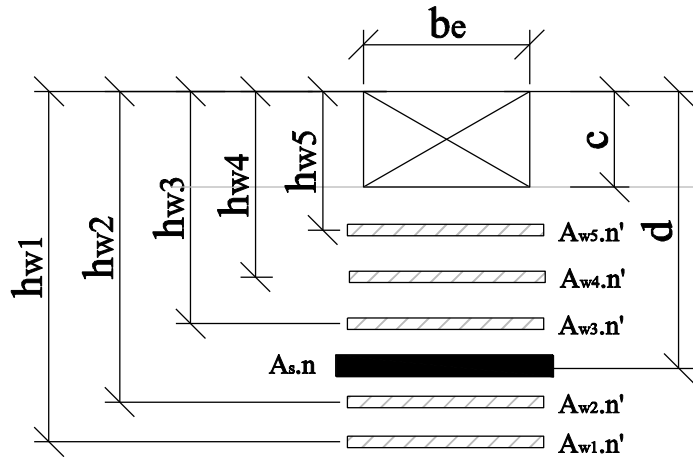
$$A_{sw3}(h_{w3}-c)^2]$$
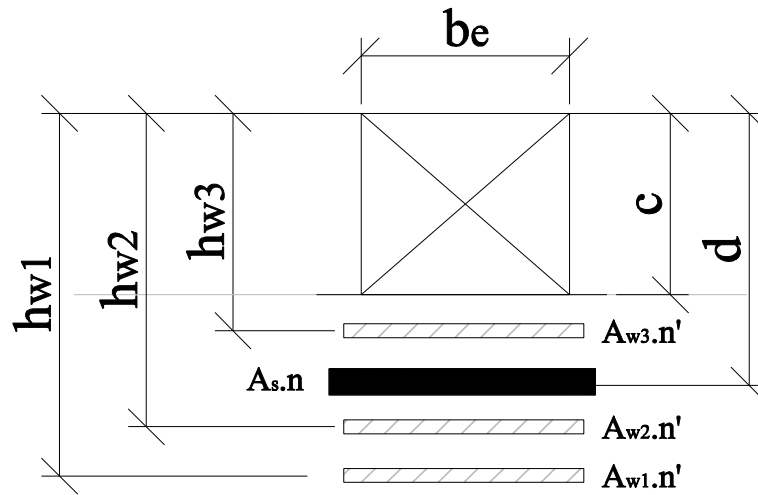
Figure 6.7 Cracked transformed Section.

The previous equation can be written as

$$I_{cr} = \frac{1}{3}b_e.c^3 + \frac{E_s}{E_c}A_s(d-c)^2 + \frac{E_w}{E_c}\sum_{i=1}^{3} A_{swi}(h_{wi}-c)^2 \qquad \text{(6-11)}$$

Where:

E_s: Elastic modulus of steel bars (MPa).

E_w: Elastic modulus of steel wires (MPa).

E_c: The elastic concrete modulus (MPa).

d: Effective depth of section (mm).

c: Depth of neutral axis (mm).

A_{swi}: Cross sectional area of the steel wires in tension at depth i (mm^2).

h_{wi}: Depth of steel wires at level i (mm).

Stage III (Ultimate Stage):

To find the bending moment at ultimate stage use the force diagram equilibrium

$$+ \rightarrow \sum F_x = 0$$

$$0.85 f_c' \cdot \beta_1 \cdot c \cdot b_e = A_s \cdot f_y + A_{sw1} \cdot f_{yw} + A_{sw2} \cdot f_{yw} + A_{sw3} \cdot f_{yw}$$

$$so \implies c = \frac{A_s \cdot f_y + f_{yw}[A_{sw1} + A_{sw2} + A_{sw3}]}{0.85 f_c' \cdot \beta_1 \cdot b_e}$$

The previous equation can be simplified as

$$c = \frac{A_s \cdot f_y + f_{yw}\left(\sum_{i=1}^{3} A_{swi}\right)}{0.85 f_c' \cdot \beta_1 \cdot b_e} \tag{6-12}$$

Where:

c: Depth of neutral axis (mm).

A_s: Cross sectional area of the steel bar in tension (mm^2).

A_{swi}: Cross sectional area of the steel wires in tension at depth i (mm^2).

f_y: Yield strength of steel bars (MPa).

f_{yw}: Yield strength of steel wires (MPa).

$f_{c'}$: Standard cylinder concrete compressive strength at 28 days (MPa).

$\mathbf{b_e}$: Width of section (mm).

$$\beta 1 = 0.85 \qquad\qquad for\ (f_c' \leq 28\ Mpa)$$

$$\beta 1 = \left[0.85 - \frac{0.05(f_c'-28)}{7}\right] \qquad for\ (f_c' > 28\ Mpa)$$

$$+ \circlearrowleft \sum M_{@\ force\ C} = 0$$

$$M_u = A_s \cdot f_u \left(d - \frac{a}{2}\right) + A_{sw1} \cdot f_{uw} \left(h_{w1} - \frac{a}{2}\right) + A_{sw2} \cdot f_{uw} \left(h_{w2} - \frac{a}{2}\right)$$
$$+ A_{sw3} \cdot f_{uw} \left(h_{w3} - \frac{a}{2}\right)$$

The previous equation can be simplified as

$$M_u = A_s \cdot f_u \left(d - \frac{a}{2}\right) + f_{uw} \cdot \Sigma_{i=1}^3 A_{swi} \left(h_{wi} - \frac{a}{2}\right) \qquad\qquad \textbf{(6-13)}$$

Where:

$\mathbf{M_u}$: Ultimate moment of beam (N.mm).

$\mathbf{d}$: Effective depth of section (mm).

$\mathbf{a}$: Depth of rectangular stress block ,Whitney Block (mm).

$\mathbf{h_{wi}}$: Depth of steel wires at level i (mm).

$\mathbf{f_u}$: Ultimate strength of steel bars (MPa).

$\mathbf{f_{uw}}$: Ultimate strength of steel wires (MPa).

At ultimate stage the mid-span deflection can be calculated as follows

$$\Delta_u = \frac{M_u}{24 \cdot E_c \cdot I_e} (3L^2 - 4a^2) \qquad\qquad \textbf{Appendix B Eq. (B-1)}$$

Where:

$\mathbf{a}$: Shear span (mm).

$\mathbf{L}$: Distance between supports (mm).

E: Elastic concrete modulus $= 4700\sqrt{f'_c}$ (MPa) **ACI Section (8.5.1)**

Δ_u: Mid-span deflection at M_u (mm).

I_e: Effective moment of inertia (mm⁴), given as follows

$$I_e = \left\{ (\tfrac{M_{cr}}{M_a})^3 I_g + [1 - (\tfrac{M_{cr}}{M_a})^3] I_{cr} \right\} \le I_g$$ **ACI Eq. (9-10)**

Where:

M_{cr}: Cracking bending moment that causes the stress in extreme tension fiber to reach the modulus of rupture (N.mm).

I_g: Moment of inertia of gross concrete section about centroidal axis (mm⁴), neglecting reinforcement $= \frac{b_e.h_e^3}{12}$.

M_a: Maximum bending moment in member at stage deflection is computed $= M_u$ (N.mm).

I_{cr}: Moment of inertia of cracked section transformed to concrete I_{cr} (mm⁴), given as follows when taking the moment of areas about the neutral axis as shown in Figure 6.7:

$$I_{cr} = \frac{1}{3} b_e.c^3 + \frac{E_w}{E_c}[A_{sw1}(h_{w1} - c)^2 + A_{sw2}(h_{w2} - c)^2 + A_{sw3}(h_{w3} - c)^2]$$

The previous equation can be written as

$$I_{cr} = \frac{1}{3} b_e.c^3 + \frac{E_w}{E_c}(\textstyle\sum_{i=1}^{3} A_{swi}(h_{wi} - c)^2)$$ **(6-14)**

the term $\left\{ \frac{E_s}{E_c} A_s(d - c)^2 \right\}$ icreased the stiffness of the section so that it is neglected in ultimate stage to get an accept value of mid-span deflection.

Where:

E_s: Elastic modulus of steel bars (MPa).

E_w: Elastic modulus of steel wires (MPa).

E_c: Elastic concrete modulus (MPa).

d: Effective depth of section (mm).

c: Depth of neutral axis (mm).

A_{swi}: Cross sectional area of the steel wires in tension at depth i (mm^2).

h_{wi}: Depth of steel wires at level i (mm).

6.4 SPECIMENS PROPERTIES

Table 6-1 illustrates the experimental results for all the specimens such as, compressive strength of concrete and SCC, actual dimension and failure mode.

Table 6.1 Beam specimen properties.

Sample	Group	f'_{c1} * (MPa)	f'_{c2} ** (MPa)	Failure Mode
CB0	Control Beams	38.607	-	Flexural
CB1		38.607	-	Flexural
CB2		38.607	-	Flexural
MA.B1	Monolithic Control Beams	39.290	-	Flexural
MA.B2		39.290	-	Flexural
MB.B1		37.258	-	Flexural
MB.B2		37.258	-	Flexural
GA.B1	Group A	39.472	44.501	Flexural
GA.B2		39.472	44.501	Flexural
GA.B3		39.470	44.501	Flexural
GA.B4		39.472	44.501	Flexural
GA.B5		38.607	42.589	Flexural
GA.B6		38.607	42.589	Flexural
GB.B1	Group B	39.973	42.884	Flexural
GB.B2		39.973	42.884	Flexural
GB.B3		39.973	42.884	Flexural
GB.B4		39.973	42.884	Flexural
GB.B5		38.607	42.589	Flexural
* f'_{c1}: The Standard cylinder compressive strength of original beam section. ** f'_{c1}: The Standards cylinder compressive strength of the SCC jacket.				

6.5 COMPARISON OF TEST RESULTS WITH THEORETICAL PREDICTIONS

As seen the experimental test results and theoretical results by the simplified analysis model are reported in Table 6.2 of bending moment for both yielding and ultimate stages as discussed in the previous sections.

Table 6.2 Comparison of experimental test results and analytical values.

Beam	Yielding Stage		M_{yC} / M_{yE}	Ultimate Stage		M_{uC} / M_{uE}
	M_{yC}^{*} (KN.m)	M_{yE}^{**} (KN.m)		$M_{uC}^{\S}$ (KN.m)	$M_{uE}^{\S\S}$ (KN.m)	
MA.B1	55.165	57.086	0.97	77.796	81.883	0.95
MA.B2	55.165	61.026	0.90	77.796	87.180	0.89
GA.B1	55.438	55.996	0.99	78.183	79.994	0.98
GA.B2	55.438	58.016	0.96	78.183	82.880	0.94
GA.B3	55.438	55.624	1.00	78.183	79.463	0.98
GA.B4	55.438	59.483	0.93	78.183	84.976	0.92
GA.B5	55.302	59.220	0.93	77.990	84.600	0.92
GA.B6	55.302	56.644	0.98	77.990	80.920	0.96
MB.B1	66.335	77.390	0.86	98.224	110.553	0.89
MB.B2	66.335	72.558	0.91	98.224	103.654	0.95
GB.B1	66.998	69.410	0.97	99.208	99.151	1.00
GB.B2	66.998	75.585	0.89	99.208	107.978	0.92
GB.B3	66.998	67.176	1.00	99.208	95.965	1.03
GB.B4	66.998	75.131	0.89	99.208	107.329	0.92
GB.B5	66.877	72.288	0.93	99.028	103.268	0.96
* Calculated bending moment at yielding stage.						
** Experimental test result of bending moment at yielding stage.						
§ Calculated bending moment at ultimate stage.						
§§ Experimental test result of bending moment at ultimate stage.						

It is noted that based on the previous table the testing program of this study was verified using the test data of 11 strengthened beams, also it was verified when compared practically with monolithic control beams, and ones can say a good agreement between experimental results and prediction values is achieved.

Figures 6.8 and 6.9 convert the previous table to bar chart model. Calculation table of all strengthened beams is available in Appendix E.
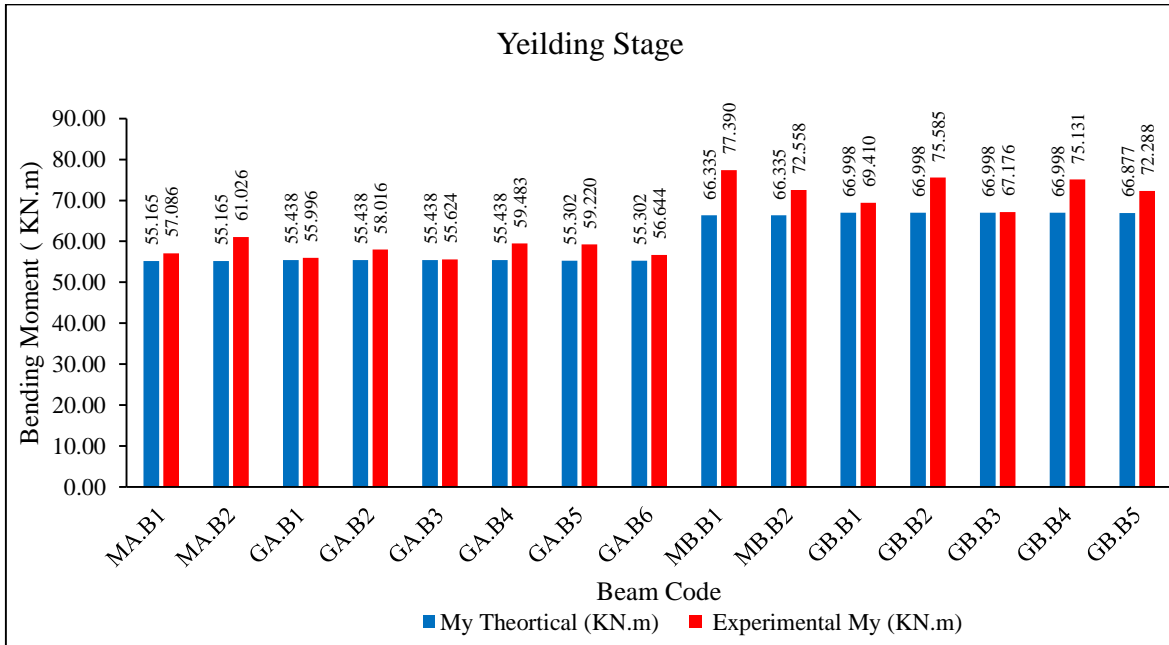
Figure 6.8   Comparison of test results and analytical values at yielding.
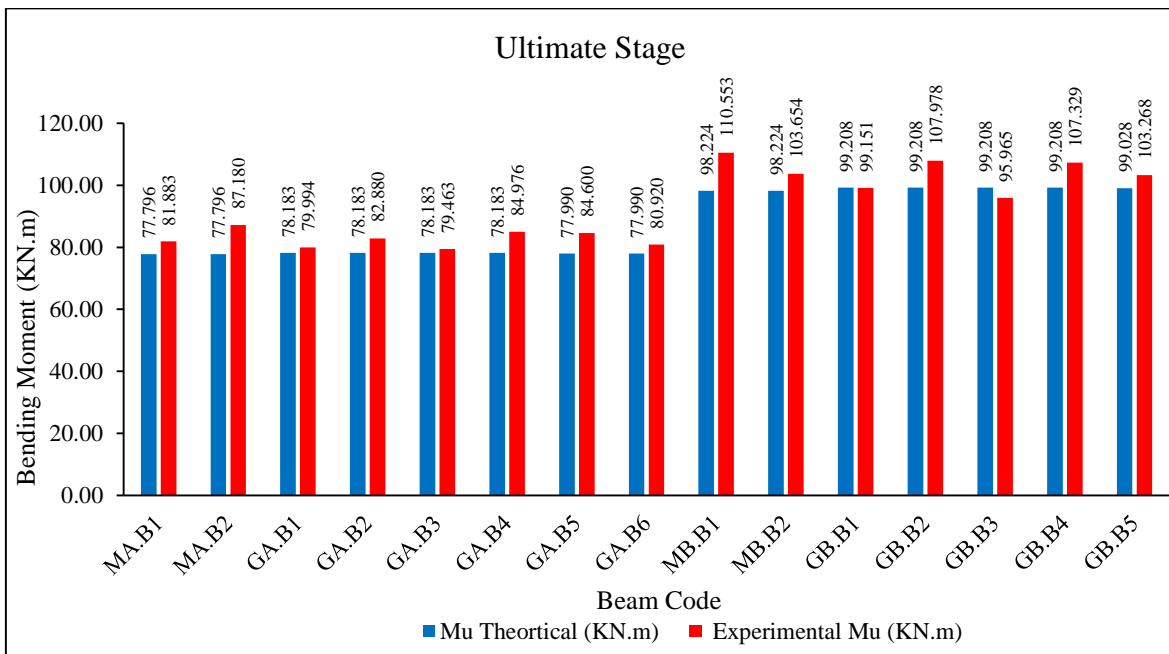
Figure 6.9   Comparison of test results and analytical values at ultimate.

As seen the experimental test results and theoretical results by the simplified analysis model are reported in Table 6.3 of mid span deflection for both yielding and ultimate stages as discussed in the previous sections.

Table 6.3 Comparison of experimental test results and analytical values.

Beam	Δyc^* (mm)	Δyt^{**} (mm)	$\Delta yc/\Delta yt$	$\Delta uc^{\S}$ (mm)	$\Delta ut^{\S\S}$ (mm)	$\Delta uc/\Delta ut$
MA.B1	2.478	4.65	0.53	16.358	13.765	1.19
MA.B2	2.478	5.13	0.48	16.358	13.11	1.25
GA.B1	2.404	4.45	0.54	15.865	11.25	1.41
GA.B2	2.404	4.8	0.50	15.865	14.815	1.07
GA.B3	2.404	4.55	0.53	15.865	12.85	1.23
GA.B4	2.404	4.68	0.51	15.865	12.465	1.27
GA.B5	2.442	5.00	0.49	16.128	20.95	0.77
GA.B6	2.442	5.2	0.47	16.128	15.29	1.05
MB.B1	3.333	5.7	0.58	18.710	13.47	1.39
MB.B2	3.333	5.32	0.63	18.710	12.196	1.53
GB.B1	3.232	5.85	0.55	18.990	15.70	1.21
GB.B2	3.232	6.6	0.49	18.990	16.99	1.12
GB.B3	3.232	6.15	0.53	18.990	14.42	1.32
GB.B4	3.232	6.18	0.52	18.990	13.08	1.45
GB.B5	3.252	6.05	0.54	18.963	13.91	1.36
* Calculated deflection at yielding stage.						
** Experimental test result of deflection at yielding stage.						
§ Calculated deflection at ultimate stage.						
§§ Experimental test result of deflection at ultimate stage.						

A good agreement between experimental results and prediction values is achieved at ultimate stage. Figures 6.10 and 6.11 convert the previous table to bar chart model. Calculation table of all strengthened beams is available in Appendix E.
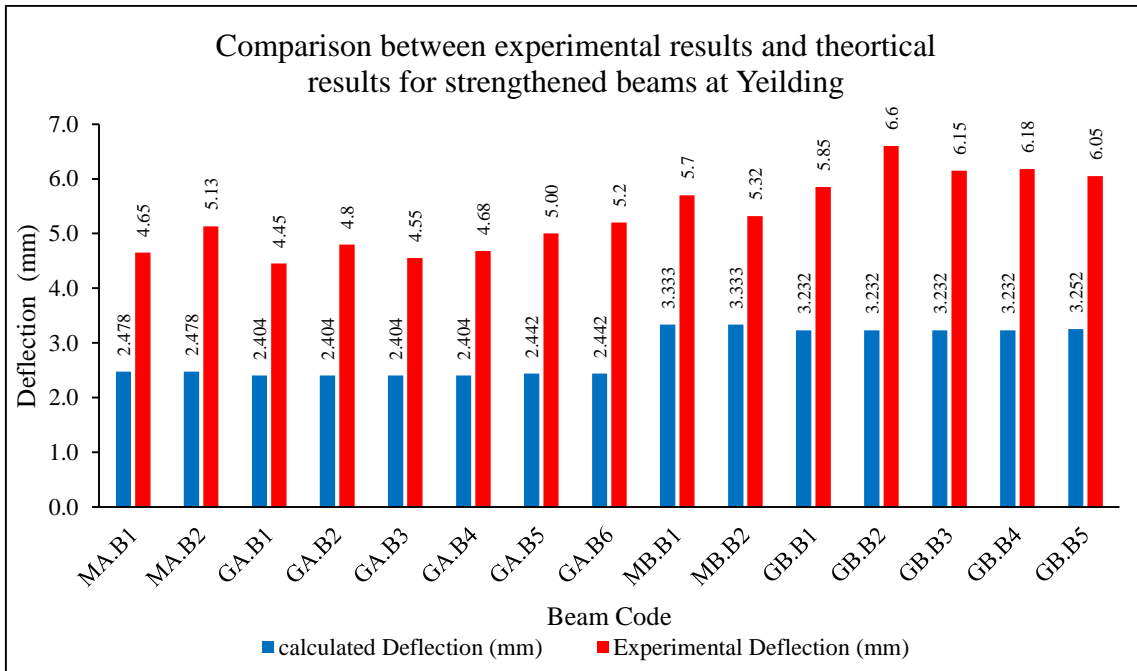
Figure 6.10 Comparison of test results and analytical values at yielding.
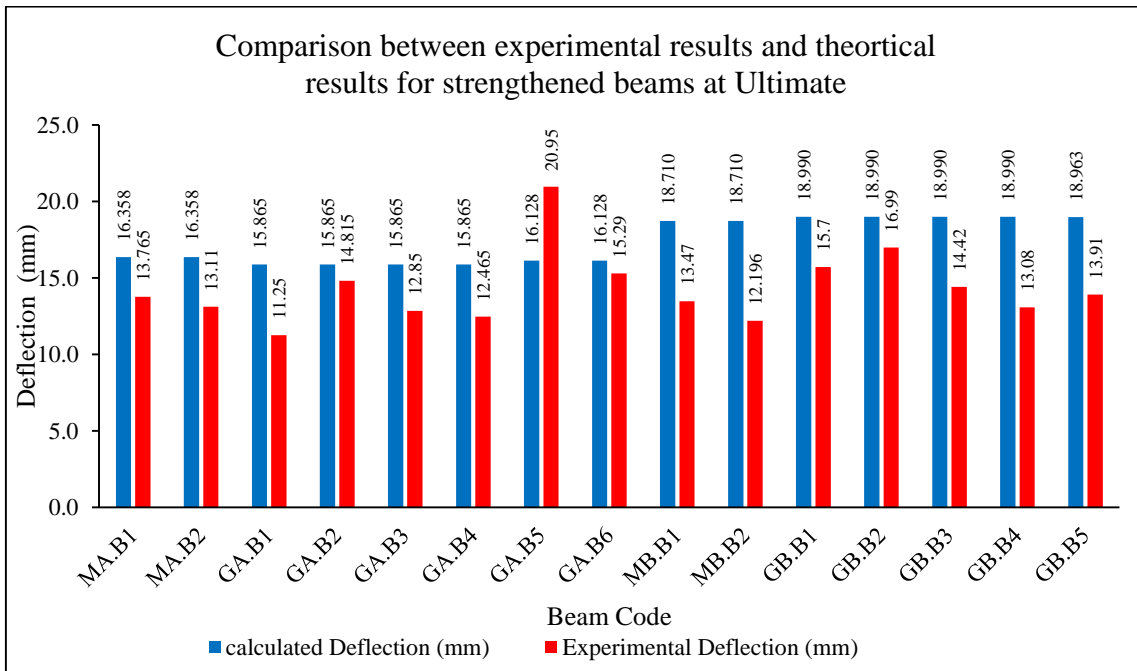
Figure 6.11 Comparison of test results and analytical values at ultimate.

7

CHAPTER

CONCLUSION AND RECOMMENDATIONS

CHAPTER 7

CONCLUSION AND RECOMMENDATIONS

7.1 INTRODUCTION

The load capacity, deflection and crack patterns of RC beams strengthened using SCC jacketing with wire mesh were studied experimentally. The study intended to assess the feasibility of strengthening RC Beams using section enlargement technique that can be applied in strengthening RC structures. The test program of the current study has been detailed in chapter three of this thesis. A series of four-point bending tests were carried out on eighteen beams. Three of these beams were tested as control beams, four were tested as monolithic control beams while eleven of beams were tested as strengthened beams. Also different mechanical bonding was investigated. Many types of bonding techniques were applied to the eleven beams even by roughening the surface or by adding shear connectors whether expansion bolts or dowel anchors with specific distribution along the interacted surfaces of the beam.

7.2 CONCLUSIONS

Based on the observations of the experimental work and the results of the theoretical analysis; the following conclusions are made for reinforced concrete beams strengthened using SCC jacketing with wire mesh:

a. The experimental results clearly proved that jacketing can upgrade the structural properties for the RC beams, which make the strengthened beams perform as monolithic construction beams.

b. The test results indicated that the use of WWM and SCC jacketing is an effective technique of strengthening RC beams in flexure.

c. It is concluded that full interaction did develop between the jackets and the existing beam. Thus separation cracks at the common interface did not occur even upon failure

during the flexural test between the concrete substrate and the SCC jacket for all strengthened beams in both groups, thus inter laminar has been prevented.

d. The main test parameters included the mesh properties based on mesh opening and nominal diameter. In addition to the bonding technique employed between old and new SCC.

e. The mix proportions of SCC that used in strengthening process is satisfied with the EFNARC 2005 limits.

f. The SCC shows accepted mechanical properties such as good workability, passing ability and remarkable filling to overcome the challenges applied in strengthening of RC beams. Further SCC flows through congested reinforcements without causing honeycombing during the practical works.

g. The flexural load capacity of the strengthened beams increased by 110.24 % of Ø 3.5mm galvanized WWM ,while increased by 162.96 % of Ø 5.5mm galvanized WWM compared with the control beams.

h. The increasing in the flexural capacity in both groups was due to the addition of WWM reinforcement within the jacket and due to the increase in the beam effective depth. This indicates that the strengthening technique satisfies its aim to increase the flexural capacity of the strengthened beams.

i. All strengthened beams have more ductility ratio compared to control beams.

j. The test results showed that in the two test groups if the diameter of the galvanized steel WWM increases as in group B the failure load capacity and ductility significantly will increase compared to other group.

k. The test results indicate that in the two test groups the opening between bars of WWM does not play a main role in decreasing the ultimate capacity of beams.

l. In Group A specimens bonded by anchors whether expansion bolts or Ø 8.00 mm dowels restore 96.80 % in average of the monolithically control specimens. While in Group B specimens bonded by anchors whether expansion bolts or Ø 8.00 mm dowels restore 95.80 % in average of the monolithically control specimens.

m. The best type of bonding technique is by adding Ø 8 mm dowels as shear connectors in Group A, while the best bonding technique is by adding Hilti expansion bolts as

shear connectors at the interacted surface to connect between old and new concrete in Group B.

n. The worst bonding technique is the surface roughening based on crack width and the stiffness at SL analysis which attributed to the surface roughening at interacted surfaces is not sufficient in the real-word application.

o. In both Group A and B in which the mechanical bonding has been used inter laminar has been prevented may be a result for using a certain number of shear connectors which make the strengthened beams perform as monolithic construction beams.

p. All the strengthened test beams were stiffer than the control beam and all were able to resist loads which exceeded the load capacity of the control beam.

q. The strengthened beams in group A of Ø3.5 mm of 25 mm opening have higher stiffness than strengthened beams in group B of Ø5.5 mm of 50 mm opening galvanized WWM at SL stage.

r. Regardless of the bonding type used in both groups, the strengthened beams have shown cracking widths and patterns similar to that obtained from the monolithic controlled beams except the strengthened beams of roughened surface they have crack width larger than others compared with monolithic control beams.

s. Regardless of the bonding type used in both groups, the strengthened beams have shown deflection values similar to that obtained from the monolithic controlled beams and at the same time have shown a deflection values more than that obtained from the controlled beams.

t. It was noticed that the jacketed beams behaved in a similar manner to their monolithic counterparts in terms of the ductility, cracking and deflection behaviors.

u. To understand the structure behavior of the strengthened beams, theoretical analysis was carried out and a simplified design procedure was presented in this thesis to predict the flexural strength and deflection at yielding and at ultimate stages of rectangular RC beams strengthened using SCC with WWM. This analysis is done based on the basics of flexural theory and its assumptions and a good agreement at ultimate stage between experiment test results and prediction values was achieved.

7.3 RECOMMENDATIONS FOR FUTURE RESEARCH

The following recommendations are proposed for further research.

a. A Larger numbers of beam specimens may be tested for every type of bonding techniques to improve the standard deviation between tests results and to improve the comparison between each type of bonding.

b. More of bonding techniques (mechanical and chemical bonding) may be tested for the section enlargement of the beams using SCC to obtain the best type of bonding between different concrete layers. In addition to obtaining the optimum combination between mechanical and chemical bonding.

c. It is recommended to study the effect of using many WWM layers and the WWM orientation on strength of beams.

d. More performance tests are recommended to be performed such as: measuring strain in concrete, measuring strain in reinforcement steel and measuring strain in WWM to study their effect on theoretical investigation.

e. Study the effect of the following factors on the behavior of strengthened beams:

   i.   Drilling holes in the beam.
   ii. Friction effect at interface in a system composed of two concrete layers.
   iii. Beam size scale effect.

f. The theoretical analysis elaborated in this thesis could be used as an indicator of expected values for flexural strength and deflection, namely provided by jacketing. More experimental models with more large scale specimens and different parameters should be developed and compared with theoretical expected values.

g. It would be also interesting to remodel the strengthening technique present in this thesis using Finite Element Method (FEM) structural analysis software likes ALGOR, ANSYS and others, and investigate the stresses, deflections, strains, loads and crack patterns of the specimens.

h. It is recommended to study the bond strength between the SCC and the concrete substrate using suitable test methods.

i. It is recommended to study the effects of shrinkage for both SCC and the concrete substrate.

REFERENCES

Abu Almjd, S. (1988), **Repair and Strengthening of Concrete Members** [online], Lecture Notes, 1-47, and Available at: http://www.gulfup.com/?OcUxX4 [Accessed: 30 May 2015]. (Arabic).

Abu Hamam, I. M. (2008), **Rehabilitation Needs for Existing Buildings in Gaza Strip**, Master Thesis, November 2008, Palestine, Islamic University Of Gaza, and Available at: http://library.iugaza.edu.ps/thesis/83327.pdf [Accessed: 24 May 2015].

ACI Committee 318, (2014), **Building Code Requirements for Structural Concrete and Commentary (ACI 318M-14)**, American Concrete Institute, P.O. Box 9094, Farmington Hills, Michigan.

ACI Committee 546, (2004), **Concrete Repair Guide (ACI 546R-04)**, American Concrete Institute, Farmington Hills, Michigan.

Ajin, M., and Gokulram, H., (2015), **Flexural Behavior of RC Beam with Welded Mesh as Shear Reinforcement**, International Journal of Engineering Science & Research Technology, pp.242-246.

AL-Kuaity, A. S., (2010), **Strengthening of Cracked Reinforced Concrete-Beam by Jacketing**, Journal of Engineering, Vol. 16, 3, pp. 5753- 5771.

Altun F., (2004), **An Experimental Study of the Jacketed Reinforced-concrete Beams under Bending**, Construction and Building Materials Vol.18, pp.611-618.

Arote P.S., Dhindale G.B., Malunjkar J.A. and Umbare A.S., (2014), **Strengthening Of PCC Beams by Using Different Types of Wire Mesh Jacketing**, International Journal Of Modern Engineering Research, Vol. 4, Issue 4, pp. 56-58.

Beeralingegowda B., and Gundakalle V. D., (2013), **The Effect of Addition of Limestone Powder on The Properties of SCC** [online], International Journal of Innovative Research in Science, Engineering and Technology, ISSN: 2319-8753, Available at: http://www.ijirset.com/upload/september/75_THE%20EFFECT.pdf [Accessed: 07 August 2015].

[Carbon Fiber Wrapping] n.d. [Image online] and Available at: http://3.imimg.com/data3/MP/BD/MY-75588/carbon-fiber-wrapping-500x500.jpg

[Accessed: 03 June 2015].

Chalioris, C.E. and Constantin, N.P., (2012), **Rehabilitation of Shear-Damaged Reinforced Concrete Beams Using Self-Compacting Concrete Jacketing**, International Scholarly Research Network, ISRN Civil Engineering, Article ID 816107.

Diab, Y.G., (1998), "**Strengthening of RC Beams by Using Sprayed Concrete Experimental Approach**." Engineering Structures Vol. 20, pp. 631-643.

EFNARC, (2005), The European guidelines for self-compacting concrete; May 2005, pp. 1-63.

El-Ebweini, M. Sh., (2009), **Structural Performance of Repaired corroded Reinforced Concrete beams**, Master Thesis, July 2009, Palestine, Islamic University of Gaza, and Available at: http://library.iugaza.edu.ps/thesis/87289.pdf [Accessed: 26 May 2015].

Huang, X., Birman, V., Nanni, A. and Tunis, G., (2006), **Properties and potential for application of steel reinforced polymer and steel reinforced grout composites**, Composites Part B: Engineering, Vol. 36, No. 1, pp. 73–82.

Jaishankar, P., and Prathima, S., (2015), **Experimental Investigation of Wired Mesh - RC Beam**, International Journal of ChemTech Research, Vol.8, No.2, pp. 815-821.

Khalaf, Q. A. (2015), **Comparative Study for Strengthening Techniques of RC Beams Using Concrete Jackets and Steel Plates**, Master Thesis, February 2015, Palestine, Islamic University Of Gaza.

Mahdy, A. S., Seleem M. H., Sallam H.E.M., Abdin E.M. and El-Ghandour N. A., (2004), **Flexural Behavior and Mode of Failure of Jacketed RC Beams**, Scientific Bulletin., Vol. 39, pp. 75-90.

Mishra, G. (2014**), Strengthening of Concrete Structures** [online], Available at: http://theconstructor.org/structural-engg/strengthening-structures/1576/ [Accessed: 22 May 2015].

Mostosi, S., Meda, A., Riva, P., and Maringoni, S., (2011), **Shear Strengthening of RC Beams with High Performance Jacket**, fib Symposium, Topic 3: Poster Session, pp.1-9.

Panda K. C., and Bal P. K., (2013), **Properties of Self Compacting Concrete Using Recycled Coarse Aggregate**, Science direct [online], Engineering (51) 159 –164, available from: http://www.sciencedirect.com/science/article/pii/S1877705813000246 [accessed 05 June 2015].

Pansal, P. P., Kumar, M., and Kaushik S.K., (2006), **Effect Of Wire Mesh Orientation On Strength Of Beams Retrofitted Using Ferrocement Jackets**, International Journal of Engineering, Volume (2) : Issue (1), pp.8-19.

Penelis G.G., and Kappos A., (1997), **Earthquake Resistant Concrete Structures**, First edition, Oxon: Taylor & Francis Group.

PMFSEL Report (1991), Reinforced Concrete Frame Connections Rehabilitated by jacketing, Sponsored by National Science Foundation, Grant No. ECE-8610946, 221 pp.

Qeshta, I. M.I., Shafigh, P., Jumaat, M. Z., Abdulla, A. I., Ibrahim, Z., and Alengaram, U. J., (2014),**The use of wire mesh–epoxy composite for enhancing the flexural performance of concrete beams**, Journal of Materials and Design , 60, pp. 250–259

Rehabcon Manual (2004), **Annex I strengthening with reinforced concrete**, [online], and Available at: http://www.cbi.se/objfiles/1/AnnexI_-1112262222.pdf [Accessed: 03 June 2015].

Rehabcon Manual (2004), **Annex K Strengthening of concrete structures using externally bonded steel plates**, [online], and Available at: http://www.cbi.se/objfiles/1/AnnexK_-935007756.PDF [Accessed: 03 June 2015].

Shehata, I., and Shehata L. (2008), **Strengthening of Reinforced Concrete Beams in Flexure by Partial Jacketing**, Materials and Structures Vol. 42, pp. 495-504.

[SIKA Carbodur] n.d. [Image online] Available at: http://www.rekocentrum.cz/data/gallery/0042.jpg [Accessed: 03 June 2015].

[Spot welding], [Image online] and Available at:
http://www.substech.com/dokuwiki/doku.php?id=resistance_welding_rw [Accessed: 07 August 2015].

Wikipedia (2015) Spot welding [online], available:

https://en.wikipedia.org/wiki/Spot_welding [Accessed: 07 August 2015].

Xing G., Wu T., Liu B., Huang H. and Gu S. (2010) **Experimental Investigation of Reinforced Concrete T-Beams Strengthened with Steel Wire Mesh Embedded in Polymer Mortar Overlay** [online], Advances in Structural Engineering, Volume 13 No.1, pp. 69-79, Available at: http://xingguohua.net/wp-content/uploads/2013/11/6-08-726_Xing.pdf [Accessed: 22 October 2014].

Yang, F. (2004) **Report #1: Self-Consolidating Concrete** [online], Available at: http://www.ce.berkeley.edu/~paulmont/241/Reports_04/SCC_report.pdf [Accessed: 17 May 2015].

Ziara, M., Touqan, S. and Naser, K. (1996) **Evaluation of Housing Affordability and conditions in Palestine**. Special Presentation, International Conference on Affordable Housing in Palestine, Birzeit University, Palestine.

Ziara, M. M. (2014), **Strengthening of Structures Lecture Notes**, ENGC 6355 Course, IUG.

A

APPENDIX A
"Repair Materials Specifications"

Standard stud anchor HSA

Base materials
- Concrete (uncracked)

Applications
- Wide range of fastening applications in concrete
- Fastening columns and beams

Advantages
- ETA approved torquing with SIW 22-A impact wrench and S-TB
- Fast and easy anchor setting with S-TB
- Excellent edge and spacing distances
- High loads (optimal utilization of the concrete strength)
- 3 embedment depths offering maximum flexibility
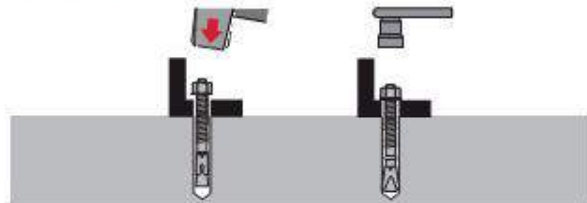
Standard stud anchor HSA

Technical data

Material composition	Steel, zinc-plated (min. 5 µm)
Head configuration	Externally threaded
PROFIS	Yes

Ordering designation	Drill bit diameter	Anchor size	Anchor length	Base plate clearance hole	Required tightening torque	Socket size	Wrench size	Sales pack quantity	Item number
HSA M6 5/-/-	6 mm	M6	50 mm	7 mm	5 Nm	10 mm	10 mm	200	2036084
HSA M6 20/10/-	6 mm	M6	65 mm	7 mm	5 Nm	10 mm	10 mm	200	2036085
HSA M8 5/-/-	8 mm	M8	55 mm	9 mm	15 Nm	13 mm	13 mm	100	2004122
HSA M8 20/10/-	8 mm	M8	70 mm	9 mm	15 Nm	13 mm	13 mm	100	2004123
HSA M8 35/25/-	8 mm	M8	85 mm	9 mm	15 Nm	13 mm	13 mm	80	2004124
HSA M10 5/-/-	10 mm	M10	68 mm	12 mm	25 Nm	17 mm	17 mm	50	2004127
HSA M10 20/10/-	10 mm	M10	83 mm	12 mm	25 Nm	17 mm	17 mm	50	2004128
HSA M10 35/25/-	10 mm	M10	98 mm	12 mm	25 Nm	17 mm	17 mm	40	2004129
HSA M10 50/40/10	10 mm	M10	113 mm	12 mm	25 Nm	17 mm	17 mm	40	2004150
HSA M12 5/ -/-	12 mm	M12	85 mm	14 mm	50 Nm	19 mm	19 mm	25	2004154
HSA M12 20/5/-	12 mm	M12	100 mm	14 mm	50 Nm	19 mm	19 mm	25	2004155
HSA M12 35/20/-	12 mm	M12	115 mm	14 mm	50 Nm	19 mm	19 mm	25	2004156
HSA M12 65/50/15	12 mm	M12	145 mm	14 mm	50 Nm	19 mm	19 mm	25	2004157
HSA M12 95/80/45	12 mm	M12	175 mm	14 mm	50 Nm	19 mm	19 mm	25	2004158
HSA M16 5/-/-	16 mm	M16	102 mm	18 mm	80 Nm	24 mm	24 mm	16	2004161
HSA M16 20/5/-	16 mm	M16	117 mm	18 mm	80 Nm	24 mm	24 mm	16	2004162
HSA M16 40/25/-	16 mm	M16	137 mm	18 mm	80 Nm	24 mm	24 mm	16	2004163
HSA M16 85/70/30	16 mm	M16	182 mm	18 mm	80 Nm	24 mm	24 mm	16	2004164
HSA M16 135/120/80	16 mm	M16	232 mm	18 mm	80 Nm	24 mm	24 mm	16	2004165
HSA M20 10/-/-	20 mm	M20	125 mm	22 mm	200 Nm	30 mm	30 mm	10	2036088
HSA M20 55/30/15	20 mm	M20	170 mm	22 mm	200 Nm	30 mm	30 mm	10	2036089

Mean ultimate resistance

Anchor size			M6			M8			M10		
Effective anchorage depth h_{ef}	[mm]		30	40	60	30	40	70	40	50	80
Tensile $N_{Ru,m}$											
HSA, HSA-BW	[kN]		8,0	9,5	9,5	11,0	17,0	17,3	17,0	23,7	29,4
HSA-R2, HSA-R	[kN]		8,0	10,0	11,9	11,0	17,0	19,2	17,0	23,7	33,2
Shear $V_{Ru,m}$											
HSA, HSA-BW	[kN]		6,8	6,8	6,8	11,0	11,1	11,1	19,8	19,8	19,8
HSA-R2, HSA-R	[kN]		7,6	7,6	7,6	11,0	12,9	12,9	23,7	23,7	23,7

Anchor size			M12			M16			M20		
Effective anchorage depth h_{ef}	[mm]		50	65	100	65	80	120	75	100	115
Tensile $N_{Ru,m}$											
HSA, HSA-BW	[kN]		23,7	35,1	43,5	35,1	48,0	66,4	43,5	67,0	82,7
HSA-R2, HSA-R	[kN]		23,7	35,1	46,5	35,1	48,0	66,4	43,5	67,0	82,7
Shear $V_{Ru,m}$											
HSA, HSA-BW	[kN]		31,0	31,0	31,0	53,6	53,6	53,6	87,1	90,1	90,1
HSA-R2, HSA-R	[kN]		30,8	30,8	30,8	59,3	59,3	59,3	87,1	96,5	96,5

Characteristic resistance

Anchor size			M6			M8			M10		
Effective anchorage depth h_{ef}	[mm]		30	40	60	30	40	70	40	50	80
Tensile N_{Rk}											
HSA, HSA-BW	[kN]		6,0	7,5	9,0	8,3	12,8	16,0	12,8	17,9	25,0
HSA-R2, HSA-R	[kN]		6,0	7,5	9,0	8,3	12,8	16,0	12,8	17,9	25,0
Shear V_{Rk}											
HSA, HSA-BW	[kN]		6,5	6,5	6,5	8,3	10,6	10,6	18,9	18,9	18,9
HSA-R2, HSA-R	[kN]		7,2	7,2	7,2	8,3	12,3	12,3	22,6	22,6	22,6

Anchor size			M12			M16			M20		
Effective anchorage depth h_{ef}	[mm]		50	65	100	65	80	120	75	100	115
Tensile N_{Rk}											
HSA, HSA-BW	[kN]		17,9	26,5	35,0	26,5	36,1	50,0	32,8	50,5	62,3
HSA-R2, HSA-R	[kN]		17,9	26,5	35,0	26,5	36,1	50,0	32,8	50,5	62,3
Shear V_{Rk}											
HSA, HSA-BW	[kN]		29,5	29,5	29,5	51,0	51,0	51,0	65,6	85,8	85,8
HSA-R2, HSA-R	[kN]		29,3	29,3	29,3	56,5	56,5	56,5	65,6	91,9	91,9

Design resistance

Anchor size			M6			M8			M10		
Effective anchorage depth	h_{ef}	[mm]	30	40	60	30	40	70	40	50	80
Tensile N_{Rd}											
HSA, HSA-BW	[kN]		4,0	5,0	6,0	5,5	8,5	10,7	8,5	11,9	16,7
HSA-R2, HSA-R	[kN]		4,0	5,0	6,0	5,5	8,5	10,7	8,5	11,9	16,7
Shear V_{Rd}											
HSA, HSA-BW	[kN]		5,2	5,2	5,2	5,5	8,5	8,5	15,1	15,1	15,1
HSA-R2, HSA-R	[kN]		5,5	5,8	5,8	5,5	9,8	9,8	18,1	18,1	18,1
Anchor size			M12			M16			M20		
Effective anchorage depth	h_{ef}	[mm]	50	65	100	65	80	120	75	100	115
Tensile N_{Rd}											
HSA, HSA-BW	[kN]		11,9	17,6	23,3	17,6	24,1	33,3	21,9	33,7	41,5
HSA-R2, HSA-R	[kN]		11,9	17,6	23,3	17,6	24,1	33,3	21,9	33,7	41,5
Shear V_{Rd}											
HSA, HSA-BW	[kN]		23,6	23,6	23,6	40,8	40,8	40,8	43,7	68,6	68,6
HSA-R2, HSA-R	[kN]		23,4	23,4	23,4	45,2	45,2	45,2	43,7	73,5	73,5

Recommended loads

Anchor size			M6			M8			M10		
Effective anchorage depth	h_{ef}	[mm]	30	40	60	30	40	70	40	50	80
Tensile N_{rec} [a]											
HSA, HSA-BW	[kN]		2,9	3,6	4,3	4,0	6,1	7,6	6,1	8,5	11,9
HSA-R2, HSA-R	[kN]		2,9	3,6	4,3	4,0	6,1	7,6	6,1	8,5	11,9
Shear V_{rec} [a]											
HSA, HSA-BW	[kN]		3,7	3,7	3,7	4,0	6,1	6,1	10,8	10,8	10,8
HSA-R2, HSA-R	[kN]		4,0	4,1	4,1	4,0	7,0	7,0	12,9	12,9	12,9
Anchor size			M12			M16			M20		
Effective anchorage depth	h_{ef}	[mm]	50	65	100	65	80	120	75	100	115
Tensile N_{rec} [a]											
HSA, HSA-BW	[kN]		8,5	12,6	16,7	12,6	17,2	23,8	15,6	24,0	29,7
HSA-R2, HSA-R	[kN]		8,5	12,6	16,7	12,6	17,2	23,8	15,6	24,0	29,7
Shear V_{rec} [a]											
HSA, HSA-BW	[kN]		16,9	16,9	16,9	29,1	29,1	29,1	31,2	49,0	49,0
HSA-R2, HSA-R	[kN]		16,7	16,7	16,7	32,3	32,3	32,3	31,2	52,5	52,5

a) With overall partial safety factor for action $\gamma = 1.4$. The partial safety factors for action depend on the type of loading and shall be taken from national regulations.

Materials

Mechanical properties

Anchor size			M6	M8	M10	M12	M16	M20
Nominal tensile strength $f_{uk,thread}$	HSA HSA-BW	[N/mm²]	650	580	650	700	650	700
	HSA- R2 HSA-R	[N/mm²]	650	560	650	580	600	625
Yield strength $f_{yk,thread}$	HSA HSA-BW	[N/mm²]	520	464	520	560	520	560
	HSA-R2 HSA-R	[N/mm²]	520	448	520	464	480	500
Stressed cross-section $A_{s,thread}$	HSA HSA-BW HSA-R2 HSA-R	[mm²]	20,1	36,6	58,0	84,3	157,0	245,0
Moment of resistance W	HSA HSA-BW HSA-R2 HSA-R	[mm³]	12,7	31,2	62,3	109,2	277,5	540,9
Char. bending resistance $M^0_{Rk,s}$	HSA HSA-BW	[Nm]	9,9	21,7	48,6	91,7	216,4	454,4
	HSA-R2 HSA-R	[Nm]	9,9	21,0	48,6	76,0	199,8	405,7

Material quality

Type	Part	Material	Coating
HSA HSA-BW Carbon Steel	Bolt	Carbon-steel	Galvanized (≥5 μm)
	Sleeve	Carbon-steel	
	Washer	HSA :carbon steel, HSA-BW: carbon steel	
	Hexagon nut	Steel, strength class 8	
HSA-R2 Stainless Steel Grade A2	Bolt	Stainless steel A2, 1.4301 or 1.4162	M6 - M20 coated
	Sleeve	Stainless steel A2, 1.4301 or 1.4404	-
	Washer	Stainless steel grade A2	-
	Hexagon nut	Stainless steel grade A2	M6 - M20 coated
HSA-R Stainless Steel Grade A4	Bolt	Stainless steel grade A4, 1.4401 or 1.4362	M6 - M20 coated
	Sleeve	Stainless steel A2, 1.4301 or 1.4404	-
	Washer	Stainless steel grade A4	-
	Hexagon nut	Stainless steel grade A4	M6 - M20 coated

180

HILTI

Geometry washer

Anchor Size			M6	M8	M10	M12	M16	M20
Inner diameter d_1								
HSA, HSA-R2/ R	d_1	[mm]	6,4	8,4	10,5	13,0	17,0	21
HSA-BW	d_1	[mm]	6,4	8,4	10,5	13,0	17,0	22
Outer diameter d_2								
HSA, HSA-R2/ R	d_2	[mm]	12,0	16,0	20,0	24,0	30,0	37,0
HSA-BW	d_2	[mm]	18,0	24,0	30,0	37,0	50,0	60,0
Thickness h								
HSA, HSA-R2/ R	h	[mm]	1,6	1,6	2,0	2,5	3,0	3,0
HSA-BW	h	[mm]	1,8	2,0	2,5	3,0	3,0	4,0

Anchor dimensions and coding

Product marking and identification of anchor

Beginning of thread: setting depth indicator for $h_{nom,1}$
$h_{nom,1}$ is reached when non-threaded part of the bolt is completely below the concrete surface

Blue ring: setting depth indicator for $h_{nom,2}$
$h_{nom,2}$ is reached when the blue ring is completely below the concrete surface

Sleeve Bolt Washer Nut Letter code

Marking:

Material code

e.g.
Hilti HSA   ... Brand and Anchor type
M12 65/50/15 ... Anchor Size and the max. $t_{fix,1}/t_{fix,2}/t_{fix,3}$ for the corresponding $h_{nom,1}/h_{nom,2}/h_{nom,3}$

181

Epoxy

EPICHOR 1768
Patch Repairing Quick Setting Epoxy

General Properties:
- **EPICHOR 1768** is two component solvent free, clear epoxy product.
- Can be mixed with graded sand to be used as a fixing dowels in concrete and repairing mortar.
- Is relatively insensitive to moisture.
- Has quick initial setting time.
- Has thyrotrophic effect, thus suitable for fixing steel dowels to concrete especially to soffits and vertical surfaces.
- Has high compressive, tensile & bond strength which ensures monolithic behavior with concrete.

Uses:
- As an adhesive mortar for fixing dowels in concrete.
- As patch repair mortar for concrete.
- In machinery & rail grouts.
- For repairing & coatings of potable water tanks.

Application:
1. Clean the holes and remove oil and grease or foreign materials.
2. Wear gloves & eye goggles before working & be sure of good ventilation.
3. Add resin **EPICHOR 1768** to hardener and mix well. Apply **EPICHOR 1768** as a primer inside the hole (the hole should be 6mm wider than the steel bar).
4. To make the mortar add resin **EPICHOR 1768** to hardener and mix well, then add the filling to the previous mixture & mix well till reaching a mortar with homogenous consistency.
5. Apply **EPICHOR 1768** mortar with the suitable tool according to usage purpose.
6. Fill 2/3 of the hole with mixed mortar, insert the steel bar in. Be sure that the bar is imbedded with enough suitable depth in the hole,
7. Failure should happen to steel before its separation from hole.
8. Clean tools using solvent ex: Thinner.

Technical Data:

ASTM (C - 580 Method A)	: Flexural test	
Flexural strength (After 7 days)		42 N/mm^2
Flexural strength (After 24 days)		67 N/mm^2
Modulus of Elasticity		2320 N/mm^2

Bs-En 1881-2006 : **PULLOUT** test

1. For pure epoxy (Resin + Hardener)

Bond strength	6.7 N / mm^2	Failure happened to steel bar
For rod Ø = 8mm, Imbedded length = 51mm		Failure load = 0.88 ton
The steel bar used is mild steel test done after 15 days from casting date.		

2. For Mortar epoxy (Resin + Hardener + filling)

Bond strength	9.70 N / mm^2	Failure happened by yield of steel bar before pullout
• For rod Ø =11mm, Imbedded length = 94 mm		Failure load = 3.0 ton
• Tests were carried after 7 days from casting date.		
• Concrete compressive strength 31.4 N /mm^2.		
• Bond between steel and concrete is achieved by **Epichor 1768** mixed with graded special sand by thickness about 3 mm around steel bar (R+H) : filling 1 - 4		

Tensile strength	: 2.90 N/mm^2 (After 7 days) ASTM (C 301)
Compressive strength	: 54.0 N/mm^2 (After 7 days) ASTM (C 579 Method B)
Initial Curing Time	: After 24 hours of mixing
Final Curing Time	: After 7 days at ambient temperature
Pot Life	: 20 min. at 24°C
Density	: 2.1 gm / cm^3 for mortar epoxy
Chemical Resistance	: Excellent resistance against water, alkalis, and detergents, moderate against acids; poor against organic solvents.
Shelf Life	: 18 months in closed container and away from sun light, heat and humidity.

Environment:　　　- Boots, rubber gloves, dust masks, and safety goggles.
　　　　　　　　　　　- Refer to MATERIAL SAFETY DATA SHEETS (MSDS)

END OF TECHNICAL DATA

YASMO MISR　　　　　　　　　　　　　　**Quality between your hands**

Sika ViscoCrete® -5920

High Performance Superplasticiser Concrete Admixture

Product Description	Sika ViscoCrete® -5920 is a third generation super plasticizer for concrete and mortar. It meets the requirements for super plasticizers according to ASTM-C- 494 Types G and F and BS EN 934 part 2: 2001.
Uses	Sika ViscoCrete® -5920 facilitates extreme water reduction, excellent flowability with at the same time optimal cohesion and highest self compacting behaviour.

Sika ViscoCrete® -5920 is used for the following types of concrete:

- Precast Concrete
- Ready Mix Concrete
- Concrete with highest water reduction (Up to 30%).
- High Strength Concrete
- Hot Weather Concrete
- Self Compacting Concrete

High water reduction, excellent flowability, coupled with high early strengths, have a positive influence on the above mentioned applications.

Advantages	Sika ViscoCrete® -5920 as a powerful superplasticiser acts by different mechanisms.

Through surface adsorption and sterical separation effect on the cement particles, in parallel to the hydration process, the following properties are obtained:

- Strong self compacting behaviour. Therefore suitable for the production of self compacting concrete.
- Extremely high water reduction (resulting in high density and strengths).
- Excellent flowability (resulting in highly reduced placing and compacting efforts).
- Increase high early strengths development.
- Improved shrinkage and creep behaviour.
- Reduced rate of carbonation of the concrete.
- Improved Water Impermeability.

Sika ViscoCrete® -5920 does not contain chloride or other ingredients promoting corrosion of steel reinforcement. It is therefore suitable to be used without any restrictions for reinforced and prestressed concrete production.

Technical Data

Base	Aqueous solution of modified Polycarboxylates
Appearance / Colour	Light brownish liquid
Density	1.09 ± 0.01 kg/lt
Solid content	36%
Packaging	5 and 20 kg pails
	220 kg drums
	Bulk Tanks packing available upon request
Storage / Shelf Life	12 months from date of production if stored properly in unopened and undamaged, original sealed packaging, in dry temperatures between +5°C and +35°C. Protected from direct sunlight and frost.

Construction

Innovation & since
Consistency 1910

Application

Dosage

■ For flowing and self compacting concrete (S.C.C.): 0.5 – 2.0% litre by weight of cement depending on desired workability and strength. It is advisable to carry out trail mixes to establish the correct dosage rate required.

Dispensing

Sika ViscoCrete® -5920 is added to the gauging water or added with it into the concrete mixer.

To take advantage of the high water reduction, a wet mixing time of at least 60 seconds is recommended.

To avoid excess water in the concrete, the final dosage must begin only after 2/3 of the wet mixing time.

Concrete Placing

The standard rules of good concreting practice, concerning production as well as placing, are to be followed.

Fresh concrete must be cured properly and as early as possible.

Compatibility

Sika ViscoCrete® -5920 may be combined with the following Sika products:

■ Sika Pump®
■ Sika Rapid®
■ Sika Ferrogard®-901
■ Sikafume®
■ Sika Fro®-V5A
■ Sika Retarder®

Pre-trials are recommended if combinations with the above products are being made.

Important Notes

If frozen and/or if precipitation has occurred, Sika ViscoCrete® -5920 may be used after thawing slowly at room temperature and after intensive mixing.

Safety Instructions

Safety Precautions

In contact with skin, wash off with soap and water.

In contact with eyes or mucous membrane, rinse immediately with clean warm water and seek medical attention without delay.

Ecology

Residues of material must be removed according to local regulations. Fully cured material can be disposed of as household waste under agreement with the responsible local authorities.

Transport

Non-hazardous

Toxicity

Non-Toxic under relevant health and safety codes.

B

APPENDIX B

"Deflection Derivation of Two Point Loading Beam"

The deriviation of mid-span deflection of a beam subjected to two point loading as shown in Figure B.1 has been calculated based on **equation of the Elastic Curve**.
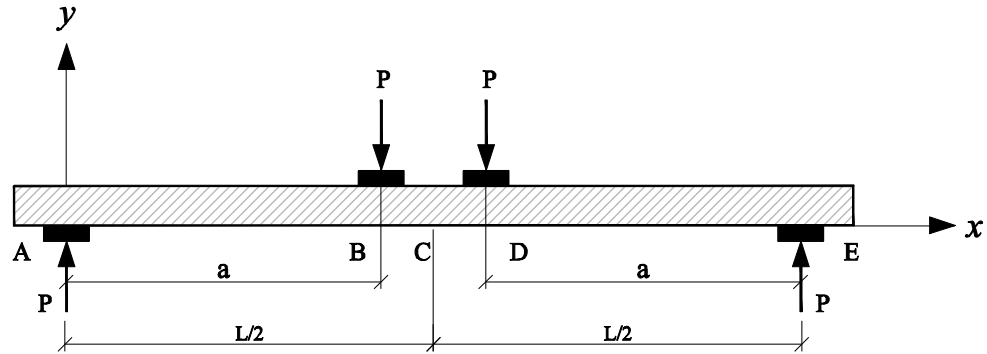
Figure B.1 Beam subjected to two point loading.

Consider porion ABC only, and consider symmetry about C.

Reaction at A and B = P

Boundary conditions:[x=0, y=0], [x=a, y=y], [x=a, $\frac{dy}{dx} = \frac{dy}{dx}$], [x=$\frac{L}{2}$, $\frac{dy}{dx} = 0$]

For $(0 < x < a)$

$$EI\frac{d^2y}{dx^2} = M = P.x$$

$$EI\frac{dy}{dx} = \frac{1}{2}P.x^2 + C_1 \qquad\qquad\qquad\qquad \textbf{(B.1)}$$

$$EI.y = \frac{1}{6}P.x^3 + C_1x + C_2 \qquad\qquad\qquad\qquad \textbf{(B.2)}$$

When $[\text{x} = 0, \text{y} = 0] \rightarrow C_2 = 0$

For $(a < x < \frac{L}{2})$

$$EI\frac{d^2y}{dx^2} = M = P.a$$

$$EI\frac{dy}{dx} = P.a.x + C_3 \qquad\qquad\qquad\qquad \textbf{(B.3)}$$

$$EI.y = \frac{1}{2}P.a.x^2 + C_3.x + C_4 \qquad\qquad\qquad\qquad \textbf{(B.4)}$$

When $[\text{x} = \frac{L}{2}, \frac{dy}{dx} = 0] \rightarrow C_3 = -\frac{1}{2}PaL$

@ Point B$\rightarrow x = a$, [x=$\frac{L}{2}, \frac{dy}{dx} = \frac{dy}{dx}$]

and equation 1 = equation 3 →

$$\frac{1}{2}P.x^2 + C_1 \quad = P.a.x + C_3$$

$$\frac{1}{2}P.a^2 + C_1 \quad = P.a^2 + \left(-\frac{1}{2}PaL\right) \quad \to \quad C_1 = (\frac{1}{2}Pa^2 - \frac{1}{2}PaL)$$

@ Point B→ $x = a$, [x=$\frac{L}{2}$, $y = y$]

and equation 2 = equation 4 →

$$\frac{1}{6}P.x^3 + C_1 x + C_2 = \frac{1}{2}P.a.x^2 + C_3.x + C_4$$

$$\frac{1}{6}P.a^3 + \left(\frac{1}{2}Pa^2 - \frac{1}{2}PaL\right)a + 0 = \frac{1}{2}P.a^3 - \frac{1}{2}Pa^2L + C_4 \quad \to \quad C_4 = (\frac{1}{6}Pa^3)$$

So that, The Elastic Curve for Portion BD is

$$EI.y = \frac{1}{2}P.a.x^2 + C_3.x + C_4$$

$$EI.y = \frac{1}{2}P.a.x^2 - \frac{1}{2}PaL.x + \frac{1}{6}Pa^3$$

$$y = \frac{P}{EI}(\frac{1}{2}a.x^2 - \frac{1}{2}aL.x + \frac{1}{6}a^3)$$

For Deflection @ C → $set\ x = \frac{L}{2}$

$$y_c = \frac{P}{EI}(\frac{1}{8}a.L^2 - \frac{1}{4}a.L^2 + \frac{1}{6}a^3)$$

$$y_c = -\frac{Pa}{24EI}(3L^2 - 4a^2) \tag{B.5}$$

C

APPENDIX C
"SCC Test Methods According to EFNARC"

C.1   Applied Tests on Fresh SCC

EFNARC defines test methods for SCC. The testing for SCC consists of tests for both the fresh and hardened concrete. The fresh concrete tests are applied to ensure the self-compacted properties for concrete. There are many different methods of testing to characterize the SCC fresh properties of filling abilities, passing abilities, workability and segregation resistance. So there are no single or combination of methods that are universally approved or achieved. At the same time there are no single method found to characterize all relevant workability aspects so each mix design should be applied to number of tests for different workability parameter. In this research we will focus on the following fresh tests:

C.1.1   Slump-flow and T500 time for SCC

The slump-flow and T500 time is a test to assess the flowability and the flow rate of SCC in the absence of obstructions (**EFNARC, 2005**). It is based on the slump test to measure two parameters the flow speed and the flow time. The result is an indication of the filling ability of SCC. The T500 time is also a measure of the speed of flow and hence the viscosity of the SCC, also the test is not suitable when the maximum size of the aggregate exceeds 40 mm.

The fresh concrete is poured into a cone as used for the normal slump test as shown in Figure (C.1). When the cone is withdrawn upwards the time from commencing upward movement of the cone to when the concrete has flowed to a diameter of 500 mm is measured; this is the T500 time. The largest diameter of the flow spread of the concrete and the diameter of the spread at right angles to it are then measured and the mean is the slump-flow.
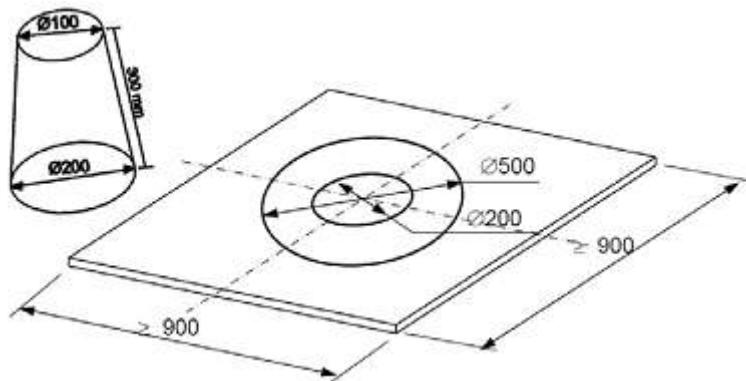
Figure C.1 Base plate & the Abrams Cone. (Source: **EFNARC, 2005**)

For detailed procedure of this test revise to the European guidelines for SCC,

(**EFNARC, 2005**), but it was concluded as follows:

The first step is to use the same basic equipment of the conventional slump test method but without using rod to stroke the concrete. Then place the cleaned base plate in a stable leveled position, fill the cone without any agitation or rodding, and strike off surplus from the top of the cone. Allow the filled cone to stand for not more than 30s; during this time remove any spilled concrete from the base plate and ensure the base plate is damp all over but without any surplus water. Lift the cone vertically in one movement without interfering with the flow of concrete. If the T500 time has been requested, start the stop watch immediately the cone ceases to be in contact with the base plate and record the time taken to the nearest 0,1 s for the concrete to reach the 500 mm circle at any point. Without disturbing the base plate or concrete, measure the largest diameter of the flow spread and record it as d_m to the nearest 10 mm. Then measure the diameter of the flow spread at right angles to d_m to the nearest 10 mm and record as dr to the nearest 10 mm as shown in Figure (C.2).

Figure C.2 SCC flow spread measurment. (Source: **EFNARC, 2005**)

Check the concrete spread for segregation. The cement paste/mortar may segregate from the coarse aggregate to give a ring of paste/mortar extending several millimeters beyond the coarse aggregate. Segregated coarse aggregate may also be observed in the central area. Report that segregation has occurred and that the test was therefore unsatisfactory. Then the slump-flow is the mean of **dm** and **dr** expressed to the nearest 10 mm, and the T500 time is reported to the nearest 0.1 s.

C.1.2 V- Funnel Test

The V-funnel test is used to assess the viscosity and filling ability of SCC (**EFNARC, 2005**). A V shaped funnel see Figure (C.3) is filled with fresh concrete and the time taken for the concrete to flow out of the funnel is measured and recorded as the V-funnel flow time. V-funnel, made to the dimensions (tolerance ± 1 mm), fitted with a quick release, Water tight gate at its base and supported so that the top of the funnel is horizontal. The V-funnel shall be made from metal; the surfaces shall be smooth, and not be readily attacked by cement paste or be liable to rusting. However container is needed to hold the test sample and having a volume larger than the volume of the funnel and not less than 12 Liter.

Figure C.3 V-Funnel apparatus, dimesnions in mm. (Source: **EFNARC,2005**)

For detailed procedure of this test revise to the European guidelines for SCC,

(**EFNARC, 2005**), but it was concluded as follows:

Clean the funnel and bottom gate, the dampen all the inside surface including the gate. Then close the gate and pour the sample of concrete into the funnel, without any agitation or rodding, then strike off the top with the straight edge so that the concrete is flush with the top of the funnel. Place the container under the funnel in order to retain the concrete to be passed. After a delay of (10 ± 2) s from filling the funnel, open the gate and measure the time t_v, to 0,1 s, from opening the gate to when it is possible to see vertically through the funnel into the container below for the first time. t_v is the V-funnel flow time.

C.1.3 L-Box Test

\The L-box test is used to assess the passing ability of SCC to flow through tight openings including spaces between reinforcing bars and other obstructions without segregation or blocking (**EFNARC, 2005**). There are two variations; the two bar test and the three bar test. The three bar test simulates more congested reinforcement. The main concept of this test is to allow a measured volume of fresh concrete to flow horizontally through the gaps between vertical, smooth reinforcing bars and the height of the concrete beyond the reinforcement is measured. L-box have the general arrangement as shown in Figure (C.4)
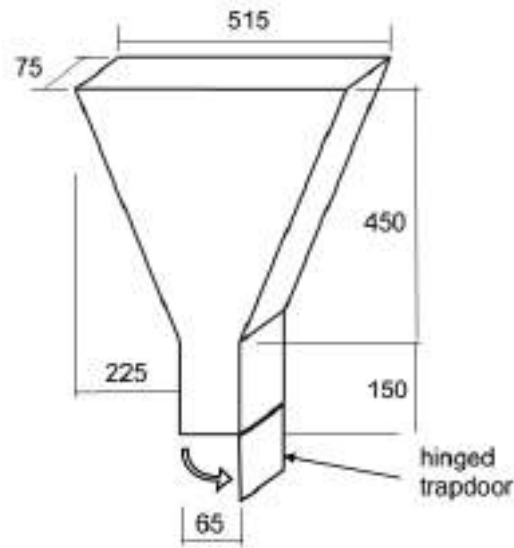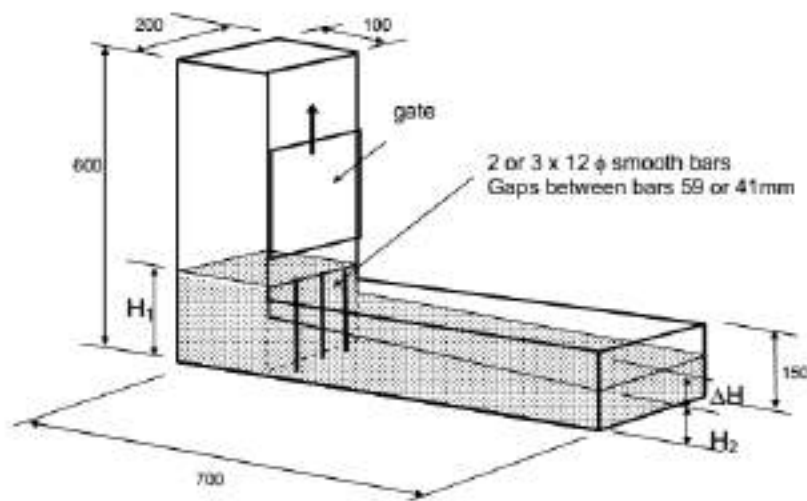

Figure C.4 L-Box apparatus, dimesnions in mm. (Source: **EFNARC,2005**)

For detailed procedure of this test revise to the European guidelines for SCC,

(**EFNARC, 2005**), but it was concluded as follows:

Support the L-box on a level horizontal base and close the gate between the vertical and horizontal sections. Pour the concrete from the container into the filling hopper of the L box and allow standing for (60 ± 10) s. Record any segregation and then raise the gate so that the concrete flows into the horizontal section of the box. When movement has ceased, measure the vertical distance, at the end of the horizontal section of the L-box, between the top of the concrete and the top of the horizontal section of the box at three positions equally spaced across the width of the box. By difference with the height of the horizontal section of the box, these three measurements are used to calculate the mean depth of concrete as H2 mm. The same procedure is used to calculate the depth of concrete immediately behind the gate as H1 mm. The passing ability PA is calculated from the following equation C.1.

$$Passing\ Ability\ (PA) = \frac{H_2}{H_1} \qquad\qquad\qquad\qquad\qquad \textbf{(C.1)}$$

The EFNARC Guidelines are not intended to provide specific detailed procedure but also gives a typical range of acceptance criteria to ensure that all aspects of SCC are fulfilled as per mentioned in table (C.1).

Table (C.1). Acceptance criteria of EFNARC for fresh properties of SCC

	Testing Method	**Characteristic**	**Unit**	**Typical Range of Values**	
				Min.	**Max.**
1	Slump Flow Test	Flowability	mm	550	850
2	T500 Slump Flow	Viscosity (assessed by rate of flow)	Sec.	2	6
3	L Box Test	Passing ability	H2/H1	0.80	1.00
4	V-Funnel Test	Viscosity / Filling ability	Sec	2	9
5	Standards molds	Compressive Strength (fc')	MPa	According to job mix design	

C.2   Applied Tests on Hardened SCC

The hardened test is applied to verify the compressive strength of concrete. This test is done according to ASTM standards to measure the compressive strength of standard cubes of hardened concrete. Standard molds 100x100x100 mm cube specimens were prepared, fully filled with fresh concrete at once without any compacting with standard rods after that the molds are covered with a plastic sheets for 24 hours to prevent moisture loss.

D

APPENDIX D

"Shear Connectors Calculations"

The laminar shear is developed in the specimen's beams due to the non-Homogeneity between two concrete layers of the main and strengthened layer. Laminar shear will be resisted only by roughening the surface and anchors. The shear capacity of the anchors is calculated according to **REHABCON ANNEX I** strengthening with RC specifications.

The load bearing capacity of a dowel can according to REHABCON ANNEX I be calculated as:

$$F = \emptyset^2 \sqrt{f_{cc} \cdot f_{st}} \qquad \text{(D.1)}$$

Where:

F: Load bearing capacity of a dowel (Pa).
Ø: Diameter of one dowel (m).
f$_{cc}$: Compressive strength of the concrete (Pa).
f$_{st}$: Tensile strength of the steel (Pa).

However, since the force acting on the dowel shall be transferred to the substrate the load-bearing capacity of a dowel never can exceed the load-bearing capacity of the concrete:

$$F = 0.2\ b\ c\ f_{ct} \qquad \text{(D.2)}$$

Where:
F: Load bearing capacity of a dowel (Pa).
b: Distance between each column of dowels ,or distance to edge (m).
c: Distance between each row of dowels (m).
f$_{ct}$: Tensile strength of the concrete which equal to 10 % of f$_{cc}$ of concrete (Pa).

To calculate the number of dowels of a beam the following calculation is required.

Ø: Diameter of one dowel = 0.008 m.
f$_{cc}$: Compressive strength of the concrete (control beams) = 38.607 x 10^6 Pa.
f$_{st}$: Tensile strength of the steel= 444.70 x 10^6 Pa.
b: Distance between each column of dowels =0.05m ,or distance to edge =0.06 m.

From **Equation D.1** can you get

$$F = \emptyset^2 \sqrt{f_{cc} \cdot f_{st}} = 0.008^2 \times \sqrt{(38.607 \times 10^6) \times (444.70 \times 10^6)}$$

$$F = 8385.84\ \text{N}$$

Take 30 % reduction factor of the load bearing capacity of a dowel for safety.

$$F = 0.7 \times (8385.84) = 5870.10 \text{ N}$$

To find the distance between two dowels equalize **D.1** with **D.2**, then:

$$F = 5870.10 \text{ N} = \ 0.2 \ b \ c \ f_{ct}$$

$$\Rightarrow 5870.10 \text{ N} = \ 0.2 \ (0.05) \times c \ \times (\frac{10}{100} \times 38.607 \times 10^6)$$

$$\Rightarrow c = 0.152 \ m$$

So that the distance between each dowels row is 0.152 m, and it was taken 0.12 m for each face of the original beam in this study as shown in Figure D.1.
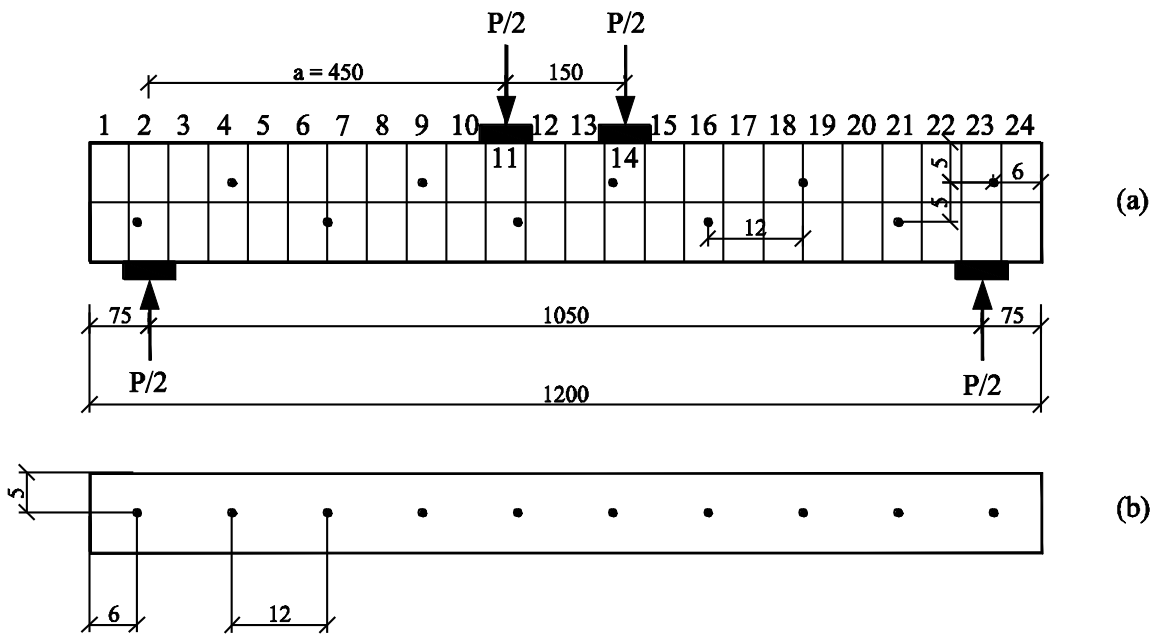

Figure D.1 Shear connector distribution at (a) both sides, (b) lower surface.

E

APPENDIX E
"Theoretical Analysis"

Table E.1 Beams Charateristics.

Beam	b (mm)	h (mm)	L (mm)	a (mm)	Es (Mpa)	Ew (Mpa)	fc' (Mpa)	Ec (MPa)	fy (Mpa)	fu (Mpa)	fyw (Mpa)	fuw (Mpa)	hw1 (mm)	hw2 (mm)	hw3 (mm)	hw4 (mm)	hw5 (mm)	As (mm2)	Asw1 (mm2)	Asw2 (mm2)	Asw3 (mm2)	Asw4 (mm2)	Asw5 (mm2)
MA.B1	160	200	1050	450	204000	25000	39.290	29460.40	444.7	689.9	250	280	181	156	127.5	99	70.5	157.1	48.11	19.25	19.25	19.25	19.25
MA.B2	160	200	1050	450	204000	25000	39.290	29460.40	444.7	689.9	250	280	181	156	127.5	99	70.5	157.1	48.11	19.25	19.25	19.25	19.25
MB.B1	160	200	1050	450	204000	25000	37.258	28688.49	444.7	689.9	300	418.6	181	137.5	82.5			157.1	75.22	50.15	50.15		
MB.B2	160	200	1050	450	204000	25000	37.258	28688.49	444.7	689.9	300	418.6	181	137.5	82.5			157.1	75.22	50.15	50.15		
GA.B1	160	200	1050	450	204000	25000	41.987	30454.59	444.7	689.9	250	280	181	156	127.5	99	70.5	157.1	48.11	19.25	19.25	19.25	19.25
GA.B2	160	200	1050	450	204000	25000	41.987	30454.59	444.7	689.9	250	280	181	156	127.5	99	70.5	157.1	48.11	19.25	19.25	19.25	19.25
GA.B3	160	200	1050	450	204000	25000	41.986	30454.59	444.7	689.9	250	280	181	156	127.5	99	70.5	157.1	48.11	19.25	19.25	19.25	19.25
GA.B4	160	200	1050	450	204000	25000	41.987	30454.59	444.7	689.9	250	280	181	156	127.5	99	70.5	157.1	48.11	19.25	19.25	19.25	19.25
GA.B5	160	200	1050	450	204000	25000	40.598	29946.78	444.7	689.9	250	280	181	156	127.5	99	70.5	157.1	48.11	19.25	19.25	19.25	19.25
GA.B6	160	200	1050	450	204000	25000	40.598	29946.78	444.7	689.9	300	280	181	156	127.5	99	70.5	157.1	48.11	19.25	19.25	19.25	19.25
GB.B1	160	200	1050	450	204000	25000	41.429	30251.54	444.7	689.9	300	418.6	181	137.5	82.5			157.1	75.22	50.15	50.15		
GB.B2	160	200	1050	450	204000	25000	41.429	30251.54	444.7	689.9	300	418.6	181	137.5	82.5			157.1	75.22	50.15	50.15		
GB.B3	160	200	1050	450	204000	25000	41.429	30251.54	444.7	689.9	300	418.6	181	137.5	82.5			157.1	75.22	50.15	50.15		
GB.B4	160	200	1050	450	204000	25000	41.429	30251.54	444.7	689.9	300	418.6	181	137.5	82.5			157.1	75.22	50.15	50.15		
GB.B5	160	200	1050	450	204000	25000	40.598	29946.78	444.7	689.9	300	418.6	181	137.5	82.5			157.1	75.22	50.15	50.15		

Table E.2 Comparisons between Theoritical & Experimental Bending Moment Results.

Beam	Theoretical Calculated						Experimental			
	M_{cr} (KN.m)	Δ_{cr} (mm)	M_y (KN.m)	Δ_y (mm)	M_u (KN.m)	Δ_u (mm)	M_y (KN.m)	Δ_y (mm)	M_u (KN.m)	Δ_u (mm)
MA.B1	18.420	0.137	55.165	2.478	77.796	16.358	57.086	4.615	81.8834	13.765
MA.B2	18.420	0.137	55.165	2.478	77.796	16.358	61.026	5.13	87.1803	13.11
MB.B1	17.941	0.137	66.335	3.333	98.224	18.710	77.39	5.7	110.553	13.47
MB.B2	17.941	0.137	66.335	3.333	98.224	18.710	72.558	5.32	103.654	12.196
GA.B1	19.046	0.137	55.438	2.404	78.183	15.865	55.996	4.45	79.994	11.25
GA.B2	19.046	0.137	55.438	2.404	78.183	15.865	58.016	4.8	82.8798	14.815
GA.B3	19.046	0.137	55.438	2.404	78.183	15.865	55.624	4.55	79.4629	12.85
GA.B4	19.046	0.137	55.438	2.404	78.183	15.865	59.483	4.68	84.976	12.465
GA.B5	18.728	0.137	55.302	2.442	77.990	16.128	59.22	5.00	84.6	20.95
GA.B6	18.728	0.137	55.302	2.442	77.990	16.128	56.644	5.2	80.9199	15.29
GB.B1	18.919	0.137	66.998	3.232	99.208	18.990	69.41	5.85	99.1512	14.7
GB.B2	18.919	0.137	66.998	3.232	99.208	18.990	75.585	6.6	107.978	16.99
GB.B3	18.919	0.137	66.998	3.232	99.208	18.990	67.176	6.15	95.9646	14.42
GB.B4	18.919	0.137	66.998	3.232	99.208	18.990	75.131	6.18	107.329	13.08
GB.B5	18.728	0.137	66.877	3.252	99.028	18.963	72.288	6.05	103.268	13.91

Table E.3 Comparisons between Theoritical & Experimental Bending Moment Results at Yelding and Ultimate Stages.

Beam	Yielding Stage		M_{yt}/M_{ye}	Ultimate Stage		M_{ut}/M_{ue}
	M_y Thoertical Calculated (KN.m)	My Experimental (KN.m)		M_u Thoertical Calculated (KN.m)	Mu Experimental (KN.m)	
MA.B1	55.165	57.086	0.97	77.796	81.883	0.95
MA.B2	55.165	61.026	0.90	77.796	87.180	0.89
GA.B1	55.438	55.996	0.99	78.183	79.994	0.98
GA.B2	55.438	58.016	0.96	78.183	82.880	0.94
GA.B3	55.438	55.624	1.00	78.183	79.463	0.98
GA.B4	55.438	59.483	0.93	78.183	84.976	0.92
GA.B5	55.302	59.220	0.93	77.990	84.600	0.92
GA.B6	55.302	56.644	0.98	77.990	80.920	0.96
MB.B1	66.335	77.390	0.86	98.224	110.553	0.89
MB.B2	66.335	72.558	0.91	98.224	103.654	0.95
GB.B1	66.998	69.410	0.97	99.208	99.151	1.00
GB.B2	66.998	75.585	0.89	99.208	107.978	0.92
GB.B3	66.998	67.176	1.00	99.208	95.965	1.03
GB.B4	66.998	75.131	0.89	99.208	107.329	0.92
GB.B5	66.877	72.288	0.93	99.028	103.268	0.96